

9-2016

Role of phosphorylation in the regulation of PRMT5

Alexsandra B. Espejo

Follow this and additional works at: http://digitalcommons.library.tmc.edu/utgsbs_dissertations

 Part of the [Molecular Biology Commons](#)

Recommended Citation

Espejo, Alexsandra B., "Role of phosphorylation in the regulation of PRMT5" (2016). *UT GSBS Dissertations and Theses (Open Access)*. 711.

http://digitalcommons.library.tmc.edu/utgsbs_dissertations/711

This Dissertation (PhD) is brought to you for free and open access by the Graduate School of Biomedical Sciences at DigitalCommons@TMC. It has been accepted for inclusion in UT GSBS Dissertations and Theses (Open Access) by an authorized administrator of DigitalCommons@TMC. For more information, please contact laurel.sanders@library.tmc.edu.

ROLE OF PHOSPHORYLATION IN THE REGULATION OF PRMT5

by

Alexsandra Beatriz Espejo Ph.D.

APPROVED:

Mark Bedford, Ph.D.
Advisory Professor

Taiping Chen, Ph.D.

Sharon Y.R. Dent, Ph.D.

Rick A. Finch, Ph.D.

David G. Johnson, Ph.D.

APPROVED:

Dean, The University of Texas
Graduate School of Biomedical Sciences at Houston

ROLE OF PHOSPHORYLATION IN THE REGULATION OF PRMT5

A

DISSERTATION

Presented to the Faculty of
The University of Texas
Health Science Center at Houston
and
The University of Texas
MD Anderson Cancer Center
Graduate School of Biomedical Sciences
in Partial Fulfillment

of the Requirements

for the Degree of

DOCTOR OF PHILOSOPHY

by

Alexandra Beatriz Espejo B.S.
Houston, Texas

December 2016

Dedication

I dedicate this thesis to my family, for their support, loving patience and encouraging me not to give up, and especially to my husband Oscar, for his unconditional love and for always being there for me.

Esta tesis esta dedicada a mi familia, por su cariñosa paciencia y apoyo, que me animaron a seguir adelante, en especial a mi esposo Oscar, por su amor incondicional, por hacerme reír y por estar siempre a mi lado.

Acknowledgements

I would like to express my sincere appreciation to my mentor, Dr. Mark Bedford for his guidance on the course to pursue my Ph.D. degree.

I also appreciate all my committee members, Drs. Taiping Chen, Sharon Dent, Rick Finch, David Johnson, Dean Tang and Gary Johanning for their support and wonderful suggestions over the years.

I would like to take this opportunity to thank all current and past members of Dr. Bedford's laboratory, Donghang Cheng, Narkhyun Bae, Jianqiang Bao, Guozhen Gao, Sitaram Gayatri, Karynne Black, Cari Sagum, Carol Mikulec, Vidyasiri Vemulapalli and Alessandra DiLorenzo, for their friendship, support and good sense of humour. My sincere gratitude to Cari Sagum and Karynne Black for working with the microarray experiments. Also, I thank Rebecca Deen for her always cordial assistance and Dr. Briana Dennehey for her tremendous help in editing my manuscript.

In addition, I would like to thank everyone at Science Park who has helped and supported me in many ways. Particularly, I would like to thank Dr. Jeusun Kim and Nicolas Veland for generating ES cells and Dr. Anup Biswas for performing CHIP experiments.

I am also very thankful to the experimental animals; they have contributed enormously not only to this study, but they have been fundamental in many aspects of science

Finally, I would like to thank my family for their love, understanding and support.

ROLE OF PHOSPHORYLATION IN THE REGULATION OF PRMT5

Alexsandra Beatriz Espejo, Ph.D.

Supervisor Professor: Mark T. Bedford, Ph.D.

Summary

PRMT5 is a member of a group of proteins that mediate arginine methylation. It is involved in diverse cellular processes, including cell differentiation, splicing, transcription elongation and epigenetic silencing, and its expression is dysregulated in many cancers. Due to its pleiotropic functions, PRMT5 is subject to multi-level regulation. Post-translational modification (PTM) of proteins can modulate an array of cellular processes by regulating both protein interactions and protein structural changes. PRMT5 is commonly found associated with other proteins; these interactions seem to control both its catalytic activity and its substrate specificity. Recently, it became clear that PRMT5 is phosphorylated at a number of residues, which prompted us to investigate whether phosphorylation of PRMT5 regulates its subcellular localization and/or substrate choice, by facilitating phospho-dependent protein-protein interactions.

To study how phosphorylation affects PRMT5 function, protein microarrays were used to identify novel phosphodependent-interacting proteins. This analysis revealed that phosphorylation mediates the interaction of PRMT5 with several SH2-domain containing proteins, 14-3-3 proteins and the FHA domain of MDC1. These novel phospho-dependent PRMT5 interactions suggest that crosstalk between kinases and arginine methyltransferases may play a pivotal role in modulating the different cellular functions of PRMT5.

Additionally, we have found that the C-terminal region of PRMT5 has a recognition motif shared by PDZ domains and 14-3-3 proteins. In order to bind to this motif, 14-3-3 proteins require the C-terminus to be phosphorylated, while PDZ domain recognition is phospho-independent. From these data, a new regulatory mechanism that affects PRMT5 behavior was proposed; the action of kinases and

phosphatases on PRMT5 may function as a switch to regulate interactions between 14-3-3 and PDZ domain-containing proteins. We additionally observed this paradigm with a number of proteins, suggesting that this phosphorylation dependent switch, regulating binding to 14-3-3 and PDZ domains, occurs in a wide range of protein-protein interactions.

Among the recently discovered PDZ-binding partners, we have found that PRMT5 interacts with NHERF2, a membrane-associated protein that regulates the sodium ion exchanger NHE3. Through this interaction, PRMT5 is placed in close proximity to the membrane and therefore may regulate the influx of ions through selective ion channels. Overall, we hypothesize that the direct interaction of PRMT5 with selected partners mediates the appropriate localization of PRMT5, allowing it to methylate specific substrates.

Physiological processes including muscle contraction, cell homeostasis and neurotransmission are controlled by the selective conduction of ions across cell membranes. Ion channels and exchangers are proteins that span cell membranes and form a channel or pore, facilitating the movement of ions in and out of cells. Abnormal response of the cell to its microenvironment is one of the key factors in the progression of many diseases. To study the role of the C-terminus of PRMT5 *in vivo*, we used CRISPR/Cas9 technology to create a mouse with the last six amino acids of PRMT5 replaced with an HA tag, as well with an altered PRMT5 C-terminus. Both mouse models lack the critical 14-3-3/PDZ binding motif. This approach revealed that the C-terminus of PRMT5 is essential for viability as no homozygous mutant embryos were recovered. Likewise, no homozygous PRMT5^{Δ+HA} ES cell lines could be created. The results described here represent progress toward understanding PRMT5 function and regulation.

Table of Contents

Approval sheet	i
Title	ii
Dedication	iii
Acknowledgements	iv
Summary	v
Table of Contents	vii
List of Illustrations	xi
List of Tables	xiii
List of Abbreviations	xiv
Chapter 1: General Introduction	1
1.1. Post-translational modification	1
1.2. Protein domains	2
1.3. Phosphorylation	4
1.4. Phosphotyrosine binding domains	5
1.4.1. SH2 and PTB domains	5
1.5. Phosphorylated serine and threonine binding domains	5
1.5.1. 14-3-3 proteins	7
1.5.2. FHA domains	8
1.5.3. BRCT domains	9
1.6. Methylation	9
1.6.1 Arginine methylation	10
1.6.2. Protein arginine methyltransferases	13
1.6.3. Arginine Mono-methyltransferases	14
1.6.4. Arginine Asymmetric-methyltransferases	14
1.6.5. Arginine Symmetric-methyltransferases	16
1.7. Multiple roles of PRMT5	17
1.7.1. PRMT5 in mRNA splicing	17
1.7.2. PRMT5 in transcriptional regulation	18
1.7.3. Association of PRMT5 and CpG methylation	18

1.7.4. Role of PRMT5 in development	19
1.7.5. Role of PRMT5 in cancer	19
1.8. Regulation of PRMT5 activity	21
1.8.1. Regulation of PRMT5 by binding partners	21
1.8.2. Existing PTMs on histones regulate PRMT5 association and specificity	22
1.8.3. Cellular localization	22
1.8.4. Crosstalk between phosphorylation and methylation	23
1.9. Topics to be covered for this study.....	24
Chapter 2: Material and Methods.....	26
2.1. Plasmid constructs	26
2.1.1. Mammalian expression vectors	26
2.1.2. Bacterial expression vector	27
2.3. shRNA knockdown	28
2.4. Protein purification.....	28
2.5. GST pulldown studies	29
2.6. Cell culture	29
2.7. immortalization and culture of MEFs.....	29
2.8. Transient transfection	30
2.9. Stable transfection.....	30
2.10. In cell phosphorylation.....	30
2.11. <i>In vitro</i> phosphorylation	31
2.12. Antibodies.....	31
2.13. Immunofluorescence microscopy	31
2.14. GFP immunoprecipitations	32
2.15. Western blots	32
2.16. Peptide synthesis	33
2.17. Peptide pull-down.....	35
2.18. Protein domain microarray	35
2.19. Membrane fractionation.....	36
2.20. Intracellular pH	36
2.21. Generation of the PRMT5 ^{Δ+HA} mouse model.....	37

2.22. Mouse genotyping	37
2.25. Derivation of mouse embryonic stem cells	38
2.24. Chromatin immunoprecipitation (ChIP) assay	38
2.26. Ionizing radiation treatment	39
Chapter 3: Regulation of PRMT5 by Tyrosine Phosphorylation	40
3.1. Introduction.....	40
3.2. Results.....	40
3.2.1. Tyrosine phosphorylation regulates PRMT5 activity	40
3.2.2. Phosphorylation of PRMT5 creates a binding motif for SH2 domains	41
3.2.3. Endogenous PRMT5 interacts with SH2 domain-containing proteins	43
3.3. Discussion	49
3.4. Future studies.....	52
Chapter 4: Phosphorylation at the C-terminus triggers a binding switch between 14-3-3 proteins and PDZ domains	55
4.1. Introduction.....	55
4.2.1. PDZ domains.....	55
4.2.2. NHERF	57
4.3. Results.....	59
4.3.1. PRMT5 is phosphorylated at the C-terminus	59
4.3.2. PRMT5 interacts with PDZ domains and 14-3-3 proteins	62
4.3.3. Endogenous PRMT5 interacts with 14-3-3 proteins and the NHERF2 PDZ domain.....	68
4.3.4. The C-terminus of PRMT5 facilitates its plasma membrane association.	70
4.3.5. PRMT5 symmetrically methylates membrane-associated proteins.....	73
4.3.6. Physiological importance of PRMT5-complexes relies on its C-terminus ...	75
4.3.7. The C-terminal motif of PRMT5 is required for mouse viability	83
4.3.8. Discussion	86
4.4. Future Studies	91
Chapter 5: Role of PRMT5 in DNA damage response	93
5.1. Introduction.....	93

5.1.1. The DNA Damage Response	93
5.2. DNA Repair Mechanisms: NHEJ and HR	95
5.2.1. Nonhomologous end-joining.....	95
5.2.2. Homologous recombination.....	95
5.3. Histone code for DNA Double-Strand Break Repair	96
5.4. Arginine methylation and DDR.....	99
5.5. Results.....	104
5.5.1. Phosphorylated PRMT5 interacts with the FHA domain of MDC1	104
5.5.2. PRMT5 is recruited to sites of DNA double-strand breaks.....	107
5.5.3. H2AR3me2s is catalyzed by PRMT5 and does not vary after IR.....	109
5.6. Discussion	114
5.7. Future studies.....	116
Chapter 6: Significance	118
Chapter 7: Bibliography	120
Chapter: 8 Vita	144

List of Illustrations

Figure 1: Protein domains that recognize particular motifs	6
Figure 2: Arginine methylation is catalyzed by PRMTs.....	12
Figure 3: PRMT5 is phosphorylated at multiple residues	41
Figure 4: PRMT5 is tyrosine-phosphorylated by the Src kinase	42
Figure 5: Phosphotyrosine-binding microarray	44
Figure 6: Identification of PRMT5 phosphotyrosine specific binding partners	45
Figure 7: Endogenous PRMT5 interacts with SH2 domain-containing proteins	47
Figure 8: Additional SH2 interactions.....	50
Figure 9: Dot blot analysis of phospho-tyrosine PRMT5 antibodies	54
Figure 10: Localization of PDZ proteins in epithelial cells.....	58
Figure 11: PRMT5 is phosphorylated at its C-terminus	60
Figure 12: Radiometric assay of the PRMT5 C-terminus peptide phosphorylation ..	61
Figure 13: AKT and SGK regulate PRMT5 phosphorylation.....	63
Figure 14: The PDZ domain and 14-3-3 proteins share a common binding motif	64
Figure 15: Map of PDZ/14-3-3 protein Array.....	66
Figure 16: C-terminal pT634 triggers a binding switch between 14-3-3 and PDZ	67
Figure 17: PRMT5 peptide pull-down assays	69
Figure 18: PRMT5 interacts with NHERF2 and 14-3-3.....	72
Figure 19: PRMT5 associates with membrane via its PDZ recognition motif	74
Figure 20: Subcellular localization of SDMA proteins	76
Figure 21: A role for PRMT5 in regulating intracellular pH	79
Figure 22: SK-CO15 PRMT5-KD rescued characterization.....	80

Figure 23: NHERF2 associates with the PRMT5-MEP50 complex	81
Figure 24: Myc-PRMT5 WT and Myc-PRMT5 ^{T634A} cellular localization	82
Figure 25: PRMT5 ^{Δ+HA} mouse generated by CRISPR/Cas9.....	85
Figure 26: Mutation in the C-terminus of PRMT5 alters 14-3-3 and PDZ recognition	90
Figure 27: DNA damage repair pathways.....	94
Figure 28: HR and NHEJ DNA Repair Mechanisms.....	97
Figure 29: PRMT5 phosphothreonine specific binding partners	105
Figure 30: PRMT5 interacts with FHA domain of MDC1	106
Figure 31. PRMT5 recruitment to DNA damage sites.....	108
Figure 32: MEF KO PRMT5 and anti-H4/H2AR3me2s characterization	110
Figure 33: Validation of H2AR3me2s using immunofluorescence.....	111
Figure 34: Symmetric methylation on H2A does not vary in response to IR.....	113

List of Tables

Table 1: Post-translational modification of amino acids.....	3
Table 2: Phosphotyrosine Interactions.....	48
Table 3: Histone modification in DDR.....	103

List of Abbreviations

4-OHT	4-hydroxy tamoxifen
53BP1	P53 binding protein1
ABL2	Abelson-related gene
ADMA	Asymmetric dimethyl arginine
AKT	Protein kinase B
ASK1	Apoptosis signal regulating kinase 1
ATM	Ataxia telangiectasia mutated
ATP	Adenosine triphosphate
ATR	Ataxia telangiectasia and Rad3-related
BBAP	The BAL-binding Protein
BCECF-AM	Bis-(2-carboxyethyl)-5-carboxyfluorescein acetoxymethyl ester
BER	Base-excision repair
Blimp	B-lymphocyte-induced maturation protein 1
BRCA1	Breast cancer type 1 susceptibility protein
BRCT	BRCA1 carboxy-terminal
BRD7	Bromodomain containing 7
Bub1	Budding uninhibited by benzimidazoles 1
CalA	Calyculin-A
CamK	Ca ²⁺ -calmodulin-dependent kinase
CAMK2	Calcium/calmodulin-dependent protein kinase II
Cas9	CRISPR associated protein 9
CBP/p300	CREB-binding protein
CDD	Conserved domain database
CFTR	Cystic fibrosis transmembrane regulator
ChIP	Chomatin immunoprecipitation
Chk1	Checkpoint kinase 1
Chk2	Checkpoint kinase 2
CK2	Casein kinase II
COPR5	Coordinator of PRMT5 and differentiation stimulator
DDR	DNA damage response
DLG	Drosophila tumor suppressor protein disks-large-1
DNA	Deoxyribonucleic acid
DNA-PKcs	DNA-dependent protein kinase
DOT1	Disruptor of telomeric silencing
DSB	DNA double-strand breaks
E6	Human Papillomavirus (HPV) E6 protein
EDTA	Ethylenediaminetetraacetic acid
EGFR	Epidermal growth factor receptor
ERBB4	Erb-b2 receptor tyrosine kinase 4
ERK	Extracellular-signal-regulated kinase 1

ERK1	Extracellular signal–regulated kinases
ERM	Ezrin-radixin-moesin Binding domain
EYA	Eyes absent
FEN1	Flap structure-specific endonuclease 1
FHA	Forkhead-associated
GCN5	General control of amino-acid synthesis
GFP	Green fluorescent protein
GRB2	Growth factor receptor-bound protein 2
GRIP1	Glutamate receptor-interacting protein 1
GST	Glutathione S-transferase
HCK	Hematopoietic cell kinase
HEPES	4-(2-hydroxyethyl)-1-piperazineethanesulfonic acid
HR	Homologous recombination
hSWI/SNF	Switch/Sucrose Non-Fermentable
HU	Hydroxyurea
I-Ppol	Intron-encoded endonuclease
IPTG	Isopropyl- β -d-thiogalactopyranoside
IRK1	Inward-rectifier potassium ion channel
KMT	Lysine methyltransferases
KO	Knockout mouse
Ku	Ku70-Ku80 heterodimer
LCK	Lymphocyte-specific protein tyrosine kinase
MBP	Myelin basic protein
MDC1	Mediator of DNA damage checkpoint 1
MEF	Mouse embryonic fibroblasts
MEP50	Methylosome protein 50
MK2	MAPKAP kinase-2
MMA	Monomethyl arginine
MMR	Mismatch repair
MMSET	Multiple myeloma SET domain
MOF	Males absent on the first
MPP7	Membrane palmitoylated protein 7
MRE11	Meiotic recombination 11 homolog 1
MRN	MRE11/RAD50/NBS1 complex
MSK1	Mitogen- and stress-activated protein kinase-1
MTAP/CDKN2A	Cyclin-dependent kinase inhibitor 2a
NHEJ	Nonhomologous end joining
NHERF	Na ⁺ /H ⁺ exchanger regulatory factor
NHEs	Sodium/hydrogen exchangers
NHK-1	Nucleosomal histone kinase 1
NM23	Nonmetastatic 23
PAM	Mimetic synthetic peptide affinity ligand
PBD	Polo-box domains

PBS	Phosphate-buffered saline
PDCD4	Suppressor of programmed cell death 4
PDZ	PSD-95/DLG/ZO-1
PGHS2	Prostaglandin-endoperoxide synthase 2
PIK3R1	Phosphatidylinositol 3-kinase regulatory subunit 1
PKA	Protein kinase A
PKB/AKT	Protein kinase B
PKC	Protein kinase C
PKG	Protein kinase G
pLCLn	Chloride conductance regulatory protein
PRC2	Polycomb repressive complex 2
PRMTs	Protein arginine methyltransferases
PSD-95	Postsynaptic density-95
PTB	Phosphotyrosine binding
PTK	Protein tyrosine kinase
PTM	Post-translational modification
RASA1	Ras p21 protein activator 1
RBBP7	Retinoblastoma binding protein 7
RBL2	Retinoblastoma-like protein 2
RioK1	Rio kinase 1
RNA	Ribonucleic acid
RNF8	RING finger protein 8
RSK	Ribosomal S6 kinase
SAM	S-adenosylmethionine
SC1	Schwann cell factor 1
SCRIB1	Scribbled planar cell polarity protein
SDMA	Symmetric dimethyl arginine
SGK	Serum/glucocorticoid regulated kinase
sgRNA	Guide RNA
SH2	Src homology 2
SH3	Src homology 3
SHIP1	Protein tyrosine phosphatase 1
SREBP	Sterol regulatory element-binding protein
ST7	Suppressor of tumorigenicity 7
TIP60	60 KDa Tat-interactive protein
TNS4	Tensin 4
TRRAP	Transformation/transcription domain associated protein
UV	Ultraviolet
VAV1	Vav guanine nucleotide exchange factor 1
vSrc	Schmidt–Rupp strain of RSV
WDR5	WD-repeat protein 5
WSTF	Williams syndrome transcription factor.
ZO-1	Zonula occludentes 1

Chapter 1: General Introduction

1.1. Post-translational modification

Although protein levels are primarily regulated by gene transcription and translation, fine-tuning the turnover and functional availability of proteins requires more dynamic control. This control is achieved in part by post-translational modifications (PTMs). The complete protein repertoire of a cell is termed the proteome (Kahn, 1995). The proteome is greatly influenced by PTMs. Indeed, immediately following protein synthesis, most proteins are modified through a series of intricate and tightly regulated steps. The resulting modifications include cleavage of the protein backbone, or modifications of specific amino acids by the covalent additions of one or more chemical groups, proteins, lipids, or sugars. PTMs can result in altered protein structure, changes in interaction with other proteins, altered protein localization, and changes in overall protein stability. Thus a relatively small number of expressed proteins lead to a much larger functional repertoire of proteins via PTMs. Consequently, PTMs are fundamental to the regulation of molecular mechanisms and cellular functions that impact the health of an entire organism.

Of the 20 standard amino acids, 15 are known to be modified totaling more than 200 different PTMs (**Table 1**). Modification of amino acids most often occurs by enzymatic reactions mediated by specialized proteins. There are a vast number of enzymes that modify the proteome, either adding or removing functional groups. These functional groups can be classified according to the cosubstrate or coenzyme they depend on, such as S-adenosylmethionine (SAM) for methylation, ATP for phosphorylation, and acetyl CoA for acetylation (Walsh et al, 2005).

One essential characteristic of most amino acid modifications is reversibility, which brings plasticity to the proteome and allows rapid response to a specific stimulus. Many PTMs alter the structure of a given protein and consequently modulate the protein's activity. For instance, phosphorylation of a conserved residue

within the activation loop of a kinase is a classical example of a covalent modification that rapidly switches protein activity on or off (Steichen et al, 2012). Likewise, the reversibility of PTMs also helps in the formation and dissociation of protein complexes. PTMs create a binding motif for specific domains, thus mediating protein interactions. Indeed, more than 60% of PTM sites contribute to protein-protein interactions mediated by protein domains (Duan & Walther, 2015).

1.2. Protein domains

Protein domains correspond to functional, structural features of proteins that are evolutionarily conserved. Domains can be identified *in silico* by comparing protein sequences and/or predicted structures. According to the NCBI Conserved Domain Database (CDD), there are more than 1000 protein domains identified to date (Marchler-Bauer et al, 2015).

Protein domains are discrete elements that fold and function independently from one another. It is common for proteins to contain multiple domains, the particular combination of domains within a protein is key for a protein's biological function and its interaction within the global protein network. Yet, a particular domain can also have an independent function, and can cooperate with other domains in multi-domain proteins.

Protein domains have a variety of functions, including recognition and binding to cellular molecules, such as DNA, RNA or other proteins (**Figure 1**). Many protein-protein interactions are mediated by the recognition of a particular motif in one protein and a domain in another. A protein motif, like a protein domain, may be conserved in a large number of proteins, however, unlike a protein domain, it only consists of a short, specific amino-acid sequence. The interactions between protein domains and protein motifs are usually transient, and are frequently regulated by PTMs (Akiva et al, 2012).

Residue	Modification
Asp	phosphorylation isomerization to isoAsp
Glu	methylation carboxylation polyglycination polyglutamylolation
Ser	phosphorylation O-glycosylation phosphopantetheinylation autocleavages
Thr	phosphorylation O-glycosylation
Tyr	phosphorylation sulfation ortho-nitration TOPA quinone
His	phosphorylation aminocarboxypropylation N-methylation
Lys	N-methylation N-acylation by acetyl, biotinyl, lipoyl, ubiquityl groups C-hydroxylation
Cys	S-hydroxylation (S-OH) disulfide bond formation phosphorylation S-acylation S-prenylation protein splicing
Met	oxidation to sulfoxide
Arg	N-methylation N-ADP-ribosylation
Asn	N-glycosylation N-ADP-ribosylation protein splicing
Gln	transglutamination
Trp	C-mannosylation
Pro	C-hydroxylation
Gly	C-hydroxylation N-myristoylation

Table 1: Post-translational modification of amino acids.

Adapted from (Walsh et al, 2005)

Each domain family recognizes motifs with similar features. Some of the examples illustrated in **Figure 1** include the acetylation or methylation of lysine residues, which creates a binding motif for bromo and chromo domains, respectively. Similarly, methyllysine and methylarginine residues can be recognized by tudor domains. These PTMs and their association with protein binding domains have gained increasing importance since scientists began to recognize that these PTMs play a key role in the epigenetic regulation of gene expression.

1.3. Phosphorylation

Phosphorylation was described over a half century ago and is the most commonly studied PTM. In eukaryotes, phosphorylation is the covalent attachment of a negatively charged phosphate group to an amino acid, mainly serine, threonine and tyrosine residues. Protein phosphorylation is highly dynamic: addition of phosphate groups is catalyzed by kinases, whereas removal of phosphate groups – dephosphorylation – is catalyzed by phosphatases. Both kinases and phosphatases regulate multiple cellular processes (Jin & Pawson, 2012).

Phosphorylation is a potent regulatory mechanism. It can modify the function of proteins by inducing conformational changes. Phosphorylation may also control the subcellular location and stability of proteins. Additionally, it can alter the activity of proteins by mediating interactions between protein domains and phosphorylated ligands, resulting in phospho-dependent protein networks. Tyrosine phosphorylation is recognized by distinct binding domains, the Src homology 2 (SH2) and phosphotyrosine binding (PTB) domains. Serine and threonine phosphorylation generate docking sites for a number of domains such as forkhead-associated (FHA) domains, Polo-box domains (PBDs), WD40 repeats, WW domains, BRCT domains and 14-3-3 proteins. (Hunter, 2014).

1.4. Phosphotyrosine binding domains

1.4.1. SH2 and PTB domains

Phosphorylation of tyrosine residues creates a binding site for phosphotyrosine recognition domains such as SH2 and PTB domains. SH2 domains are present in more than a hundred distinct proteins (Liu et al, 2006), comprising the largest class of known phosphotyrosine-recognition domains. PTB domain are present in 79 human proteins; however, only a fraction of them have the capacity to recognize the phosphotyrosine-motif. The others recognize nonphosphorylated peptide ligands or phosphoinositides (Liu et al, 2006).

The SH2 domain consists of about 100 amino acids organized into six beta-sheets and two alpha-helices. The phosphopeptide binding site lies perpendicular to the central beta-sheets (Liu et al, 2006; Yaffe, 2002). The specificity of the SH2 domain is given by the recognition of not only the phosphotyrosine but also the adjacent carboxy-terminal residues (Liu et al, 2006; Yaffe, 2002).

SH2 domains play a critical role as adaptor proteins and signaling molecules downstream of receptor tyrosine kinase (RTK) activity, and protein-protein interactions (Yaffe, 2002). Several human diseases are associated with mutations in SH2-encoding genes (Liu et al, 2006), arising from either the loss- or the gain-of-function of SH2. Additionally, developmental studies using knockout mouse models of SH2 proteins show a variety of phenotypes, ranging from early embryonic lethality to no visible abnormality.

1.5. Phosphorylated serine and threonine binding domains

Serine and threonine phosphorylation plays an important role in multiple cellular processes, either directly, by regulating the activity of enzymes, or indirectly, by promoting specific protein-protein interactions. 14-3-3 proteins were the first family of phosphoserine- or phosphothreonine- binding proteins to be discovered.

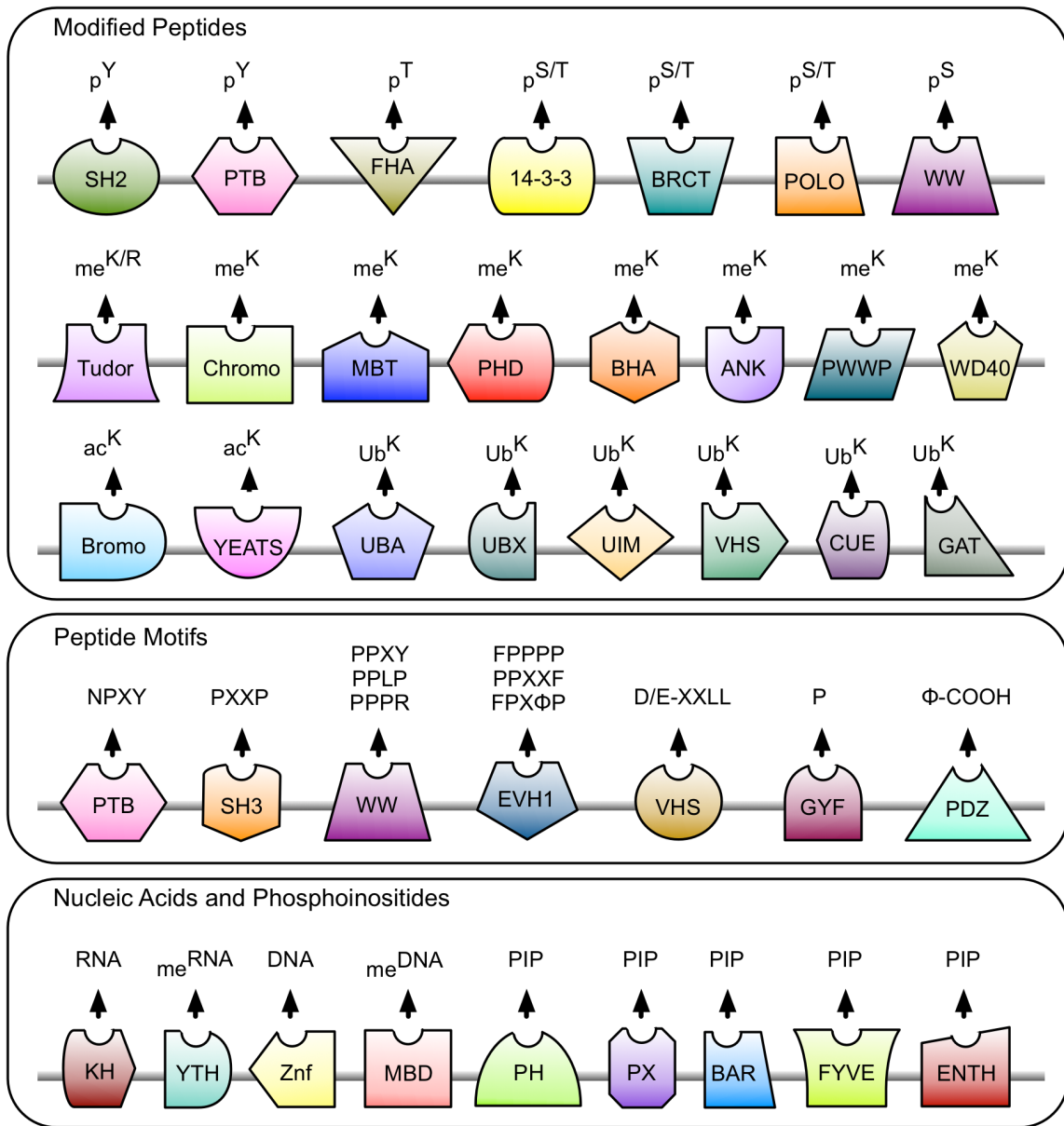


Figure 1: Protein domains that recognize particular motifs

Distinct domains, depicted with different colors and shapes are able to recognize specific motifs. Some domains recognize motifs that harbor PTMs, while others recognize distinct molecules such as DNA or RNA. ϕ , hydrophobic residue; p, phosphorylation; me, methylation; ac, acetylation; ub, ubiquitination; PIP, phosphoinositides.

Subsequently, other proteins have been identified as integral components of these phospho-binding domain networks.

1.5.1. 14-3-3 proteins

First identified as abundant brain proteins, 14-3-3 proteins are found in almost all human tissues, predominantly in the cytoplasm of cells (Uhlen et al, 2015). There are seven distinct 14-3-3 isoforms that are encoded by different genes, denoted α/β , γ , ϵ , η , σ , τ/θ , and ζ . They are small proteins of 28 to 33 KDa, forming homo- and heterodimers that resemble a horseshoe-shaped structure (Wilker et al, 2005). Each monomeric unit is formed by nine alpha helices. The dimerization interface is present at the N-terminal alpha helices. The central channel forms the binding groove, which is highly conserved across the different 14-3-3 isoforms (Xiao et al, 1995; Yaffe et al, 1997). Each unit contains an independent binding groove; consequently, the dimer can interact with two motifs simultaneously (Uhart & Bustos, 2013).

14-3-3 proteins have two canonical consensus binding motifs RSXpSXP (Motif I) and RX[Y/F]XpSXP (Motif II) (Yaffe et al, 1997) as well as a C-terminal binding motif p(S/T)X₁₋₂-COOH (Motif III), in which an upstream arginine residue is frequently present, likely facilitating 14-3-3 interaction and kinase recognition (Coblitz et al, 2006; Ganguly et al, 2005).

Phosphorylation on either serine or threonine is required for 14-3-3 binding. Accordingly, the 14-3-3-binding site has several common features with the optimal substrate sequences for many kinases, including protein kinase A (PKA), protein kinase G (PKG), protein kinase C (PKC), protein kinase B (PKB/Akt), Ca²⁺-calmodulin-dependent kinase (CamK), serum- and glucocorticoid-induced kinase (SGK) family members, and the checkpoint effector kinases: Chk1, Chk2, and MK2 (Kobayashi et al, 1999; Mohammad & Yaffe, 2009; Smith et al, 2011).

Interestingly, motif III located at the extreme C-terminus of 14-3-3 ligands has a notable similarity with the PDZ binding motif. However, 14-3-3 interactions require phosphorylation, whereas PDZ binding does not.

Via its phospho-dependent binding groove, 14-3-3 proteins interact with hundreds of proteins implicated in cell cytoskeleton organization, cell cycle regulation, signal transduction, protein metabolism, protein synthesis, chromatin structure, protein folding, apoptosis, and several other cellular processes (Chen et al, 2010; Jin et al, 2004; Meek et al, 2004; Pozuelo Rubio et al, 2004).

Mechanistically, 14-3-3 proteins regulate cellular processes by obstructing specific motifs, thus blocking protein-protein interactions; retaining proteins in the cytoplasm; regulating the catalytic activity of its bound ligand; linking enzymes and substrates; and preventing protein degradation (Morrison, 2009).

1.5.2. FHA domains

FHA domains are phospho-binding domains, commonly found in DNA repair-associated proteins, and specifically recognize only phosphothreonine motifs. Based on sequence analysis, the FHA domain core homology region is about 55 to 75 amino acids. However, based on structural analysis, the FHA domain extends to include 95 to 121 residues. Although FHA domains may have low sequence homology, structurally, they adopt a similar fold that consists of 11 beta strands. The phosphothreonine-binding region in a FHA domain includes the loops and turns between β 3- β 7 and β 10- β 11 strands (Mahajan et al, 2008).

The binding motif of FHA domains consists of four different types: i) “pT+3 rule”, in which the FHA domain recognizes phosphothreonine and the 3 adjacent C-terminal residues pTXX(I/L/V), and favors a nonpolar residue at the pT+3 position; ii) The “N- and C-terminus to pT” encompasses amino acid residues both N-terminal and C-terminal to the phosphothreonine residue; iii) The “pT-pT+3” includes two phosphothreonine residues and the 3 C-terminal residues pTXXpTXXS; and iv) The “pT + an extended binding surface”, which is considerably different from the other FHA domain binding motifs, as the ligand interaction requires a longer binding surface (Mahajan et al, 2008).

1.5.3. BRCT domains

The BRCT domain (breast cancer 1 (BRCA1) C-terminus) was originally identified as a tandem repeat on the C-terminus of BRCA1. BRCT domains are composed of 85–95 amino acids, and are arranged as either a single domain or multiple tandem domains, usually together with other domains in multidomain proteins (di Masi et al, 2011). BRCT motifs are arranged in a parallel four-stranded β sheet flanked on one side by α helices 1 and 3, and on the other side by α helix 2. BRCT domains have a binding preference for phosphoserine present in a pSXXF motif (Glover et al, 2004; Yu et al, 2003).

In humans, at least 23 proteins harbor BRCT domains. BRCT mediated protein–protein interactions are essential for DNA replication and repair as well as cell cycle regulation (Gerloff et al, 2012; Glover et al, 2004). BRCT domain function is important for cell homeostasis since cancer susceptibility is linked to mutations found within the BRCT domains of BRCA1, Nijmegen breakage syndrome (NBS) protein and microcephalin (MCPH1) protein (Glover et al, 2004).

1.6. Methylation

In the mid-sixties, researchers anticipated the existence of at least two methyl-enzyme systems, one that methylates lysine and one that methylates arginine residues. With a visionary interpretation of their experimental results, these researchers suggested a possible role of methyltransferases during repression or derepression of gene expression (Paik & Kim, 1968). Methylation is a widespread post-translational modification affecting many cellular processes.

In the case of lysine, this modification is mediated by lysine methyltransferases (KMT). KMTs possess an evolutionarily conserved catalytic domain named the SET domain. Lysine residues of both histones and non-histone proteins can be monomethylated, dimethylated and trimethylated. The addition of more than one methyl group can be catalyzed by a single enzyme or sequentially by different enzymes. Thus, each methylation status is regulated by the interplay of dedicated

KMTs (Boriack-Sjodin & Swinger, 2016). In contrast, arginine residues can be monomethylated and symmetrically- or asymmetrically-dimethylated. These reactions are catalyzed by enzymes called protein arginine methyl transferases (PRMTs) (**Figure 2A**) (Cheng et al, 2007).

Until recently, it was unclear whether demethylation of methylarginine residues exists. However, a new detailed analysis indicates that this modification is reversible. The removal of arginine methylation occurs via oxidation of the arginine guanidino nitrogen-methyl groups and loss of formaldehyde in a reaction similar to that of lysine demethylation (Walport et al, 2016). Therefore, the methyl group of both lysine and arginine residues can be removed by specialized JmjC-domain containing enzymes, lysine demethylases (KDMs) and arginine demethylases (RDMs).

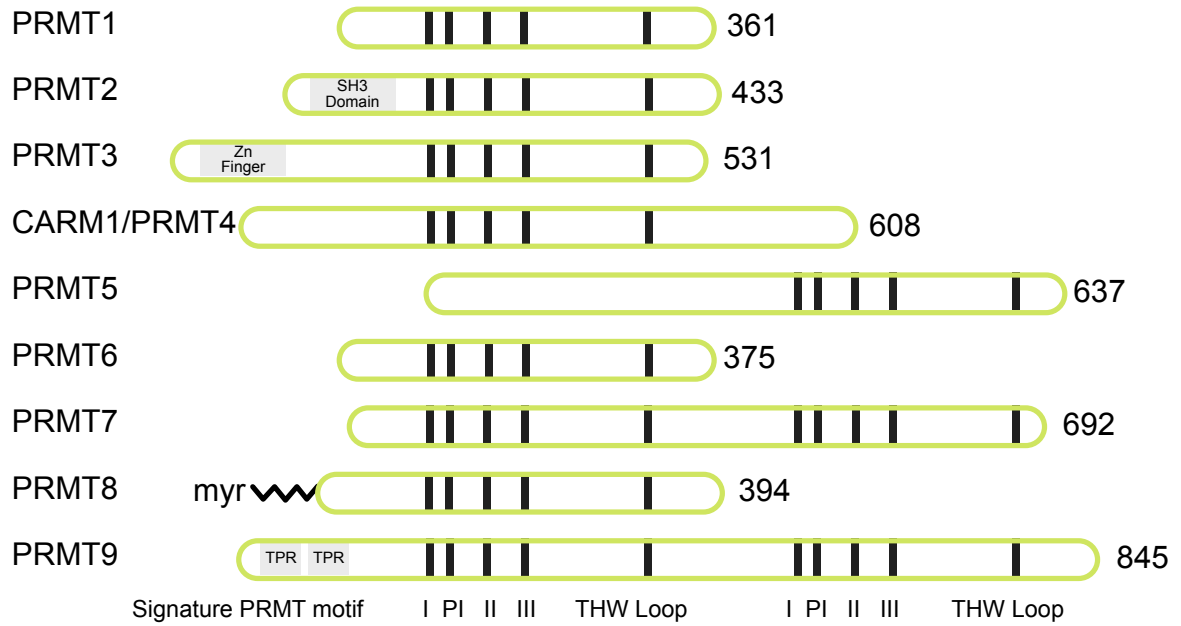
Like other PTMs, methyl-arginine and -lysine generate binding motifs for specific protein domains. Lysine methylation creates a binding motif for chromo, chromo barrel, plant homeodomain (PHD), tudor, malignant brain tumor (MBT), PWWP, and bromo adjacent homology (BAH) domains, whereas methylated arginine is recognized only by tudor domains (Chao Xu, 2015; Kim et al, 2006; Kuo et al, 2012).

The addition of methyl groups to arginine residues of histones and non-histone proteins not only modulates transcription, but also many distinct cellular functions, such as signal transduction, mRNA splicing, DNA repair, and protein translocation (Bedford & Clarke, 2009).

1.6.1 Arginine methylation

Of the 20 amino acids, arginine has the longest side chain with the end of the side chain carrying a net positive charge. It has two potential hydrogen bond donors that promote interactions with negatively charged molecules, hydrogen bond acceptors, such as DNA, RNA and proteins (Lakowski & Frankel, 2009). The addition of a methyl group to arginine residues does not alter the total charge;

A



B

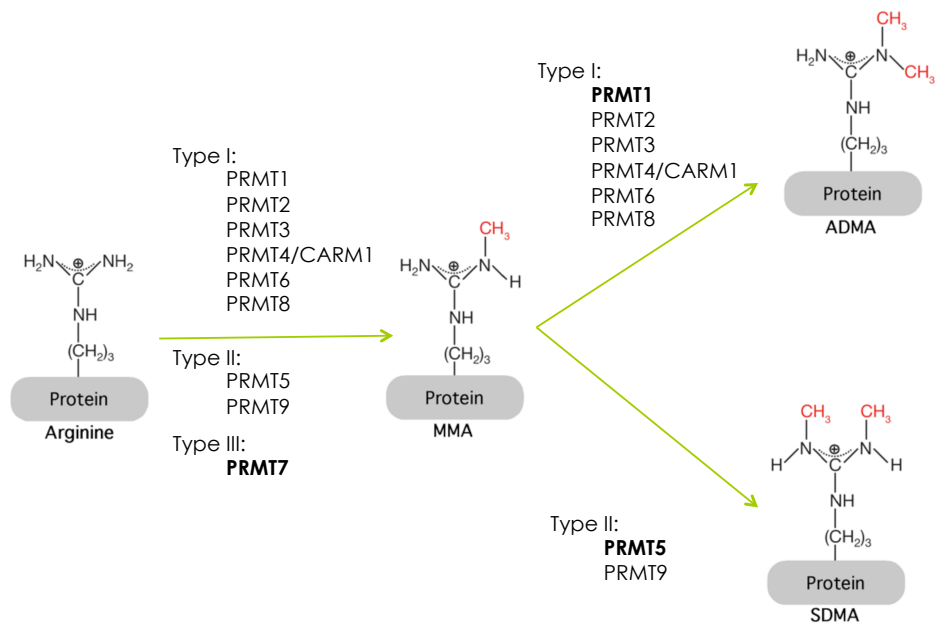


Figure 2: Arginine methylation is catalyzed by PRMTs

(A) PRMT family members. Conserved catalytic core region containing the signature motifs I, post-I (PI), II, and III, and the conserved THW loop.

(B) PRMT family members catalyze the formation of monomethylarginine (MMA), asymmetric dimethylarginine (ADMA) and symmetric dimethylarginine (SDMA). Type I catalyzes ADMA and is comprised by PRMT1, PRMT2, PRMT3, PRMT4/CARM1, PRMT6 and PRMT8. Type II enzymes mediate SDMA and include PRMT5 and PRMT9. In addition, type I and type II enzymes can catalyze the formation of MMA as an intermediate. PRMT7 is the only type III enzyme, which mainly generates MMA. Whether PRMT7 catalyzes SDMA is controversial. The main enzymes for each form of methylation are indicated. Adapted from Molecular Cell. Bedford MT, Clarke SG. Protein arginine methylation in mammals: who, what, and why. 33: 1-13 (2009), with permission from Elsevier.

instead, it removes a potential hydrogen bond donor through replacement of the available hydrogen atoms by methyl groups (Raman et al, 2001).

Methyl groups in terminal guanidino nitrogen atoms of arginine residues can be incorporated in three distinct forms: monomethylarginine (MMA) contains only one methyl group; symmetric dimethylated arginine (SDMA) contains two methyl groups placed on each of the terminal nitrogen atoms; and asymmetric dimethylarginine (ADMA) contains two methyl groups positioned on the same terminal nitrogen atom (**Figure 2B**). All three forms are created by PRMTs.

1.6.2. Protein arginine methyltransferases

PRMTs are classified according to the type of methylation they catalyze. Types I, II and III are all able to generate MMA, however, type III solely catalyzes MMA at the terminal nitrogen of arginine residues (Zurita-Lopez et al, 2012). Further methylation is carried out once more by type I enzymes (PRMT1, PRMT2, PRMT3, PRMT4/CARM1, PRMT6, and PRMT8) to generate ADMA, or by type II enzymes (PRMT5 and PRMT9) to generate SDMA. Of these, PRMT5 is the major enzyme that generates SDMA.

Sequence analysis of all PRMTs shows a highly conserved catalytic core region containing the signature methyltransferase motifs I, post-I, II and III. Motif I mediates the binding of SAM and contains the double-E loop (two glutamate residues). The C-terminus of the core region harbors the most highly conserved sequence of this domain the THW (threonine-histidine-tryptophan) loop. These sequences arrange the methyltransferase active site in this family of enzymes (**Figure 2A**) (Bedford & Richard, 2005; Weiss et al, 2000; Zhang et al, 2000).

The structure of the catalytic core is also highly conserved, as shown by the crystal structures of PRMT1, PRMT3, PRMT4 and PRMT5 (Antonysamy et al, 2012; Ho et al, 2013; Sun et al, 2011; Troffer-Charlier et al, 2007; Yue et al, 2007; Zhang et al, 2000).

1.6.3. Arginine Mono-methyltransferases

PRMT7 harbors two AdoMet-binding motifs and is the only enzyme described as having primarily type III activity. PRMT7 substrates are also substrates for all of the other characterized PRMTs (PRMT1, -2, -3, -4, -5, -6 and -8), including histone substrates (Zurita-Lopez et al, 2012). This correlates with the notion that monomethylarginine is the precursor for subsequent methylation by type I and II PRMTs (Dhar et al, 2013).

1.6.4. Arginine Asymmetric-methyltransferases

ADMA is the predominant type of arginine methylation, and is mediated by type I enzymes, largely PRMT1 (Tang et al, 2000). In the absence of PRMT1 and the consequent reduction of ADMA, an increase of SDMA and MMA marks was observed, indicating that the pre-existence of the ADMA mark can block the formation of SDMA and MMA marks on the same substrate (Dhar et al, 2013). PRMT1 substrates harbor a conserved glycine- and arginine-rich (GAR) motif (Lee & Bedford, 2002; Tang et al, 2000). Mouse embryos lacking PRMT1 die shortly after implantation and before gastrulation (Pawlak et al, 2000). PRMT1 is predominantly nuclear, and is involved in transcription activation, presumably by mediating the methylation of several transcription factors, cofactors, and histone H4 on arginine 3 (H4R3).

PRMT2 was identified by its homology with PRMT1 (Katsanis et al, 1997; Scott et al, 1998) and is the only PRMT containing a Src homology 3 (SH3) domain. PRMT2 binds to estrogen receptor α (ER α) and the androgen receptor (AR), enhancing ER α and AR-mediated transcription (Meyer et al, 2007; Qi et al, 2002). PRMT2 has been classified as a type I enzyme, although its activity is low in comparison with other PRMTs, and its optimal substrate is still unknown. However, it has been shown to have weak activity towards histones and proteins containing GAR motifs (Lakowski & Frankel, 2009). This weak activity correlates with the lack of phenotype associated with PRMT2 null mice living under normal physiological

conditions (Yoshimoto et al, 2006). This lack of phenotype could be explained by the loss of PRMT2 being compensated by other PRMTs.

Like PRMT2, PRMT3 was discovered based on its sequence similarity to PRMT1. The catalytic regions of the two proteins are highly similar, however, the PRMT3 N-terminus contains a zinc-finger domain, which is responsible for its substrate specificity (Frankel & Clarke, 2000; Tang et al, 1998). Ribosomal protein RPS2 interacts with the zinc finger of PRMT3 and thus mediates methylation of its N-terminal GAR motif, making RPS2 an optimal substrate for PRMT3 (Swiercz et al, 2005). Indeed, RPS2 methylation is decreased by 80% in *Prmt3*^{-/-} MEFs (Swiercz et al, 2007). In contrast to PRMT1, PRMT3 is predominantly cytoplasmic (Tang et al, 1998), consistent with its role in association with ribosomal proteins. *Prmt3* deficient embryos are smaller than wild-type embryos; however, no size differences are observed between mutants and wild-types at weaning age (Swiercz et al, 2007).

Another type I family member is co-activator-associated arginine methyltransferase 1 (CARM1). CARM1, also known as PRMT4, not only functions as a methyl transferase but also enhances transcriptional activation by binding to nuclear hormone receptor (NR) co-activators (Stallcup et al, 2000). CARM1 substrates, unlike PRMT1 substrates, lack GAR motifs. Recent studies indicate that CARM1 methylates arginine residues within proline and glycine-rich (PGM) motifs (Gayatri et al, 2016). CARM1 substrates include TARPP, PABP1, CA150, H3R17 and H3R26 (An et al, 2004; Bauer et al, 2002; Chen et al, 1999; Cheng et al, 2007; Lee & Bedford, 2002). Knock-out experiments showed that E12.5 CARM1 null mice are smaller than wild-type and die just after birth (Yadav et al, 2003). The lethality is driven by the lack of CARM1 enzymatic activity as catalytically-dead knock-in CARM1 mice phenocopy the null mouse phenotype (Kim et al, 2010).

PRMT6, like PRMT1, is mainly localized to the nucleus and methylates GAR motifs (Frankel et al, 2002). An early characterization of PRMT6 identified it as a repressor of transcription, mainly because that study indicated that PRMT6 predominantly methylated histone H3 arginine 2. Methylation of H3R2 prevents the formation of H3K4 trimethylation, which is correlated with activation of transcription (Guccione et al, 2007; Hyllus et al, 2007; Iberg et al, 2008). Additionally, PRMT6

catalyzes R11 and R29 methylation sites in H2A, and H2AR29me2 is specifically enriched at genes repressed by PRMT6 (Waldmann et al, 2011). However, PRMT6 activity could be regulating transcription via other arginine residues on histone H2A and H4 (Hyllus et al, 2007).

PRMT8 is the family member most closely related to PRMT1. It harbors a myristoylation motif on its distinctive N-terminal region. PRMT8 distribution is largely limited to the brain. More specifically, it is localized to the plasma membrane by N-terminal myristoylation (Lee et al, 2005a). The N-terminus may also provide an autoregulatory function to this enzyme (Sayegh et al, 2007).

1.6.5. Arginine Symmetric-methyltransferases

PRMT9 and PRMT5 have symmetric methyl transferase activity (Hadjikyriacou et al, 2015; Lee et al, 2005b). Almost two decades ago, PRMT5 was described as a 72 KDa protein interacting with the chloride conductance regulatory protein (pLCln) (Krapivinsky et al, 1998). Pollack et al, described PRMT5 as a Jak2 binding protein, characterized its biochemical function as a methyltransferase, and identified three of its substrates: histone H2A, histone H4 and myelin basic protein (MBP) (Pollack et al, 1999). Further biochemical characterization, carried out by the Clarke group, showed that PRMT5 catalyzes the formation of SDMA, thus identifying the first enzyme of this type (Branscombe et al, 2001). Four years later, Lee et al. identified a second symmetric dimethyltransferase, PRMT7 (Lee et al, 2005b). Recently, PRMT9 has also been identified as catalyzing SDMA (Hadjikyriacou et al, 2015). It is important to note that PRMT5 is the major enzyme responsible for the SDMA of a diverse number of proteins, (Hadjikyriacou et al, 2015) and its biological function is essential; loss of PRMT5 function causes early embryonic lethality (Tee et al, 2010). PRMT5 protein is conserved from yeast to humans (Boulanger et al, 2004; Hung & Li, 2004; Krapivinsky et al, 1998; Lee et al, 2000), suggesting that PRMT5 has a pivotal role that has been preserved throughout speciation.

PRMT5 functions as part of a multimeric complex, engaged with a variety of partner proteins that regulate its activity and specificity. The major binding partner of

PRMT5 is MEP50. The structure of the PRMT5-MEP50 complex has been studied independently by two groups, revealing consistent results (Antonyamy et al, 2012; Ho et al, 2013). The PRMT5-MEP50 interface forms between the N-terminal domain of PRMT5 and the second and third of the seven β -propeller blades of MEP50. Four PRMT5-MEP50 heterodimers form an octameric complex whose surface is negatively charged, a convenient feature for recognition of positively-charged substrates, such as the canonical GAR motifs (Antonyamy et al, 2012; Ho et al, 2013).

1.7. Multiple roles of PRMT5

1.7.1. PRMT5 in mRNA splicing

The diversity of the cell proteome is greatly increased by alternative splicing; however, improper functioning of proteins involved in RNA processing is linked to neurodegenerative disorders such as spinal muscular atrophy (Zhang et al, 2008). PRMT5 plays a crucial role in mRNA processes. It methylates multiple members of the splicing machinery, including fibrillarin, which is a protein that methylates RNA. The engagement of PRMT5 with a fibrillarin-associated subcomplex may be coordinating the methylation of both RNA and protein substrates during mRNA processing in Cajal bodies (Yanagida et al, 2004). Additionally, PRMT5-MEP50 mediates the methylation of substrates within the methylosome, such as Sm proteins D1 and D3, thus promoting their interaction with the survival motor neuron (SMN) complex and its assembly into the pre-mRNA splicing core (Friesen et al, 2001; Friesen et al, 2002; Meister et al, 2001; Meister & Fischer, 2002). Absence of PRMT5 triggers defects in the core splicing machinery, causing the generation of unstable products. In particular, alternatively spliced *Mdm4* acts as a sensor of splicing defects. Normally MDM4 inhibits p53 activity, however, abnormal splicing results in unstable *Mdm4* transcripts, leading to a reduction in MDM4 protein levels, thus activating the p53 signaling pathway (Bezzi et al, 2013).

1.7.2. PRMT5 in transcriptional regulation

PRMT5 plays an important role in transcription. By chromatin immunoprecipitation (ChIP) experiments, it was shown that association of PRMT5 at the transcription start site of the Cyclin E1 gene represses its expression, providing the first evidence that PRMT5 is involved in transcription regulation and proliferation (Fabbrizio et al, 2002). In addition, PRMT5 was found in two chromatin-remodeler complexes involved in gene silencing, hSWI/SNF and mSin3A/HDAC2 (Pal et al, 2003). hSWI/SNF-associated PRMT5 targets histones H3R8 and H4R3 as substrates for symmetric dimethylation. Using microarray analysis, it was found that PRMT5 represses a number of genes, among them suppressor of tumorigenicity 7 (ST7) and nonmetastatic 23 (NM23), thus indicating the involvement of PRMT5 in cell growth and proliferation (Pal et al, 2004).

Although PRMT5 is mainly associated with transcriptional repression by selectively methylating histones H2AR3, H4R3, and H3R8 (Pal et al, 2004), new data indicate that it may function as an activator as well. Histone H3R2 is monomethylated and symmetrically dimethylated by PRMT5, promoting the binding of WDR5, a component of coactivator complexes (Chen et al, 2016a; Migliori et al, 2012).

1.7.3. Association of PRMT5 and CpG methylation

Symmetric dimethylation of histone H4R3, mediated by PRMT5, creates a docking site for the DNA methyltransferase DNMT3, well known for its ability to repress transcription (Rank et al, 2010; Zhao et al, 2009). In addition, PRMT5 interacts with and methylates MBD2, a protein that binds methylated DNA (Le Guezennec et al, 2006; Tan & Nakielny, 2006). MBD2 can be symmetrically and asymmetrically dimethylated. High levels of methylation reduce the affinity of MBD2 for methylated DNA, suggesting that methylation of MBD2 inhibits its function as a transcriptional repressor (Tan & Nakielny, 2006). Thus, PRMT5 fine-tunes transcription via its interactions with different protein complexes.

1.7.4. Role of PRMT5 in development

PRMT5 is essential for development. PRMT5 RNA is maternally loaded and is degraded as the blastula stage progresses, but is synthesized *de novo* in the developing embryo by the 16-cell and blastocyst stages (McGraw et al, 2007). During preimplantation and in primordial germ cells, PRMT5 helps defend the genome during global DNA demethylation, which leaves cells vulnerable to the activation of transposable elements (TE). Enrichment of the PRMT5 mediated methylation of H2A/H4R3 might have a specific role in the repression of TE (Kim et al, 2014).

The absence of PRMT5 results in early embryonic lethality (Tee et al, 2010). To overcome the early embryonic lethality of *Prmt5* knockout mouse model, new investigations made use of a conditional deletion allele of *Prmt5*. *Prmt5* inducible germline-specific knockout mice showed that PRMT5 is required in primordial germ cell development and survival between E10.5 and E13.5 (Li et al, 2015). Inactivation of PRMT5 in adult skeletal muscle stem cells resulted in a severe loss of muscle volume, indicating that PRMT5 is required for muscle regeneration (Zhang et al, 2015). Targeted deletion of *Prmt5* in the central nervous system resulted in mouse lethality 14 days after birth (Bezzi et al, 2013), and a conditional deletion of *Prmt5* in adult hematopoietic stem cells caused severe anemia, and mice were moribund shortly after PRMT5 loss (Liu et al, 2015).

1.7.5. Role of PRMT5 in cancer

PRMT5 expression is elevated in many cancers including gastric cancer, gliomas, lymphoma, and epithelial ovarian cancer (Bao et al, 2013; Han et al, 2014; Kanda et al, 2016; Pal et al, 2007), and correlates with tumor growth, invasion and migration, and consequently with poor prognosis. One of the factors that may

contribute to the overexpression of PRMT5 is the nuclear transcription factor Y (NF-Y), which causes the elevated expression of oncogenes in many cancers. NF-Y binds to two inverted CCAAT boxes present in the proximal promoter of PRMT5 (Zhang et al, 2014). Furthermore, the proto-oncogene Myc upregulates the transcription of PRMT5 and the core small nuclear ribonucleoprotein, both of which are key regulatory elements of pre-messenger-RNA splicing. Absence of Myc results in a partial reduction of PRMT5, thereby causing aberrant splicing, increases in apoptosis and reduced tumorigenic potential in hematopoietic malignancies (Koh et al, 2015).

PRMT5 can exert its oncogenic effect directly via methylation of a particular substrate, or indirectly as a transcriptional regulator. For example, PRMT5 methylates the tumor suppressor programmed cell death 4 (PDCD4) protein at R110, altering its function. Coexpression of PRMT5 and PDCD4 reverses the tumor suppressive properties of PDCD4 in an orthotopic model of breast cancer. These observations were consistent with the poor outcome of a cohort of breast cancer patients displaying elevated expression of PRMT5 and PDCD4 (Powers et al, 2011).

Additionally, methylation of Sm proteins by PRMT5 controls the splicing machinery and maintains splicing fidelity in several genes associated with cell proliferation (Koh et al, 2015; Lacquet, 1985). As a transcriptional regulator, the roles of PRMT5 have been extensively studied in the last few years. Transcriptional regulation mediated by PRMT5 enhances malignant phenotypes in many cancers such as lung adenocarcinoma, lung squamous cell carcinoma, breast carcinoma, acute myeloid leukemia and nasopharyngeal carcinoma (Chen et al, 2016a; Tarighat et al, 2016; Yang et al, 2016).

Several studies have placed PRMT5 not only as a potential prognostic marker, but also as a therapeutic target. Inhibition of PRMT5 may aid in the treatment of many cancers, such as MTAP/CDKN2A-deleted tumors, MYCN oncogene driven neuroblastoma, and glioblastoma (Kryukov et al, 2016; Mavrakis et al, 2016; Park et al, 2015; Yan et al, 2014). Recently, a potent inhibitor of PRMT5, EPZ015666, has demonstrated dose-dependent antitumor activity in mantle cell lymphoma (MCL) xenograft models (Chan-Penebre et al, 2015). Additionally,

another PRMT5 inhibitor, GSK591/EPZ015866, has been recently studied in cancer and normal cells. In the A549 human lung adenocarcinoma epithelial cell line, GSK591/EPZ015866 treatment abrogated cell migration and cell invasion, but did not effect normal IMR90 fetal lung fibroblasts (Chen et al, 2016a). Moreover, these PRMT5 inhibitors not only promise to become a potential therapeutic drug, but also valuable probes for investigating the biological functions of PRMT5.

1.8. Regulation of PRMT5 activity

1.8.1. Regulation of PRMT5 by binding partners

Early studies indicated that the formation of multimers activates PRMT5 catalytic function toward MBP (Lim et al, 2005). Today, it is well known that MEP50 is the major binding partner of PRMT5 and together they form an octameric complex. The PRMT5-MEP50 complex promotes histone methylation; however, nucleosomes are not a substrate for PRMT5-MEP50 (Burgos et al, 2015). Other PRMT5 protein cofactors, such as Blimp1 (Ancelin et al, 2006), COPR5 (Lacroix et al, 2008), Menin/Men1 (Gurung et al, 2013), and the hSWI/SNF chromatin remodeling complex (Pal et al, 2004), may trigger methylation activity toward nucleosomes. Also, other components of hSWI-SNF complexes, such as BRD7 interacts with PRMT5 and colocalizes with PRC2 on the promoter of ST7 and retinoblastoma-like protein 2 (RBL2) (Tae et al, 2011). In addition, it was shown that Schwann cell factor 1 (SC1) recruits PRMT5 to mediate symmetric dimethylation of histone H4R3 (Chittka et al, 2012).

The transcription repressor protein Blimp1 associates with PRMT5 and regulates its methyltransferase activity in a time- and stage-dependent manner. In mouse primordial germ cells (E8.5), PRMT5-Blimp1 is localized to the nucleus, and is correlated with high levels of H2A/H4R3 methylation; however, by E11.5 PRMT5-Blimp1 translocates to the cytoplasm and levels of H2A/H4 R3 methylation decrease (Ancelin et al, 2006).

RioK1 and pICln interact with PRMT5 in a similar manner, but have distinct outcomes. The association of RioK1 or pICln with the PRMT5-MEP50 complex is mutually exclusive and directs PRMT5 substrate specificity. Whereas PRMT5-MEP50-RioK1 targets nucleolin, PRMT5-MEP50-pICln targets Sm proteins (Guderian et al, 2011). The pICln mediated methylation of Sm proteins is inhibited by the interaction of PRMT5 with DAL-1/4.1B (Jiang et al, 2005).

1.8.2. Existing PTMs on histones regulate PRMT5 association and specificity

At the chromatin level, pre-existing acetyl marks modulate arginine methylation on histones. H4K5ac facilitates symmetrical dimethylation of H4R3. In contrast, H4K16ac weakens the binding affinity of PRMT5 to H4. Interestingly, H4K5ac together with H4K8ac and/or H4K12ac decreases the asymmetric dimethylation of H4R3; Conversely, H4K16ac alone or in combination with H4K5ac or H4K8ac increases it (Feng et al, 2011). This indicates that acetylation coordinates the type of arginine methylation deposited on the histones, by making histones a more suitable substrate either for PRMT5 or PRMT1. In addition, histone H2AS1 and H4S1 phosphorylation may sterically block the arginine residues of histone H2A/H4 tail region, thus preventing PRMT5-mediated methylation (Stopa et al, 2015).

1.8.3. Cellular localization

PRMT5 is predominantly cytoplasmic, but is also found in the nucleus. The ratio of cytoplasmic to nuclear PRMT5 varies depending on the cell type. Cytoplasmic or nuclear localization of PRMT5 results in distinct functionalities and outcomes. In zygotes and two-cell-stage embryos, PRMT5 is cytoplasmic, but from the four- to eight-cell stage until the early E3.5 blastocyst stage, PRMT5 is nuclear. Thereafter, PRMT5 is mostly cytoplasmic. Notably, the nuclear localization of

PRMT5 coincides with an enrichment of H2A/H4R3me2s in the nucleus (Kim et al, 2014).

PRMT5-MEP50 cellular localization changes according to cell type (Liang et al, 2007). In fetal germ cells, PRMT5-MEP50 is cytoplasmic, whereas in Leydig cells and in adult non-neoplastic testes, it is nuclear. However in human seminoma and Leydig tumor cells, MEP50-PRMT5 shows an increased cytoplasmic localization, indicating a particular role within the subcellular localization of this complex (Liang et al, 2007). In lung adenocarcinoma, cytoplasmic localization of PRMT5 correlates with poor prognosis, but strong nuclear localization was frequently identified in low-grade adenocarcinomas (Ibrahim et al, 2014). Likewise, in non-small cell lung carcinomas and pulmonary neuroendocrine tumors, cytoplasmic PRMT5 was associated with poorly differentiated tumors, whereas nuclear PRMT5 expression was frequently observed in well-differentiated tumors (Shilo et al, 2013). Finally, in prostate cells, cytoplasmic PRMT5 promotes cancer cell growth, whereas nuclear PRMT5 inhibits cell growth (Gu et al, 2012).

These data indicate that the function of PRMT5 is altered by its localization and plays an important role in cancer. However, these differences may be cell type dependent and regulated by factors that are yet to be identified. Among other mechanisms, PTMs or interaction with other proteins may regulate its localization and substrate choice. Further studies are necessary to determine the mechanism of PRMT5 localization as this may lead to a more robust understanding of the oncogenic role of PRMT5.

1.8.4. Crosstalk between phosphorylation and methylation

Recent studies indicate possible connections between the methylation and phosphorylation status of proteins. Methylation may influence the phosphorylation of nearby residues. Such is the case for the sterol regulatory element-binding protein (SREBP) and apoptosis signal-regulating kinase 1 (ASK1), both substrates of PRMT5. When symmetrically dimethylated, SREBP (R321me2s), prevents S430 phosphorylation by GSK3, thus stabilizing SREBP and promoting the growth of

cancer cells *in vivo* and *in vitro* (Liu et al, 2016). There are other examples where methylation occurs near phosphorylation sites. For example, PRMT5 also interacts with and methylates ASK1 (R89). ASK1 methylation promotes its interaction with Akt, which then phosphorylates ASK1 on S83, thereby inhibiting its apoptotic function (Chen et al, 2016b).

Additionally, PRMT5 may influence cell signaling and differentiation. Experimental work by two independent groups revealed that methylation plays an important role in signaling through the ERK1/2 pathway. Indeed, PRMT5 methylates the transmembrane cell-surface receptor tyrosine kinase EGFR at R1175, which induces phosphorylation at Y1173. pY1173 serves as a docking site for SH2-domain-containing protein tyrosine phosphatase 1 (SHP1). The interaction of EGFR with SHP1 results in attenuation of EGFR-dependent ERK activation. Therefore, methylation of EGFR suppresses ERK activation. Moreover, PRMT5 affects MAPK signaling cascades by methylating RAF proteins. PRMT5-dependent methylation enhances the degradation of CRAF and BRAF, consequently decreasing activation of downstream kinases including MEK1/2 and ERK1/2. Methylation of RAF proteins by PRMT5 results in hypo-phosphorylation of ERK1/2, which in turn culminates in cell proliferation. Interestingly, inhibition of methylation leads to augmentation of ERK1/2 phosphorylation and switches the biological effect from proliferation to differentiation (Andreu-Perez et al, 2011; Hsu et al, 2011).

Lastly, PRMT5 itself can be phosphorylated. PRMT5 has been shown to be phosphorylated at three tyrosine sites, which affects its binding with MEP50, its main co-activator, consequently reducing PRMT5 enzymatic activity (Liu et al, 2011). Tyrosine phosphorylation of PRMT5 will be addressed in more detail in Chapter 3.

1.9. Topics to be covered for this study

This study is based on the hypothesis that phosphorylation of PRMT5 regulates its subcellular localization and/or substrate choice, by facilitating phospho-dependent protein-protein interactions. The topics to be covered will include: (1) The identification of phosphodependent-interacting proteins and data showing that

phosphorylation of PRMT5 mediates its interaction with several SH2-domain containing proteins, 14-3-3 proteins and the FHA domain of MDC1. (2) The delineation of mechanisms underlying 14-3-3 and PDZ C-terminal motif recognition. We showed that the C-terminal region of PRMT5 has a recognition motif shared by PDZ domains and 14-3-3 proteins. 14-3-3 protein interaction requires a phosphorylated residue at the C-terminus, while PDZ domain recognition occurs when the C-terminus is unphosphorylated. (3) The examination of the interaction of the PRMT5 with the PDZ domain of NHERF2 and its functional consequences. The rationale is that membrane-associated NHERF2 binding to the PRMT5 C-terminal region, positions PRMT5 near the cell membrane. We also investigate the effect of PRMT5 on ion exchanger activity. These studies will provide better understanding of the cell biology of PRMT5 and provide mechanistic insights into regulation of its function.

Chapter 2: Material and Methods

2.1. Plasmid constructs

2.1.1. Mammalian expression vectors

All expression constructs containing PRMT5 are derivatives of human wild-type cDNA. The Myc-PRMT5 construct was cloned into the pVAK vector containing an N-terminal myc epitope tag (EQKLISEEDL). EcoRI sites flank PRMT5 sequences. PRMT5, Myc-PRMT5^{T634}, and Myc-PRMT5^Δ were generated by mutagenesis using the QuikChange site-directed mutagenesis kit according to the manufacturer's protocol (Agilent). Primers were generated harboring the desired mutation, the presence of the desired mutation was verified by sequencing.

List of primers used for mutagenesis:

PRMT5 Y280A#1: 5'-AGA GAA GGA GTT CTG CTC CGC CCT CCA ATA CCT GGA ATA C-3'

PRMT5 Y280A#2: 5'-GTA TTC CAG GTA TTG GAG GGC GGA GCA GAA CTC CTT CTC T-3'

PRMT5 Y283A#1: 5'-AGG AGT TCT GCT CCT ACC TCC AAG CCC TGG AAT ACT TAA GC-3'

PRMT5 Y283A#2: 5'-GCT TAA GTA TTC CAG GGC TTG GAG GTA GGA GCA GAA CTC CT-3'

PRMT5 Y286A#1: 5'-CTA CCT CCA ATA CCT GGA AGC CTT AAG CCA GAA CCG TCC T-3'

PRMT5 Y286A#2: 5'-AGG ACG GTT CTG GCT TAA GGC TTC CAG GTA TTG GAG GTA G-3'

PRMT5 Y283A-Y286A#1: 5'-TCT GCT CCG CCC TCC AAG CCC TGG AAG CCT TAA GCC AGA ACC GTC-3'

PRMT5 Y283A-Y286A#2: 5'-GAC GGT TCT GGC TTA AGG CTT CCA GGG CTT GGA GGG CGG AGC AGA-3'

PRMT5 Delta276-309#1: 5'-CAA CCA CCA CTC AGA GAA AGG ATC CCC GCT TCA-3'

PRMT5 Delta276-309#2: 5'-TGA AGC GGG GAT CCT TTC TCT GAG TGG TGG TTG-3'

PRMT5 T634A#1: 5'-CCACAGGCCGCTCATATGCCATTGGCCTCTA-3'

PRMT5 T634A#2: 5'-TAGAGGCCAATGGCATATGAGCGGCCTGTGG-3'

PRMT5 Δ#1: 5'-ATAACCCACAGGCCGCTGACATATACCATTGG-3'

PRMT5 Δ#2: 5'-CCAATGGTATATGTGACAGCGGCCTGTGGGGTTAT-3'

GFP-PRMT5: cDNA fragments encoding PRMT5 amino acids 340 to 637 were cloned into the EcoRI site of pEGFP-C1 (Clontech). GFP-PRMT5^{T634A} was created using site-directed mutagenesis using the primers described above.

pBabe-Myc-PRMT5 constructs were generated by PCR using pVAK-PRMT5 as template, including the Myc-tag. Fragments were subcloned into the BamHI site of the pBabe-hygromycin vector.

For expression of PRMT5 in PRMT5-KD cells, we generated shRNA resistant PRMT5 constructs by mutating the shRNA target sequence without changing the amino acid sequence. Primers were generated harboring silent point mutation for the shRNA target sequence KD4. An EcoRI restriction site was created to screen for the desired mutation.

PRMT5 KD4r#1:

5'-TGTCTTCCATCCGCGGTTTAAACGAGAATTCATTCAGGAACCTGC-3'

PRMT5 KD4r#2:

5'-GCAGGTTCTGAATGAATTCTCGTTTAAACCGCGGATGGAAGACA-3'

The mouse Myc-PRMT5 constructs were generated by PCR using cDNA template extracted from a heterozygous female PRMT5^{Δ+HA} mouse. An N-terminal myc-tag was inserted in PRMT5^{WT} and PRMT5^{Δ+HA} and then cloned into pLOC (Thermo Scientific) using BamHI and NheI sites. Myr-Akt delta4-129 was obtained from Addgene (plasmid # 10841) (Kohn et al, 1996).

2.1.2. Bacterial expression vector

The constructs pDEST15-SH2 domains were a kind gift from Dr. Shawn Li from Western University.

The PDZ domain array content was selected considering the biophysical interactions described by Stiffler et al, 2007. The protein content is listed in Appendix B. 14-3-3 proteins encoded the full-length sequence. cDNAs that contained the codon-optimized sequence for expression in bacteria were synthesized by Biomatik with flanking BamHI and XhoI restriction sites, used for cloning into pGEX 6P-1. Human NHERF2 constructs were amplified by PCR and cloned into pGEX 6p-1 using BamHI and EcoRI. The plasmid named NHERF2 PDZ FL encodes full-length NHERF2, whereas NHERF2-PDZ 1 encodes amino acids 1 to 152, and NHERF2-PDZ 2 encodes amino acids 107 to 337.

2.3. shRNA knockdown

HeLa PRMT5 stable knockdown cell lines and shRNAs for PRMT5 were a kind gift from Dr. Sharon Dent, MD Anderson Cancer Center. The lentivirus based PRMT5 shRNA targeting codons were CCAGTTTGAGATGCCTT (KD2) and GTTTC AAGAGGGAGTTC (KD4). SK-CO15 PRMT5 stable knockdown cell lines were generated using pLKO.1-shPRMT5. HEK 293T cells were co-transfected with pLKO.1 shPRMT5-KD2 or -KD4 along with pMD2.G and psPAX2 (viral envelope and packaging plasmids) using Lipofectamine 2000. After 48 hours, viral supernatants were harvested and filtered through a 0.45- μ m pore filter. SK-CO15 cells were infected with viral supernatants with the addition of 8 μ g/ml polybrene (Sigma-Aldrich). Clones stably expressing the shRNAs were selected with medium containing 5 μ g/ml puromycin. Empty vector control cell lines were generated by infecting with pLKO.1 and selecting for puromycin resistance. SK-CO15 cell were a gift from Dr. Rodriguez-Boulan, Weil Cornell Medical College.

2.4. Protein purification

GST fusion proteins were purified following standard methods. Briefly, protein was expressed in BL21 cells for 4 h at 37°C with 0.1 mM isopropyl- β -D-thiogalactopyranoside (IPTG). For SH2 containing constructs, BL21-AI cells were induced with 0.2 % L-arabinose and 0.1 mM IPTG for protein expression. Cells were

resuspended in PBS buffer, then lysed by sonication (30% amplitude) for 10 sec. Lysates were cleared by centrifugation and incubated with Glutathione Sepharose 4B resin at 4°C with tumbling (GE Life Science). Subsequently, Sepharose-immobilized GST-tagged proteins were washed with PBS and eluted with Elution Buffer (100 mM Tris HCl pH8.0; 120 mM NaCl and 40 mM reduced glutathione).

2.5. GST pulldown studies

GST-tagged proteins (~10 µg) were incubated with cell lysates (from one confluent 10 cm dish, lysed with 1 ml of mild buffer [50 mM Tris-HCl, pH 7.5, 150 mM NaCl, 0.1% Nonidet P-40 (NP-40), 5mM EDTA, 5 mM EGTA, 15 mM MgCl₂ and Proteinase inhibitor cocktail (Roche)] for 2 h at 4°C with tumbling in a final volume of 1 ml. Equilibrated Glutathione Sepharose 4B resin was then added for an additional 1 h with tumbling. Samples were washed 4 times with mild lysis buffer prior to elution, SDS-PAGE, and Western blotting.

2.6. Cell culture

MCF7, U2OS, Src-deficient MEF (SYF^{-/-}) (ATCC CRL-2459) and MEF-Src^{+/+} (ATCC CRL-2498) cells were cultured in high glucose Dulbecco's modified Eagle's medium (DMEM, Sigma) containing 1X PenStrep (Gibco), 1X MEM non-essential amino acids (Gibco), and 10% newborn calf serum (NCS) under standard conditions (37°C and 5% CO₂).

HeLa and SK-CO15 cells, were cultured in high glucose Dulbecco's modified Eagle's medium (DMEM, Sigma) supplemented with 1X PenStrep (Gibco), 1X MEM non-essential amino acids (Gibco), 15 mM HEPES, and 10% heat-inactivated fetal bovine serum (FBS), under standard conditions (37°C and 5% CO₂).

2.7. Immortalization and culture of MEFs

The inducible PRMT5 KO MEF cell line was generated from primary MEFs derived from a conditional knockout mouse harboring LoxP (^{F/F}) sequences flanking exon 7 of the *Prmt5* gene and expressing tamoxifen-inducible Cre (kind gift from Dr.

Ernesto Guccione, Institute of Molecular and Cell Biology, A*STAR Singapore). Immortalized MEFs were created according to the standard 3T3 protocol. Cells were grown in DMEM containing 10% FBS. Immortalized cells were treated every 3 days with 2 μ M 4-hydroxy tamoxifen for 21 days.

2.8. Transient transfection

Cells were transfected with various mammalian expression constructs using Lipofectamine 2000 (Invitrogen, Carlsbad, CA, USA) according to manufacturer's specification. Cells were transfected overnight and harvested the following day for analysis.

2.9. Stable transfection

The pBabe-hygromycin retroviral constructs were transfected with FuGENE into the Phoenix-Eco packaging cell line. Forty-eight hours later, the supernatant was harvested and filtered through a 0.45- μ m filter. SK-CO15 PRMT5 KD cells were incubated with filtered transducing supernatant and 8 μ g/ml polybrene (Sigma). Clones stably expressing the pBabe-Myc-PRMT5 constructs were selected with medium containing 1 mg/ml hygromycin.

2.10. In cell phosphorylation

For induction of threonine phosphorylation, SK-CO15 cells were transiently transfected with either GFP-PRMT5 or GFP-PRMT5^{T634A} and treated with one of the following: 30 μ M forskolin (CST) for 30 min; 1 nM angiotensin II (Sigma) for 45 min; 1 μ M dexamethasone (Sigma) for 24 hrs; or overexpression of constitutive active myr-AKT. All treatments were followed by a 10 min 0.05 μ M Calyculin A treatment. Samples were immunoprecipitated with anti-GFP antibody and blotted with a pan anti-phosphothreonine antibody. Quantification was performed using ImageJ software, measuring the band intensities of immunoprecipitated samples as detected by both an anti-pT-specific antibody and an anti-GFP antibody.

For Induction of tyrosine phosphorylation, MCF7 or NIH-3T3 cell were treated with sodium pervanadate, (2 mM Na₃VO₄ dissolved in H₂O pH 10, 88 mM H₂O₂) and incubated at 37°C in a CO₂ incubator for 1 hour.

2.11. *In vitro* phosphorylation

In vitro phosphorylation assays of PRMT5 [T634] were conducted by Kinexus laboratory using a radiometric method with [gamma-³³P]-ATP (Appendix A). In the first stage, phosphorylation of the PRMT5 wild type C-terminus peptide (KKPTGRSYTIGL-COOH) was assayed against 295 protein kinases. In the second stage, kinases from the first stage that generated signals greater than 250 cpm were used for further examination against the wild type PRMT5 [T634] and its mutated peptide, PRMT5 [A634] (KKPTGRSYAIGL-COOH). *In vitro* kinase assays were performed at ambient temperature for 20-40 min in a final volume of 25 µl containing a mixture of 10-50 nM active protein kinase, peptide and 5 µl of [gamma-³³P] ATP in a suitable buffer. After the incubation period, 10 µl of the reaction mixture was spotted onto a phosphocellulose P81 plate and counted in the presence of scintillation fluid in a Trilux scintillation counter.

2.12. Antibodies

The following antibodies were used in this study: anti-PRMT5 (Active Motif 61001), anti-PRMT5 (Millipore 07-405), Pan Phospho-Akt S/T Substrate (CST 9614), Pan Symmetric Di-Methyl Arginine (anti-SDMA) [CST D2C3D6 not commercially available], anti-NHERF2 (CST 9568), 14-3-3 (CST 8312), Pan-Cadherin (CST 4068), myc (9E10) (Sigma M4439), GFP (Santa Cruz sc-9996), AKT (CST 9272), anti-HA (CST-37245) and anti-MEP50 (CST 2823).

2.13. Immunofluorescence microscopy

Epifluorescence microscopy was performed using a Zeiss Observer.D1 microscope. Methanol fixed cells were incubated with primary antibodies overnight at 4°C. Secondary antibodies (Molecular Probes) were diluted 1:1,000 and incubated with cells for 1 h at RT. Alternatively, cells growing on glass coverslips

were fixed with 4% paraformaldehyde at RT for 10 min. Cells were permeabilized in a solution containing 0.5% Triton X-100 in PBS for 15 min. After permeabilization, cells were blocked with 10% newborn calf serum in PBS for 1 hour at RT. Mouse anti- γ H2AX (1:1,000), mouse anti-Myc (1:1,000), rabbit anti-NHERF2 (1:1,000) or rabbit anti-H4/H2AR3me2s (1:500) antibodies were incubated with fixed cells overnight at 4°C. After three washes, the cells were stained with Alexa Fluor 488-conjugated anti-rabbit and Alexa Fluor 555-conjugated anti-mouse secondary antibodies. DNA was stained with DAPI (4',6'-diamidino-2-phenylindole).

2.14. GFP immunoprecipitations

For GFP immunoprecipitations, GFP-nAb magnetic Sepharose and agarose resin (Allele Biotech) were used following the manufacturer's procedures. Briefly, cells were harvested in PBS, then cleared by centrifugation. Cell pellets were resuspended in 200 μ l of lysis buffer (20 mM Tris-HCl pH 7.5, 150 mM NaCl, 1 mM EDTA, 0.5% NP-40, proteinase inhibitor cocktail and phosphatase inhibitors) and then lysed by sonication (10 cycles of 30 sec on/off using Bioruptor, Diagenode). After centrifugation at 20,000 x g for 10 min at 4°C, the supernatant was collected and diluted with binding buffer (10 mM Tris-HCl pH 7.5, 150 mM NaCl, and proteinase inhibitor cocktail and phosphatase inhibitors) to a final volume of 700 μ l. Equilibrated beads were incubated with lysate with tumbling for 1 h at 4°C. The immunoprecipitated samples were cleared using wash buffer (10 mM Tris-HCl pH 7.5, 500 mM NaCl and proteinase inhibitor cocktail and phosphatase inhibitors) using either a magnetic stand or spin columns. The harvested beads were then resuspended in 30 μ l of loading buffer and boiled for 5 min to elute the proteins. Samples were separated by SDS-PAGE and transferred onto PVDF membranes for western blot analysis.

2.15. Western blots

Lysates were separated on SDS-polyacrylamide gels (SDS-PAGE). Proteins were transferred onto PVDF membrane using a semi-dry transfer apparatus. Blots were

blocked in blocking buffer (PBS, 0.1 %Tween-20 and 5% milk) for 1 h at RT, then incubated with primary antibody diluted in the blocking buffer, overnight at 4°C. The blots were washed with PBS 0.1% Tween-20, probed with the appropriate HRP-conjugated secondary antibody and detected by enhanced chemiluminescence (GE Healthcare Life Sciences).

2.16. Peptide synthesis

Biotinylated peptides were synthesized by the W.M. Keck Center (KC) and CPC Scientific, Inc. (CPC). Peptides are listed below. Phosphorylated residues are indicated as pY/T/S:

(KC) PRMT5 273-293:

Free –SEKEFCSYLQYLEYLSQNRPP-(biotin)-COOH

(KC) PRMT5 pY280:

Free –SEKEFCSpYLQYLEYL(biotin)-COOH

(KC) PRMT5 pY283:

Free –EFCSYLQpYLEYLSQN (biotin)-COOH

(KC) PRMT5 pY286:

Free –SYLQYLEpYLSQNRPP(biotin)-COOH

(KC) PRMT5 pY280 pY283:

Free –SEKEFCSpYLQpYLEYLSQNRPP(biotin)-COOH

(KC) PRMT5 pY280 pY286:

Free –SEKEFCSpYLQYLEpYLSQNRPP(biotin)-COOH

(KC) PRMT5 pY283 pY286:

Free –SEKEFCSYLQpYLEpYLSQNRPP(biotin)-COOH

(KC) PRMT5 pY280 pY283 pY286:

Free –SEKEFCSpYLQpYLEpYLSQNRPP(biotin)-COOH

(KC) PRMT5 623-637:

Biotin – SAIHNPTGRSYTIGL-COOH

(KC) PRMT5 pT634:

Biotin – SAIHNPTGRSYpTIGL-COOH

(KC) E6 (HPV16):

Biotin – SSRTRRETQL-COOH

(KC) E6 (HPV16) pT156:

Biotin – SSRTRREpTQL-COOH

(KC) ERBB4*:

Biotin – GTVLPPPPYRHRNTVV -COOH

(KC) ERBB4 pT1306*:

Biotin – GTVLPPPPYRHRNpTVV-COOH

(KC) PGHS-2 :

Biotin – SGSGVLIKRRSTEL-COOH

(KC) PGHS-2 pT602:

Biotin – SGSGVLIKRRSpTEL-COOH

(KC) IRK-1:

Biotin – SGSGPRPLRRESEI-COOH

(KC) IRK-1 pS425:

Biotin – SGSGPRPLRREpSEI-COOH

(CPC) PRMT5 623-636:

Biotin – SAIHNPTGRSYTIG-COOH

(CPC) PRMT5 623-636 pT634:

Biotin – SAIHNPTGRSYpTIG-COOH

(CPC) PRMT5 623-637 R631K:

Biotin – SAIHNPTGKSYTIGL-COOH

(CPC) PRMT5 623-637 R631K pT634:

Biotin – SAIHNPTGLSYpTIGL-COOH

(CPC) PRMT5 623-637 R631A:

Biotin – SAIHNPTGASYTIGL-COOH

(CPC) PRMT5 623-637 R631A pT634:

Biotin –SAIHNPTGASYpTIGL-COOH

(* kind gift from Dr. Marius Sudol)

2.17. Peptide pull-down

15 µg of biotin-labeled peptides were immobilized on streptavidin-agarose beads (Sigma) in peptide-binding buffer (50 mM Tris-HCl at pH 7.5, 150 mM NaCl, 1 mM EDTA, 2 mM dithiothreitol, 0.5% NP-40) overnight at 4°C and washed three times with binding buffer to remove unbound peptides. To reduce nonspecific binding, GST-fusion proteins were preincubated with streptavidin-agarose beads overnight. Beads were harvested by centrifugation, and the supernatants were incubated with immobilized peptide in 300 µl of binding buffer overnight. The beads were washed with binding buffer, harvested by centrifugation and then resuspended in 30 µl of loading buffer and boiled for 5 minutes. The samples were resolved by SDS-PAGE prior to transfer to PVDF membrane and detection with anti-GST antibody.

2.18. Protein domain microarray

Protein domain microarrays were generated as previously described (Espejo et al, 2002). Briefly, proteins were arrayed in duplicate using a Flexys robotic workstation (Genomic Solution) or an Aushon 2470 Microarrayer (Aushon Biosystems). GST fusion proteins were arrayed from a 384-well plate, which contained 10 µl of each protein at an approximate concentration of 1 µg/ul. The protein arrays are composed of blocks, each organized in a matrix of columns and rows as shown in Figures 5, 15 and 29. Each protein is printed in duplicate with a unique orientation. Samples are printed with a distance of 600 µm between spots. GST alone is printed on each block as negative control. Proteins were printed on nitrocellulose coated glass slides (Grace Bio-labs).

Peptides were synthesized by Keck Biotechnology or by CPC Scientific, Inc., 10 µg of biotinylated peptides were bound to Cy3-streptavidin or Cy5-streptavidin (GE Healthcare) in 500 µl PBST- 0.1% Tween 20). Labeled peptides were cleared of unconjugated straptavidin label by incubation with biotin-agarose beads (Sigma, St. Louis, MO, U.S.A.) Arrays were probed with fluorescently labeled peptides overnight at 4°C, unbound peptides were washed away with PBST-0.1% Tween 20.

The fluorescent peptide bound signal was detected using a GenePix 4200A microarray scanner (Molecular Devices). 550 nm and 675 nm filters were used for the detection of Cy3 and Cy5-labeled probes. GST signal was detected with anti-GST and 555-conjugated rabbit secondary antibodies.

2.19. Membrane fractionation

This protocol was adapted from (Jorgensen, 1988). Three 15 cm plates at 80 to 100% confluency were used. Cells were washed 3 times with homogenization buffer (25 mM imidazole, 250 mM sucrose, 1 mM EDTA, pH 7.2 and protease inhibitors), and harvested by scraping into 10 ml of homogenization buffer.

Cells were lysed with six passages through an 18 gauge needle, followed by six passages through a 27 gauge needle. Lysate were cleared by centrifugation (5,800 x g for 15 minutes at 4°C). Supernatants were collected and the pellets were resuspended into 5 ml of ice-cold homogenization buffer by vortexing, and then centrifuged at (5,800 x g for 15 minutes at 4°C). Supernatants were combined and cleared again by centrifugation (47,800 x g, 30 minutes at 4°C). The resulting supernatant contained the cytoplasmic proteins and the pellet contained the membrane and membrane-associated proteins. Pellets were resuspended in 1 ml of homogenization buffer containing protease inhibitors. The samples were analyzed by immunoblotting after resolution on SDS-PAGE gels.

2.20. Intracellular pH

Intracellular pH (pH_i) was determined using the fluorometric, pH-sensitive dye 2',7'-bis-(2-carboxyethyl)-5-carboxyfluorescein acetoxymethyl ester (BCECF-AM) (Invitrogen Molecular Probes), according to (Levine et al, 1993) with modifications. Briefly, cells were grown to 70-80% confluence in a 96 well plates. Cells were incubated with 5 μM BCECF-AM in Hank's Balanced Salt Solution (HBSS) (Gibco) for 1 h at RT, then washed with "Na⁺-free" medium (130 mM tetramethylammonium-Cl, 5 mM KCl, 2 mM CaCl₂, 1 mM MgSO₄, 10 mM glucose, and 20 mM HEPES, pH 7.4) to remove the excess of dye. Medium was replaced with 30 mM NH₄Cl in

“Na+free” for 5 min at 37°C, in a CO₂ cell culture chamber. NH₄Cl was removed by washing with Na+free medium. Then Na+ medium (130 mM NaCl, 5 mM KCl, 2 mM CaCl₂, 1 mM MgSO₄, 1 mM NaPO₄, 25 mM glucose and 20mM HEPES, pH 7.4) was added and data points were collected approximately every 90 sec for 20 min. Fluorescence was measured using a filter for detecting emission at 520 nm and at 620 nm (the isosbestic point) when excited at 488 nm. Experimental fluorescence was adjusted by subtracting the background intensity. All the fluorescence intensity measurements after NH₄Cl recovery were normalized by the fluorescence intensity at time zero.

2.21. Generation of the PRMT5^{Δ+HA} mouse model

We used CRISPR/Cas9 to generate a mouse model in which we replaced the last 6 amino acids of PRMT5 with an HA tag, which we refer to as PRMT5^{Δ+HA}. To generate the PRMT5^{Δ+HA} knock-in mice, we co-injected sgRNA, Cas9 mRNA, and an oligo donor into one-cell stage mouse embryos.

The oligo donor is a double-stranded gBlock fragment that has 80 bp of homology in each arm, with DNA encoding the HA tag (60 bp) in the middle:

```
TGCAGCAATTCCAAGAAAGTGTGGTACGAGTGGGCGGTGACGGCCCCCGTCT
GTTCTTCTATTACAACCCTACCGGCCGGGGATATCCATATGATGTTTCTGATT
ATGCTTAGCCCTGCACACAGTGTCAAACCTTGGGAAGCAGCTCTGAGTTCTCTT
CCTACAGCACAGAAGGTGTAGAACA. The guide RNA and Cas9 were generated
by Sage Laboratories, gRNA/PAM sequence: ATGGTATAGGAGCGGCCGGTAGG.
Guide RNA and donor sequence were generated by Sage laboratory (Appendix C).
```

2.22. Mouse genotyping

All mouse procedures were performed in accordance with The University of Texas MD Anderson Cancer Center guidelines. Genomic DNA was isolated from tail biopsies and analyzed by PCR. The PRMT5 C-terminus WT and Δ+HA alleles were identified using the following oligonucleotides:

5'- CCGCCTGTGTCTTTCGTATT -3'

5'- GTTGGCCACCATGACATTAG -3'

PCR reactions generated a 336 bp band for the wild-type allele and a 348 bp band for the PRMT5^{Δ+HA} allele. The PCR products for founder mice were sequenced to verify the fidelity of the mutation.

2.25. Derivation of mouse embryonic stem cells

Mouse embryonic stem cells were derived from pregnant female mice essentially as described elsewhere (Czechanski et al, 2014). Briefly, heterozygous PRMT5^{Δ+HA} mice were mated 48 hours after intraperitoneal injection with 5 IU of pregnant mare's serum gonadotropin (PMSG), and checked for the presence of vaginal plugs. At embryonic day 3.5 (E3.5), mice were euthanized and blastocysts were collected by flushing them out of the uterine horn with M2 medium (Sigma). Blastocysts were plated in feeder-coated wells with serum-free ES medium containing LIF, CHIR99021 and PD0325901 inhibitors, and then incubated at 37 °C with 5% CO₂ for 48 hours. Serum-free medium was replaced after blastocysts hatched from the zona pellucida. Once inner cell mass outgrowths were prominent, the entire well was disaggregated with 0.05% trypsin and pipetting, and then plated in a new feeder-coated well with ES medium containing FBS, LIF, CHIR99021 and PD0325901 inhibitors. ES colonies were generally visible 5 days after disaggregation. Once the wells reached 70-90% confluency, ES cells were passed into a 0.2% gelatin-coated well (labeled as passage 1), and further cultured in feeder-free conditions. ES cells were harvested for genotyping and western blot analysis after at least 4 passages in feeder-free conditions. Experiments were performed by Dr. Jeusun Kim and Nicolas Veland, B.S. in Dr. Taiping Chen's Laboratory.

2.24. Chromatin immunoprecipitation (ChIP) assay

The ChIP assay was performed as described previously (Biswas et al, 2014). Briefly, U2OS expressing ER-I-Ppol control or 4-hydroxy tamoxifen treated cells were cross-linked with 1% formaldehyde for 10 min at RT. Cross-linking reactions

were quenched by the addition of glycine followed by incubation for 5 min at RT. Nuclei were isolated and sonicated in ChIP buffer containing a protease inhibitor cocktail (Roche) and a phosphatase inhibitor cocktail (Roche) to generate DNA fragments of approximately 200 to 1000 bp. Primers for sequences flanking an I-Ppol cut site was used to examine enrichment at a DNA double-strand break.

2.26. Ionizing radiation treatment

Cells were irradiated at a dose of 5 Gy at RT using a RS-2000 Biological Irradiator (Rad Source). After IR treatment, the cells were returned to an incubator and maintained at 37 °C for further analysis.

Chapter 3: Regulation of PRMT5 by Tyrosine Phosphorylation

3.1. Introduction

Distinct PTMs, including acetylation, ubiquitination and phosphorylation, have been experimentally identified across PRMT5, and have been deposited in PhosphoSitePlus (Hornbeck et al, 2015) (**Figure 3**). In addition to these, we have identified new phosphoserine and phosphothreonine sites on PRMT5 by means of mass spectrometric analysis of PRMT5 purified from hyperphosphorylated cells (**Figure 3**). However, the functions of modified PRMT5 are largely unknown. Here, we investigate the significance of some of these phosphotyrosine sites, with respect to whether they play a role in mediating protein-protein interactions.

3.2. Results

3.2.1. Tyrosine phosphorylation regulates PRMT5 activity

We were particularly interested in the phosphotyrosine sites located in the central region of PRMT5. There are at least six tyrosine residues potentially phosphorylated in this region and all are conserved between humans and mice. Phosphorylation of Y297, Y304 and Y307 of PRMT5 had already been established by Dr. Nimer's group (Liu et al, 2011). Phosphorylation on these residues impairs MEP50-PRMT5 interaction and consequently, PRMT5 activity is diminished (Liu et al, 2011). Additionally, phosphorylation of Y280, Y283 and Y286 has been found multiple times by mass spectrometry and at least one residue is predicted to be a substrate for Src. Experimental data from our laboratory showed that immunoprecipitated Myc-PRMT5 from cells co-transfected with vSrc was phosphorylated, indicating that PRMT5 is a substrate for vSrc kinase (**Figure 4A**). Moreover, an *in vitro* methylation assay performed with Myc-PRMT5

immunoprecipitated from cells with or without cotransfected vSrc, demonstrated that the activity of PRMT5 towards H3, H4 and MBP was reduced when PRMT5 was phosphorylated by vSrc (**Figure 4B**). This indicates that the methyltransferase activity of PRMT5 might be regulated by its tyrosine phosphorylation.

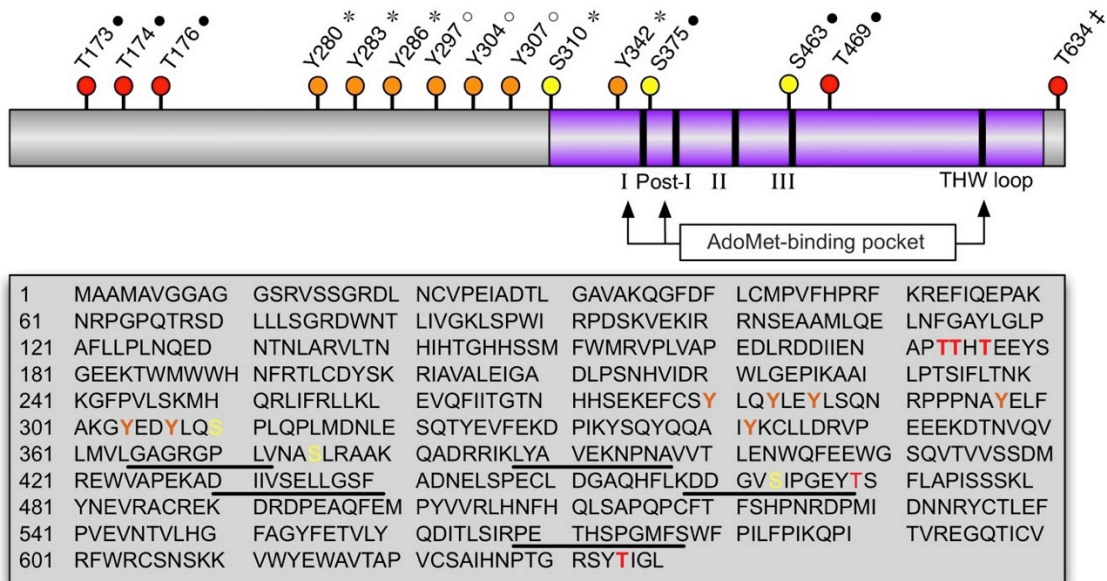


Figure 3: PRMT5 is phosphorylated at multiple residues

Schematic representation of PRMT5. The relative positions of predicted and observed phosphorylated residues are indicated; • observed by mass spectrometry-based analysis in hyperphosphorylated samples, * observed by mass spectrometry reported at PhosphoSite Plus, ○ reported in literature, ‡ predicted AKT phospho-site. The catalytic core is indicated in purple. The signature methyltransferase motifs are boxed in the following order: I, post-I, II, III and THW loop.

3.2.2. Phosphorylation of PRMT5 creates a binding motif for SH2 domains

We postulate that phosphorylation of PRMT5 regulates its enzymatic activity and substrate specificity by mediating phospho-dependent protein-protein

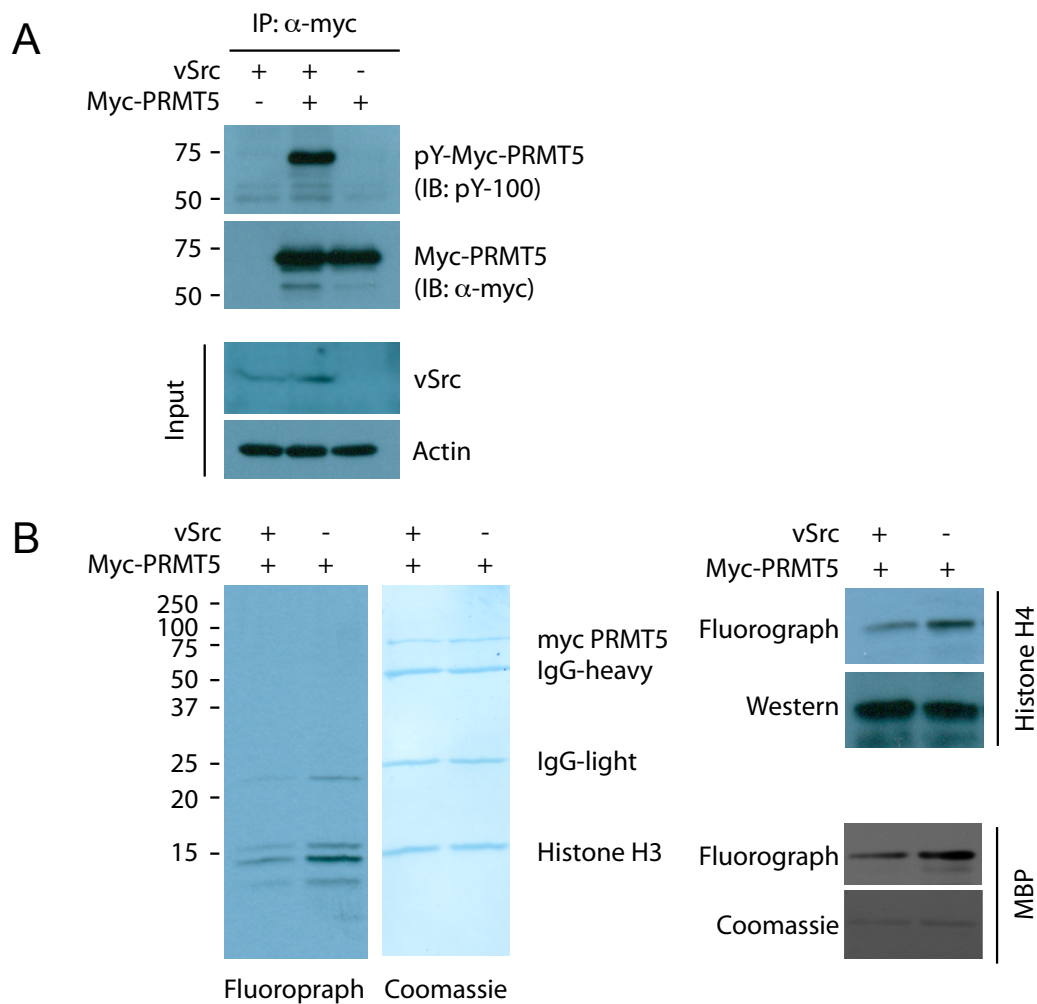


Figure 4: PRMT5 is tyrosine-phosphorylated by the Src kinase

A) Myc-PRMT5 was co-transfected into HeLa cells with or without a vSrc plasmid as indicated. A western blot analysis for vSrc, using an actin loading control is shown. Phosphorylated tyrosine in myc-PRMT5 immunoprecipitates was detected using a pan-phosphotyrosine antibody (pY-100). The phosphorylation level of Myc-PRMT5 increased with vSrc overexpression.

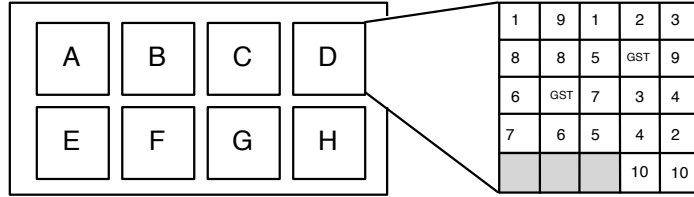
B) To test whether the tyrosine phosphorylation of PRMT5 can affect its enzymatic activity, an *in vitro* methylation assay using H3, H4 and MBP substrates was performed using immunopurified myc-PRMT5 from HeLa cells with or without vSrc overexpression. Overexpression of vSrc led to a decrease in PRMT5 activity, indicating that the methyltransferase activity of PRMT5 might be regulated by its tyrosine phosphorylation. Experiments were performed by Dr. Yong Kee Kim.

interactions. SH2 domains are the major protein module that recognizes phosphotyrosine motifs. To perform a comprehensive and unbiased screen of phosphotyrosine-dependent interactions, we purified over 70 different GST-fusions of SH2-containing protein domains and generated an SH2-domain array (**Figure 5**). The use of protein microarrays for studying protein interactions with peptide ligands has been well-validated, and is a reliable and reproducible approach for identifying binding partners (Espejo et al, 2002; Kim et al, 2006; Yang et al, 2010). Using the online database PhosphoSite Plus we observed a cluster of three putative tyrosine phosphorylation sites (Y280, 283 and 286). To identify PRMT5 phosphorylation-dependent binding partners and determine whether these were functional phosphorylation sites, we used peptides harboring phospho-tyrosine residues to screen for potential SH2 domain-containing proteins that could bind each of these three phospho-motifs.

These PRMT5 peptides were fluorescently labeled and probed on a protein SH2-array (**Figure 6**). We observed that the combination of two or more pY sites enhanced the interaction with SH2-domains, but overall, did not show an exclusive preference for a specific combination of pY residues, for example, PIK3R1_N (magenta oval). However, a few interactions only occurred with a particular combination of phosphotyrosines, for example PTK6 (yellow oval), which interacted only with the peptide containing both pY280 and pY283 (**Figure 6**). In conclusion, SH2 domains recognize one or more phosphotyrosine residues on PRMT5 either singly or in combination. This suggests that PRMT5 may be regulated by SH2 domain containing proteins for a variety of cellular functions, or that these SH2-containing proteins may themselves be substrates of PRMT5.

3.2.3. Endogenous PRMT5 interacts with SH2 domain-containing proteins

Our comprehensive SH2 domain array screen revealed a broad set of SH2-domains that interact with PRMT5 phosphotyrosine peptides. As a result of this screen, 25 phosphorylation-dependent protein-peptide interactions were discovered



<u>Kinases</u> A1 LYN (P07948) A2 HCK (P08631) A3 LCK (P06239) A4 BLKSH2 (P51451) A5 FYN (P06241) A6 YES (P07947) A7 SRC (P12931) A8 PTK6 (Q13882) A9 FRK (P42685)	<u>Kinases</u> B1 ABL1 (P00519) B2 ABL2 (P42684) B3 FER (PI6591) B4 FES (P07332) B5 TXK (P42681) B6 ITK (Q08881) B7 BTK (Q06187) B8 TEC (P42680) B9 BMX (P51813)	<u>Kinases</u> C1 SYK-C (Q5T6N8) C2 SYK-N (Q5T6N8) C3 ZAP70-C (P43404) C4 ZAP70-N (P43404) C5 MATK (P42679) C6 CSK (P41240) <u>Phosphatases</u> C7 PTPN11-C (Q06124) C8 PTPN11-N (Q06124) C9 PTPN6-C (P29350)	<u>Scaffolds</u> D1 BLNK (Q8WV28) D2 SLNK (Q7Z4S9) D3 SHC1 (P29353) D4 SHC3 Q92529) D5 SHC4 (Q8IYW3) <u>Small GTPase signalling</u> D6 RASA1-N (P20936) D7 RASA1-C (P20936) D8 VAV1(P15498) D9 VAV2 (P52735)
<u>Signal Regulation</u> E1 DAPP1 (Q9UN19) E2 HSH2D (Q96JZ2) E3 GRB7 (Q14451) E4 GRB10 (Q13322) E5 GRB14 (Q14449) E6 SHB (Q15464) E7 SHD (Q96IW2) E8 SHE (Q5VZ18) E9 SHF (Q96IE8)	<u>Cytoskeletal Regulation</u> F1 BRDG1(Q9ULZ2) F2 SH3BP2 (P78314) F3 SH2D1A (O60880) F4 SH2D1B (O14796) F5 TNS1 (Q9HBL0) F6 TNS2 (Q76MW6) F7 TNS3 (Q8IZW7) F8 TNS4 (Q8IZW8) <u>Signal Regulation</u> F9 APS (O14492)	<u>Adapters</u> G1 GRAP (Q13588) G2 GRAP2 (O75791) G3 GRB2 (P62993) G4 CRK (P46108) G5 CRKL (P41240) G6 NCK1 (P16333) G7 NCK2(O43639) <u>Phospholipid signaling</u> G8 SHIP1 (O00145) G9 SHIP2 (O15357)	<u>Phospholipid signaling</u> H1 PIK3R1_C (P27986) H2 PIK3R1_N (P27986) H3 PIK3R2_C (O00459) H4 PIK3R2_N (O00459) H5 PIK3R3_C (Q92569) H6 PIK3R3_N (Q92569) H7 PLCg1-C (P19174) H8 PLCg1-N (P19174) H9 PLCg2-C (P16885) H10 PLCg2-N (P16885)

Plasmids were kindly provided by Dr. Shawn Li, Department of Biochemistry, University of Western Ontario

Figure 5: Phosphotyrosine-binding microarray

Protein microarray containing 73 different GST-fusion SH2 domains. Each protein is printed in duplicate in a specific orientation as designated in the key. Each block harbors up to 10 GST-fusion proteins, plus GST protein as negative control.

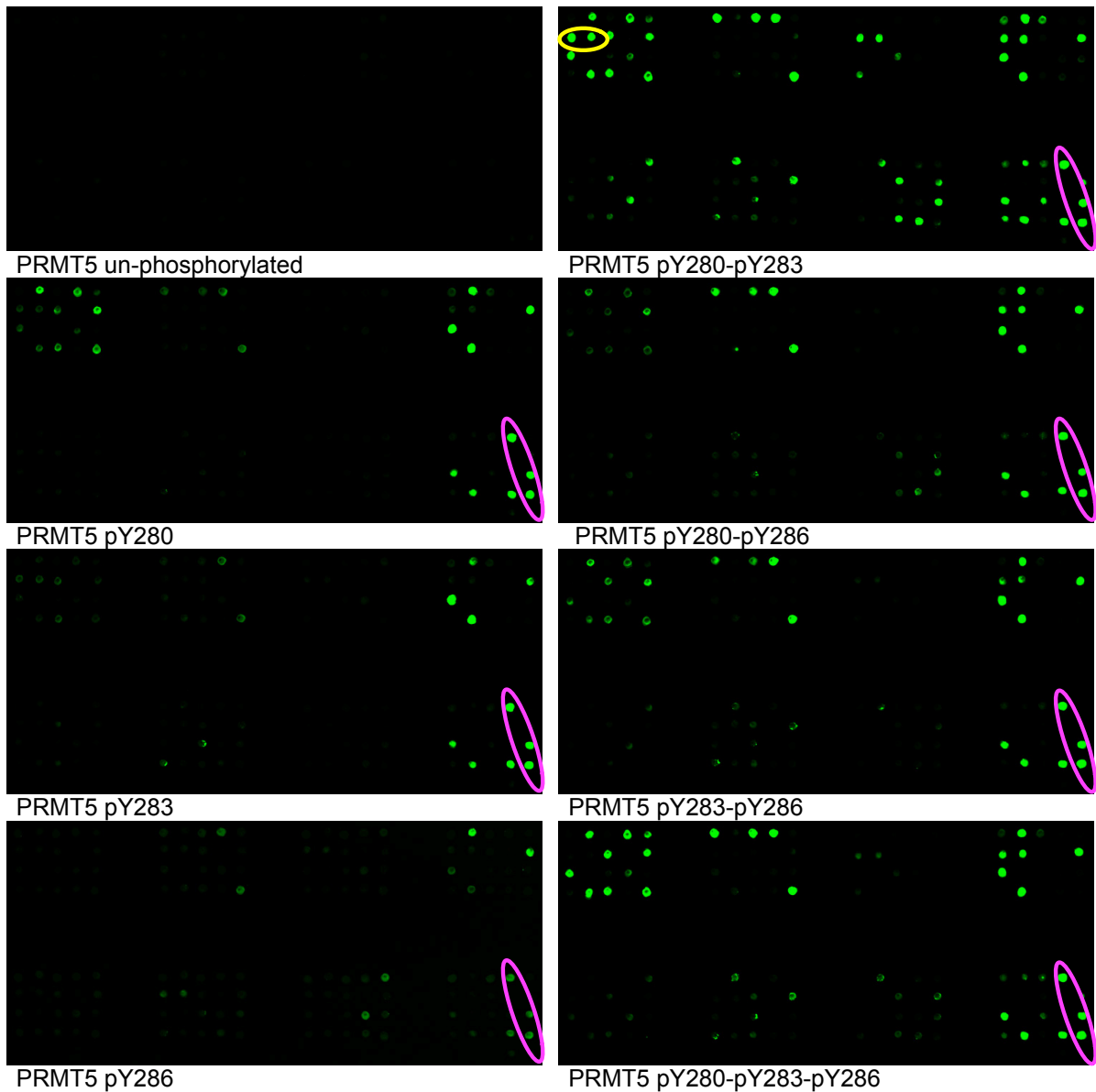


Figure 6: Identification of PRMT5 phosphotyrosine specific binding partners

Tyrosine phosphorylation of PRMT5 regulates its interactions with SH2 domain containing proteins. Tyrosine phosphorylated peptides harboring pY280, pY283, pY286 and all possible combinations were probed on a protein microarray harboring 73 different SH2 domains-containing proteins. Ovals highlight two of the 27 putative binding partners; PTK6 (yellow) and PIK3R1_N (magenta). It is important to note that while PTK6 binds exclusively with the PRMT5 pY280-Y283 peptide, PIK3R1_N does not show such preference. A List of the arrayed proteins is shown in Figure 5.

(Table 2). To validate these PRMT5-binding interactions, we used purified GST-SH2 domains and performed pull-down assays. We selected four representative samples from the array results; PIK3R1_N (which interacted with all the phosphotyrosine peptides), PTK6 (which bound only the peptide containing pY280 and pY283), Abl1 (which bound peptides containing pY280 together with other combinations of pY) and VAV1 (which bound only to peptides containing multiple combinations of pY). GST-SH2 domains were incubated with the lysates of cells that were hyperphosphorylated using sodium pervanadate treatment, which specifically increases the levels of phosphotyrosine by inhibiting endogenous phosphatase activity. This pull-down verified the interaction of PTK6-SH2 with PRMT5 and revealed a weak interaction with PIK3R1 (**Figure 7A**). PTK6 and PIK3R1 were not only able to pull-down PRMT5, but also other phosphotyrosine-containing proteins from sodium pervanadate-treated cells (**Figure 7C**). In a similar experiment, we treated NIH-3T3 cells and confirmed the interaction of PRMT5 with PTK6 along with the SH2 domains of Fyn, HCK, LCK, RASA1, and Yes (**Figure 7B**). The summary of the interactions validated by GST pull-down is shown in **Table 2**, column 1.

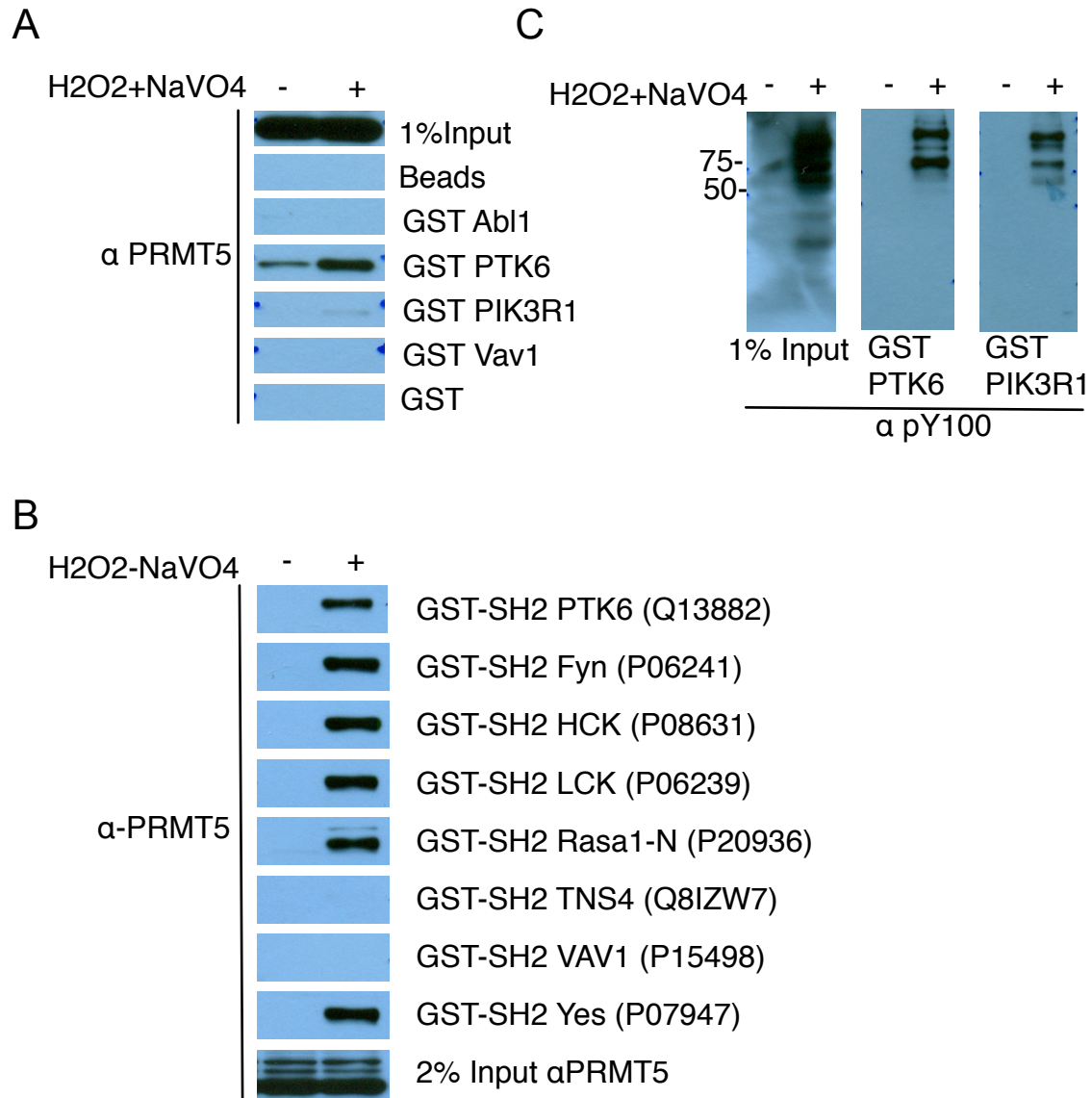


Figure 7: Endogenous PRMT5 interacts with SH2 domain-containing proteins

To validate the PRMT5 binding proteins found in the protein microarrays, we purified GST-fusion proteins of candidate phospho-dependent partners and incubated these with MCF7 and NIH-3T3 whole cell lysates and performed western blotting with anti-PRMT5 antibody. (A) GST-fusion proteins were incubated with lysates from untreated or sodium pervanadate-treated MCF7 cells and (B) NIH-3T3 cells. (C) Inputs are shown to demonstrate hyperphosphorylation in cells using α -phosphotyrosine antibody. Molecular size markers (in kilodaltons) are indicated.

		Peptide-SH2 Domain Interaction Using Array							
GST Pull-down	peptide protein	Unphosphorylated	Y280	Y283	Y286	Y280-Y283	Y280-Y286	Y283-Y286	Y280-Y283-Y286
yes	A3 LCK (P06239)	no	no	no	no	yes	no	no	yes
yes	A5 FYN (P06241)	no	no	no	no	yes	yes	yes	yes
yes	A6 YES (P07947)	no	no	no	no	yes	no	yes	yes
yes	A8 BRK/PTK6 (Q13882)	no	no	no	no	yes	no	no	no
N/T	A9 FRK (P42685)	no	yes	no	no	yes	yes	yes	yes
no	B1 ABL1 (P00519)	no	yes	no	no	yes	yes	yes	yes
N/T	B2 ABL2 (P42684)	no	yes	yes	yes	yes	yes	yes	yes
N/T	C7 PTPN11-C (Q06124)	no	no	no	no	yes	no	no	no
N/T	C8 PTPN11-N (Q06124)	no	no	no	no	yes	no	no	yes
N/T	D1 BLNK (Q8WV28)	no	no	no	no	yes	no	no	no
yes	D6 RASA1-N (P20936)	no	yes	yes	no	yes	yes	yes	yes
no	D8 VAV1(P15498)	no	no	no	no	yes	yes	yes	yes
N/T	D9 VAV2 (P52735)	no	yes	yes	yes	yes	yes	yes	yes
N/T	E3 GRB7 (Q14451)	no	no	no	no	yes	no	no	no
N/T	F7 TNS3 (Q8IZW7)	no	no	yes	no	yes	no	no	no
no	F8 TNS4 (Q8IZW8)	no	no	no	yes	no	no	no	no
N/T	F9 APS (O14492)	no	no	no	no	yes	no	no	yes
N/T	G3 GRB2 (P62993)	no	no	no	yes	no	no	no	no
N/T	G4 CRK (P46108)	no	no	no	no	yes	yes	no	no
N/T	G5 CRKL (P41240)	no	no	no	no	yes	no	no	no
N/T	G9 SHIP2 (O15357)	no	no	no	no	yes	no	no	yes
yes	H2 PIK3R1_N (P27986)	no	yes	yes	yes	yes	yes	yes	yes
yes	H4 PIK3R2_N (O00459)	no	yes	yes	yes	yes	yes	yes	yes
yes	H6 PIK3R3_N (Q92569)	no	yes	yes	no	yes	yes	yes	yes

Table 2: Phosphotyrosine Interactions

Summary of SH2 domain interactions detected using the protein domain microarray with positive interactions highlighted in green. The first column indicates whether the interaction was validated by GST pull-down experiments. Positive interactions are highlighted in yellow, negative in red and N/T: not tested. A letter followed by a number before the protein name indicates the array code position. Protein accession numbers are indicated in parentheses.

3.3. Discussion

In this work, we used comprehensive and unbiased approaches to define phosphotyrosine-dependent interactions between PRMT5 and SH2 domain containing-proteins. First, we found that Src phosphorylates PRMT5 and that tyrosine phosphorylation reduces PRMT5 activity. Second, we established that Y280, Y283 and Y286 are functional phosphorylation sites, allowing interaction with over 20 distinct PRMT5 phosphotyrosine-dependent binding partners. Third, we showed that multiple combinations of PRMT5 phosphotyrosine may form a code to recruit specific effectors.

Phosphorylation of PRMT5 regulates its association with MEP50. Phosphorylation of Y297, Y304 and Y307 negatively affects the interaction of PRMT5 with MEP50, and therefore impedes PRMT5 catalytic function (Liu et al, 2011). However, these sites are phosphorylated by a mutated form of Jak2 and not by the wild type kinases. On the other hand, the tyrosine phosphorylation sites we have described here, Y280, Y283 and Y286, have been identified numerous times by mass spectrometry (reported in PhosphositePlus), while the tyrosine sites investigated by Dr. Nimer's group have not been observed using this technique. These data lead us to believe that phosphorylation occurs predominantly at Y280, Y283 and Y286 and that these sites may play a pivotal role in PRMT5 function. Nonetheless, we have also observed that phosphorylation on Y297, Y304 and Y307 promotes PRMT5 interaction with a number of SH2 domains (**Figure 8**). Interestingly, PRMT5 activity regulates kinases involved in signaling pathways, suggesting regulatory crosstalk between kinases and arginine-methyltransferases. (Andreu-Perez et al, 2011; Hsu et al, 2011).

Here, we observed that the activity of PRMT5 was reduced when phosphorylated by Src. Src is one of many phosphotyrosine kinases that is associated with the plasma membrane via amino terminal myristoylation. We also showed that PRMT5 is phosphorylated by Src, and in the next chapter, we will show that PRMT5 is associated with the plasma membrane via its C-terminus. These observations support the idea that PRMT5 could be a target for Src kinase.

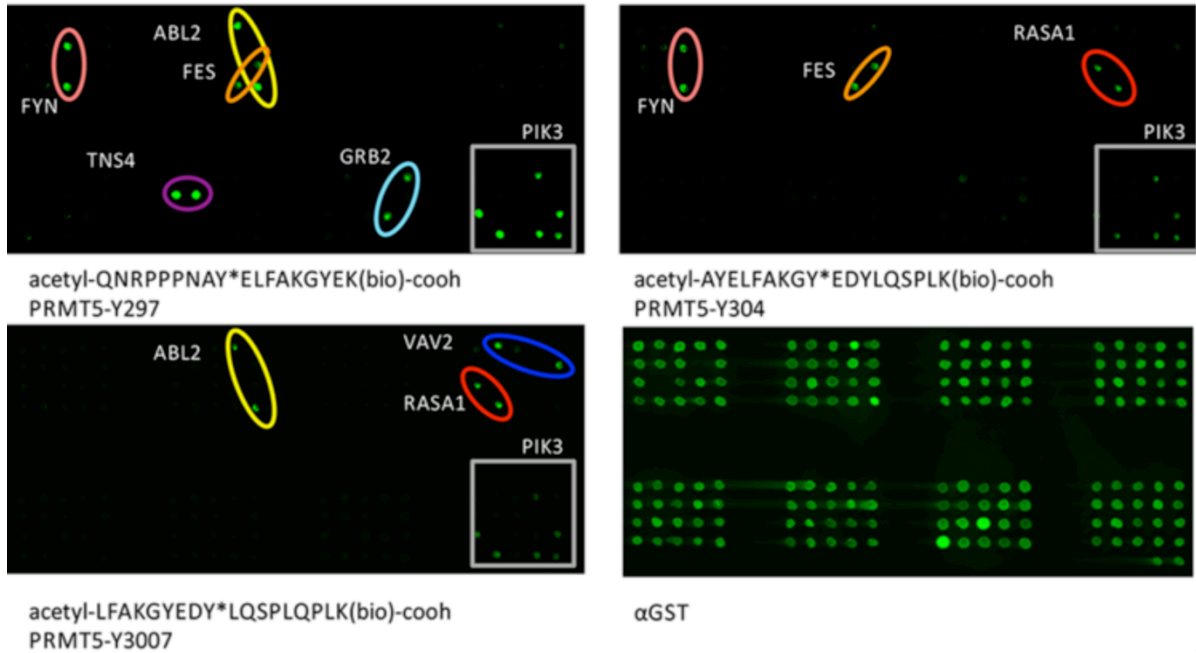


Figure 8: Additional SH2 interactions

Tyrosine phosphorylated peptides harboring pY297, pY304 and pY307 were probed on a SH2 protein microarray. Positive interactions are circled. List of SH2 domain proteins represented on the array is shown in Figure 5.

Many signaling processes are mediated by three components, a writer enzyme that post-translationally modified proteins, one or more erasers that reverse the effect of the writer, and one or more readers that can sense and respond to a change in the condition of the system. This three component model can be applied to many cellular functions, from cell membrane signaling to the histone code. Post-translational modifications play fundamental roles in regulating molecular pathways, and tyrosine phosphorylation is a central component of molecular signaling pathways, governed by kinases (writers), phosphatases (erasers) and SH2-domain containing proteins (readers).

Tyrosine phosphorylated proteins make up a small proportion of the proteome relative to the much more abundant serine and threonine phosphorylated proteins (Hunter, 1989). The presence of constitutively activated PTK in cancer cells increases the levels of phosphotyrosine-containing proteins causing deleterious effects. Therefore, in healthy cells, proper regulation of PTK is a critical process, and the number and diversity of phosphotyrosine-motif readers may provide the necessary precision to regulate the outcomes of PTK. Thus, SH2 domains play a critical role in signaling by mediating the formation of protein complexes.

PTK6 is one of 25 novel SH2 domain-containing phosphotyrosine-dependent PRMT5 binding partners. PTK6 belongs to a family of non-receptor tyrosine kinases, somewhat similar to the Src family, but lacking a N-terminal myristoylation site of the Src kinase (Brauer & Tyner, 2010). In addition to the tyrosine kinase domain, PTK6 contains both SH2 and SH3 domains, which bind to phosphotyrosine and proline-rich sequences (PXXP), respectively.

PTK6 is known to associate with and phosphorylate a small number of substrates, including Src-associated in mitosis 68 kDa protein (Sam68) (Derry et al, 2000). Sam68 is an RNA-binding protein, which binds RNA via its KH domain. It also contains a recognition motif for SH2 domains and for SH3 or WW domains, both of which bind to PXXP motifs. Interestingly, these proline-rich sequences are flanked by a glycine- and arginine-rich (GAR) motif, which is also characteristic of PRMT1 and PRMT5 substrates. Indeed, Sam68 is predominantly methylated by PRMT1 (Bedford et al, 2000; Cote et al, 2003). Methylation of Sam68 is required for its

nuclear localization, but also prevents SH3 domain binding, yet has no effect on WW domain binding (Bedford et al, 2000; Cote et al, 2003).

One can hypothesize that the phosphotyrosine-dependent interaction of PRMT5 with PTK6 may place Sam68 into close proximity with PRMT5, where it becomes a target for symmetric methylation. This suggests that PRMT1 and PRMT5 may compete for the same substrate, which can be asymmetrically and symmetrically dimethylated. The simultaneous occurrence of both asymmetrically and symmetrically methylated arginine has been reported on another protein, MBD2 (Tan & Nakielny, 2006). MBD2 interacts with the HDAC complex and specifically binds to methylated DNA. Arginine methylation of MBD2 inhibits both its protein-protein and protein-DNA interaction (Tan & Nakielny, 2006).

Both asymmetric arginine dimethylation and phosphorylation of Sam68, mediated by PRMT1 and PTK6, respectively, abolishes the ability of Sam68 to bind RNA (Derry et al, 2000; Rho et al, 2007). Because we speculate that PRMT5 and PTK6 are in the same complex as Sam68, it would be interesting to understand what is the biological significance of symmetric versus asymmetric arginine methylation. ADMA affects the RNA binding function of another protein, the trans-activating regulatory (TAT) protein of the Human immunodeficiency virus (HIV-1). TAT studies revealed that both forms of arginine methylation reduce the affinity of the protein-RNA interaction, with the biggest reduction occurring with ADMA, and only a weak reduction with SDMA (Kumar & Maiti, 2013). Further studies will be necessary to determine whether Sam68 contains SDMA and what the specific roles of ADMA and SDMA are.

3.4. Future studies

These studies raise several questions that need to be experimentally addressed. In particular, it remains to be determined whether the *in silico* identified phosphorylation sites are present *in vivo* on PRMT5. To address this question, we attempted to develop an antibody using a peptide containing pY280, pY283 and pY286. Unfortunately, this antibody was not phosphospecific, (**Figure 9A and C**).

However, pan phosphotyrosine 4G10 recognized all combinations of phosphotyrosine studied here. Despite that, some pY combinations were better recognized than others (**Figure 9B**), this antibody proved suitable for identification of phosphorylated sites in immunoprecipitated PRMT5 (**Figure 9C**).

Additionally, we generated several myc-tagged PRMT5 constructs. These included constructs with a single Y substitution (Y280, Y283, or Y286), all three substitutions and a construct deleted for residues 276 to 309, thus removing our sites of interest as well as the sites identified by Dr. Nimer's group (Y297, Y304 and Y307). The use of these constructs together with the 4G10 antibody may reveal whether tyrosine phosphorylated sites of PRMT5 exist *in vivo*.

Finally, considering our preliminary data, we can hypothesize that the absence of Src may reduce PRMT5 interaction with SH2 domains. To further analyze the contribution of Src to PRMT5 phosphorylation, GST fusion pull-down experiments will be performed with purified PTK6- and PIK3R1- proteins incubated with lysates from either untreated or pervanadate-treated Src-deficient MEF (SYF^{-/-}) cells and c-Src expressing MEF cells (Src^{+/+}). We expect that the levels of co-precipitated PRMT5 will be reduced in Src-deficient MEFs compared to the control cells.

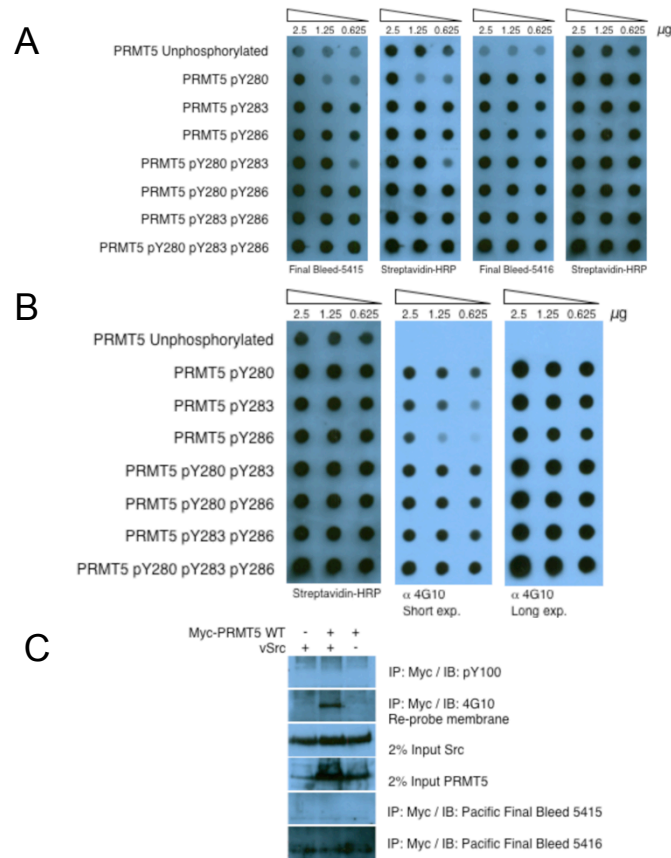


Figure 9: Dot blot analysis of phospho-tyrosine PRMT5 antibodies

(A) Antibodies were developed using a peptide containing all phospho-tyrosine residues (pY280, pY283 and pY286). Peptides containing single modifications and all possible combination were spotted onto nitrocellulose membranes and probed with (A) final bleed 5415 and 5416 and (B) pTyr mAb 4G10. Streptavidin-HRP was used as a loading control. 4G10 antibody detects phosphotyrosine peptides, although it shows a weaker signal for PRMT5-pY280 and -pY283. (C) Myc-PRMT5 was co-transfected into HeLa cells with a vSrc expressing plasmid as indicated. Immunoprecipitated Myc-PRMT5 was analyzed with all three antibodies sources. The 4G10 antibody produced a stronger signal in conditions leading to myc-PRMT5 hyperphosphorylation (+ vSrc).

Chapter 4: Phosphorylation at the C-terminus triggers a binding switch between 14-3-3 proteins and PDZ domains

4.1. Introduction

PRMT5 is commonly found associated with other proteins, and these interactions control its catalytic activity and substrate specificity. Recently, it has become clear that PRMT5 is phosphorylated at several residues, which prompted us to investigate whether phosphorylation of PRMT5 regulates its subcellular localization and substrate choice by mediating phospho-dependent protein-protein interactions. While investigating the role of phosphorylation on the regulation of PRMT5, we found that the phosphorylated C-terminal tail of PRMT5 interacts with 14-3-3 proteins. However, what is more interesting is that the unphosphorylated C-terminus binds the PDZ domains of a membrane-associated protein, NHERF2, as well as other PDZ containing proteins. Thus, the C-terminus of PRMT5 has a shared recognition motif for PDZ domain and 14-3-3 proteins. In order to bind to this motif, 14-3-3 proteins require the site to be phosphorylated. In contrast, PDZ domain recognition is phospho-independent. We also observed this phenomenon in a number of proteins, suggesting that this potential phosphorylation-dependent switch between binding to 14-3-3 and PDZ domains occurs among a wider range of proteins.

4.2.1. PDZ domains

The PDZ domain was identified as a set of conserved sequence repeats in three related proteins; the postsynaptic density-95 (PSD-95) protein, the *Drosophila* tumor suppressor protein disks-large-1 (DLG), and the tight junction protein zonula occludens 1 (ZO-1), and named for these three proteins in which the repeats were

initially observed (Kennedy, 1995). PDZ domains constitute one of the largest families of interaction domains in eukaryotes and are found in more than 400 human proteins (Zhang & Wang, 2003). PDZ domains are typically between 80-90 amino acids in length, and are composed of 5 to 6 β strands and 2 α helices.

PDZ domains preferentially recognize a short peptide motif at the extreme carboxyl terminus of their target proteins. Recognition is mediated through a binding pocket formed by the second β strand, second α helix and the carboxylate-binding loop which contains the conserved sequence motif K/R-X-X-X-G- Φ -G- Φ (X represents any natural amino acid and Φ is a hydrophobic residue) (Lee & Zheng, 2010; Zhang & Wang, 2003). Based on the sequence of their preferred ligands, PDZ domains are grouped into numerous classes, nonetheless, the most classical organization consists of 3 classes: X[T/S]X Φ -COOH (Class I motif), X Φ X Φ -COOH (Class II motif) and X[D/E]X Φ -COOH (Class III motif) (Lee & Zheng, 2010). Interestingly, the PDZ class I motif has remarkable similarity to 14-3-3 binding motif III.

PDZ domains are often organized in a tandem arrangement. Recent studies have shown that in order to fold properly, some PDZ domains require contact with other PDZ domains. This association may occur intramolecularly with a neighboring tandem repeat or intermolecularly by PDZs forming heterodimers via their PDZ domains. The structural rearrangements can either leave the binding pockets of both PDZs open, or preserve only one open pocket for interaction with the target protein (Lee & Zheng, 2010).

For most PDZ-containing proteins, individual domains are usually well folded and their presence in tandem repeats allows the association with other proteins through each PDZ domain. Such PDZ-containing scaffold proteins can assemble large molecular complexes. Interestingly, most of the PDZ domains are associated with the cell membrane, despite lacking a transmembrane domain (Zhang & Wang, 2003). PDZ scaffolds play an important function in the establishment of epithelial polarity, clustering ion transporters and signaling receptors on membranes, connecting plasma membrane and cytoskeletal proteins, and regulating protein

trafficking (Kiela & Ghishan, 2009; Kim & Sheng, 2004; Kundu & Backofen, 2014; Nourry et al, 2003; Romero et al, 2011).

4.2.2. NHERF

NHERF family proteins (Na^+/H^+ exchanger regulatory factor) are PDZ containing proteins that comprise a group of structurally related adapter proteins that are highly expressed in the apical portion of the plasma membrane of polarized epithelial cells. Members of this group include NHERF-1 (also known as NHERF, EBP50), NHERF-2 (E3KARP), NHERF-3 (CAP70, PDZ-dc1), and NHERF-4 (IKEPP) (**Figure 10**). NHERF1 and NHERF2 are highly homologous, containing a C-terminal sequence that binds to the ezrin-radixin-moesin (ERM-Binding domain) family of membrane-cytoskeletal proteins and two tandem PDZ domains.

NHERF proteins interact with many cellular proteins via their PDZ domains. Moreover, the NHERF family of proteins homodimerize and heterodimerize, suggesting they can form a mesh at the apical region of epithelial cells that binds and modulates protein complexes (Wade et al, 2003). The multi-PDZ domain structure permits them to interact with multiple binding partners to mediate the formation of large protein networks (Donowitz et al, 2005). NHERF members can associate with a number of membrane proteins, including the cystic fibrosis transmembrane regulator (CFTR) anion channel and the sodium/hydrogen exchanger NHE3 (Ghishan & Kiela, 2012). Indeed, NHERF proteins were originally identified as regulators of NHE3 through its association via PDZ domains and the C-terminus of NHE3 (Kiela & Ghishan, 2009).

NHE3 belongs to a family of sodium/hydrogen exchangers (NHEs) ubiquitous transmembrane proteins that maintain cellular volume, intracellular sodium concentration and whole-organism acid-base homeostasis. NHE3 is expressed predominantly in the plasma membrane of renal and intestinal epithelia where it mediates the majority of sodium absorption (Zachos et al, 2005).

NHERF1 and NHERF2 regulate the localization of NHE3 activity in intestinal microvilli by organizing signaling complexes (Yang et al, 2015). Although all NHERF

members are present in a single cell, their localization varies. NHERF1 and NHERF3 are localized at the outer-most apical region of the microvillus, NHERF2 and NHERF4 are present in the inner part of the microvillus, and NHERF4 is also cytoplasmic (Hryciw et al, 2006; Murtazina et al, 2011) (Donowitz et al, 2005). (Figure 10).

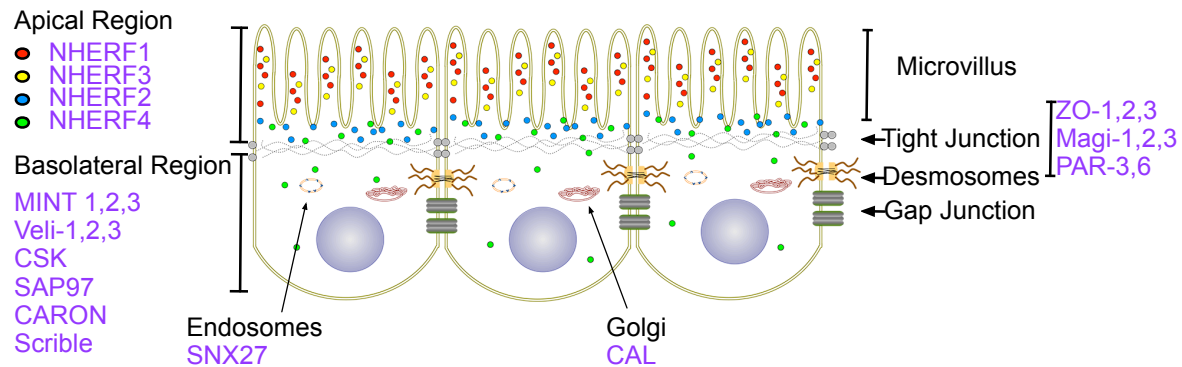


Figure 10: Localization of PDZ proteins in epithelial cells

NHERF family proteins homodimerize and heterodimerize, suggesting that they form a mesh at the apical region. The localization of PDZ domain-containing proteins (purple) is indicated.

Ion exchangers play an important role during the normal digestive process. The epithelium of the gastrointestinal tract secretes and absorbs large quantities of anions and fluid. This process is predominantly mediated by the Na^+/H^+ exchanger NHE3 and the CFTR Cl^- channel (Lamprecht & Seidler, 2006). Interestingly, both proteins, NHE3 and CFTR, interact with NHERF2 and other PDZ containing proteins, suggesting the importance of interactions between PDZ proteins and epithelial ion transporters (Lamprecht & Seidler, 2006).

A number of NHERF2 null mouse models have been generated. NHERF2 KO mice are born phenotypically normal (Seidler et al, 2009), but models developed by two different groups are inconsistent with regard to the role of NHERF2 in regulating the subcellular localization of NHE3, and the role of cAMP in the inhibition of NHE3 (Chen et al, 2010; Murtazina et al, 2011). Despite these discrepancies, the collective data indicate that loss of NHERF2 presents no obvious phenotype, but that NHERF2

is necessary for Ca²⁺- and cGMP-mediated inhibition of NHE3 (Chen et al, 2010; Murtazina et al, 2011).

4.3. Results

4.3.1. PRMT5 is phosphorylated at the C-terminus

Members of the PRMT family are phosphorylated and this modification regulates their activity. In particular, PRMT5 is phosphorylated at three tyrosine sites, which affect its binding with MEP50, its main co-activator. Moreover, additional phosphorylatable tyrosine, threonine and serine sites have been discovered either experimentally or *in silico*. Using bioinformatics, we identified the C-terminal residue T634 as having a high probability of being phosphorylated by AKT (**Figure 11A**).

To validate the phosphorylation of T634, we generated a GFP-PRMT5 construct harboring PRMT5 amino acids 340 to 637 (**Figure 11A**). Using this construct, we exclude other putative phosphothreonine sites located on the N-terminal half of PRMT5. GFP-PRMT5 and GFP-PRMT5^{T634A} were co-expressed with constitutively active myr-AKT in HeLa cells. We observed that GFP-PRMT5 but not GFP-PRMT5^{T634A} was detected by a pan-phosphothreonine antibody (**Figure 11B**), suggesting that PRMT5 is phosphorylated at T634 *in vivo*. We next investigated additional kinases that could potentially phosphorylate PRMT5 at T634. We conducted *in vitro* kinase assay experiments to test over 250 kinases for their ability to phosphorylate a peptide harboring the last 10 amino acids of PRMT5 (**Figure 12A**).

Because the C-terminus of PRMT5 contains additional residues that could be phosphorylated, a second *in vitro* kinase assay was performed, using those kinases that generated signals greater than 250 cpm in the first stage. WT and mutant-A634 peptides were used for further comparison of their phosphorylation efficiency with 18

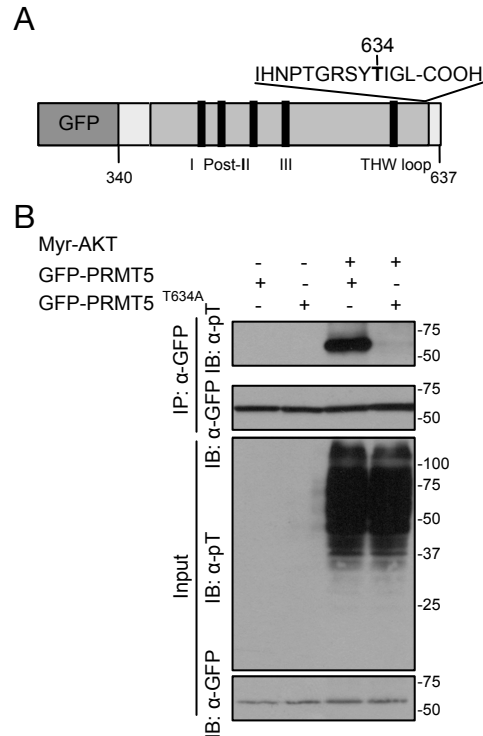


Figure 11: PRMT5 is phosphorylated at its C-terminus

A) Schematic representation of N-terminally truncated PRMT5. Position of predicted AKT-phosphorylated residue T634 is indicated. The sequence of the C-terminus, which includes the recognition motifs for 14-3-3 and PDZ binding is shown. The signature methyltransferase motifs are marked by black boxed in the following order: I, post-I, II, III and THW loop.

B) A threonine to alanine substitution at position 634 abrogates the Akt/Calyculin-A induced phosphorylation of GFP-PRMT5 WT. GFP-PRMT5 harbors amino acids 340 to 637. HeLa cells were transiently transfected with GFP-tagged WT or mutant (T634A) expression plasmids with or without constitutively active Akt (myr-Akt). Cells were treated with 0.1 μ M Calyculin-A (a phosphatase inhibitor) for 1 hour prior to lysis. Proteins were immunoprecipitated with anti-GFP agarose resin and immunoblotted with pan anti-phosphothreonine and anti-GFP antibodies. Input lysates were immunoblotted with antibodies specific to GFP-tagged proteins and phosphor-threonine residues.

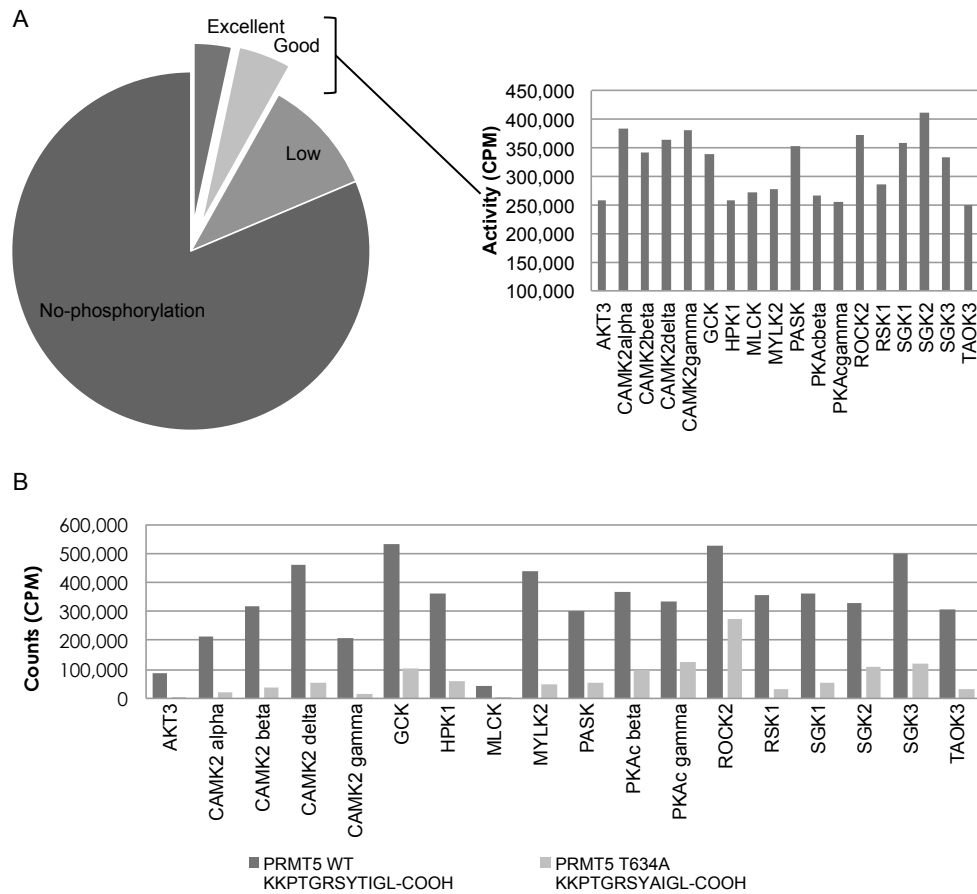


Figure 12: Radiometric assay of the PRMT5 C-terminus peptide phosphorylation

A) The activity of 295 protein kinases was tested against a PRMT5 C-terminal peptide. These assays were based on the direct quantification of radiolabeled phosphate transferred from ATP (gamma-33P) to the peptide substrate. *In vitro* kinase activity was ranked as excellent (over 300 cpm), good (299-250 cpm), low (249-100 cpm), and non-phosphorylated (under 99 cpm).

B) The 18 most active kinases (excellent and good ranking) were used to validate the initial *in vitro* phosphorylation screen using PRMT5 WT and T634A C-terminal peptides as substrates. Kinase assays were performed by Kinexus.

previously identified kinases (**Figure 12B**). This assay confirmed that the T634 of PRMT5 can be phosphorylated not only by Akt, but also by calcium/calmodulin-dependent protein kinase II (CAMK2), ribosomal S6 kinase (RSK) and by serum/glucocorticoid regulated kinase (SGK) family members.

To confirm and extend the results of our *in vitro* kinase experiments, we determined whether PRMT5 is phosphorylated in cells. We studied PRMT5 phosphorylation using agents capable of increasing kinase activity. To test the involvement of PKA, we used forskolin, which increases intracellular cAMP, thus activating PKA (Kocinsky et al, 2007). CaMKII activity was stimulated with angiotensin II, which induces the elevation of calcium, to activate CaMKII (Costa-Pessoa et al, 2013). Since SGKs are regulated by glucocorticoid, dexamethasone (a synthetic glucocorticoid compound) was used to assess PRMT5 C-terminal phosphorylation induced by SGK kinases.

Preliminary experiments indicated that AKT strongly phosphorylates PRMT5, therefore we compared the levels of PRMT5 phosphorylation when induced by AKT, PKA, CamKII and SGK. As expected, overexpression of constitutively active AKT induced PRMT5 phosphorylation in the WT but not in GFP-PRMT5^{T634A} construct. Additionally SGK activation induced an increase of threonine phosphorylation at the C-terminus of PRMT5 (**Figure 13**).

4.3.2. PRMT5 interacts with PDZ domains and 14-3-3 proteins

Phosphorylation of serine and threonine residues generates docking sites for a number of proteins including 14-3-3 proteins. 14-3-3 proteins binding sites share several common features with optimal AKT phosphorylation sites, hence many Akt substrates are 14-3-3 ligands (Smith et al, 2011). Given that PRMT5 contains a 14-3-3 consensus binding motif at its C-terminus (**Figure 14A and 14B**), which overlaps with an AKT phosphorylation sites, we wanted to study the interaction of PRMT5 with 14-3-3 proteins and whether phosphorylation by Akt might affect those interactions. Notably, the 14-3-3 consensus binding site is nested within a PDZ

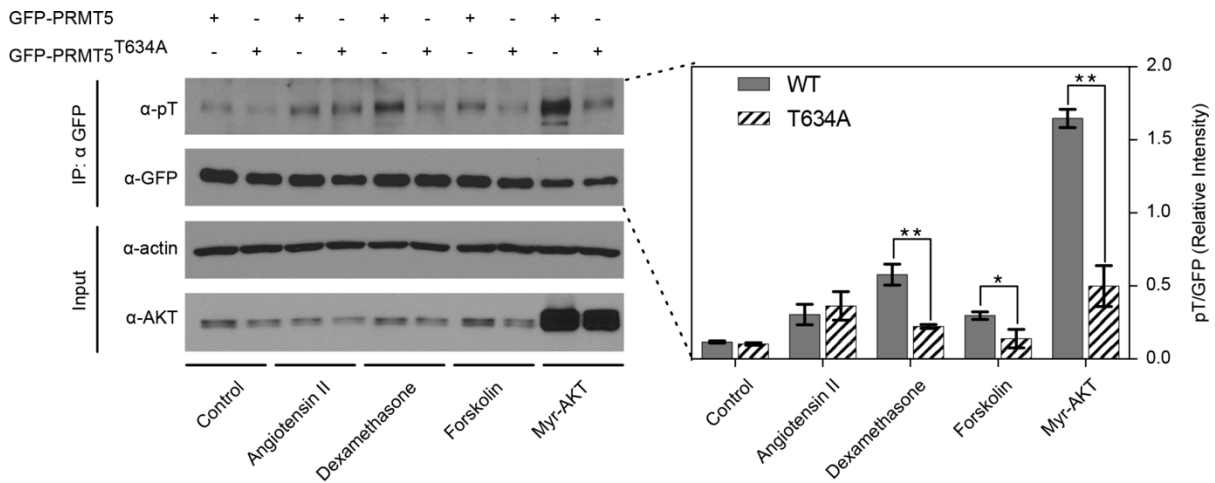


Figure 13: AKT and SGK regulate PRMT5 phosphorylation

SK-CO15 cells were transfected with GFP-PRMT5 WT or the point mutant GFP-PRMT5 T634A. Cells were exposed to the indicated agents to induce specific kinases; angiotensin II (induces the elevation of calcium activating CaMKII); dexamethasone, a synthetic glucocorticoid compound (glucocorticoid regulates SGK); forskolin (increases intracellular cAMP, activating PKA); and overexpression of constitutively active AKT. Samples were immunoprecipitated with anti-GFP antibody followed by western blotting using anti-pT and anti-GFP antibodies. The input samples were probed with anti-AKT. β -actin was used as a loading control. The bar graph represents the normalized ratio of phosphorylated GFP-PRMT5 (anti-pT) and total GFP-PRMT5 (anti-GFP). Quantification was performed by densitometry of the top two panels and a duplicate experiment. Three independent measurements were taken for each band from the two different blots. S.D. is denoted by error bars, * $P < 0.01$ and ** $P < 0.001$, generated by an unpaired Student's t test.

A

BINDING MOTIFS	
PDZ	14-3-3
X[S/T]X ϕ -COOH Motif I	RSX p SXP Motif I
X ϕ X ϕ -COOH Motif II	RX[Y/F]X p SXP Motif II
XEDX ϕ -COOH Motif III	RXX[p S/ p T]XX-COOH Motif III

B

PROTEINS	PDZ / 14-3-3 MOTIF
PRMT5	634 ...PTGRSY p TIGL-COOH
E6 (HPV16)	156 ...SSRTRRE p TQL-COOH
ERBB4	1306* ...PPYRHRN p TVV-COOH
PGHS2	602* ...VLIKRRS p TEL-COOH
IRK1	425 ...PRPLRRE p SEI-COOH

Figure 14: The PDZ domain and 14-3-3 proteins share a common binding motif

A) A comparison of 14-3-3 and PDZ domain binding motifs. The consensus binding sequences of PDZ motif I and the distal C-terminal motif III of 14-3-3 are highly similar, differing only in the phosphorylation-dependent characteristic of 14-3-3 binding. Single-letter amino acid code or symbols are shown, where X is any residue, ϕ is a hydrophobic residue and *p* represents a phosphorylated residue.

B) Proteins harboring PDZ and 14-3-3 binding motifs. Schematic diagram of predicted (*) phosphorylation sites (ERBB4 & PGHS2) and reported phosphorylation sites (PRMT5, IRK1 & E6). Predictions were performed using iGPS1.0 software.

domain binding site, which differs only in the phosphorylation status of the serine or threonine present in the motif, leading us to hypothesize that phosphorylation of PRMT5 T634 would steer the interaction towards 14-3-3 proteins at the expense of PDZ domain proteins.

To explore our hypothesis, we generated phosphorylated and unphosphorylated peptides corresponding to the C-terminus of PRMT5 harboring the threonine 634 site, and used protein microarray technology to investigate whether the association between PDZ domain/14-3-3 proteins and the C-terminus of PRMT5 is mediated by phosphorylation. To do this, we developed a customized microarray consisting of more than 70 purified GST-tagged PDZ domains and all seven 14-3-3 isoforms (**Figure 15**) (Appendix B). The GST-PDZ microarray content was selected based on the functional analysis performed by the MacBeath group (Stiffler et al, 2007).

As predicted, the phosphorylated peptide (but not the unphosphorylated peptide) bound 14-3-3 proteins (α , γ , ϵ , and ζ). In contrast, the unphosphorylated peptide bound a selected group of PDZ domains (GRIP1, MPP7, PDZ-LIM5, NHERF1 FL, NHERF2 FL, SCRIB1 and PDZ-LIM2), whereas the phospho-peptide only showed interaction with PDZ-LIM2 (**Figure 16A and B**).

It was recently reported that the C-terminus of the human papillomavirus E6 oncoprotein undergoes PDZ/14-3-3 interaction switching in a phospho-dependent manner (Boon & Banks, 2013). Our results indicate that PRMT5 can switch between PDZ and 14-3-3 binding modes in a similar phospho-dependent fashion. This prompted us to hypothesize that this signaling paradigm may occur in other mammalian proteins. To explore this idea using other proteins with predicted overlapping Akt phosphorylation sites and 14-3-3/PDZ binding sites, we used Scansite and NetPhorest. We selected three such proteins: 1) the receptor tyrosine kinase ERBB4, 2) the inward rectifier potassium channel IRK1 (Kir2.1), and 3) the prostaglandin-endoperoxide synthase PGHS-2 (COX2) (**Figure 164B**).

Using the protein domain microarray platform, we tested peptide sets from these three candidate proteins together with E6 as control and observed that they all undergo PDZ/14-3-3 switching (**Figure 16A and B**). This finding suggests that this

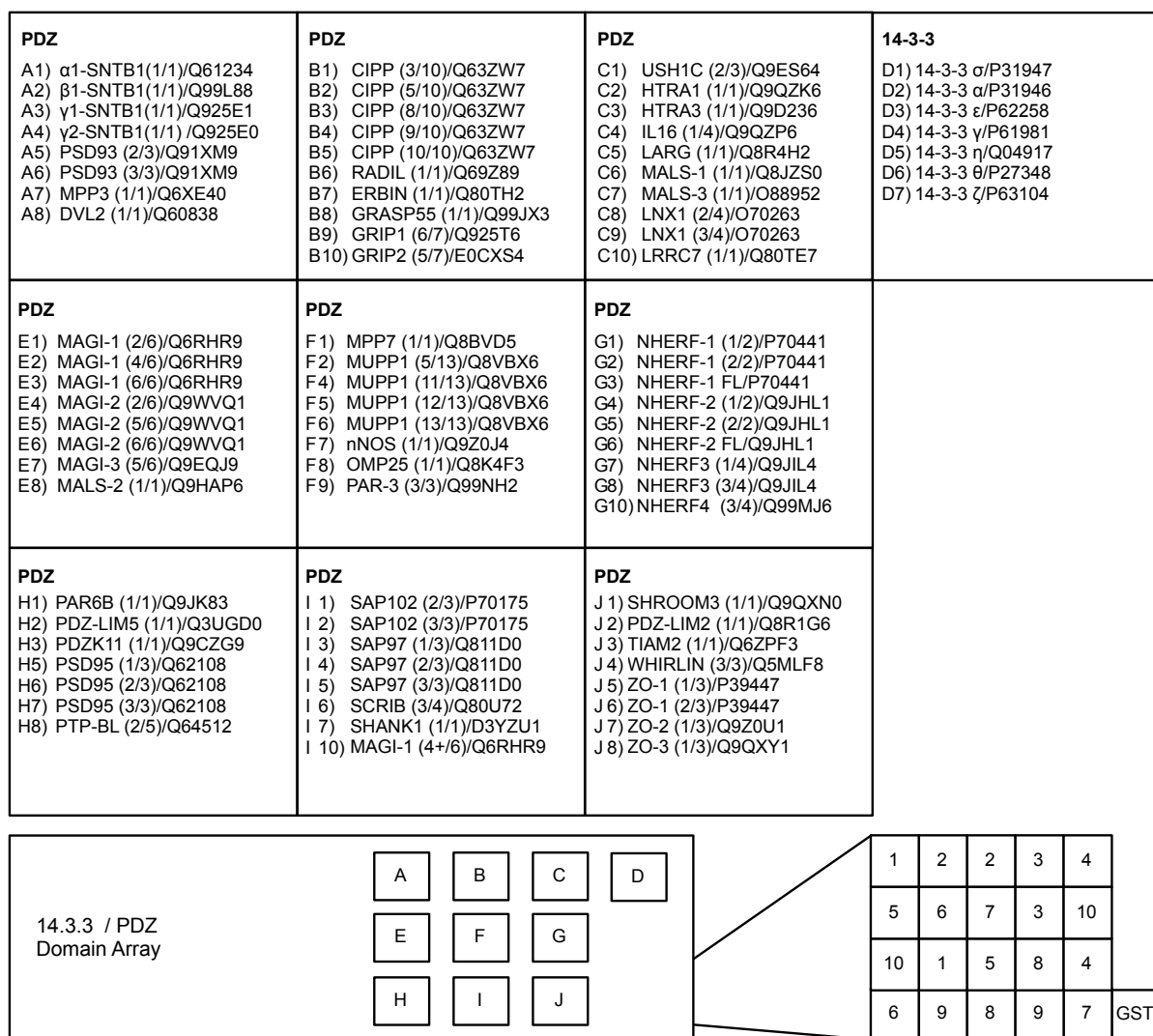


Figure 15: Map of PDZ/14-3-3 protein Array

The protein domain microarray consisting of GST-fusion proteins of all 14-3-3 isoforms, and 76 PDZ domains. Each GST fusion protein was arrayed in duplicate, at a different angle to facilitate the identification of the spots. Within each block, unfused GST protein was used as negative control.

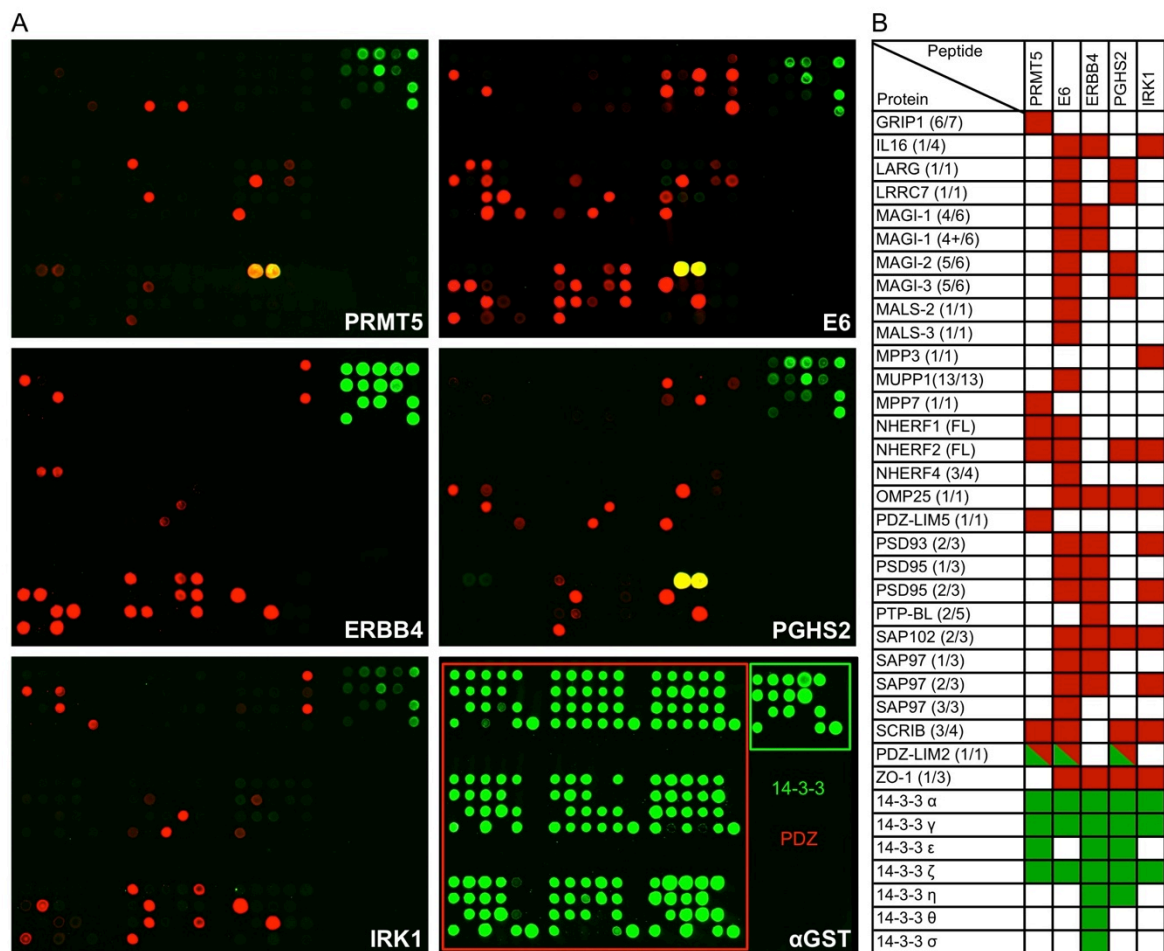


Figure 16: C-terminal pT634 triggers a binding switch between 14-3-3 and PDZ

(A) Phosphorylated and unphosphorylated PRMT5, ERBB4, E6 (HPV16), PGHS2 and IRK1 peptides were labeled with Cy5 (red) and Cy3 (green), respectively, and probed on a protein microarray containing 14-3-3 and PDZ domains. Bottom right panel shows the array probed with α -GST as a loading control. The position of the PDZ domains (red block) and 14-3-3 (green block) proteins are indicated. A complete list of protein is displayed in Figure 15.

(B) Graphical depiction of the interactions observed in (A). Red and green squares indicate interactions with unphosphorylated and phosphorylated peptides, respectively. (Experiments were performed by Karynne Black in Dr. Bedford's laboratory).

signaling paradigm may be a broad mechanism used by biological systems to modulate protein-protein interactions, and that it is not limited to viral proteins like E6.

Following this screening step, we confirmed these interactions using peptide pull-down assays with the seven GST-PDZs identified in the protein microarrays, using GST as a negative control (**Figure 17**). The results of the peptide pull-down experiment confirmed the direct interaction of the unphosphorylated PRMT5 peptide with the GST-PDZ proteins and also allowed the detection of the relative strength of the peptide-protein interaction (**Figure 17 – bottom panel**). This result indicates that the stronger interaction occurs with GST fused to full-length NHERF2, which harbors two PDZ domains (**Figure 17**).

4.3.3. Endogenous PRMT5 interacts with 14-3-3 proteins and the NHERF2 PDZ domain.

As mentioned earlier, the presence of tandem PDZ repeats in proteins is a common feature of PDZ containing-proteins, facilitating the formation of protein complexes. NHERF2 contains two PDZ domains; therefore we speculated that one would interact with PRMT5, while the other would bind to another protein, thus creating a complex. To investigate which of the NHERF2 PDZ domains interacted with the PRMT5 C-terminal peptide and to confirm the PDZ/14-3-3 phospho-switch, we performed a peptide pull-down assay with the proteins described in Figure 16A. Given that NHERF2 mouse and human orthologs share an 86% identity, we wanted to validate this interaction using human proteins. Therefore we generated NHERF2 constructs encoding individual PDZ domains as well as the full-length human NHERF2 protein (**Figure 18A**). This analysis revealed that the PRMT5-NHERF2 interaction occurs via the first PDZ domain, but that the interaction is stronger with the GST-NHERF2 full-length proteins, suggesting that other parts of the proteins contribute to binding. In contrast, phosphorylation of the PRMT5 peptide prevented

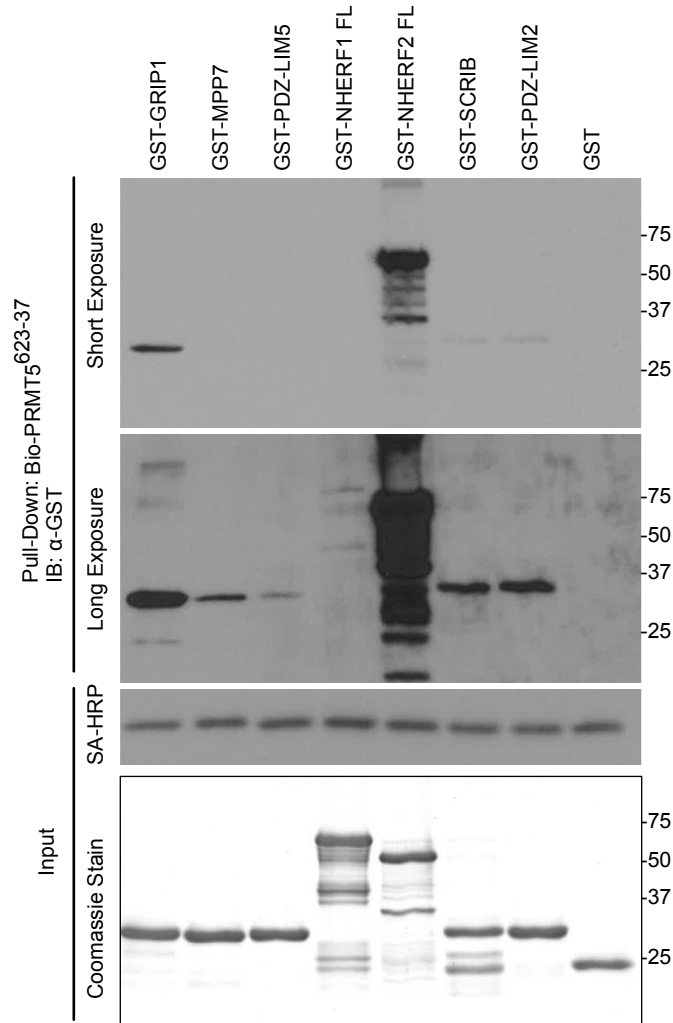


Figure 17: PRMT5 peptide pull-down assays

GST-fused PDZ domains of GRIP1 (672-754), MPP7 (139-220), PDZ-LIM5 (2-85), NHERF1 FL (1-355), NHERF2 FL (1-337), SCRIB1 (714-801), PDZ-LIM2 (1-84) and GST were incubated with biotinylated PRMT5 unphosphorylated peptide. Bound proteins were detected by western blot with anti-GST antibody (short and long exposure are shown). Peptide loading was assessed by western blot with HRP-conjugated streptavidin. Relative GST-fused PDZ domain quantities were analyzed by Coomassie stain.

NHERF2 binding, but enable 14-3-3 ϵ binding (**Figure 18B**). This data supports the phospho-switch paradigm we first observed in our microarray experiments.

To determine whether interactions between endogenous PRMT5 and NHERF2 or 14-3-3 ϵ could be detected in cells, we performed GST pull-downs with NHERF2 and 14-3-3 ϵ from lysates of HeLa cells cultured in the presence or absence of the phosphatase inhibitor, calyculin A. Under hypophosphorylated conditions, endogenous PRMT5 interacted with NHERF2, but in calyculin A-treated cells, it interacted with the 14-3-3 ϵ protein (**Figure 18C**). PRMT5 knockdown cells were used as a control to confirm that the bands we see by western analysis correspond to the PRMT5 protein.

To confirm that the NHERF2 and 14-3-3 ϵ interactions observed by GST Pull-down were driven by direct binding with the C-terminal region of PRMT5, we performed a similar experiment using full-length myc-tagged PRMT5 WT, and two different Myc-PRMT5 C-terminus mutants: one with a deletion of the last 6 residues of PRMT5 (Δ), and the other with a single amino acid change (T634A).

It is important to note that PRMT5 homodimerizes (Stopa et al, 2015), and to reduce the influence of the myc-tagged PRMT5 proteins interacting with endogenous PRMT5, we performed these experiments in PRMT5 shRNA knock-down HeLa cells, using shRNA resistant expression vectors. These experiments demonstrated that the hyperphosphorylation induced by calyculin A treatment is required for the 14-3-3 interaction and inhibits the NHERF2 interaction with PRMT5 (**Figure 18D**). Additionally, the intact C-terminus is necessary as either truncation or the substitution of a single amino acid resulted in the total loss of both NHERF2 and 14-3-3 binding (**Figure 18D**).

4.3.4. The C-terminus of PRMT5 facilitates its plasma membrane association.

The majority of PDZ domain containing proteins are associated with the plasma membrane, where they function as scaffolding for membrane proteins such as receptors and ion channels (Ivarsson, 2012). That is the case for six of the seven

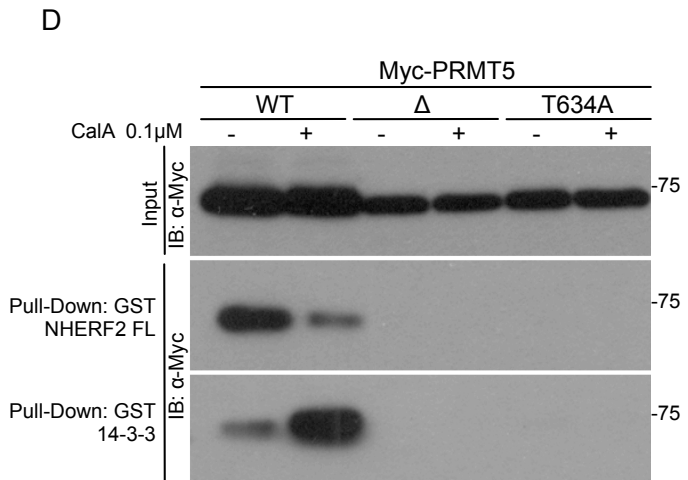
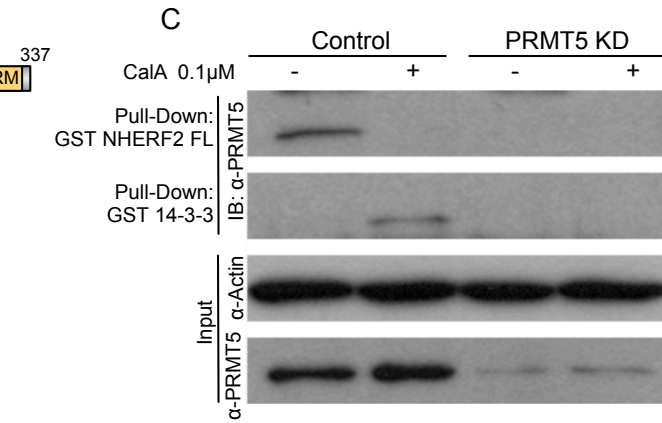
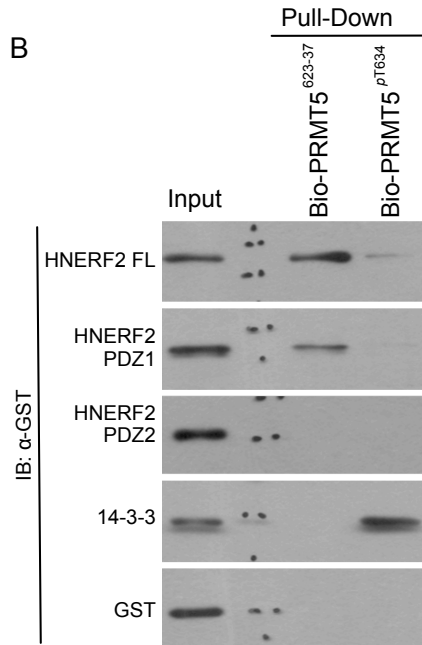
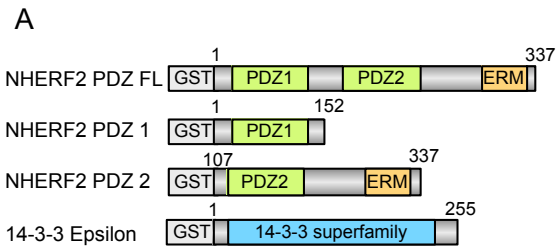


Figure 18: PRMT5 interacts with NHERF2 and 14-3-3

A) Schematic representation of the constructs used for peptide pull-down.

B) PRMT5 interacts with the first PDZ domain of NHERF2. Purified recombinant GST, GST-tagged full-length NHERF2, PDZ1 (amino acids 1 to 152 NHERF2-PDZ 1), PDZ2 (amino acids 107 to 337 NHERF2-PDZ 2) and 14-3-3 ϵ were incubated with biotinylated unphosphorylated PRMT5 peptide bound to streptavidin–agarose beads and detected by anti-GST immunoblot. The C-terminal peptide of PRMT5 interacted with GST-fusion proteins containing the full-length or with only the first PDZ domain of NHERF2, indicating that the interaction between PRMT5 and NHERF2 requires the first PDZ domain. The left lane shows the GST fusion protein inputs.

C) Endogenous PRMT5 proteins are pulled-down by GST_14-3-3 and GST_PDZ proteins in the presence or absence of phosphatase inhibitors. GST pull-downs were carried out to validate protein microarray findings. Wild-type and knock-down PRMT5 HeLa cells were treated with and without calyculin A. GST pull-down confirmed the interaction observed in the microarray system.

D) GST-pull-down of myc-PRMT5 proteins. GST-Pull-down of myc-PRMT5 from HeLa cells. shRNA PRMT5 (KD4) transiently transfected with sh4 resistant Myc-PRMT5 WT, Δ (6 amino acid deletion of the C-terminus) and mutant T634A.

PDZ domain proteins that interacted with the C-terminal region of PRMT5, including the strong binder NHERF2. Interestingly, a number of membrane associated proteins are symmetrically methylated by PRMT5 (Beltran-Alvarez et al, 2013; Boisvert et al, 2003; Guo & Bao, 2010; Hsu et al, 2011; Likhite et al, 2015). Hence, we reasoned that the C-terminus of PRMT5 may bring it to the plasma membrane. To explore this idea we performed cell fractionations from the intestinal epithelial cell line SK-CO15, which expresses NHERF2 (Yoo et al, 2012). The results indicate that endogenous PRMT5 is preferentially localized in the cytoplasm, but a portion of PRMT5 is clearly distinguishable in the membrane fraction (**Figure 19A**).

Whilst the above results indicate that PRMT5 associates with the plasma membrane, it does not indicate whether this process is mediated by the C-terminal motif. To address this issue, cell fractionation were performed using full-length myc-PRMT5 and the C-terminal deletion mutant (PRMT5^Δ) transfected into SK-CO15 cells. This approach revealed a dramatic reduction of the myc-PRMT5^Δ present in the membrane fraction (**Figure 19B**) relative to myc-PRMT5, which remained associated with the membrane. This result confirmed that PRMT5 is membrane associated, and it requires its C-terminus for this sub-cellular localization.

4.3.5. PRMT5 symmetrically methylates membrane-associated proteins.

PRMT5 symmetrically methylates membrane proteins such as EGF receptor, Nav.1.5 and srGAP2, GPCRs, and dopamine receptor D2, (Beltran-Alvarez et al, 2013; Boisvert et al, 2003; Guo & Bao, 2010; Hsu et al, 2011; Likhite et al, 2015), as well as membrane associated proteins such as MBP (Branscombe et al, 2001). Additionally, a systematic characterization of arginine-methylated proteins has identified numerous monomethylated receptor and membrane proteins in mouse brain that play an important role in synaptic transmission (Guo et al, 2014). Because PRMT5 is able to catalyze the symmetric dimethylation and monomethylation of arginine residues, (Branscombe et al, 2001), it may contribute to the methylation of proteins involved in synaptic transmission. Because NHERF2 is highly expressed in the apical portion of the plasma membrane of polarized epithelial cells, we wanted to

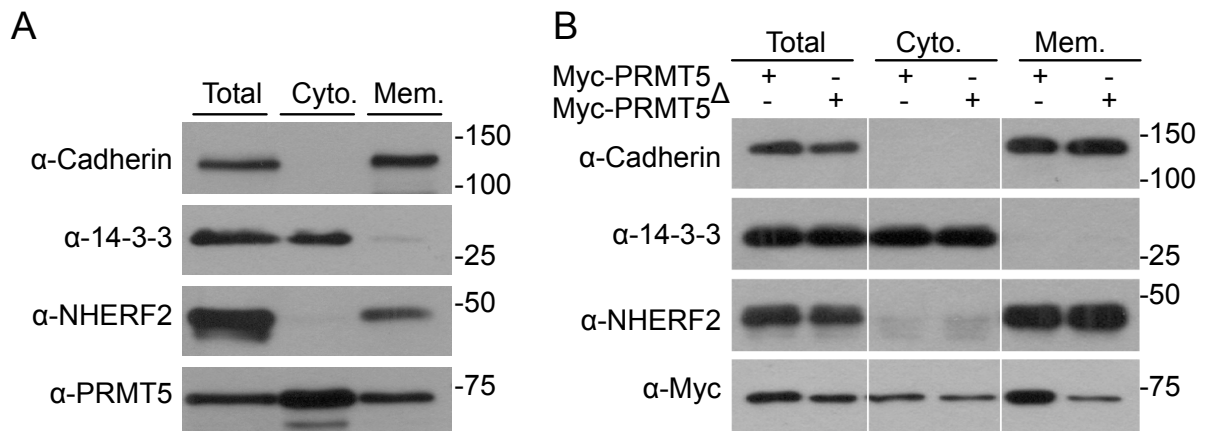


Figure 19: PRMT5 associates with membrane via its PDZ recognition motif

A) PRMT5 is a membrane-associated protein. Human intestinal epithelial cell line SK-CO15 expresses high levels of NHERF2. Cellular membranes were fractionated by ultracentrifugation. Fractions were immunoblotted with antibodies against PRMT5, members of the cadherin family as integral membrane markers, NHERF2, which is membrane associated, and 14-3-3 as cytosolic protein marker.

B) The C-terminus of PRMT5 positions it at the plasma membrane. Myc-tagged PRMT5 and PRMT5 Δ were transiently transfected into SK-CO15 cells. Myc-tagged PRMT5 is present in the membrane fraction, while the mutant construct lacking the last 6 amino acids, myc-PRMT5 Δ , has its membrane localization impaired. The low levels of Myc-PRMT5 Delta protein observed at the membrane fraction could be a result of homodimerization with endogenous PRMT5. Fractionation was tested with the indicated antibodies. Anti-pan 14-3-3 and anti-pan cadherin antibodies are shown as quality controls for cytoplasmic and membrane fractions, respectively.

investigate whether PRMT5 symmetrically methylates membrane-associated proteins in these types of cells. To explore this idea, we generated stable SK-CO15 PRMT5 knockdown (SK-CO15 PRMT5-KD) cells using shRNA and repeated the cell fractionations as described above. Levels of PRMT5 are significantly reduced in SK-CO15 PRMT5-KD cell lines (**Figure 20, top panel**). To assess the effects of PRMT5 depletion on symmetric dimethylarginine content on membranes, cell fractions were probed with a pan antibody that specifically binds to symmetrically methylated arginine residues. This result showed that symmetric methylation is present in the membrane fraction; moreover, some proteins are only enriched in the membrane but not cytoplasmic or total cell fractions (**Figure 20**). Depletion of PRMT5 clearly decreases the level of methylation of these proteins, indicating that they are substrates of PRMT5.

4.3.6. Physiological importance of PRMT5-complexes relies on its C-terminus

Na⁺/H⁺ exchanger regulatory factor 2 (NHERF2) plays an important role in linking Na⁺/H⁺ exchanger 3 (NHE3) to the cytoskeleton. NHE3 accounts for most Na⁺ absorption and pH homeostasis in the renal and intestinal epithelia. NHEs are membrane transporters that mediate the simultaneous efflux of hydrogen ions and influx of sodium ions across the plasma membrane to regulate intracellular pH and cell volume. Hence, NHE3 function is highly regulated and can be modulated by its interaction with multiple regulatory proteins and by post-translational modifications, particularly phosphorylation (Alexander & Grinstein, 2009). The second PDZ domain of NHERF2 interacts with NHE3 (Park et al, 2005), and we have demonstrated that the first PDZ domain of NHERF2 binds to PRMT5. Therefore, PRMT5 may be recruited to an NHE3-associated complex.

To determine the physiological importance of membrane-associated PRMT5, we tested the ability of PRMT5 to affect the intracellular pH (pHi) of SK-CO15 intestinal epithelial cells. To evaluate the activity of the Na⁺/H⁺ exchange system, we tested SK-CO15 control and PRMT5 KD cells using the fluorescent probe 2',7'-bis-(2-carboxyethyl)-5-(and-6)-carboxyfluorescein BCECF-AM (Invitrogen) that can

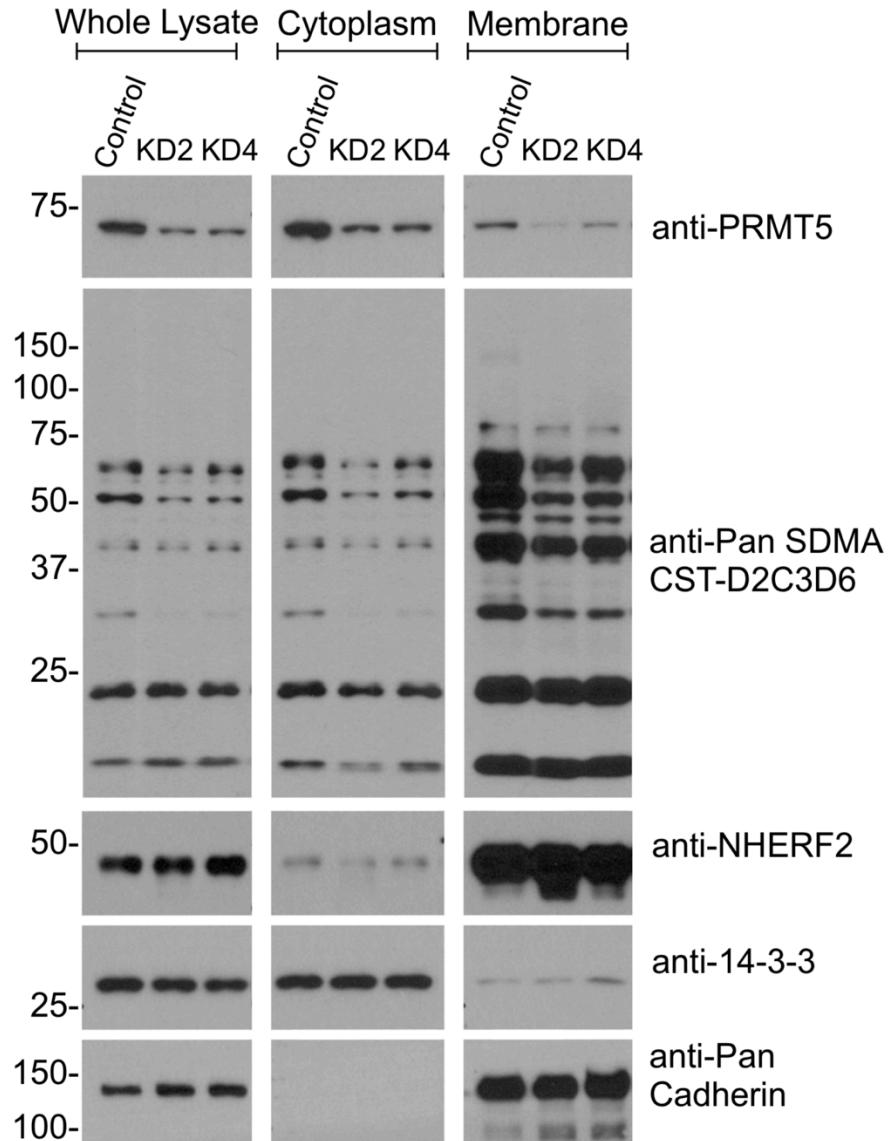


Figure 20: Subcellular localization of SDMA proteins

Whole-cell extracts, cytoplasm and membrane were fractionated by ultracentrifugation. Fractions from SK-CO15 control and knocked down PRMT5 cells were assessed using a pan-SDMA antibody. The antibodies against PRMT5, NHERF2, pan-14-3-3 and pan-Cadherin were used to demonstrate the compartmentalization of different proteins with the cellular fractions.

be used to monitor changes in pHi. PRMT5 KD cells displayed lower fluorescence than SK-CO15 control cells, indicating a more acidic pHi. As expected, cells treated with the PRMT5 inhibitor EPZ01566 also displayed a lower fluorescence (**Figure 21A**).

The Na⁺/H⁺ exchange activity of NHE3 is determined by the rate of pH recovery after the addition of NH₄Cl, which causes intracellular acidification of BCECF-loaded SK-CO15 cells, and its recovery depends on the Na⁺ influx regulated by NHEs. After acidification induced by NH₄Cl, the rise of the pHi indicates an increase in Na⁺ influx across the membrane (**Figure 21B**). This influx can be inhibited in both PRMT5 deficient cells and cells treated with PRMT5 inhibitor, indicating that PRMT5 regulates, in part, the activity of NHE3.

To evaluate the specific contribution of the PRMT5-NHERF2 complex to pHi, myc-tagged PRMT5 and PRMT5^{T634A} constructs were stably transfected into SK-CO15 PRMT5 KD cells. Expression of myc-tagged PRMT5 effectively increased the pHi of SK-CO15 PRMT5 KD cells. Notably, expression of Myc-PRMT5^{T634A} failed to rescue the pHi. This data further supports the idea that PRMT5 may have multiple roles at the plasma membrane (**Figure 21C**).

To determine whether the intrinsic methyltransferase activity of Myc-PRMT5 is altered by mutation of the T634 site, we evaluated the SDMA levels on total cell lysates from SK-CO15 PRMT5 KD cells rescued with either Myc-PRMT5 or Myc-PRMT5^{T634A}. We observed no differences in the levels of symmetric dimethylarginine in cells rescued with either Myc-PRMT5 or Myc-PRMT5^{T634A} (**Figure 22**), indicating that the activity of both myc-PRMT5 forms is comparable. It is important to note that the interaction of PRMT5 with NHERF2 does not exclude MEP-50 from the complex, since MEP50 is also detected by a pull-down with GST-NHERF2 (**Figure 23**).

Additionally, the subcellular localization of myc-tagged PRMT5 and Myc-PRMT5^{T634A}, as examined by immunofluorescence microscopy were indistinguishable. Further, PRMT5 membrane localization was not observed, probably because its was masked by the predominant cytosolic localization of PRMT5 (**Figure 24**).

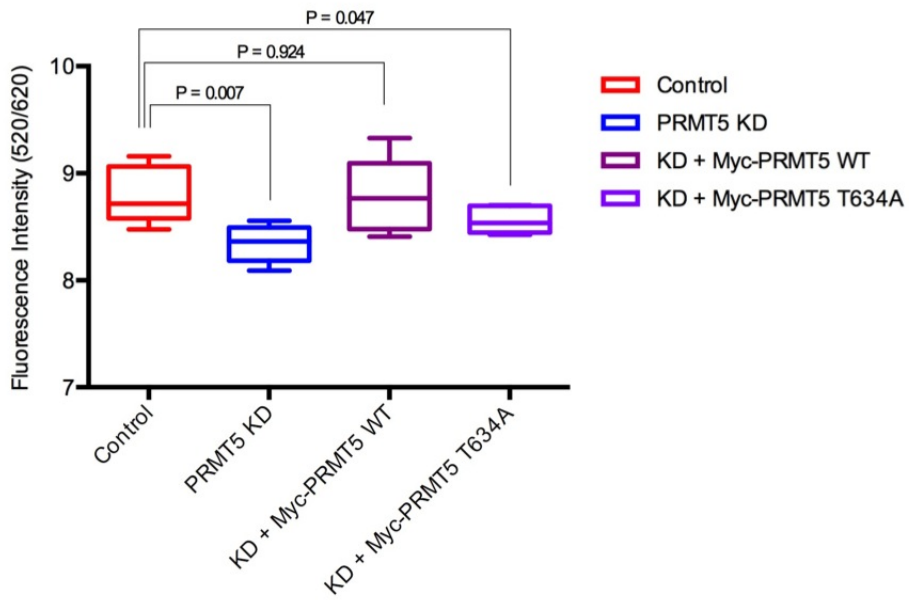
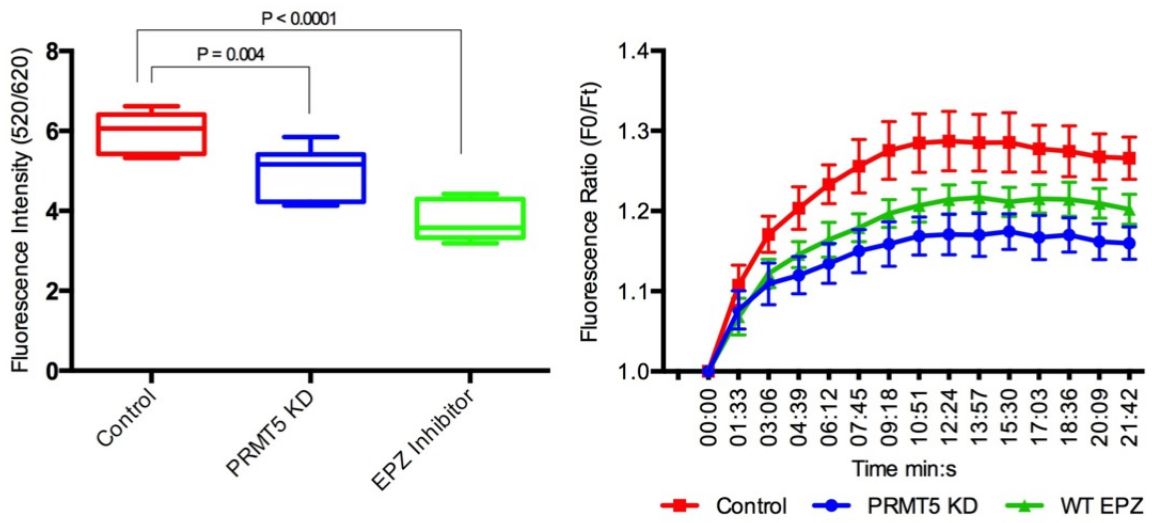


Figure 21: A role for PRMT5 in regulating intracellular pH

A) Intracellular pH was measured using the pH-sensitive dye BCECF-AM. The fluorescence of control SK-CO15 cells, PRMT5-KD cells or cells treated with 5 μ M of PRMT5 inhibitor EPZ015666 for 48 h. pHi is determined by obtaining the ratio of fluorescence emission at 520 and 620 nm excited at 488 nm. The box plot represents the mean \pm standard deviation (SD) of the ratio of fluorescence among the different cell lines. The p-values are indicated, $p < 0.05$ indicates significant differences between two groups. 520/620 nm fluorescence emission ratios excited at 488 nm.

B) Na⁺/H⁺ exchange activity in SK-CO15 cells was determined by measuring the rate of Na-dependent pH recovery after acid loading induced by 30 mM NH₄Cl.

C) SK-CO15 PRMT5-KD cells were transfected with either Myc-PRMT5 or Myc-PRMT5^{T634A}, and selected with hygromycin to obtain stably transfected cell lines. Expression of Myc-PRMT5^{T634A} in SK-CO15 PRMT5-KD cells resulted in a reduction in pHi, while the introduction of Myc-PRMT5 rescued the steady-state pHi observed in control SK-CO15 cells. pHi was measured as in A.

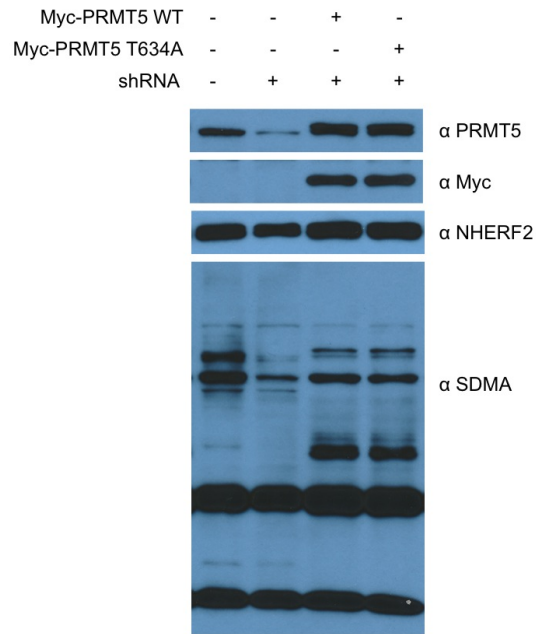


Figure 22: SK-CO15 PRMT5-KD rescued characterization

SK-CO15 PRMT5 KD cells were transfected with shRNA-resistant constructs for Myc-PRMT5 WT or Myc-PRMT5 T634A and stable cell lines were generated. Cell lysates from SK-CO15 control, KD and rescued lines were characterized by western blotting followed by incubation with anti-PRMT5, anti-myc and anti-NHERF2 antibodies. The activity of the myc-PRMT5 constructs was evaluated with pan anti-SDMA antibody.

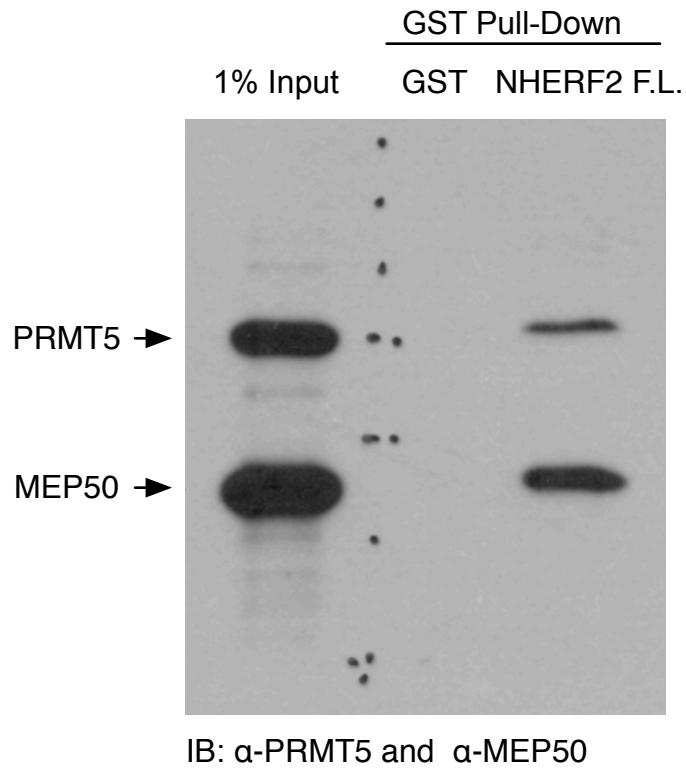
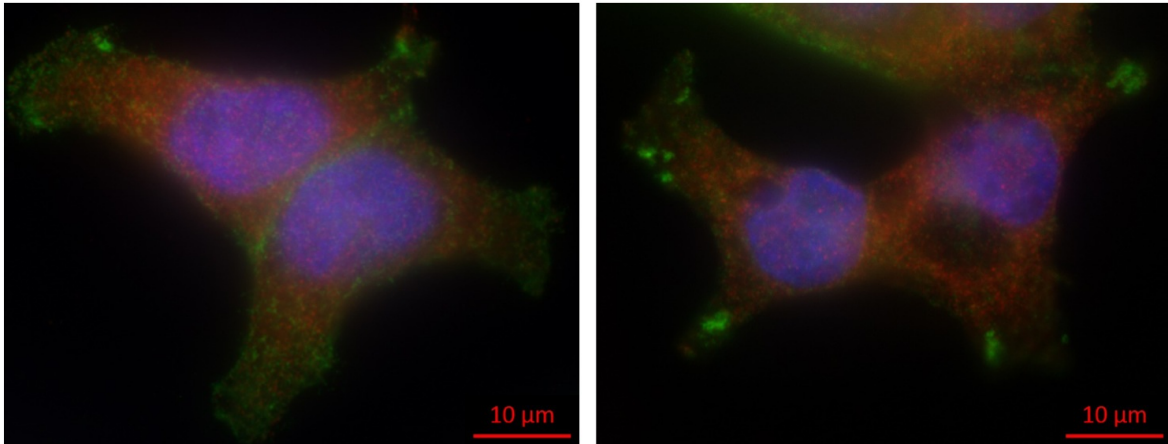


Figure 23: NHERF2 associates with the PRMT5-MEP50 complex

Purified full length NHERF2 FL fused to GST and GST alone were incubated with SK-CO15 lysates. GST-NHERF2 FL, but not GST alone, was able to interact with endogenous PRMT5 and MEP50.



Red: Myc-PRMT5 WT
Green: NHERF2
Blue: Dapi

Red: Myc-PRMT5 T634A
Green: NHERF2
Blue: Dapi

Figure 24: Myc-PRMT5 WT and Myc-PRMT5^{T634A} cellular localization

SK-CO15 PRMT5-KD cells stably transfected with either Myc-PRMT5 WT or Myc-PRMT5 T634A were fixed and stained with anti-Myc (red), and anti-NHERF2 (green) antibodies, DAPI was used for nuclear localization (blue).

4.3.7. The C-terminal motif of PRMT5 is required for mouse viability

To evaluate the biological function of the C-terminus of PRMT5 *in vivo*, we used CRISPR/Cas9 to generate a mouse model in which we replaced the last 6 amino acids of PRMT5 with an HA tag (PRMT5^{Δ+HA}). A guide RNA was generated by Sage laboratories and injected in a one-cell embryo together with a donor sequence that encoded PRMT5^{Δ+HA}. Two founders for PRMT5^{Δ+HA} knock-in mice (#2 & #6) that had the expected insertion of a HA-tag and the concomitant removal of the last 6 residues of PRMT5 were obtained (**Figure 25A**). Two additional founders (#8 & #10) had distinct C-termini due to the presence of indels that generated frameshifts (**Figure 25A**). PRMT5^{Δ+HA} lines #6 & #10 were bred to homozygosity, but of 71 E9.5 and E11.5 embryos analyzed, none were PRMT5^{Δ+HA} homozygotes. This indicates that an intact PRMT5 C-terminus is required for mouse viability, given that the HA-tagged truncated protein is expressed in heterozygotes (**Figure 25B**).

Analysis of heterozygous embryos demonstrated not only that the PRMT5^{Δ+HA} protein is expressed, but also that the total levels of PRMT5 and MEP50 are similar between heterozygous PRMT5^{Δ+HA} and wild-type littermates (**Figure 25B**). This is important because MEP50 is PRMT5 main co-activator for methylation. Further, the levels of H2AR3me2s are identical, but the total levels of symmetric methylation, examined using a pan-SDMA antibody, are different between heterozygous PRMT5^{Δ+HA} and wild-type littermates, suggesting that a subset of proteins is not methylated efficiently in the heterozygous PRMT5^{Δ+HA} embryos (**Figure 25B**). Neither heterozygous adults (data not shown) nor E11.5 embryos displayed an obvious phenotype (**Figure 25C**).

To overcome the limits of our homozygous PRMT5^{Δ+HA} mouse model, we attempted to develop homozygous PRMT5^{Δ+HA} ES cell lines derived from intercrosses of heterozygous PRMT5^{Δ+HA} mice. We established four wild-type and six heterozygous lines, but no homozygous lines. This suggests that the PDZ/14-3-3 switching motif is required for the derivation of ES cells. The function that depends upon the PRMT5 C-terminus may account for our inability and the inability of other groups to generate PRMT5 null ES cells (Li et al, 2015; Tee et al, 2010).

A

Sequence	Founder #
...SIHNPTGR SYTIGL	WT
...SIHNPTGR GYPYDVPDYA	2 & 6
...SIHNPTG PLLYHWPLALHTVSKPWKQL	8
...S PAHSVKALEAALSSLPTAQKV	10

 WT HA-Tag Additional sequence

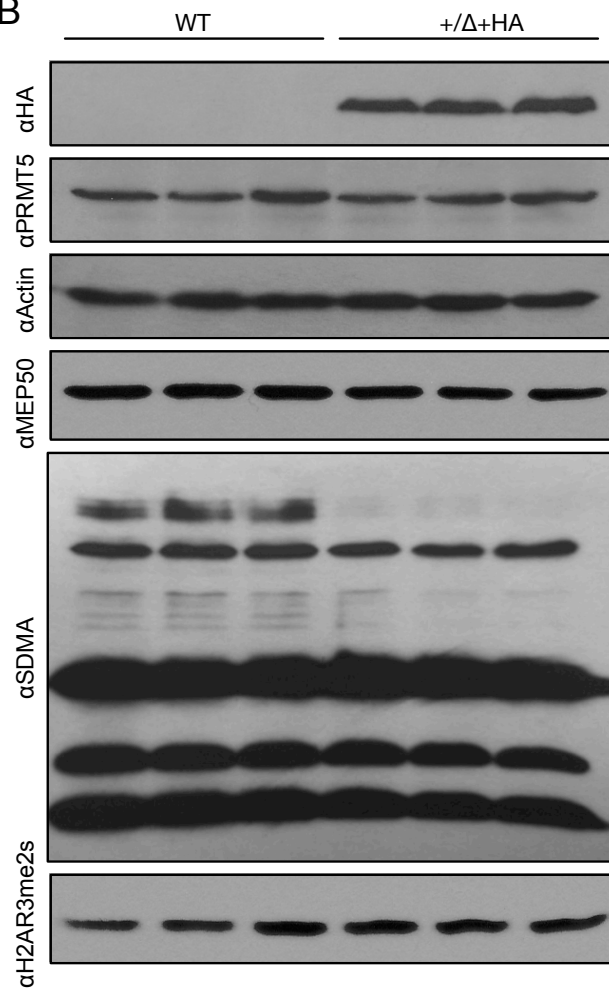
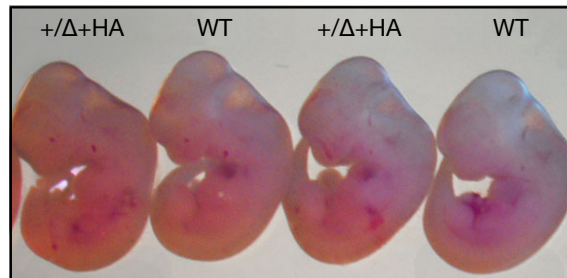
B**C**

Figure 25: PRMT5^{Δ+HA} mouse generated by CRISPR/Cas9

(A) Schematic showing PRMT5 C-terminal sequences of the founder mice. Four founder mice were obtained, #2 & #6 display the expected insertion of HA-tag, while mouse #8 & #10 represent alterations at the C-terminus due to indels, resulting in a shift of reading frame.

(B) Western blot analysis of PRMT5^{Δ+HA} in E11.5 WT and heterozygous embryo lysates using anti-HA, anti-PRMT5, anti-MEP50, anti-SDMA and anti-H2AR3me2s (BL14494 M12-5079) antibodies. β-actin was used as a loading control.

(C) WT and heterozygous PRMT5^{Δ+HA} embryos at E11.5 show no obvious phenotype.

4.3.8. Discussion

PRMT5 by itself is catalytically inactive, as shown by its failure to methylate its preferred substrates when recombinant PRMT5 is expressed in bacteria. Yet, PRMT5 immunoprecipitated from either mammalian or insect cells is catalytically active in *in vitro* methylation assays, implying that PRMT5 activity depends upon the formation of protein complexes and/or post translational modifications in eukaryotic cells. As such, understanding the mechanisms that govern the formation of the PRMT5 complex is critical in the field of arginine methylation.

Phospho-dependent protein-protein interactions can regulate PRMT5 enzymatic activity by either serving as a platform for different binding partners, thus dictating substrate recognition, or by blocking the binding sites of PRMT5 co-activators. Indeed, PRMT5 has been shown to be phosphorylated at three tyrosine residues, which alters its binding with MEP50, its main co-activator, consequently reducing PRMT5 enzymatic activity (Liu et al, 2011).

In our current work, we have examined the phosphorylation of PRMT5. Through the use of protein microarrays, we showed that phosphorylation at the C-terminus serves to switch between two binding module interactions, PDZ and 14-3-3. That is, when PRMT5 is unphosphorylated, its interaction with PDZ domain-containing proteins is promoted, but when it is phosphorylated, it dissociates from PDZ domain proteins and preferentially binds 14-3-3 proteins. The 14-3-3/PDZ overlapping binding motif exists in other proteins, suggesting that this binding switch may be a common protein binding paradigm.

We have demonstrated that PRMT5 is phosphorylated by AKT and SGK at the C-terminus, creating a binding motif that controls its interaction with other proteins, including 14-3-3 proteins. Although PRMT5 has been previously identified as a 14-3-3 interacting protein by two independent groups, neither the motif that mediated the interaction nor the kinase that phosphorylated PRMT5 was known. (Jin et al, 2004; Weimann et al, 2013). Our studies provide a guide for future investigations of PRMT5 in the context of its phosphodependent interactions with 14-3-3 proteins.

We have also observed the interaction between PRMT5 and the PDZ domain of NHERF2, which contrary to the interaction with 14-3-3 proteins, is inhibited by phosphorylation. The study of PRMT5 interaction with the PDZ domain of NHERF2 has enabled us to investigate, for the first time, the membrane association of PRMT5. Furthermore, we demonstrate the existence of PRMT5's substrate at the plasma membrane, suggesting that they may play a role in the regulation of membrane associated proteins, such as ion exchangers.

Indeed, NHE3 and CFTR are ion exchangers that play an important role during the normal digestive process, which is regulated by PDZ-containing proteins. In fact, the CFTR Cl⁻ channel is one of the best known ion transport proteins involved in anion secretion, and NHE3 is the predominant Na⁺/H⁺ exchanger for sodium absorption. Both CFTR and NHE3 proteins interact with NHERF2 and other PDZ-containing proteins (Lamprecht & Seidler, 2006). Therefore, we hypothesize that PRMT5 may regulate the function of ion exchangers by engaging protein complexes assembled via NHERF2.

Alteration of the pHi results in response to changes in NHE3-mediated sodium influx. Our studies evaluating pHi clearly demonstrate that in cells lacking PRMT5, the intracellular pH is significantly reduced and its recovery after an acidic load is altered. Additionally, rescue experiments using myc-tagged mutant PRMT5^{T634A} fail to recover the pHi when compared with myc-tagged PRMT5.

Interestingly, NHERF2 has a high affinity for Ezrin, a important protein in cell surface structure (Yang et al, 2015), and this association is regulated through phosphorylation of NHERF2 on serine 303 by SGK. This phosphorylation decreases the affinity between NHERF2 and Ezrin and induces the redistribution of NHERF2 toward the cytosolic compartment (Yang et al, 2015). Thus, simultaneous phosphorylation of NHERF2 and PRMT5 by SGK may be a combined mechanism to prevent the interaction of PRMT5 with NHERF2 in the cytoplasm, thereby promoting the interaction of PRMT5 with 14-3-3 proteins and preventing its re-engagement with PDZ domain-containing proteins.

Finally, we explored whether the C-terminus of PRMT5 is essential for its *in vivo* functions by creating CISPR/Cas9 mice with the last six amino acids replaced

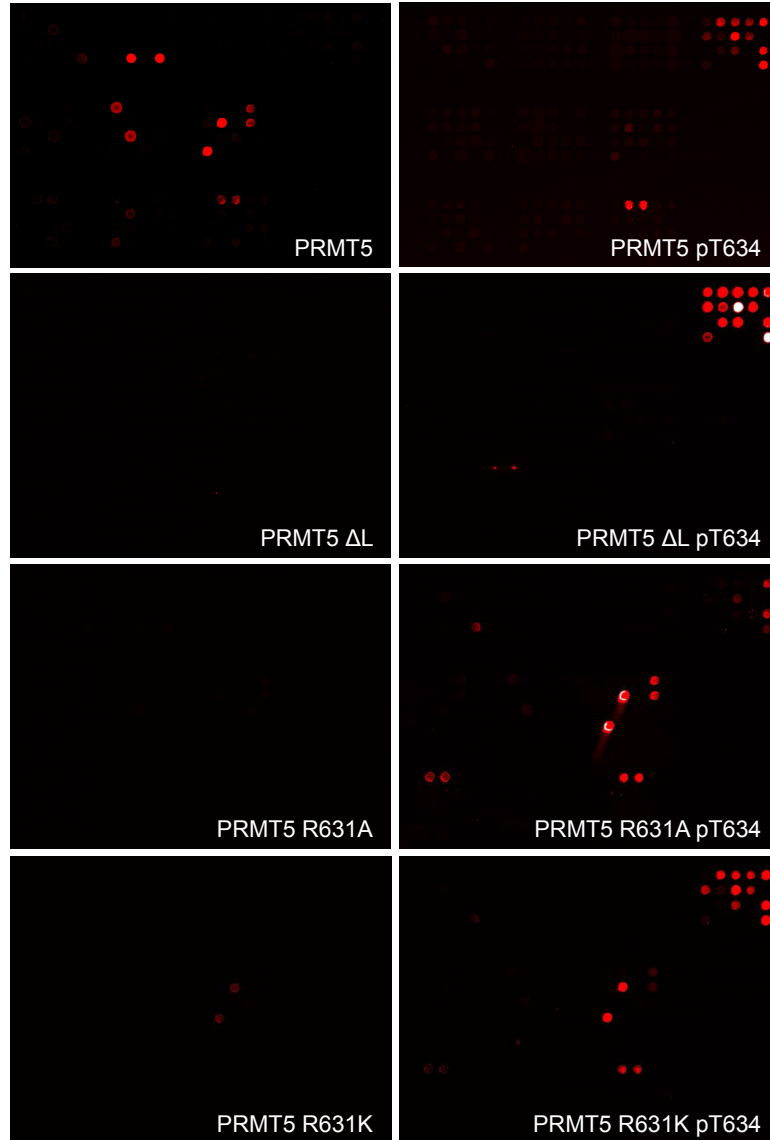
with an HA tag, as well as mice with an altered C-terminus. Both set of mice lacked the critical 14-3-3/PDZ binding motif. We found that the C-terminus of PRMT5 is essential for viability as no homozygous mutants embryos were recovered. Likewise, no homozygous PRMT5^{Δ+HA} ES cell lines could be created. The precise reason for this lethality remains to be explored.

We further investigated the nature of the C-terminal motif of PRMT5 by studying its interaction with 14-3-3 proteins and PDZ domains by utilizing protein microarrays and a number of modified peptides (**Figure 26A**). First we removed the last C-terminal hydrophobic residue required for the interaction with PDZ domains. As expected, this modification blocked the binding of this peptide with PDZ domains and greatly enhances the interaction with 14-3-3 proteins. Because an upstream arginine residue is frequently present in the 14-3-3 motif III (Coblitz et al, 2006; Ganguly et al, 2005), we wanted to investigate whether it is necessary for interaction with 14-3-3 proteins. Mutation of R631 to alanine reduces 14-3-3 interactions, but enhances PDZ interaction with the PRMT5 peptides, whereas mutation of R631 to lysine, thus preserving the positive charge of the residue, slightly reduces the interactions with 14-3-3 and PDZ. Interestingly, the mutation of arginine to alanine or lysine enhances the interaction with PDZ but only when the peptide is phosphorylated (**Figure 26B**). This result was unexpected and further research will be needed to understand the nature of this motif, and will help us to design mouse models that block either 14-3-3 or PDZ binding, but not both. The summary of observed interactions are listed in **Figure 26C**.

A

PRMT5	Biotin-SAIHNPTGRSYTIGL
PRMT5 ΔL	Biotin-SAIHNPTGRSYTIG_
PRMT5 R631K	Biotin-SAIHNPTGKSYTIGL
PRMT5 R632A	Biotin-SAIHNPTGASYTIGL

B



C

Peptide \ Protein	Protein												
	GRIP1	MPP7	NHERF1 FL	NHERF2 FL	PDZ-LIM2	PDZ-LIM5	14-3-3α	14-3-3γ	14-3-3ε	14-3-3ζ	14-3-3η	14-3-3θ	14-3-3σ
PRMT5													
PRMT5 pT634													
PRMT5 ΔL													
PRMT5 ΔL pT634													
PRMT5 R631A													
PRMT5 R631A pT634													
PRMT5 R631K													
PRMT5 R631K pT634													

Figure 26: Mutation in the C-terminus of PRMT5 alters 14-3-3 and PDZ recognition

A) Sequence of peptides. Red residues indicate mutations the underscore indicates a missing residue.

B) 14-3-3/PDZ microarray probed with Cy-5 labeled peptides. Phosphorylated peptides (right) and unphosphorylated peptides (left). List of proteins in Figure 15.

C) Graphical depiction of the interactions observed in (B). Red squares indicate interactions with phosphorylated peptides. (Experiments were performed by Karynne Black in Dr. Bedford's laboratory).

4.4. Future Studies

From our PRMT5^{Δ+HA} mouse model study we can infer that the C-terminus of PRMT5 is vital for its full biological function. However, because the homozygous PRMT5^{Δ+HA} model was embryonic lethal, we could not investigate the precise role of this motif. Therefore, to evaluate the function of the PRMT5 C-terminus in adult tissues displaying an abundance of PDZ domain activity, such as heart, kidney and neurons, we need to generate a conditional knock-in mouse. By crossing our PRMT5^{Δ+HA} mouse with a PRMT5^{flox} mouse, we will generate PRMT5^{Δ+HA/flox} mice, which can then be crossed to a tissue-specific Cre line to obtain tissues that only express the C-terminally truncated form of PRMT5.

For example, by using a Nestin-Cre/PRMT5^{Δ+HA/flox} cross, a conditional knock-in will be generated in neurons, where the PDZ domain plays an important role in neuron function (Kim & Sheng, 2004). The unphosphorylated C-terminus of PRMT5 interacts with the PDZ domain containing proteins NHERF2, Grip1, Pdlim5 and Scrb1, which have been shown to play a role in neuronal development and at nerve synapses (Filippov et al, 2010; Geiger et al, 2014; Murdoch et al, 2003; Ren et al, 2015).

Because the C-terminus harbors both the 14-3-3 and PDZ binding motif, it is difficult to assess the separate functions of PRMT5 related to either the 14-3-3 binding module or PDZ domain binding module. To investigate the role of each binding module independently, it will be necessary to disrupt the interaction with one protein module without disturbing the other. This could be done by introducing single amino acid changes into the PDZ/14-3-3 binding motif. We used our protein domain array platform to assess this option (**Figure 26**).

By removing the last amino acid (L), we could successfully preserve phospho-dependent interactions with 14-3-3 proteins, while still disrupting the PDZ interaction. On the other hand, mutation of an arginine that is usually present on 14-3-3 binding motifs, partially disrupted the interaction with these proteins, however future studies will be needed to establish a mutation that will effectively alter the binding with 14-3-3 proteins.

The establishment of mutations that will shift PRMT5 interaction toward 14-3-3 or PDZ domain-containing proteins will allow us to create knock-in mice with sgRNA and Cas9 mRNA as before. These mouse models will give us the opportunity to evaluate the role of each binding module *in vivo*.

Chapter 5: Role of PRMT5 in DNA damage response

5.1. Introduction

5.1.1. The DNA Damage Response

Cells must respond appropriately to DNA damage and replication stress for their survival. Genomic integrity is crucial to preserve life, and not surprisingly the basic mechanisms to cope with DNA damage are conserved among species. Organisms are continuously exposed to DNA-damaging agents present in the environment. These include DNA damaging compounds released from our own metabolic processes, and exogenous agents like ultraviolet (UV) radiation, ionizing radiation (IR), and other agents that attack DNA and produce a variety of alterations in the chemical structure of DNA (De Bont & van Larebeke, 2004).

To cope with genomic instability, cells count on DNA repair protein complexes, orchestrated in defined signaling pathways termed DNA damage response (DDR) pathways. However, DDR faces a complicated challenge: DNA compaction. In eukaryotic cells, a high level of compaction is necessary to accommodate the DNA inside the nucleus. Although necessary, compaction of DNA into chromatin represent a barrier for accessing DNA for various cellular processes, including DNA repair. Thus, DDR studies should not only take chromatin structure into consideration, but also the mechanisms involved in its compaction or relaxation.

The coordination of different molecular processes that activate DDR will determine cell destiny, either DNA repair or cell death. Unfortunately, improperly repaired damage can generate mutations and chromosomal aberrations, leading to oncogenic transformation and tumor progression. Understanding the molecular basis of DDR is crucial not only for gaining insight into the molecular mechanisms of carcinogenesis, but also to establish the effect of genotoxic drugs in cancer therapy.

Cells can withstand a large number of DNA lesions per day, and repair can occur via diverse pathways, as depicted in **Figure 27**: direct repair (DR), base-excision repair (BER), nucleotide-excision repair (NER), mismatch repair (MMR), homologous recombination (HR), and nonhomologous end joining (NHEJ). DNA double-strand breaks (DSBs) are the most dangerous form of DNA damage and are one of the most common events that cause genomic instability. Efficient repair of DNA damage is particularly important for dividing cells, that is why in response to a DSB, the cell has acquired an intricate signaling system to detect the lesion, initiate repair, and also to stop the cell cycle thus enabling the repair to be completed. To effectively repair a DSB, there are two different DDR pathways: nonhomologous end-joining (NHEJ) and homologous recombination (HR) (Chapman et al, 2012).

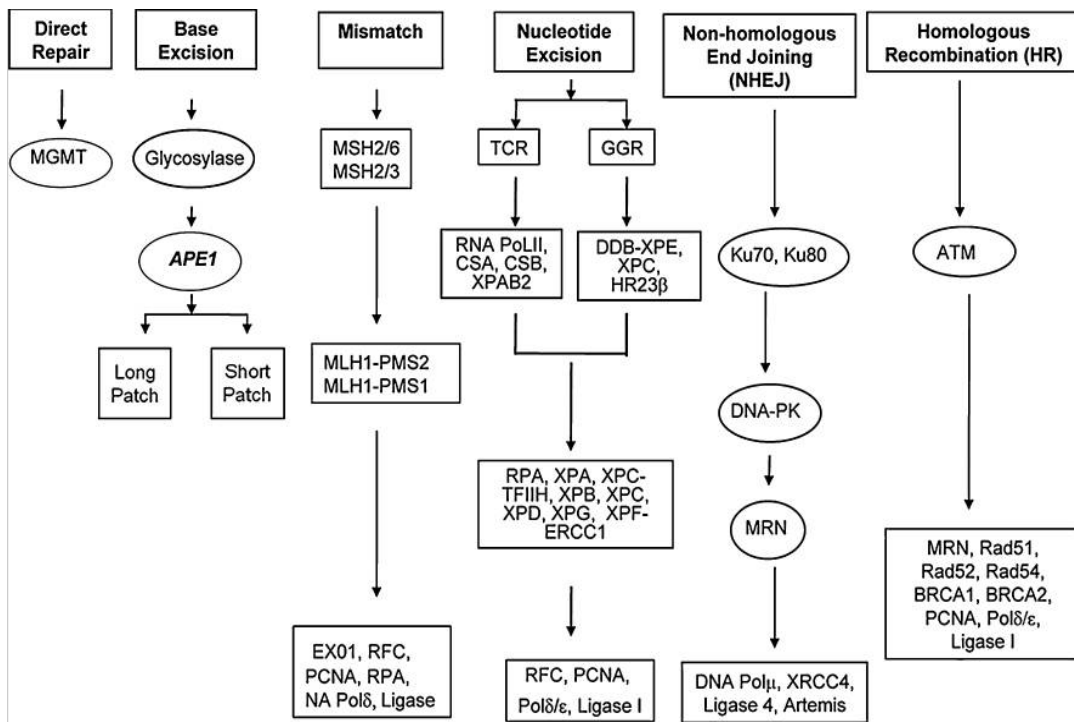


Figure 27: DNA damage repair pathways

From Luo M, He H, Kelley MR, Georgiadis MM (2010) Redox regulation of DNA repair: implications for human health and cancer therapeutic development. *Antioxid Redox Signal* 12: 1247-1269. Reprinted with permission of Mary Ann Liebert, Inc.

5.2. DNA Repair Mechanisms: NHEJ and HR

5.2.1. Nonhomologous end-joining

NHEJ is a process used to repair DNA ends at double-strand breaks (DSBs). It is particularly important when a homology donor is not in close proximity, such as in nondividing haploid organisms or in diploid organisms that are not in S phase. When a double-strand break occurs in eukaryotes, the broken DNA ends are bound by the Ku70-Ku80 heterodimer (Ku). Then the KU-DNA end complex can recruit the nuclease, polymerase and ligase, which work together to promote direct ligation of the DSB ends in an error-prone manner (Lieber, 2010). However, during S phase where the sister chromatid is available, homologous recombination is the preferred pathway (Scully & Xie, 2013).

5.2.2. Homologous recombination

In HR, the MRN (MRE11/RAD50/NBS1) complex localizes to the break site, recruiting ATM (ataxia telangiectasia–mutated protein) through the interaction with a C-terminal motif in NBS1. ATM phosphorylates multiple downstream proteins, including histone H2AX molecules, adjacent to the break site, thus marking nearby chromatin with γ -H2AX, and signaling the beginning of DSB recognition. The initial signal is spread and amplified by the recruitment of MDC1, which functions as a platform that mediates complex formation after the initial signal. MDC1 comprises a FHA domain at the extreme N-terminus, followed by a series of STD repeats, a series of TQXF motifs, and finally two tandem BRCT domains at the C-terminus. All these components are known to mediate MDC1 interaction with other proteins, thus BRCT domains bind to γ H2AX; phosphorylated TQXF binds to the FHA domain of RNF8; phosphorylated STD repeats bind to the FHA and BRCT domains of NBS1; and the FHA domain interacts with phosphorylated CHK2 and with N-terminus of

MDC1 itself mediating a head-to-tail dimerization (Jungmichel et al, 2012; Lou et al, 2003; Mohammad & Yaffe, 2009). A number of other downstream factors involved in HR or NHEJ assemble on the γ H2AX-MDC1 chromatin complex (**Figure 28**). These factors include BRCA1, RAP80 and 53BP1, which aid in forming larger complexes at the double strand break to allow its repair (Coster & Goldberg, 2010; Panier & Boulton, 2014; Scully & Xie, 2013).

HR and NHEJ are orchestrated through a cascade of events requiring DNA damage sensors, transducers, and effectors. All of these events take place within the context of chromatin. Likewise, synchronized post-translational modifications occur on the histone N-terminal tails, which themselves help regulate the recruitment of DDR factors (Panier & Boulton, 2014) (**Table 3**).

5.3. Histone code for DNA Double-Strand Break Repair

Chromatin structure is well regulated in order to control the compaction of and accessibility to DNA. The basic structural unit of chromatin is the nucleosome. The nucleosome is composed of 146 bp of DNA wrapped around two units each of canonical histones H2A, H2B, H3, and H4. Different mechanisms cooperate to regulate chromatin structure and DNA accessibility. These include: remodeling complexes that will slide the nucleosomes and exchange or remove histones from the chromatin; histone chaperones that control the supply and distribution of histones and histone variants (Gurard-Levin et al, 2014); and post-translational modifications (PTMs) of histones. The N-terminal tail of each histone protrudes from the nucleosome and bears modifications such as acetylation, methylation, phosphorylation and ubiquitination. These modifications modulate docking sites that facilitate the interaction with non-histone proteins serving as readers, writers and erasers. The combinations of PTMs on the histone tail constitute what is known as the “histone code”. This code helps control DSB repair in a spatial and temporal manner.

Almost two decades ago, the phosphorylation of histone H2A variant H2AX

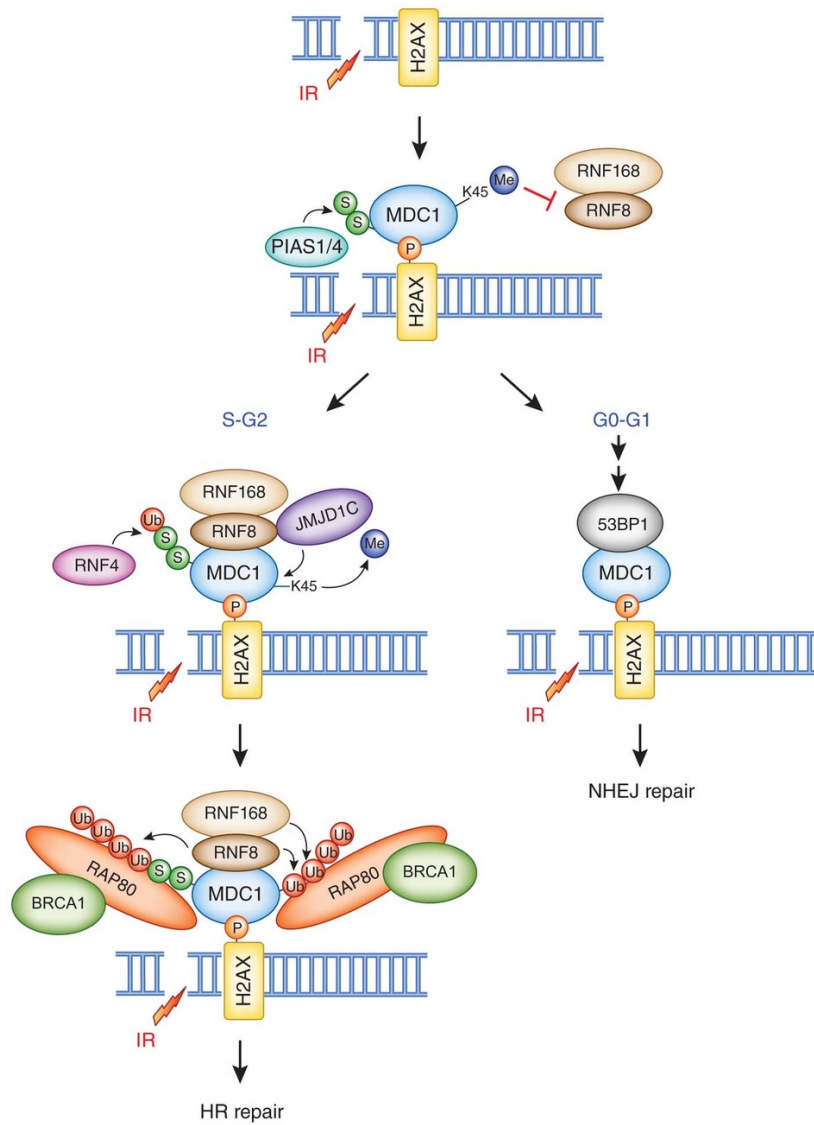


Figure 28: HR and NHEJ DNA Repair Mechanisms

Two DDR pathways are depicted, homologous recombination (HR) and non-homologous end joining (NHEJ). Both pathways depend on recruitment of MDC1 to sites of DNA damage marked previously with γ -H2AX. Reprinted by permission from Macmillan Publishers Ltd: Nature Structural & Molecular Biology (Lu & Matunis, 2013), Copyright (2013).

on serine 139 (termed γ -H2AX) was shown to be involved in DNA DSB repair (Rogakou et al, 1998). This provided the first indication of the importance of histone variants and PTMs on the histone tail in the context of DDR. In mammalian cells, phosphorylation of H2AX serine 139 is mediated by ATM, ATR, and DNA PKcs (Williamson et al, 2012).

Not only do phosphorylated histone variants play a role in regulating chromatin structure at the site of DNA damage, the phosphorylation of canonical histones are also important in DNA damage response (**Table 3**). Likewise, histone acetylation at sites of DNA damage is an important chromatin modification in DNA repair. Histone H4 and H3 acetylation on lysine is crucial for both NHEJ and HR (**Table 3**) (Tamburini & Tyler, 2005; Williamson et al, 2012).

Another PTM, ubiquitination is essential for the recruitment of proteins during DDR. The E3 ubiquitin ligase RNF8 is recruited to chromatin following the incorporation of MDC1 to the break site by γ -H2AX. RNF8 ubiquitinates H2AX and other proteins leading to the focal accumulation of 53BP1 (Mailand et al, 2007). However, recruitment of 53BP1 is mediated not only by ubiquitination, but also by dimethylation of histone H4 lysine 20 of (H4K20me2) as well as other factors that provide a docking site for the binding of the 53BP1 tandem Tudor domain (Hsiao & Mizzen, 2013; Schotta et al, 2008).

H4K20me2 is abundant and its levels do not appear to change following DNA damage when examined by using conventional techniques (Pei et al, 2011), suggesting a regulatory mechanism to limit the interaction of 53BP1 and H4K20me2 (Hsiao & Mizzen, 2013). Dr. Durocher's group showed that 53BP1 is a bivalent histone modification reader in which H4K20me2 and H2AK15ub are necessary for 53BP1 recruitment to chromatin (Fradet-Turcotte et al, 2013), suggesting that ubiquitination of H2AK15 could be the limiting factor for the localization of 53BP1 to sites of DNA damage.

H3 harbors four lysine residues that are methylated in response to DNA damage: K4, K9, K36 and K79 (**Table 3**). As was observed for H4K20, H3K4 and H3K9 methylation are not exclusively dedicated to DDR. It has recently been suggested that after DNA damage, euchromatin takes on a structure more similar to

heterochromatin as it also bears H3K9 methylation and forms a repressive structure, thus inhibiting local transcription. However, after DDR is established, this repressive structure is removed via a negative feedback mechanism that regulates release of the repressive complex associated with H3K9 methylation, thus leading to relaxation of chromatin structure (Ayrapetov et al, 2014).

Methylation is a widespread modification occurring on lysine and arginine residues. Although arginine methylation on histones has been linked to other processes, including transcription regulation, it is currently unknown whether histone arginines are modified during or in response to DNA damage repair. Nevertheless, arginine methylation is observed on non-histone proteins associated with DDR, such as MRE11, 53BP1, BRCA1, PolBeta, P53, FEN1 and RAD9 (Auclair & Richard, 2013).

5.4. Arginine methylation and DDR

As discussed earlier, arginine methylation is a common post-translational modification. In mammals, this modification is catalyzed by nine-known protein arginine methyltransferases (PRMT 1 - 9). These enzymes transfer one or two methyl groups to the side-chain nitrogen atoms of arginine residues. Recent studies have shown that PRMT7 is an epigenetic regulator of DDR: PRMT7 symmetrically dimethylates histones H2A and H4 to form H2AR3 and H4R3 at the promoter of DNA repair genes (Karkhanis et al, 2012). Hence, PRMT7 deficiency results in the enhanced expression of these DNA repair genes thereby increasing cellular resistance to genotoxic drugs (Karkhanis et al, 2012). PRMTs also play a role in DNA damage response by modifying non-histone proteins involved in DNA damage repair.

Asymmetric dimethylation of arginine mediated by PRMT1 is found in a broad range of proteins, especially those bearing glycine and arginine-rich RGG/RG motifs (Tang et al, 2000). PRMT1 deficiency results in spontaneous DNA damage, checkpoint defects, hypersensitivity to DNA-damaging agents and chromosomal instability, as observed in conditional PRMT1 knockout MEFs (Yu et al, 2009).

These observations show that PRMT1 has an important role in DDR. Proteins involved in DDR that are modified by PRMT1 include MRE11, 53BP1, BRCA1, hnRNPUL1 and Pol β (Boisvert et al, 2005a; Boisvert et al, 2005b; El-Andaloussi et al, 2007; Guendel et al, 2010; Gurunathan et al, 2015).

PRMT5 associates with a large number of proteins, and these interactions regulate its catalytic activity, generating SDMA on a variety of substrates, including DNA damage response proteins (Auclair & Richard, 2013). Like PRMT1, PRMT5 also preferentially methylates RGG/RG motifs. PRMT5 targets proteins involved in the DNA damage response including p53, FEN1 and Rad9a (Guo et al, 2010; He et al, 2011; Jansson et al, 2008).

The tumor suppressor p53 and its role as a transcriptional activator are of great importance for human health, thus, enormous effort has been dedicated to understanding the mechanisms of its regulation. A major advance in this area occurred following the discovery of PTMs on p53, which were shown to modulate its function, including arginine methylation mediated by PRMT5. p53 methylation occurs on arginines 333, 335 and 337 and increases in response to DNA damage. This event induces cell cycle arrest that depends on the activation of p21 expression in response to DNA damage (Jansson et al, 2008).

The endonuclease FEN1 is also methylated by PRMT5. This endonuclease removes 5-prime overhanging flaps created during normal DNA replication and during DDR (Hosfield et al, 1998). The nuclease function of FEN1 must be regulated precisely, both temporally and spatially. A repertoire of PTMs regulates FEN1, including acetylation, phosphorylation, sumoylation, ubiquitination and methylation (Guo et al, 2012; Guo et al, 2010; Hasan et al, 2001). Methylation of FEN1 at arginine 192 facilitates PCNA binding and the recruitment of FEN1 to the replication fork and also enhances DNA repair (Guo et al, 2010).

RAD9 is a cell cycle checkpoint exonuclease that arrests the cell cycle upon DNA damage. Rad9 forms a checkpoint protein complex with RAD1 and HUS1

RESIDUE	PTM	MODIFIER	FUNCTION IN DDR	REFERENCES
H2AK15	Ub	ENF168	Promotes the recruitment of 53BP1 to DSB	(Fradet-Turcotte et al, 2013)
H2AK119	Ub	RNF8, RNF168	Leads to the release of H2AX from damaged chromatin upon DSB	(Ikura et al, 2007)
H2AT120	Pho	Bub1, NHK-1	DDR sensitivity Activates the spindle checkpoint	(Kawashima et al 2010; Yang et al 2012)
H2AXK5	Ac	TIP60	Necessary for H2AX K119ub	(Ikura et al, 2007)
H2AXK36	Ac	CBP/p300	Regulates radiation sensitivity	(Jiang et al, 2010)
H2AXS139	Pho	ATM, ATR, DNA-PKcs	Recruits and accumulates MDC1 and promotes histone acetylation	(Paull et al, 2000 Rogakou et al 1998)
H2AXK119	Ub	RNF8, RNF168, TIP60-UBC13	Recruits DDR proteins	(Mailand et al 2007)
H2AXY142	Pho	WSTF, EYA	Regulates foci formation upon DNA damage. Dephosphorylation favors recruitment of MDC1 to the tail of γ -H2AX	(Xiao et al, 2009 (Cook et al, 2009)
H2BS14	Pho	CK2	Detected upon DNA	(Fernandez-

			damage induced by IR	Capetillo et al 2004)
H2BK120	Ub	RNF20- RNF40	Recruitment of NHEJ and HR proteins Chromatin remodeling during HR	(Moyal et al, 2011 Nakamura et al 2011)
H3K4	Me3	SET1	Stimulates V(D) J recombination via RAG complex. Required for DNA cleavage during Ig class switch recombination	(Shimazaki et al 2009; Stanlie et al 2010)
H3K9, K14, K23, K27	Ac	GCN5, CBP/p300	Essential for viability following HR	(Tamburini & Tyler 2005)
H3K9	Me3	Suv3- 9H1/Suv3-9H2	Activates TIP60	(Ayrapetov et al 2014; Sun et al 2009)
H3K18	Ac	GCN5, CBP/p300	Regulates Ku protein recruitment during NHEJ	(Ogiwara et al 2011)
H3K36	Me2	Metnase/SET MAR	Recruits NBS1 and the KU complex during NHEJ	(Fnu et al, 2011)
H3K56	Ac	GCN5, CBP/p300 RTT109	K56ac is reduced upon DNA damage. K56ac is required to reinstate the chromatin structure after DDR	(Chen et al, 2008 Miller et al, 2010)
H3K79	Me3	DOT1	Repair of UV damage in budding yeast	(Bostelman et al 2007)

H3S10	Pho	Ipl1 (Sc), AuroraB (Hs), RSK2, MSK1, ERK1, p38, Fyn, Chk1, PRK1	Decrease of phosphorylation following DNA damage induced by UV irradiation	(Shimada et al 2008)
H3T11	Pho	Chk1	Decrease of phosphorylation following DNA damage induced by UV irradiation	(Shimada et al 2008)
H4S1	Pho	CK2	Regulates chromatin acetylation	(Cheung et al 2005; Utley et al 2005)
H4K5, K8, K12, K16	Ac	MOF, TIP60, TRRAP, CBP/p300	Recruits DDR factors	(Ogiwara et al 2011; Sharma et al, 2010)
H4K20	Me2	Suv420H1/Su v420H2, MMSET	Recruits DDR factors	(Sanders et al 2004)
H4K91	Ub	BBAP	Promotes H4K20me and recruits 53BP1	(Yan et al, 2009)

Table 3: Histone modification in DDR

Adapted from Hunt et al, 2013

(Volkmer & Karnitz, 1999). RAD9 is methylated at Arg172, Arg174 and Arg175.

Arginine methylation occurs on proteins involved in the DNA damage response. In this study, we will demonstrate that PRMT5 interacts with the FHA domain of MDC1, and will show the localization of PRMT5 at induced DSB as well as an enrichment of H4R3 methylation at these sites. The regulatory role of histone modifications in DNA damage repair response is well established; however, despite the large number of arginine methylation sites identified on histones, none have yet been connected to DDR.

5.5. Results

5.5.1. Phosphorylated PRMT5 interacts with the FHA domain of MDC1

We have demonstrated that the C-terminus of PRMT5 is phosphorylated at threonine 634 and that this modification allows the interaction of PRMT5 with 14-3-3 proteins. In addition to 14-3-3 proteins, threonine phosphorylation generates docking sites for a number of domains such as, WD40 repeats, WW, BRCT and FHA domains. To identify additional phospho-dependent interactions, we created a phospho-threonine binding protein microarray containing FHA, WW and BRCT domains in addition to the seven 14-3-3 protein isoforms (**Figure 29**).

To discover novel PRMT5 phospho-threonine binding partners, a synthetic PRMT5 peptide harboring pT634 was tested on this phospho-threonine binding array. As expected, the phosphorylated peptide (**Figure 29 top panel**) binds most of the 14-3-3 isoforms. Moreover, the PRMT5 pT634 peptide interacted with the FHA domain of MDC1, whereas the unphosphorylated peptide (**Figure 29 middle panel**) showed no interactions. We confirmed these interactions using peptide pull-down assays (**Figure 30A**).

In order to investigate whether endogenous PRMT5 could interact with the FHA domain of MDC1, we performed a GST pull-down experiment. We could

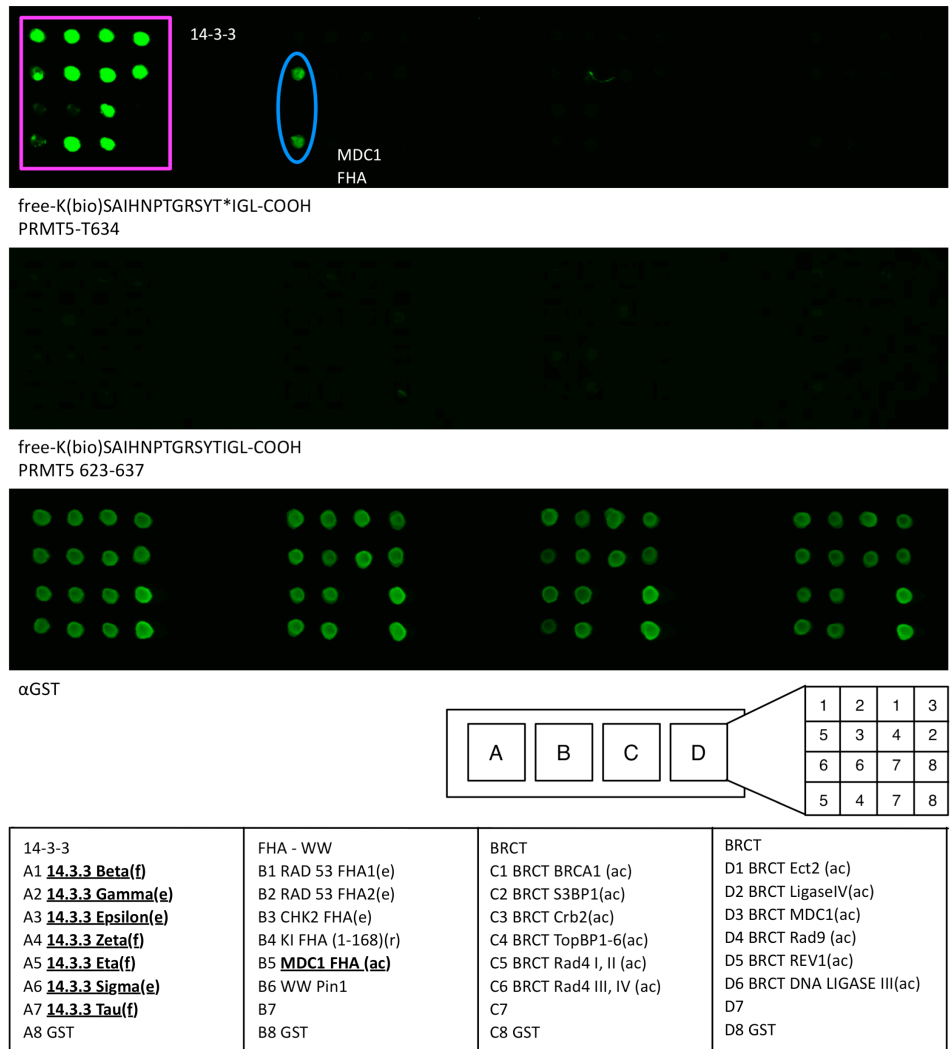


Figure 29: PRMT5 phosphothreonine specific binding partners

To identify the binding partner for phosphothreonine, a PRMT5 peptide harboring pT634 was tested using a protein microarray containing 14-3-3 proteins as well as FHA and BRCT domains. The phosphorylated peptide (top panel) binds 14-3-3 isoforms as well as the FHA domain of MDC1. The unphosphorylated peptide (middle panel) shows no interactions. Anti-GST (bottom panel) is used as a protein microarray loading control.

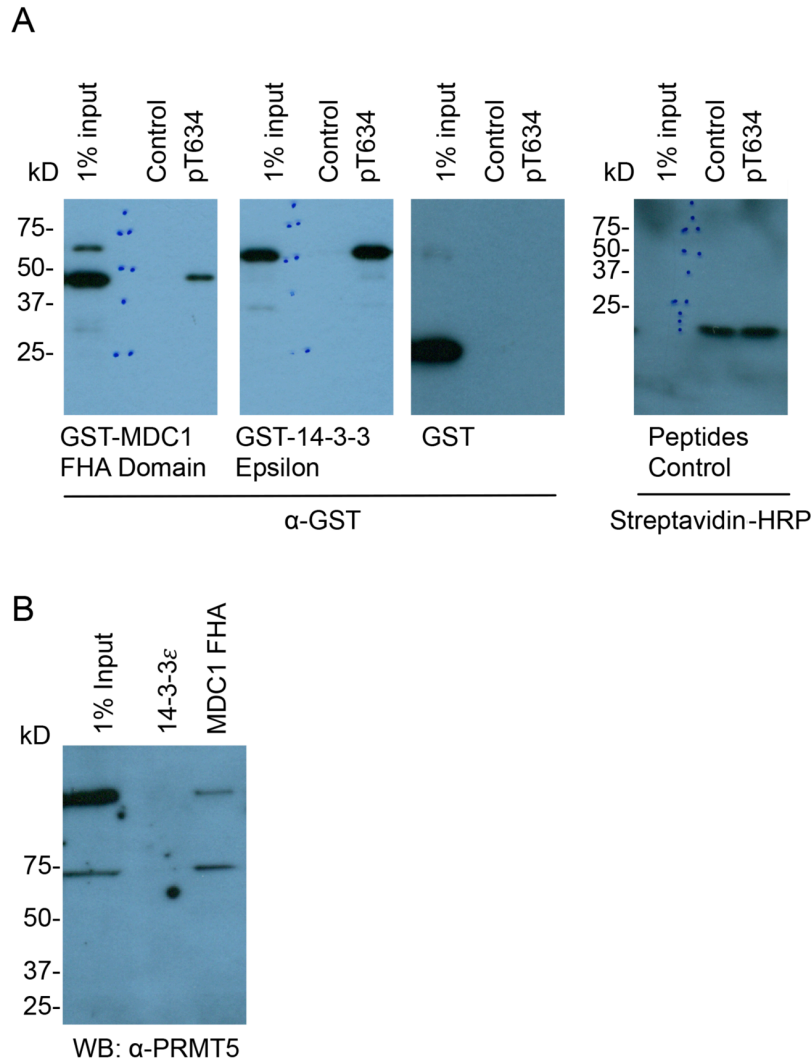


Figure 30: PRMT5 interacts with FHA domain of MDC1

(A) Peptide pull-down corroborates protein microarray findings. GST-fusion proteins of candidate phospho-dependent binding partners identified by protein domain microarray analysis were incubated with biotinylated PRMT5 phospho-threonine 643 (pT634) or unphosphorylated (control) peptides bound to streptavidin–agarose and detected by anti-GST immunoblot. Inputs of the GST fusion proteins are shown.

(B) Purified 14-3-3 ϵ and MDC1 FHA domain GST-fusion proteins were incubated with whole embryo lysates.

detect the interaction between endogenous PRMT5 and the FHA domain of MDC1 fused to GST in untreated whole embryo (E12.5) lysates (**Figure 30B**). It is important to note that this interaction occurs in an embryonic lysate that was not chemically hyperphosphorylated. However we did not see this interaction using HeLa, U2OS or MCF7 cells regardless of hypo- or hyperphosphorylated (data not shown).

5.5.2. PRMT5 is recruited to sites of DNA double-strand breaks

MDC1 binds to gamma-H2AX through its BRCT domain. Subsequently, it functions as an assembly platform, expanding the signal for DNA repair. To understand the functional implications of the MDC1-PRMT5 interaction, we examined whether PRMT5 is recruited to DNA double-strand breaks. To explore this idea, we used an inducible system that takes advantage of a rare cutting endonuclease I-PpoI. Expression of I-PpoI specifically cleaves a limited number of target sites, generating DSBs in the genome, at well defined locations. In this system, I-PpoI is fused to a mutant estrogen receptor (ER) hormone-binding domain that promotes rapid nuclear localization in response to 4-hydroxytamoxifen (4-OHT) (**Figure 31A**) (Berkovich et al, 2008). Using this system we analyzed whether PRMT5 is recruited to DSBs upon the induction of I-PpoI by performing ChIP assays.

We found that upon induction of I-PpoI, PRMT5 was recruited to an I-PpoI cleavage site in U2OS cell. As expected we also observed the recruitment of phosphorylated ATM (**Figure 31B**). Interestingly, we identified an increase in symmetric methylation of histone 4 at arginine 3 (H4R3me2s), which correlates with the presence of PRMT5 at the site of damage. In contrast, no difference in the levels of asymmetric dimethylation of H4R3 (**Figure 31B**) was observed. These results demonstrate that PRMT5 is recruited to sites of DNA double-strand breaks and that its substrate, H4R3, is predominantly symmetrically dimethylated at the site of damage.

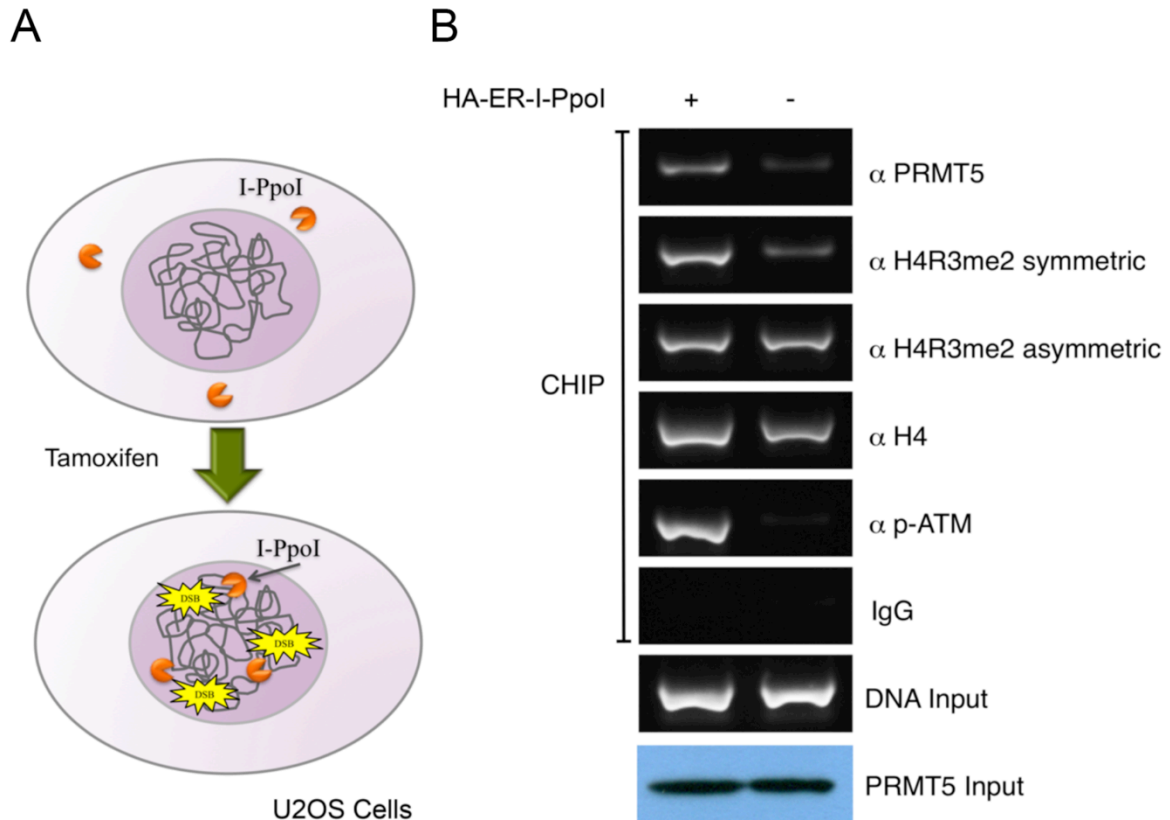


Figure 31. PRMT5 recruitment to DNA damage sites

A) U2OS cells were infected with HA-ER-I-PpoI retrovirus. 24 h after infection, cells were induced with 4-OHT for 12 h. ChIP analysis was carried out using the indicated antibodies and a primer pair adjacent to a single I-PpoI cleavage site.

B) Schematic representation of the I-PpoI system. I-PpoI is an endonuclease that has ~300 target sites in the human genome. This system allows for the examination of events occurring at a defined DNA DSB site. (Experiments were performed by Dr. Anup Biswas in Dr. Johnson’s laboratory).

5.5.3. H2AR3me2s is catalyzed by PRMT5 and does not vary after IR

To further investigate the role of the interaction between PRMT5 and the FHA domain of MDC1, we developed a tamoxifen-inducible PRMT5 KO MEF cell line. After 4-OHT treatments for 21 days, cells were lysed and the protein levels of PRMT5 were analyzed by western blot using anti-PRMT5 antibody (**Figure 32A**). We also investigated whether the H4/H2AR3me2s mark was affected by the loss of PRMT5. We used a panel of antibodies generated by CST, together with a commercially available H4R3me2s antibody. We observed that the levels of symmetric dimethylation on H2A were reduced to a greater extent than on H4R3 (**Figure 32B**). We have also further characterized, using immunofluorescence microscopy, one of the antibodies that by western blot specifically recognized H2AR3me2s. The signal of this antibody shows a strong nuclear localization in control MEF cells and is notably reduced in the absence of PRMT5 (**Figure 33**).

Having characterized this antibody, we explored whether this PRMT5 mediated mark changed after IR. Untreated MEF PRMT5 *LoxP*^(F/F) cells were irradiated (5 Gy), then stained with the previously characterized antibody. Gamma-H2AX was used as positive control for nuclear foci formation. The localization and intensity of H2AR3me2s staining did not considerably vary after IR. In contrast, gamma-H2AX was rapidly visualized after IR increasing to a maximum intensity at 1 hour, and gradually disappeared by 12 hours (**Figure 34**). These results suggest that the activity of PRMT5 toward H2A does not change with the induction of DNA double strand breaks by IR.

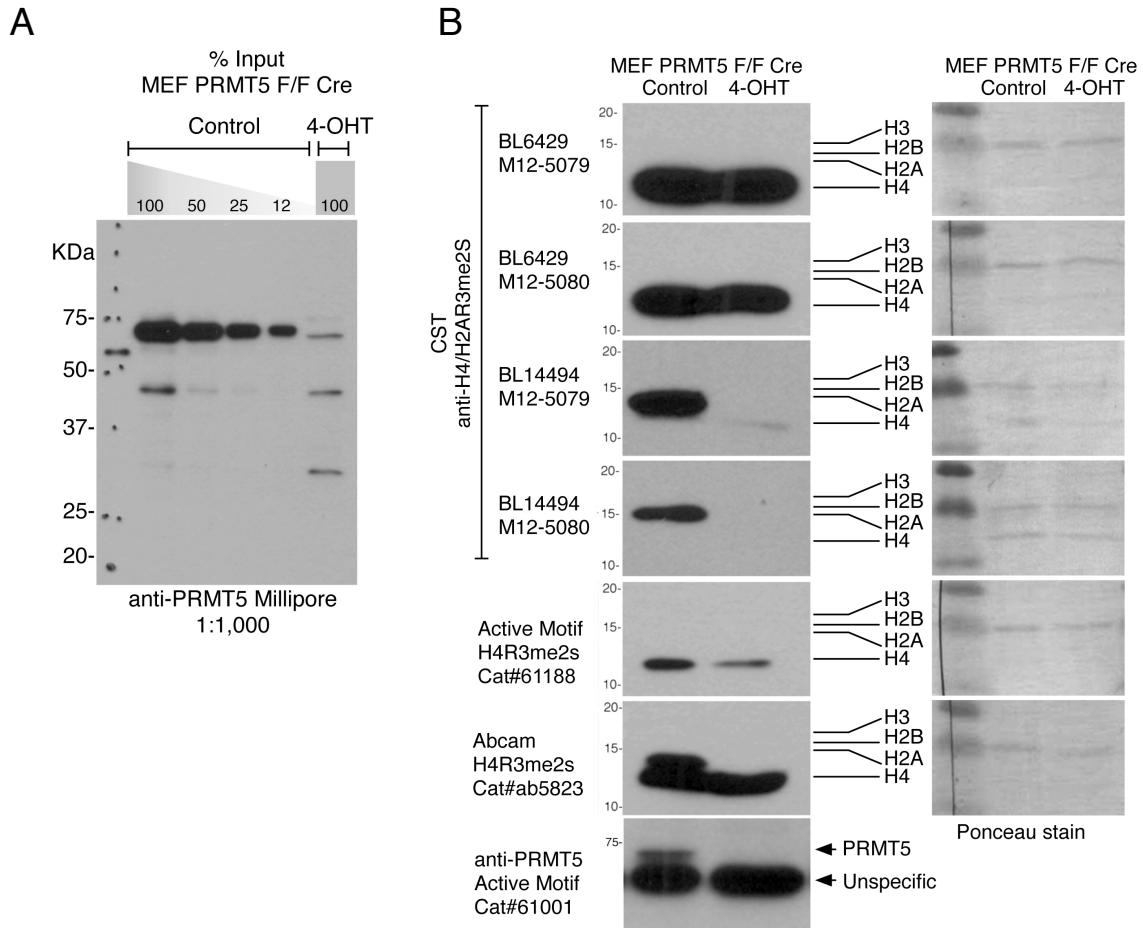


Figure 32: MEF KO PRMT5 and anti-H4/H2AR3me2s characterization

A) Cells were obtained from a conditional knockout mouse harboring LoxP (F/F) sequences flanking exon 7 in the Prmt5 gene (Bezzi et al, 2013) and expressing tamoxifen-inducible Cre. Cells were immortalized using the 3T3 protocol. Immortalized cells were treated every 3 days with 2uM 4-hydroxy tamoxifen 4-OHT for 21 days. Whole cell lysates from tamoxifen-treated or untreated cells were subjected to western blotting and probed with an anti-PRMT5 antibody. The percentage of total control and treated cell lysate loaded are indicated.

B) The indicated antibodies were tested on nuclear extracts from tamoxifen-treated and untreated cells (left panel). Equal loading of histones was verified by Ponceau S staining (right panel).

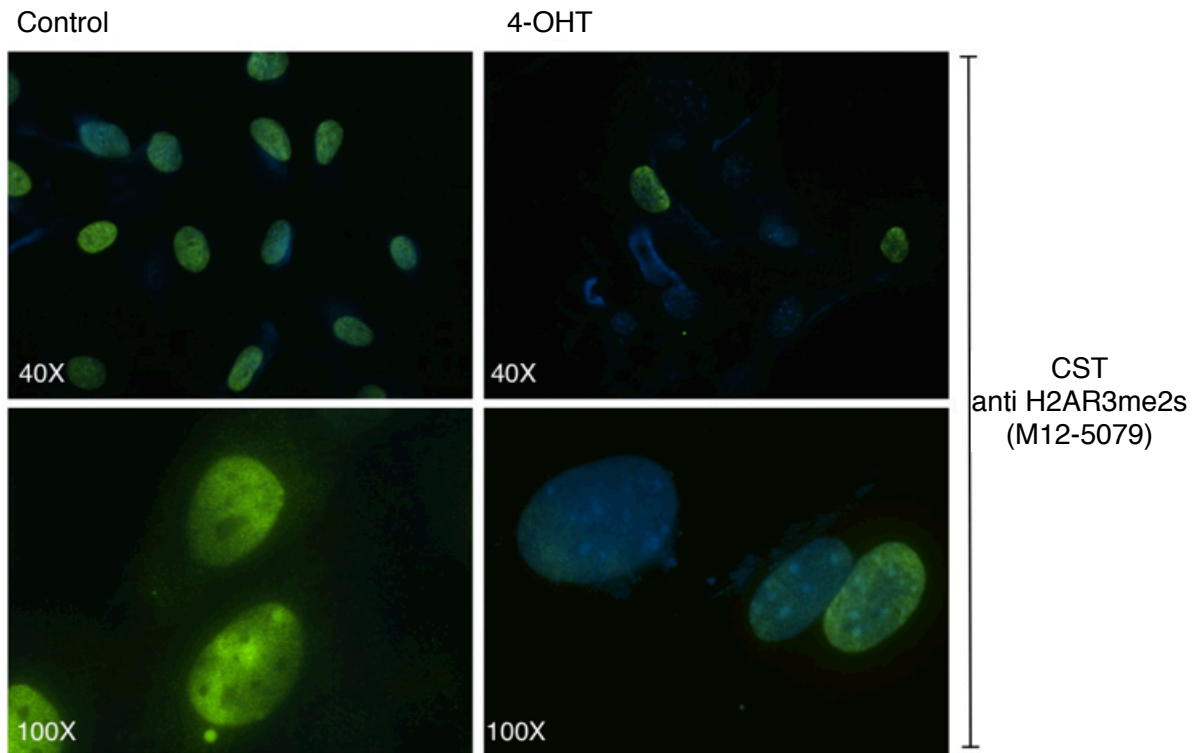


Figure 33: Validation of H2AR3me2s using immunofluorescence

MEF PRMT5 LoxP (^{F/F}) untreated (control) or 4-OHT treated for 21 days were examined by immunofluorescence microscopy following staining with H2AR3me2s antibody (BL14494 M12-5079). DAPI was used to stain DNA.

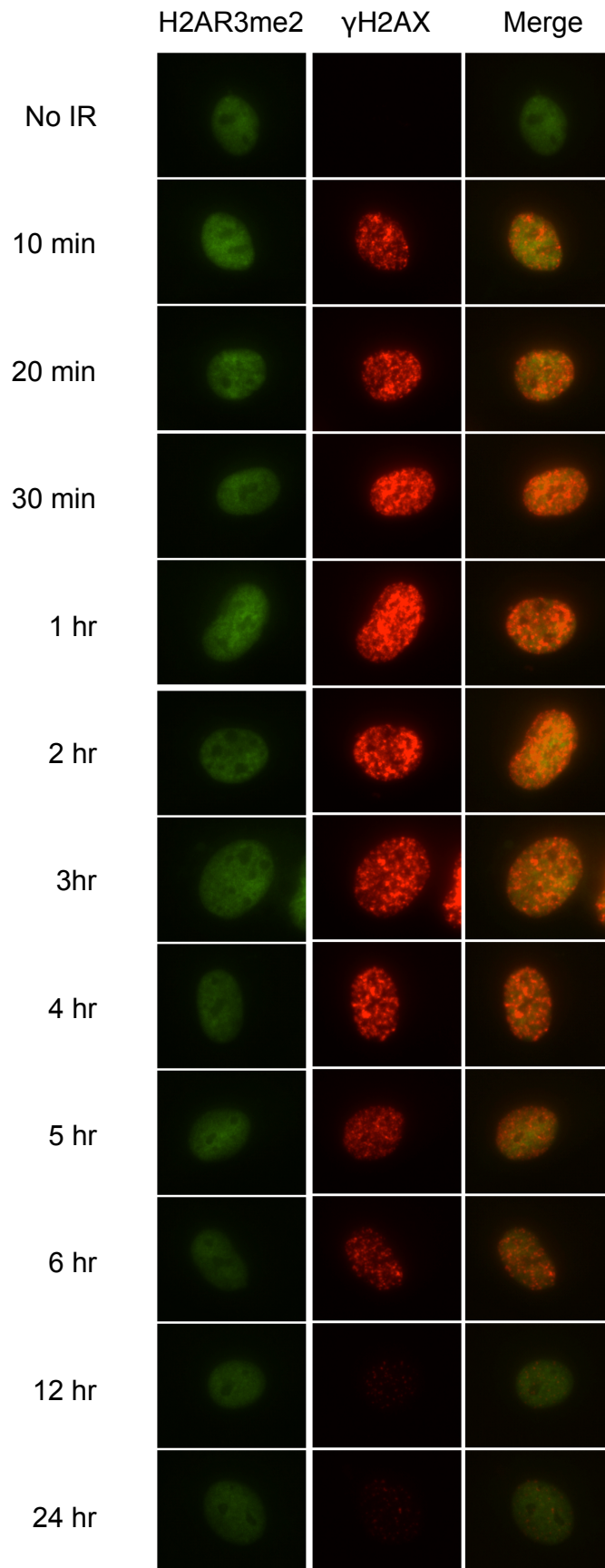


Figure 34: Symmetric methylation on H2A does not vary in response to IR

MEF PRMT5 LoxP^(F/F) cells were irradiated with gamma rays (5 Gy) and cultured under normal conditions for the indicated times. Cells were fixed and co-immunostained with anti-H2AR3me2s and γ -H2AX antibodies.

5.6. Discussion

The basic mechanisms involved in DNA repair have been extensively studied. However, it is becoming more and more evident that there is a strong interconnection between chromatin status and DNA repair. In the context of chromatin, it has been suggested that after DNA damage, euchromatin and heterochromatin have similar attributes, such as the presence of H3K9me3, thus inhibiting local transcription (Ayrapetov et al, 2014). PRMT5 is also present in repressive chromatin supporting the possibility that PRMT5 may be recruited to DNA damage sites via its interaction with MDC1, in order to deposit repressive chromatin marks such as H3R8me2s, H4R3me3s, and H2AR3me2s, thus strengthening transcription inhibition at sites of DNA damage.

It is also important to consider that recent studies have revealed that MDC1 has a role as a transcriptional co-activator. MDC1 associates with the androgen receptor (AR) and estrogen receptor α (ER α) (Wang et al, 2015; Zou et al, 2015). The interaction of MDC1 with ER α and AR activates the transcription of hormone receptor-mediated genes and functions as tumor suppressor. Moreover, interaction of MDC1 with AR facilitates the association between AR and histone acetyltransferase GCN5, increasing histone H3 acetylation levels, thus activating androgen-induced target genes (Wang et al, 2015). Taking into consideration the transcription function of MDC1, the interaction of PRMT5 and MDC1 could also serve to modulate gene expression via arginine methylation of histones.

In this section of our study, we have demonstrated that the FHA domain of MDC1 interacts with PRMT5 phosphorylated at T634. We further showed by CHIP that PRMT5 is localized to sites of DNA damage, coincident with the enrichment of H4R3me2. This result is consistent with a role for PRMT5 in DDR.

MDC1 is recruited to gamma-H2AX foci, forming complexes with a number of proteins involved in DDR such as RNF8, 53BP1 and NBS1 (Lu & Matunis, 2013; Melander et al, 2008). MDC1 functions as an assembly platform, amplifying the signal for DNA repair. We have demonstrated that PRMT5 interacts with the FHA domain of MDC1 and that it may be recruited to DNA double-strand breaks. We also

observed an increase in symmetric methylation of H4R3me2s at the site of damage, indicating that the loading of PRMT5 may result in the rapid formation of repressive chromatin at the DSB.

In addition, we investigated the presence of symmetric methylation of H2AR3 over time following IR, by immunofluorescence microscopy. We observed no major change in H2AR3me2s localization or intensity during DNA repair (**Figure 34**). However, it is possible that because the H2AR3me2s mark has a strong presence in the nucleus of MEF cells, as is shown in **Figures 33 and 34**, subtle changes, perhaps precisely overlapping sites of damage, cannot be detected via immunofluorescence microscopy. H4K20me2, which is also highly abundant and does not appear to change in abundance following DNA damage as assessed by conventional techniques such as western blot, was detected by immunofluorescence only after DNA damage was induced by laser irradiation (Pei et al, 2011).

In the previous chapter, we demonstrated the interaction of 14-3-3 proteins with PRMT5 in the context of cytoplasmic proteins. In the nucleus, 14-3-3 isoforms mediate G1/S and G2/M cell cycle checkpoints after DNA damage (Mohammad & Yaffe, 2009). While we have previously shown that pT634 mediates 14-3-3 interactions, in this chapter we have demonstrated that phosphorylation of threonine 634 in PRMT5 also mediates its interaction with the FHA domain of MDC1.

ATM, ATR and DNA-PKcs substrates are thought to be involved in the formation of foci, whereas checkpoint effector kinases (Chk1, Chk2 and MK2) ensure that the cell cycle arrests to allow time for repair prior to cell division. 14-3-3 proteins interact with substrates of checkpoint kinases, while FHA domains have been shown to interact with substrates of “foci” kinases (Mohammad & Yaffe, 2009). Our studies indicate that PRMT5 pT634 interacts with both the FHA domain of MDC1 and 14-3-3 proteins. Consistently, the C-terminus of PRMT5 contains motifs known to interact with FHA domains and 14-3-3 proteins: motif III of 14-3-3 (RXX [pS/pT]XX-COOH) and the pThr+3 rule of FHA binding modules (pTXX(I/L/V) (Ganguly et al, 2005; Mahajan et al, 2008). This dual motif may indicate that PRMT5 could be involved in both processes. Indeed, PRMT5 methylates at least two proteins with key functions in cell cycle checkpoint control, p53 and Rad9.

In collaboration with Dr. Stephan Richard, we observed that loss of PRMT5 did not alter the activation of the DNA damage checkpoint that leads to cell cycle arrest, or sensitize cells to etoposide-induced cell death (Data not shown). One possible explanation is that very little PRMT5 is necessary to support its functions. This is evidenced by the notion that PRMT5 null mice are not viable and that no ES null cells could be generated. In contrast, PRMT5 KD cells are relatively easy to maintain in culture. In addition, our experience working with inducible PRMT5 KO MEF cells indicates that the levels of SDMA remained stable long after PRMT5 was depleted. Until recently, it was thought that arginine methylation may be a semi-permanent PTM; however, recent findings indicate otherwise. Yet, these findings show that although ADMA was removed by a subset of JmjC-containing enzymes, MMA and SDMA are not greatly suitable to be demethylated by these enzymes (Walport et al, 2016). Considering the nature of SDMA and that little PRMT5 is needed for its biological function, we can deduce that cells would not be strongly affected by PRMT5 deficiency in knockdown experiments, thus explaining the lack of phenotype following DNA damage. Simultaneous suppression of PRMT5 by shRNA and a PRMT5 inhibitor may help to overcome this problem and clarify the role of PRMT5 in DDR.

5.7. Future studies

Although our knowledge of the role of PRMT5 as an epigenetic writer continues to grow, there are still many mechanistic details that remain to be clarified. Development of antibodies specifically recognizing PRMT5 pT634 modifications would help to clarify many of these questions. Additionally, we generated stable inducible MEF PRMT5 KO cells and lentiviral vectors harboring myc-tagged PRMT5 and PRMT5^{T634A}. These will be useful for future rescue experiments that will provide valuable information on the role of phosphorylation in foci formation and cell cycle arrest, using more precise methods such as ChIP analysis of I-Ppol induced cells.

We cannot rule out the possibility that an impaired checkpoint response might be observed in other cell models. PRMT5 localization changes during development

and in cancer (Gu et al, 2012; Kim et al, 2014; Liang et al, 2007; Shilo et al, 2013). In malignant neoplasms, cytoplasmic localization of PRMT5 is usually correlated with the worst outcome. Our experiments were carried out in cancer cell lines where PRMT5 is mostly cytoplasmic. The fact that these are cancer cells could mean that the machineries necessary for the “normal” behavior of PRMT5 could be already compromised in these cells. Repeating these experiments using other cell types could strengthen the results.

Additionally, transcriptional regulation by PRMT5 may alter DDR. Indeed p53 signaling genes (*Cdkn1a*, *Mdm2*, *Ccng1*) and DDR genes (*Ercc5*, *Btg2*, *Rev1*) are upregulated in *Prmt5* mouse null primordial germ cells (Kim et al, 2014). In *Arabidopsis*, PRMT5 deficiency in root stem cells causes cell death and defective cell cycle progression in response to DNA damage. Also, loss of PRMT5 function increases DNA damage-induced apoptosis in *C. elegans* (Li et al, 2016; Yang et al, 2009). However, the precise role of PRMT5 in DSB repair remains unclear. We observed an interaction between PRMT5 and MDC1, under certain conditions, and we detected elevated levels of the H4R3me2s mark at DSBs. These preliminary observations suggest that a temporary repressive chromatin structure may be formed at the site of damage, which could be partially regulated by the phosphorylation of PRMT5.

Chapter 6: Significance

Post-translational modifications play a pivotal role in the function of proteins, in part by mediating protein-protein interactions, which promote the assembly of multiprotein complexes. We investigated the function of a subset of phosphorylated residues on PRMT5, with special emphasis on new discoveries related to potential cross-talk between arginine methylation and protein kinases.

This study increased our scientific knowledge regarding arginine methylation. We observed that Src mediated phosphorylation of PRMT5 facilitates the interaction of PRMT5 with many SH2-domain containing proteins. Likewise, we have determined that PRMT5 is phosphorylated by AKT and SGK near the C-terminus at threonine 634. This creates a binding motif that allows interaction with 14-3-3 proteins. We also observed that under unphosphorylated conditions, the C-terminus of PRMT5 interacts with the PDZ domain of NHERF2, which has enabled us to investigate, for the first time, the membrane association of PRMT5, the existence of PRMT5's substrate at the plasma membrane, and the role of PRMT5 in the regulation of ion exchangers. Moreover, phosphorylation of PRMT5 at T634, also promotes its interaction with the FHA domain of MDC1, which may bring it to sites of DSBs, therefore connecting the phosphorylation of PRMT5 to DDR.

Consequently, we propose the existence of kinase-mediated signaling networks that coordinate PRMT5 interactions with several binding partners and in turn, position it as a key player for many different biological functions. Regulation of protein-RNA binding, DNA repair, and ion-exchanger function are just a few examples where PRMT5 phosphorylation may be an integral part of cellular regulatory mechanisms. Since PRMT5 phosphorylation is mediated by Src and Akt, which are frequently dysregulated in many cancers and are linked to cell growth and survival pathways, future studies will aim to clarify the events regulated by phosphorylated PRMT5 in cancer.

One of the major roles of PRMT5 phosphorylation that we have identified is the PDZ/14-3-3 switch, which may regulate many biological functions. The importance of the PDZ/14-3-3 binding switch in mammalian cells was first suggested after discovering that the HPV E6 oncoprotein has adopted this mechanism to facilitate host infection (Boon & Banks, 2013). This prompted us to speculate that many more proteins may possess this unique C-terminal motif and could switch their binding between 14-3-3 proteins and PDZ domain interaction networks. Indeed, we have identified other mammalian proteins, ERBB4, PGHS2 and IRK1, which just like PRMT5, possess this dual C-terminal regulatory motif and switch from binding PDZ domains to binding 14-3-3 proteins upon phosphorylation.

Both 14-3-3 and PDZ-domain containing proteins have been strongly implicated in synaptic functions (Berg et al, 2003; Foote & Zhou, 2012; Paquet et al, 2006). We expected to explore the role of this switch in synapses using a mouse knock-in model. However, the 14-3-3/PDZ dual motif at the C-terminus of PRMT5 was essential for viability as no homozygous mutant embryos were alive in our knock-in mouse models. Therefore, developing a conditional knock-in Nestin-Cre/PRMT5^{Δ+HA/flox} mouse and/or knock-in mouse that can separate the interaction of PRMT5 with 14-3-3 proteins and PDZ domains will be a valuable tool to explore the roles of PRMT5 in synaptic transmission and other cellular processes.

Chapter 7: Bibliography

Akiva E, Friedlander G, Itzhaki Z, Margalit H (2012) A dynamic view of domain-motif interactions. *PLoS computational biology* **8**: e1002341

Alexander RT, Grinstein S (2009) Tethering, recycling and activation of the epithelial sodium-proton exchanger, NHE3. *The Journal of experimental biology* **212**: 1630-1637

An W, Kim J, Roeder RG (2004) Ordered cooperative functions of PRMT1, p300, and CARM1 in transcriptional activation by p53. *Cell* **117**: 735-748

Ancelin K, Lange UC, Hajkova P, Schneider R, Bannister AJ, Kouzarides T, Surani MA (2006) Blimp1 associates with Prmt5 and directs histone arginine methylation in mouse germ cells. *Nature cell biology* **8**: 623-630

Andreu-Perez P, Esteve-Puig R, de Torre-Minguela C, Lopez-Fauqued M, Bech-Serra JJ, Tenbaum S, Garcia-Trevijano ER, Canals F, Merlino G, Avila MA, Recio JA (2011) Protein arginine methyltransferase 5 regulates ERK1/2 signal transduction amplitude and cell fate through CRAF. *Science signaling* **4**: ra58

Antonyssamy S, Bonday Z, Campbell RM, Doyle B, Druzina Z, Gheyi T, Han B, Jungheim LN, Qian Y, Rauch C, Russell M, Sauder JM, Wasserman SR, Weichert K, Willard FS, Zhang A, Emtage S (2012) Crystal structure of the human PRMT5:MEP50 complex. *Proceedings of the National Academy of Sciences of the United States of America* **109**: 17960-17965

Auclair Y, Richard S (2013) The role of arginine methylation in the DNA damage response. *DNA repair* **12**: 459-465

Ayrapetov MK, Gursoy-Yuzugullu O, Xu C, Xu Y, Price BD (2014) DNA double-strand breaks promote methylation of histone H3 on lysine 9 and transient formation of repressive chromatin. *Proceedings of the National Academy of Sciences of the United States of America* **111**: 9169-9174

Bao X, Zhao S, Liu T, Liu Y, Liu Y, Yang X (2013) Overexpression of PRMT5 promotes tumor cell growth and is associated with poor disease prognosis in epithelial ovarian cancer. *The journal of histochemistry and cytochemistry : official journal of the Histochemistry Society* **61**: 206-217

Bauer UM, Daujat S, Nielsen SJ, Nightingale K, Kouzarides T (2002) Methylation at arginine 17 of histone H3 is linked to gene activation. *EMBO reports* **3**: 39-44

Bedford MT, Clarke SG (2009) Protein arginine methylation in mammals: who, what, and why. *Molecular cell* **33**: 1-13

Bedford MT, Frankel A, Yaffe MB, Clarke S, Leder P, Richard S (2000) Arginine methylation inhibits the binding of proline-rich ligands to Src homology 3, but not WW, domains. *The Journal of biological chemistry* **275**: 16030-16036

Bedford MT, Richard S (2005) Arginine methylation an emerging regulator of protein function. *Molecular cell* **18**: 263-272

Beltran-Alvarez P, Espejo A, Schmauder R, Beltran C, Mrowka R, Linke T, Batlle M, Perez-Villa F, Perez GJ, Scornik FS, Benndorf K, Pagans S, Zimmer T, Brugada R (2013) Protein arginine methyl transferases-3 and -5 increase cell surface expression of cardiac sodium channel. *FEBS letters* **587**: 3159-3165

Berg D, Holzmann C, Riess O (2003) 14-3-3 proteins in the nervous system. *Nature reviews Neuroscience* **4**: 752-762

Berkovich E, Monnat RJ, Jr., Kastan MB (2008) Assessment of protein dynamics and DNA repair following generation of DNA double-strand breaks at defined genomic sites. *Nature protocols* **3**: 915-922

Bezzi M, Teo SX, Muller J, Mok WC, Sahu SK, Vardy LA, Bonday ZQ, Guccione E (2013) Regulation of constitutive and alternative splicing by PRMT5 reveals a role for Mdm4 pre-mRNA in sensing defects in the spliceosomal machinery. *Genes & development* **27**: 1903-1916

Biswas AK, Mitchell DL, Johnson DG (2014) E2F1 responds to ultraviolet radiation by directly stimulating DNA repair and suppressing carcinogenesis. *Cancer research* **74**: 3369-3377

Boisvert FM, Cote J, Boulanger MC, Richard S (2003) A proteomic analysis of arginine-methylated protein complexes. *Molecular & cellular proteomics : MCP* **2**: 1319-1330

Boisvert FM, Dery U, Masson JY, Richard S (2005a) Arginine methylation of MRE11 by PRMT1 is required for DNA damage checkpoint control. *Genes & development* **19**: 671-676

Boisvert FM, Rhie A, Richard S, Doherty AJ (2005b) The GAR motif of 53BP1 is arginine methylated by PRMT1 and is necessary for 53BP1 DNA binding activity. *Cell cycle* **4**: 1834-1841

Boon SS, Banks L (2013) High-risk human papillomavirus E6 oncoproteins interact with 14-3-3zeta in a PDZ binding motif-dependent manner. *J Virol* **87**: 1586-1595

Boriack-Sjodin PA, Swinger KK (2016) Protein Methyltransferases: A Distinct, Diverse, and Dynamic Family of Enzymes. *Biochemistry* **55**: 1557-1569

Bostelman LJ, Keller AM, Albrecht AM, Arat A, Thompson JS (2007) Methylation of histone H3 lysine-79 by Dot1p plays multiple roles in the response to UV damage in *Saccharomyces cerevisiae*. *DNA repair* **6**: 383-395

Boulanger MC, Miranda TB, Clarke S, Di Fruscio M, Suter B, Lasko P, Richard S (2004) Characterization of the *Drosophila* protein arginine methyltransferases DART1 and DART4. *The Biochemical journal* **379**: 283-289

Branscombe TL, Frankel A, Lee JH, Cook JR, Yang Z, Pestka S, Clarke S (2001) PRMT5 (Janus kinase-binding protein 1) catalyzes the formation of symmetric dimethylarginine residues in proteins. *The Journal of biological chemistry* **276**: 32971-32976

Brauer PM, Tyner AL (2010) Building a better understanding of the intracellular tyrosine kinase PTK6 - BRK by BRK. *Biochimica et biophysica acta* **1806**: 66-73

Burgos ES, Wilczek C, Onikubo T, Bonanno JB, Jansong J, Reimer U, Shechter D (2015) Histone H2A and H4 N-terminal tails are positioned by the MEP50 WD repeat protein for efficient methylation by the PRMT5 arginine methyltransferase. *The Journal of biological chemistry* **290**: 9674-9689

Chan-Penebre E, Kuplast KG, Majer CR, Boriack-Sjodin PA, Wigle TJ, Johnston LD, Rioux N, Munchhof MJ, Jin L, Jacques SL, West KA, Lingaraj T, Stickland K, Ribich SA, Raimondi A, Scott MP, Waters NJ, Pollock RM, Smith JJ, Barbash O, Pappalardi M, Ho TF, Nurse K, Oza KP, Gallagher KT, Kruger R, Moyer MP, Copeland RA, Chesworth R, Duncan KW (2015) A selective inhibitor of PRMT5 with in vivo and in vitro potency in MCL models. *Nature chemical biology* **11**: 432-437

Chao Xu GC, Maria Victoria Botuyan, Georges Mer (2015) Methyllysine Recognition by the Royal Family Modules: Chromo, Tudor, MBT, Chromo Barrel, and PWWP Domains. In *Histone Recognition*, Zhou M-M (ed), pp 49-82. Springer

Chapman JR, Taylor MR, Boulton SJ (2012) Playing the end game: DNA double-strand break repair pathway choice. *Molecular cell* **47**: 497-510

Chen CC, Carson JJ, Feser J, Tamburini B, Zabaronick S, Linger J, Tyler JK (2008) Acetylated lysine 56 on histone H3 drives chromatin assembly after repair and signals for the completion of repair. *Cell* **134**: 231-243

Chen D, Ma H, Hong H, Koh SS, Huang SM, Schurter BT, Aswad DW, Stallcup MR (1999) Regulation of transcription by a protein methyltransferase. *Science* **284**: 2174-2177

Chen H, Lorton B, Gupta V, Shechter D (2016a) A TGFbeta-PRMT5-MEP50 axis regulates cancer cell invasion through histone H3 and H4 arginine methylation coupled transcriptional activation and repression. *Oncogene*

Chen M, Qu X, Zhang Z, Wu H, Qin X, Li F, Liu Z, Tian L, Miao J, Shu W (2016b) Cross-talk between Arg methylation and Ser phosphorylation modulates apoptosis signal-regulating kinase 1 activation in endothelial cells. *Molecular biology of the cell* **27**: 1358-1366

Chen M, Sultan A, Cinar A, Yeruva S, Riederer B, Singh AK, Li J, Bonhagen J, Chen G, Yun C, Donowitz M, Hogema B, de Jonge H, Seidler U (2010) Loss of PDZ-adaptor protein NHERF2 affects membrane localization and cGMP- and [Ca²⁺]- but not cAMP-dependent regulation of Na⁺/H⁺ exchanger 3 in murine intestine. *The Journal of physiology* **588**: 5049-5063

Cheng D, Cote J, Shaaban S, Bedford MT (2007) The arginine methyltransferase CARM1 regulates the coupling of transcription and mRNA processing. *Molecular cell* **25**: 71-83

Cheung WL, Turner FB, Krishnamoorthy T, Wolner B, Ahn SH, Foley M, Dorsey JA, Peterson CL, Berger SL, Allis CD (2005) Phosphorylation of histone H4 serine 1 during DNA damage requires casein kinase II in *S. cerevisiae*. *Current biology : CB* **15**: 656-660

Chittka A, Nitarska J, Grazini U, Richardson WD (2012) Transcription factor positive regulatory domain 4 (PRDM4) recruits protein arginine methyltransferase 5 (PRMT5) to mediate histone arginine methylation and control neural stem cell proliferation and differentiation. *The Journal of biological chemistry* **287**: 42995-43006

Coblitz B, Wu M, Shikano S, Li M (2006) C-terminal binding: an expanded repertoire and function of 14-3-3 proteins. *FEBS letters* **580**: 1531-1535

Cook PJ, Ju BG, Teles F, Wang X, Glass CK, Rosenfeld MG (2009) Tyrosine dephosphorylation of H2AX modulates apoptosis and survival decisions. *Nature* **458**: 591-596

Costa-Pessoa JM, Figueiredo CF, Thieme K, Oliveira-Souza M (2013) The regulation of NHE(1) and NHE(3) activity by angiotensin II is mediated by the activation of the angiotensin II type I receptor/phospholipase C/calcium/calmodulin pathway in distal nephron cells. *European journal of pharmacology* **721**: 322-331

Cote J, Boisvert FM, Boulanger MC, Bedford MT, Richard S (2003) Sam68 RNA binding protein is an in vivo substrate for protein arginine N-methyltransferase 1. *Molecular biology of the cell* **14**: 274-287

Czechanski A, Byers C, Greenstein I, Schrode N, Donahue LR, Hadjantonakis AK, Reinholdt LG (2014) Derivation and characterization of mouse embryonic stem cells from permissive and nonpermissive strains. *Nature protocols* **9**: 559-574

De Bont R, van Larebeke N (2004) Endogenous DNA damage in humans: a review of quantitative data. *Mutagenesis* **19**: 169-185

Derry JJ, Richard S, Valderrama Carvajal H, Ye X, Vasioukhin V, Cochrane AW, Chen T, Tyner AL (2000) Sik (BRK) phosphorylates Sam68 in the nucleus and negatively regulates its RNA binding ability. *Molecular and cellular biology* **20**: 6114-6126

Dhar S, Vemulapalli V, Patananan AN, Huang GL, Di Lorenzo A, Richard S, Comb MJ, Guo A, Clarke SG, Bedford MT (2013) Loss of the major Type I arginine methyltransferase PRMT1 causes substrate scavenging by other PRMTs. *Scientific reports* **3**: 1311

di Masi A, Gullotta F, Cappadonna V, Leboffe L, Ascenzi P (2011) Cancer predisposing mutations in BRCT domains. *IUBMB life* **63**: 503-512

Donowitz M, Cha B, Zachos NC, Brett CL, Sharma A, Tse CM, Li X (2005) NHERF family and NHE3 regulation. *The Journal of physiology* **567**: 3-11

Duan G, Walther D (2015) The roles of post-translational modifications in the context of protein interaction networks. *PLoS computational biology* **11**: e1004049

El-Andaloussi N, Valovka T, Toueille M, Hassa PO, Gehrig P, Covic M, Hubscher U, Hottiger MO (2007) Methylation of DNA polymerase beta by protein arginine methyltransferase 1 regulates its binding to proliferating cell nuclear antigen. *FASEB journal : official publication of the Federation of American Societies for Experimental Biology* **21**: 26-34

Espejo A, Cote J, Bednarek A, Richard S, Bedford MT (2002) A protein-domain microarray identifies novel protein-protein interactions. *The Biochemical journal* **367**: 697-702

Fabrizio E, El Messaoudi S, Polanowska J, Paul C, Cook JR, Lee JH, Negre V, Rousset M, Pestka S, Le Cam A, Sardet C (2002) Negative regulation of transcription by the type II arginine methyltransferase PRMT5. *EMBO reports* **3**: 641-645

Feng Y, Wang J, Asher S, Hoang L, Guardiani C, Ivanov I, Zheng YG (2011) Histone H4 acetylation differentially modulates arginine methylation by an in Cis mechanism. *The Journal of biological chemistry* **286**: 20323-20334

Fernandez-Capetillo O, Allis CD, Nussenzweig A (2004) Phosphorylation of histone H2B at DNA double-strand breaks. *The Journal of experimental medicine* **199**: 1671-1677

Filippov AK, Simon J, Barnard EA, Brown DA (2010) The scaffold protein NHERF2 determines the coupling of P2Y1 nucleotide and mGluR5 glutamate receptor to different ion channels in neurons. *J Neurosci* **30**: 11068-11072

Fnu S, Williamson EA, De Haro LP, Brenneman M, Wray J, Shaheen M, Radhakrishnan K, Lee SH, Nickoloff JA, Hromas R (2011) Methylation of histone H3 lysine 36 enhances DNA repair by nonhomologous end-joining. *Proceedings of the National Academy of Sciences of the United States of America* **108**: 540-545

Foote M, Zhou Y (2012) 14-3-3 proteins in neurological disorders. *Int J Biochem Mol Biol* **3**: 152-164

Fradet-Turcotte A, Canny MD, Escribano-Diaz C, Orthwein A, Leung CC, Huang H, Landry MC, Kitevski-LeBlanc J, Noordermeer SM, Sicheri F, Durocher D (2013) 53BP1 is a reader of the DNA-damage-induced H2A Lys 15 ubiquitin mark. *Nature* **499**: 50-54

Frankel A, Clarke S (2000) PRMT3 is a distinct member of the protein arginine N-methyltransferase family. Conferral of substrate specificity by a zinc-finger domain. *The Journal of biological chemistry* **275**: 32974-32982

Frankel A, Yadav N, Lee J, Branscombe TL, Clarke S, Bedford MT (2002) The novel human protein arginine N-methyltransferase PRMT6 is a nuclear enzyme displaying unique substrate specificity. *The Journal of biological chemistry* **277**: 3537-3543

Friesen WJ, Paushkin S, Wyce A, Massenet S, Pesiridis GS, Van Duyne G, Rappsilber J, Mann M, Dreyfuss G (2001) The methylosome, a 20S complex containing JBP1 and pICln, produces dimethylarginine-modified Sm proteins. *Molecular and cellular biology* **21**: 8289-8300

Friesen WJ, Wyce A, Paushkin S, Abel L, Rappsilber J, Mann M, Dreyfuss G (2002) A novel WD repeat protein component of the methylosome binds Sm proteins. *The Journal of biological chemistry* **277**: 8243-8247

Ganguly S, Weller JL, Ho A, Chemineau P, Malpoux B, Klein DC (2005) Melatonin synthesis: 14-3-3-dependent activation and inhibition of arylalkylamine N-acetyltransferase mediated by phosphoserine-205. *Proceedings of the National Academy of Sciences of the United States of America* **102**: 1222-1227

Gayatri S, Cowles MW, Vemulapalli V, Cheng D, Sun ZW, Bedford MT (2016) Using oriented peptide array libraries to evaluate methylarginine-specific antibodies and arginine methyltransferase substrate motifs. *Scientific reports* **6**: 28718

Geiger JC, Lipka J, Segura I, Hoyer S, Schlager MA, Wulf PS, Weinges S, Demmers J, Hoogenraad CC, Acker-Palmer A (2014) The GRIP1/14-3-3 pathway coordinates cargo trafficking and dendrite development. *Dev Cell* **28**: 381-393

Gerloff DL, Woods NT, Farago AA, Monteiro AN (2012) BRCT domains: A little more than kin, and less than kind. *FEBS letters* **586**: 2711-2716

Ghishan FK, Kiela PR (2012) Small intestinal ion transport. *Current opinion in gastroenterology* **28**: 130-134

Glover JN, Williams RS, Lee MS (2004) Interactions between BRCT repeats and phosphoproteins: tangled up in two. *Trends in biochemical sciences* **29**: 579-585

Gu Z, Li Y, Lee P, Liu T, Wan C, Wang Z (2012) Protein arginine methyltransferase 5 functions in opposite ways in the cytoplasm and nucleus of prostate cancer cells. *PloS one* **7**: e44033

Guccione E, Bassi C, Casadio F, Martinato F, Cesaroni M, Schuchlantz H, Luscher B, Amati B (2007) Methylation of histone H3R2 by PRMT6 and H3K4 by an MLL complex are mutually exclusive. *Nature* **449**: 933-937

Guderian G, Peter C, Wiesner J, Sickmann A, Schulze-Osthoff K, Fischer U, Grimm M (2011) RioK1, a new interactor of protein arginine methyltransferase 5 (PRMT5), competes with pICln for binding and modulates PRMT5 complex composition and substrate specificity. *The Journal of biological chemistry* **286**: 1976-1986

Guendel I, Carpio L, Pedati C, Schwartz A, Teal C, Kashanchi F, Kehn-Hall K (2010) Methylation of the tumor suppressor protein, BRCA1, influences its transcriptional cofactor function. *PloS one* **5**: e11379

Guo A, Gu H, Zhou J, Mulhern D, Wang Y, Lee KA, Yang V, Aguiar M, Kornhauser J, Jia X, Ren J, Beausoleil SA, Silva JC, Vemulapalli V, Bedford MT, Comb MJ (2014) Immunoaffinity enrichment and mass spectrometry analysis of protein methylation. *Molecular & cellular proteomics : MCP* **13**: 372-387

Guo S, Bao S (2010) srGAP2 arginine methylation regulates cell migration and cell spreading through promoting dimerization. *The Journal of biological chemistry* **285**: 35133-35141

Guo Z, Kanjanapangka J, Liu N, Liu S, Liu C, Wu Z, Wang Y, Loh T, Kowolik C, Jamsen J, Zhou M, Truong K, Chen Y, Zheng L, Shen B (2012) Sequential posttranslational modifications program FEN1 degradation during cell-cycle progression. *Molecular cell* **47**: 444-456

- Guo Z, Zheng L, Xu H, Dai H, Zhou M, Pascua MR, Chen QM, Shen B (2010) Methylation of FEN1 suppresses nearby phosphorylation and facilitates PCNA binding. *Nature chemical biology* **6**: 766-773
- Gurard-Levin ZA, Quivy JP, Almouzni G (2014) Histone chaperones: assisting histone traffic and nucleosome dynamics. *Annu Rev Biochem* **83**: 487-517
- Gurunathan G, Yu Z, Coulombe Y, Masson JY, Richard S (2015) Arginine methylation of hnRNPUL1 regulates interaction with NBS1 and recruitment to sites of DNA damage. *Scientific reports* **5**: 10475
- Gurung B, Feng Z, Iwamoto DV, Thiel A, Jin G, Fan CM, Ng JM, Curran T, Hua X (2013) Menin epigenetically represses Hedgehog signaling in MEN1 tumor syndrome. *Cancer research* **73**: 2650-2658
- Hadjikyriacou A, Yang Y, Espejo A, Bedford MT, Clarke SG (2015) Unique Features of Human Protein Arginine Methyltransferase 9 (PRMT9) and Its Substrate RNA Splicing Factor SF3B2. *The Journal of biological chemistry* **290**: 16723-16743
- Han X, Li R, Zhang W, Yang X, Wheeler CG, Friedman GK, Province P, Ding Q, You Z, Fathallah-Shaykh HM, Gillespie GY, Zhao X, King PH, Nabors LB (2014) Expression of PRMT5 correlates with malignant grade in gliomas and plays a pivotal role in tumor growth in vitro. *Journal of neuro-oncology* **118**: 61-72
- Hasan S, Stucki M, Hassa PO, Imhof R, Gehrig P, Hunziker P, Hubscher U, Hottiger MO (2001) Regulation of human flap endonuclease-1 activity by acetylation through the transcriptional coactivator p300. *Molecular cell* **7**: 1221-1231
- He W, Ma X, Yang X, Zhao Y, Qiu J, Hang H (2011) A role for the arginine methylation of Rad9 in checkpoint control and cellular sensitivity to DNA damage. *Nucleic acids research* **39**: 4719-4727
- Ho MC, Wilczek C, Bonanno JB, Xing L, Seznec J, Matsui T, Carter LG, Onikubo T, Kumar PR, Chan MK, Brenowitz M, Cheng RH, Reimer U, Almo SC, Shechter D (2013) Structure of the arginine methyltransferase PRMT5-MEP50 reveals a mechanism for substrate specificity. *PloS one* **8**: e57008
- Hornbeck PV, Zhang B, Murray B, Kornhauser JM, Latham V, Skrzypek E (2015) PhosphoSitePlus, 2014: mutations, PTMs and recalibrations. *Nucleic acids research* **43**: D512-520
- Hosfield DJ, Mol CD, Shen B, Tainer JA (1998) Structure of the DNA repair and replication endonuclease and exonuclease FEN-1: coupling DNA and PCNA binding to FEN-1 activity. *Cell* **95**: 135-146

Hryciw DH, Ekberg J, Ferguson C, Lee A, Wang D, Parton RG, Pollock CA, Yun CC, Poronnik P (2006) Regulation of albumin endocytosis by PSD95/Dlg/ZO-1 (PDZ) scaffolds. Interaction of Na⁺-H⁺ exchange regulatory factor-2 with CIC-5. *The Journal of biological chemistry* **281**: 16068-16077

Hsiao KY, Mizzen CA (2013) Histone H4 deacetylation facilitates 53BP1 DNA damage signaling and double-strand break repair. *Journal of molecular cell biology* **5**: 157-165

Hsu JM, Chen CT, Chou CK, Kuo HP, Li LY, Lin CY, Lee HJ, Wang YN, Liu M, Liao HW, Shi B, Lai CC, Bedford MT, Tsai CH, Hung MC (2011) Crosstalk between Arg 1175 methylation and Tyr 1173 phosphorylation negatively modulates EGFR-mediated ERK activation. *Nature cell biology* **13**: 174-181

Hung CM, Li C (2004) Identification and phylogenetic analyses of the protein arginine methyltransferase gene family in fish and ascidians. *Gene* **340**: 179-187

Hunter T (1989) Protein modification: phosphorylation on tyrosine residues. *Current opinion in cell biology* **1**: 1168-1181

Hunter T (2014) The genesis of tyrosine phosphorylation. *Cold Spring Harbor perspectives in biology* **6**: a020644

Hyllus D, Stein C, Schnabel K, Schiltz E, Imhof A, Dou Y, Hsieh J, Bauer UM (2007) PRMT6-mediated methylation of R2 in histone H3 antagonizes H3 K4 trimethylation. *Genes & development* **21**: 3369-3380

Iberg AN, Espejo A, Cheng D, Kim D, Michaud-Levesque J, Richard S, Bedford MT (2008) Arginine methylation of the histone H3 tail impedes effector binding. *The Journal of biological chemistry* **283**: 3006-3010

Ibrahim R, Matsubara D, Osman W, Morikawa T, Goto A, Morita S, Ishikawa S, Aburatani H, Takai D, Nakajima J, Fukayama M, Niki T, Murakami Y (2014) Expression of PRMT5 in lung adenocarcinoma and its significance in epithelial-mesenchymal transition. *Human pathology* **45**: 1397-1405

Ikura T, Tashiro S, Kakino A, Shima H, Jacob N, Amunugama R, Yoder K, Izumi S, Kuraoka I, Tanaka K, Kimura H, Ikura M, Nishikubo S, Ito T, Muto A, Miyagawa K, Takeda S, Fishel R, Igarashi K, Kamiya K (2007) DNA damage-dependent acetylation and ubiquitination of H2AX enhances chromatin dynamics. *Molecular and cellular biology* **27**: 7028-7040

Ivarsson Y (2012) Plasticity of PDZ domains in ligand recognition and signaling. *FEBS letters* **586**: 2638-2647

Jansson M, Durant ST, Cho EC, Sheahan S, Edelman M, Kessler B, La Thangue NB (2008) Arginine methylation regulates the p53 response. *Nature cell biology* **10**: 1431-1439

Jiang W, Roemer ME, Newsham IF (2005) The tumor suppressor DAL-1/4.1B modulates protein arginine N-methyltransferase 5 activity in a substrate-specific manner. *Biochemical and biophysical research communications* **329**: 522-530

Jiang X, Xu Y, Price BD (2010) Acetylation of H2AX on lysine 36 plays a key role in the DNA double-strand break repair pathway. *FEBS letters* **584**: 2926-2930

Jin J, Pawson T (2012) Modular evolution of phosphorylation-based signalling systems. *Philosophical transactions of the Royal Society of London Series B, Biological sciences* **367**: 2540-2555

Jin J, Smith FD, Stark C, Wells CD, Fawcett JP, Kulkarni S, Metalnikov P, O'Donnell P, Taylor P, Taylor L, Zougman A, Woodgett JR, Langeberg LK, Scott JD, Pawson T (2004) Proteomic, functional, and domain-based analysis of in vivo 14-3-3 binding proteins involved in cytoskeletal regulation and cellular organization. *Current biology* : **CB 14**: 1436-1450

Jorgensen PL (1988) Purification of Na⁺,K⁺-ATPase: enzyme sources, preparative problems, and preparation from mammalian kidney. *Methods in enzymology* **156**: 29-43

Jungmichel S, Clapperton JA, Lloyd J, Hari FJ, Spycher C, Pavic L, Li J, Haire LF, Bonalli M, Larsen DH, Lukas C, Lukas J, MacMillan D, Nielsen ML, Stucki M, Smerdon SJ (2012) The molecular basis of ATM-dependent dimerization of the Mdc1 DNA damage checkpoint mediator. *Nucleic acids research* **40**: 3913-3928

Kahn P (1995) From genome to proteome: looking at a cell's proteins. *Science* **270**: 369-370

Kanda M, Shimizu D, Fujii T, Tanaka H, Shibata M, Iwata N, Hayashi M, Kobayashi D, Tanaka C, Yamada S, Nakayama G, Sugimoto H, Koike M, Fujiwara M, Koder Y (2016) Protein arginine methyltransferase 5 is associated with malignant phenotype and peritoneal metastasis in gastric cancer. *International journal of oncology* **49**: 1195-1202

Karkhanis V, Wang L, Tae S, Hu YJ, Imbalzano AN, Sif S (2012) Protein arginine methyltransferase 7 regulates cellular response to DNA damage by methylating promoter histones H2A and H4 of the polymerase delta catalytic subunit gene, POLD1. *The Journal of biological chemistry* **287**: 29801-29814

Katsanis N, Yaspo ML, Fisher EM (1997) Identification and mapping of a novel human gene, HRMT1L1, homologous to the rat protein arginine N-methyltransferase

1 (PRMT1) gene. *Mammalian genome : official journal of the International Mammalian Genome Society* **8**: 526-529

Kawashima SA, Yamagishi Y, Honda T, Ishiguro K, Watanabe Y (2010) Phosphorylation of H2A by Bub1 prevents chromosomal instability through localizing shugoshin. *Science* **327**: 172-177

Kennedy MB (1995) Origin of PDZ (DHR, GLGF) domains. *Trends in biochemical sciences* **20**: 350

Kiela PR, Ghishan FK (2009) Ion transport in the intestine. *Current opinion in gastroenterology* **25**: 87-91

Kim D, Lee J, Cheng D, Li J, Carter C, Richie E, Bedford MT (2010) Enzymatic activity is required for the in vivo functions of CARM1. *The Journal of biological chemistry* **285**: 1147-1152

Kim E, Sheng M (2004) PDZ domain proteins of synapses. *Nature reviews Neuroscience* **5**: 771-781

Kim J, Daniel J, Espejo A, Lake A, Krishna M, Xia L, Zhang Y, Bedford MT (2006) Tudor, MBT and chromo domains gauge the degree of lysine methylation. *EMBO reports* **7**: 397-403

Kim S, Gunesdogan U, Zylicz JJ, Hackett JA, Cougot D, Bao S, Lee C, Dietmann S, Allen GE, Sengupta R, Surani MA (2014) PRMT5 protects genomic integrity during global DNA demethylation in primordial germ cells and preimplantation embryos. *Molecular cell* **56**: 564-579

Kobayashi T, Deak M, Morrice N, Cohen P (1999) Characterization of the structure and regulation of two novel isoforms of serum- and glucocorticoid-induced protein kinase. *The Biochemical journal* **344 Pt 1**: 189-197

Kocinsky HS, Dynia DW, Wang T, Aronson PS (2007) NHE3 phosphorylation at serines 552 and 605 does not directly affect NHE3 activity. *American journal of physiology Renal physiology* **293**: F212-218

Koh CM, Bezzi M, Low DH, Ang WX, Teo SX, Gay FP, Al-Haddawi M, Tan SY, Osato M, Sabo A, Amati B, Wee KB, Guccione E (2015) MYC regulates the core pre-mRNA splicing machinery as an essential step in lymphomagenesis. *Nature* **523**: 96-100

Kohn AD, Takeuchi F, Roth RA (1996) Akt, a pleckstrin homology domain containing kinase, is activated primarily by phosphorylation. *The Journal of biological chemistry* **271**: 21920-21926

Krapivinsky G, Pu W, Wickman K, Krapivinsky L, Clapham DE (1998) pICln binds to a mammalian homolog of a yeast protein involved in regulation of cell morphology. *The Journal of biological chemistry* **273**: 10811-10814

Kryukov GV, Wilson FH, Ruth JR, Paulk J, Tsherniak A, Marlow SE, Vazquez F, Weir BA, Fitzgerald ME, Tanaka M, Bielski CM, Scott JM, Dennis C, Cowley GS, Boehm JS, Root DE, Golub TR, Clish CB, Bradner JE, Hahn WC, Garraway LA (2016) MTAP deletion confers enhanced dependency on the PRMT5 arginine methyltransferase in cancer cells. *Science* **351**: 1214-1218

Kumar S, Maiti S (2013) Effect of different arginine methylations on the thermodynamics of Tat peptide binding to HIV-1 TAR RNA. *Biochimie* **95**: 1422-1431

Kundu K, Backofen R (2014) Cluster based prediction of PDZ-peptide interactions. *BMC genomics* **15 Suppl 1**: S5

Kuo AJ, Song J, Cheung P, Ishibe-Murakami S, Yamazoe S, Chen JK, Patel DJ, Gozani O (2012) The BAH domain of ORC1 links H4K20me2 to DNA replication licensing and Meier-Gorlin syndrome. *Nature* **484**: 115-119

Lacquet LK (1985) Surgical correction of congenital deformities of the anterior chest wall. *Verhandelingen - Koninklijke Academie voor Geneeskunde van België* **47**: 27-47

Lacroix M, El Messaoudi S, Rodier G, Le Cam A, Sardet C, Fabrizio E (2008) The histone-binding protein COPR5 is required for nuclear functions of the protein arginine methyltransferase PRMT5. *EMBO reports* **9**: 452-458

Lakowski TM, Frankel A (2009) Kinetic analysis of human protein arginine N-methyltransferase 2: formation of monomethyl- and asymmetric dimethyl-arginine residues on histone H4. *The Biochemical journal* **421**: 253-261

Lamprecht G, Seidler U (2006) The emerging role of PDZ adapter proteins for regulation of intestinal ion transport. *American journal of physiology Gastrointestinal and liver physiology* **291**: G766-777

Le Guezennec X, Vermeulen M, Brinkman AB, Hoeijmakers WA, Cohen A, Lasonder E, Stunnenberg HG (2006) MBD2/NuRD and MBD3/NuRD, two distinct complexes with different biochemical and functional properties. *Molecular and cellular biology* **26**: 843-851

Lee HJ, Zheng JJ (2010) PDZ domains and their binding partners: structure, specificity, and modification. *Cell communication and signaling : CCS* **8**: 8

- Lee J, Bedford MT (2002) PABP1 identified as an arginine methyltransferase substrate using high-density protein arrays. *EMBO reports* **3**: 268-273
- Lee J, Sayegh J, Daniel J, Clarke S, Bedford MT (2005a) PRMT8, a new membrane-bound tissue-specific member of the protein arginine methyltransferase family. *The Journal of biological chemistry* **280**: 32890-32896
- Lee JH, Cook JR, Pollack BP, Kinzy TG, Norris D, Pestka S (2000) Hsl7p, the yeast homologue of human JBP1, is a protein methyltransferase. *Biochemical and biophysical research communications* **274**: 105-111
- Lee JH, Cook JR, Yang ZH, Mirochnitchenko O, Gunderson SI, Felix AM, Herth N, Hoffmann R, Pestka S (2005b) PRMT7, a new protein arginine methyltransferase that synthesizes symmetric dimethylarginine. *The Journal of biological chemistry* **280**: 3656-3664
- Levine SA, Montrose MH, Tse CM, Donowitz M (1993) Kinetics and regulation of three cloned mammalian Na⁺/H⁺ exchangers stably expressed in a fibroblast cell line. *The Journal of biological chemistry* **268**: 25527-25535
- Li Q, Zhao Y, Yue M, Xue Y, Bao S (2016) The Protein Arginine Methylase 5 (PRMT5/SKB1) Gene Is Required for the Maintenance of Root Stem Cells in Response to DNA Damage. *Journal of genetics and genomics = Yi chuan xue bao* **43**: 187-197
- Li Z, Yu J, Hosohama L, Nee K, Gkoutela S, Chaudhari S, Cass AA, Xiao X, Clark AT (2015) The Sm protein methyltransferase PRMT5 is not required for primordial germ cell specification in mice. *The EMBO journal* **34**: 748-758
- Liang JJ, Wang Z, Chiriboga L, Greco MA, Shapiro E, Huang H, Yang XJ, Huang J, Peng Y, Melamed J, Garabedian MJ, Lee P (2007) The expression and function of androgen receptor coactivator p44 and protein arginine methyltransferase 5 in the developing testis and testicular tumors. *The Journal of urology* **177**: 1918-1922
- Lieber MR (2010) The mechanism of double-strand DNA break repair by the nonhomologous DNA end-joining pathway. *Annu Rev Biochem* **79**: 181-211
- Likhite N, Jackson CA, Liang MS, Krzyzanowski MC, Lei P, Wood JF, Birkaya B, Michaels KL, Andreadis ST, Clark SD, Yu MC, Ferkey DM (2015) The protein arginine methyltransferase PRMT5 promotes D2-like dopamine receptor signaling. *Science signaling* **8**: ra115
- Lim Y, Kwon YH, Won NH, Min BH, Park IS, Paik WK, Kim S (2005) Multimerization of expressed protein-arginine methyltransferases during the growth and differentiation of rat liver. *Biochimica et biophysica acta* **1723**: 240-247

Liu BA, Jablonowski K, Raina M, Arce M, Pawson T, Nash PD (2006) The human and mouse complement of SH2 domain proteins-establishing the boundaries of phosphotyrosine signaling. *Molecular cell* **22**: 851-868

Liu F, Cheng G, Hamard PJ, Greenblatt S, Wang L, Man N, Perna F, Xu H, Tadi M, Luciani L, Nimer SD (2015) Arginine methyltransferase PRMT5 is essential for sustaining normal adult hematopoiesis. *The Journal of clinical investigation* **125**: 3532-3544

Liu F, Zhao X, Perna F, Wang L, Koppikar P, Abdel-Wahab O, Harr MW, Levine RL, Xu H, Tefferi A, Deblasio A, Hatlen M, Menendez S, Nimer SD (2011) JAK2V617F-mediated phosphorylation of PRMT5 downregulates its methyltransferase activity and promotes myeloproliferation. *Cancer cell* **19**: 283-294

Liu L, Zhao X, Zhao L, Li J, Yang H, Zhu Z, Liu J, Huang G (2016) Arginine Methylation of SREBP1a via PRMT5 Promotes De Novo Lipogenesis and Tumor Growth. *Cancer research* **76**: 1260-1272

Lou Z, Minter-Dykhouse K, Wu X, Chen J (2003) MDC1 is coupled to activated CHK2 in mammalian DNA damage response pathways. *Nature* **421**: 957-961

Lu J, Matunis MJ (2013) A mediator methylation mystery: JMJD1C demethylates MDC1 to regulate DNA repair. *Nature structural & molecular biology* **20**: 1346-1348

Mahajan A, Yuan C, Lee H, Chen ES, Wu PY, Tsai MD (2008) Structure and function of the phosphothreonine-specific FHA domain. *Science signaling* **1**: re12

Mailand N, Bekker-Jensen S, Faustrup H, Melander F, Bartek J, Lukas C, Lukas J (2007) RNF8 ubiquitylates histones at DNA double-strand breaks and promotes assembly of repair proteins. *Cell* **131**: 887-900

Marchler-Bauer A, Derbyshire MK, Gonzales NR, Lu S, Chitsaz F, Geer LY, Geer RC, He J, Gwadz M, Hurwitz DI, Lanczycki CJ, Lu F, Marchler GH, Song JS, Thanki N, Wang Z, Yamashita RA, Zhang D, Zheng C, Bryant SH (2015) CDD: NCBI's conserved domain database. *Nucleic acids research* **43**: D222-226

Mavrakis KJ, McDonald ER, 3rd, Schlabach MR, Billy E, Hoffman GR, deWeck A, Ruddy DA, Venkatesan K, Yu J, McAllister G, Stump M, deBeaumont R, Ho S, Yue Y, Liu Y, Yan-Neale Y, Yang G, Lin F, Yin H, Gao H, Kipp DR, Zhao S, McNamara JT, Sprague ER, Zheng B, Lin Y, Cho YS, Gu J, Crawford K, Ciccone D, Vitari AC, Lai A, Capka V, Hurov K, Porter JA, Tallarico J, Mickanin C, Lees E, Pagliarini R, Keen N, Schmelzle T, Hofmann F, Stegmeier F, Sellers WR (2016) Disordered methionine metabolism in MTAP/CDKN2A-deleted cancers leads to dependence on PRMT5. *Science* **351**: 1208-1213

McGraw S, Vigneault C, Sirard MA (2007) Temporal expression of factors involved in chromatin remodeling and in gene regulation during early bovine in vitro embryo development. *Reproduction* **133**: 597-608

Meek SE, Lane WS, Piwnica-Worms H (2004) Comprehensive proteomic analysis of interphase and mitotic 14-3-3-binding proteins. *The Journal of biological chemistry* **279**: 32046-32054

Meister G, Eggert C, Buhler D, Brahms H, Kambach C, Fischer U (2001) Methylation of Sm proteins by a complex containing PRMT5 and the putative U snRNP assembly factor pICln. *Current biology* : **CB 11**: 1990-1994

Meister G, Fischer U (2002) Assisted RNP assembly: SMN and PRMT5 complexes cooperate in the formation of spliceosomal UsnRNPs. *The EMBO journal* **21**: 5853-5863

Melander F, Bekker-Jensen S, Falck J, Bartek J, Mailand N, Lukas J (2008) Phosphorylation of SDT repeats in the MDC1 N terminus triggers retention of NBS1 at the DNA damage-modified chromatin. *The Journal of cell biology* **181**: 213-226

Meyer R, Wolf SS, Obendorf M (2007) PRMT2, a member of the protein arginine methyltransferase family, is a coactivator of the androgen receptor. *The Journal of steroid biochemistry and molecular biology* **107**: 1-14

Migliori V, Muller J, Phalke S, Low D, Bezzi M, Mok WC, Sahu SK, Gunaratne J, Capasso P, Bassi C, Cecatiello V, De Marco A, Blackstock W, Kuznetsov V, Amati B, Mapelli M, Guccione E (2012) Symmetric dimethylation of H3R2 is a newly identified histone mark that supports euchromatin maintenance. *Nature structural & molecular biology* **19**: 136-144

Miller KM, Tjeertes JV, Coates J, Legube G, Polo SE, Britton S, Jackson SP (2010) Human HDAC1 and HDAC2 function in the DNA-damage response to promote DNA nonhomologous end-joining. *Nature structural & molecular biology* **17**: 1144-1151

Mohammad DH, Yaffe MB (2009) 14-3-3 proteins, FHA domains and BRCT domains in the DNA damage response. *DNA repair* **8**: 1009-1017

Morrison DK (2009) The 14-3-3 proteins: integrators of diverse signaling cues that impact cell fate and cancer development. *Trends Cell Biol* **19**: 16-23

Moyal L, Lerenthal Y, Gana-Weisz M, Mass G, So S, Wang SY, Eppink B, Chung YM, Shalev G, Shema E, Shkedy D, Smorodinsky NI, van Vliet N, Kuster B, Mann M, Ciechanover A, Dahm-Daphi J, Kanaar R, Hu MC, Chen DJ, Oren M, Shiloh Y (2011) Requirement of ATM-dependent monoubiquitylation of histone H2B for timely repair of DNA double-strand breaks. *Molecular cell* **41**: 529-542

Murdoch JN, Henderson DJ, Doudney K, Gaston-Massuet C, Phillips HM, Paternotte C, Arkell R, Stanier P, Copp AJ (2003) Disruption of scribble (*Scrb1*) causes severe neural tube defects in the circletail mouse. *Hum Mol Genet* **12**: 87-98

Murtazina R, Kovbasnjuk O, Chen TE, Zachos NC, Chen Y, Kocinsky HS, Hogema BM, Seidler U, de Jonge HR, Donowitz M (2011) NHERF2 is necessary for basal activity, second messenger inhibition, and LPA stimulation of NHE3 in mouse distal ileum. *American journal of physiology Cell physiology* **301**: C126-136

Nakamura K, Kato A, Kobayashi J, Yanagihara H, Sakamoto S, Oliveira DV, Shimada M, Tauchi H, Suzuki H, Tashiro S, Zou L, Komatsu K (2011) Regulation of homologous recombination by RNF20-dependent H2B ubiquitination. *Molecular cell* **41**: 515-528

Nourry C, Grant SG, Borg JP (2003) PDZ domain proteins: plug and play! *Science's STKE : signal transduction knowledge environment* **2003**: RE7

Ogiwara H, Ui A, Otsuka A, Satoh H, Yokomi I, Nakajima S, Yasui A, Yokota J, Kohno T (2011) Histone acetylation by CBP and p300 at double-strand break sites facilitates SWI/SNF chromatin remodeling and the recruitment of non-homologous end joining factors. *Oncogene* **30**: 2135-2146

Paik WK, Kim S (1968) Protein methylase I. Purification and properties of the enzyme. *The Journal of biological chemistry* **243**: 2108-2114

Pal S, Baiocchi RA, Byrd JC, Grever MR, Jacob ST, Sif S (2007) Low levels of miR-92b/96 induce PRMT5 translation and H3R8/H4R3 methylation in mantle cell lymphoma. *The EMBO journal* **26**: 3558-3569

Pal S, Vishwanath SN, Erdjument-Bromage H, Tempst P, Sif S (2004) Human SWI/SNF-associated PRMT5 methylates histone H3 arginine 8 and negatively regulates expression of ST7 and NM23 tumor suppressor genes. *Molecular and cellular biology* **24**: 9630-9645

Pal S, Yun R, Datta A, Lacomis L, Erdjument-Bromage H, Kumar J, Tempst P, Sif S (2003) mSin3A/histone deacetylase 2- and PRMT5-containing Brg1 complex is involved in transcriptional repression of the Myc target gene *cad*. *Molecular and cellular biology* **23**: 7475-7487

Panier S, Boulton SJ (2014) Double-strand break repair: 53BP1 comes into focus. *Nature reviews Molecular cell biology* **15**: 7-18

Paquet M, Kuwajima M, Yun CC, Smith Y, Hall RA (2006) Astrocytic and neuronal localization of the scaffold protein Na⁺/H⁺ exchanger regulatory factor 2 (NHERF-2) in mouse brain. *The Journal of comparative neurology* **494**: 752-762

Park JH, Szemes M, Vieira GC, Melegh Z, Malik S, Heesom KJ, Von Wallwitz-Freitas L, Greenhough A, Brown KW, Zheng YG, Catchpoole D, Deery MJ, Malik K (2015) Protein arginine methyltransferase 5 is a key regulator of the MYCN oncoprotein in neuroblastoma cells. *Molecular oncology* **9**: 617-627

Park KS, Jeong MS, Kim JH, Jang SB (2005) Overexpression, purification, and characterization of PDZ domain proteins NHERF and E3KARP in Escherichia coli. *Protein expression and purification* **40**: 197-202

Paull TT, Rogakou EP, Yamazaki V, Kirchgessner CU, Gellert M, Bonner WM (2000) A critical role for histone H2AX in recruitment of repair factors to nuclear foci after DNA damage. *Current biology : CB* **10**: 886-895

Pawlak MR, Scherer CA, Chen J, Roshon MJ, Ruley HE (2000) Arginine N-methyltransferase 1 is required for early postimplantation mouse development, but cells deficient in the enzyme are viable. *Molecular and cellular biology* **20**: 4859-4869

Pei H, Zhang L, Luo K, Qin Y, Chesi M, Fei F, Bergsagel PL, Wang L, You Z, Lou Z (2011) MMSET regulates histone H4K20 methylation and 53BP1 accumulation at DNA damage sites. *Nature* **470**: 124-128

Pollack BP, Kotenko SV, He W, Izotova LS, Barnoski BL, Pestka S (1999) The human homologue of the yeast proteins Skb1 and Hsl7p interacts with Jak kinases and contains protein methyltransferase activity. *The Journal of biological chemistry* **274**: 31531-31542

Powers MA, Fay MM, Factor RE, Welm AL, Ullman KS (2011) Protein arginine methyltransferase 5 accelerates tumor growth by arginine methylation of the tumor suppressor programmed cell death 4. *Cancer research* **71**: 5579-5587

Pozuelo Rubio M, Geraghty KM, Wong BH, Wood NT, Campbell DG, Morrice N, Mackintosh C (2004) 14-3-3-affinity purification of over 200 human phosphoproteins reveals new links to regulation of cellular metabolism, proliferation and trafficking. *The Biochemical journal* **379**: 395-408

Qi C, Chang J, Zhu Y, Yeldandi AV, Rao SM, Zhu YJ (2002) Identification of protein arginine methyltransferase 2 as a coactivator for estrogen receptor alpha. *The Journal of biological chemistry* **277**: 28624-28630

Raman B, Guarnaccia C, Nadassy K, Zakhariyev S, Pintar A, Zanuttin F, Frigyes D, Acatrinei C, Vindigni A, Pongor G, Pongor S (2001) N(omega)-arginine dimethylation modulates the interaction between a Gly/Arg-rich peptide from human nucleolin and nucleic acids. *Nucleic acids research* **29**: 3377-3384

Rank G, Cerruti L, Simpson RJ, Moritz RL, Jane SM, Zhao Q (2010) Identification of a PRMT5-dependent repressor complex linked to silencing of human fetal globin gene expression. *Blood* **116**: 1585-1592

Ren B, Li X, Zhang J, Fan J, Duan J, Chen Y (2015) PDLIM5 mediates PKCepsilon translocation in PMA-induced growth cone collapse. *Cell Signal* **27**: 424-435

Rho J, Choi S, Jung CR, Im DS (2007) Arginine methylation of Sam68 and SLM proteins negatively regulates their poly(U) RNA binding activity. *Archives of biochemistry and biophysics* **466**: 49-57

Rogakou EP, Pilch DR, Orr AH, Ivanova VS, Bonner WM (1998) DNA double-stranded breaks induce histone H2AX phosphorylation on serine 139. *The Journal of biological chemistry* **273**: 5858-5868

Romero G, von Zastrow M, Friedman PA (2011) Role of PDZ proteins in regulating trafficking, signaling, and function of GPCRs: means, motif, and opportunity. *Advances in pharmacology* **62**: 279-314

Sanders SL, Portoso M, Mata J, Bahler J, Allshire RC, Kouzarides T (2004) Methylation of histone H4 lysine 20 controls recruitment of Crb2 to sites of DNA damage. *Cell* **119**: 603-614

Sayegh J, Webb K, Cheng D, Bedford MT, Clarke SG (2007) Regulation of protein arginine methyltransferase 8 (PRMT8) activity by its N-terminal domain. *The Journal of biological chemistry* **282**: 36444-36453

Schotta G, Sengupta R, Kubicek S, Malin S, Kauer M, Callen E, Celeste A, Pagani M, Opravil S, De La Rosa-Velazquez IA, Espejo A, Bedford MT, Nussenzweig A, Busslinger M, Jenuwein T (2008) A chromatin-wide transition to H4K20 monomethylation impairs genome integrity and programmed DNA rearrangements in the mouse. *Genes & development* **22**: 2048-2061

Scott HS, Antonarakis SE, Lalioti MD, Rossier C, Silver PA, Henry MF (1998) Identification and characterization of two putative human arginine methyltransferases (HRMT1L1 and HRMT1L2). *Genomics* **48**: 330-340

Scully R, Xie A (2013) Double strand break repair functions of histone H2AX. *Mutat Res* **750**: 5-14

Seidler U, Singh A, Chen M, Cinar A, Bachmann O, Zheng W, Wang J, Yeruva S, Riederer B (2009) Knockout mouse models for intestinal electrolyte transporters and regulatory PDZ adaptors: new insights into cystic fibrosis, secretory diarrhoea and fructose-induced hypertension. *Experimental physiology* **94**: 175-179

Sharma GG, So S, Gupta A, Kumar R, Cayrou C, Avvakumov N, Bhadra U, Pandita RK, Porteus MH, Chen DJ, Cote J, Pandita TK (2010) MOF and histone H4 acetylation at lysine 16 are critical for DNA damage response and double-strand break repair. *Molecular and cellular biology* **30**: 3582-3595

Shilo K, Wu X, Sharma S, Welliver M, Duan W, Villalona-Calero M, Fukuoka J, Sif S, Baiocchi R, Hitchcock CL, Zhao W, Otterson GA (2013) Cellular localization of protein arginine methyltransferase-5 correlates with grade of lung tumors. *Diagnostic pathology* **8**: 201

Shimada M, Niida H, Zineldeen DH, Tagami H, Tanaka M, Saito H, Nakanishi M (2008) Chk1 is a histone H3 threonine 11 kinase that regulates DNA damage-induced transcriptional repression. *Cell* **132**: 221-232

Shimazaki N, Tsai AG, Lieber MR (2009) H3K4me3 stimulates the V(D)J RAG complex for both nicking and hairpinning in trans in addition to tethering in cis: implications for translocations. *Molecular cell* **34**: 535-544

Smith AJ, Daut J, Schwappach B (2011) Membrane proteins as 14-3-3 clients in functional regulation and intracellular transport. *Physiology* **26**: 181-191

Stallcup MR, Chen D, Koh SS, Ma H, Lee YH, Li H, Schurter BT, Aswad DW (2000) Co-operation between protein-acetylating and protein-methylating co-activators in transcriptional activation. *Biochemical Society transactions* **28**: 415-418

Stanlie A, Aida M, Muramatsu M, Honjo T, Begum NA (2010) Histone3 lysine4 trimethylation regulated by the facilitates chromatin transcription complex is critical for DNA cleavage in class switch recombination. *Proceedings of the National Academy of Sciences of the United States of America* **107**: 22190-22195

Steichen JM, Kuchinskas M, Keshwani MM, Yang J, Adams JA, Taylor SS (2012) Structural basis for the regulation of protein kinase A by activation loop phosphorylation. *The Journal of biological chemistry* **287**: 14672-14680

Stiffler MA, Chen JR, Grantcharova VP, Lei Y, Fuchs D, Allen JE, Zaslavskaja LA, MacBeath G (2007) PDZ domain binding selectivity is optimized across the mouse proteome. *Science* **317**: 364-369

Stopa N, Krebs JE, Shechter D (2015) The PRMT5 arginine methyltransferase: many roles in development, cancer and beyond. *Cellular and molecular life sciences* : *CMLS* **72**: 2041-2059

Sun L, Wang M, Lv Z, Yang N, Liu Y, Bao S, Gong W, Xu RM (2011) Structural insights into protein arginine symmetric dimethylation by PRMT5. *Proceedings of the National Academy of Sciences of the United States of America* **108**: 20538-20543

Sun Y, Jiang X, Xu Y, Ayrapetov MK, Moreau LA, Whetstine JR, Price BD (2009) Histone H3 methylation links DNA damage detection to activation of the tumour suppressor Tip60. *Nature cell biology* **11**: 1376-1382

Swiercz R, Cheng D, Kim D, Bedford MT (2007) Ribosomal protein rpS2 is hypomethylated in PRMT3-deficient mice. *The Journal of biological chemistry* **282**: 16917-16923

Swiercz R, Person MD, Bedford MT (2005) Ribosomal protein S2 is a substrate for mammalian PRMT3 (protein arginine methyltransferase 3). *The Biochemical journal* **386**: 85-91

Tae S, Karkhanis V, Velasco K, Yaneva M, Erdjument-Bromage H, Tempst P, Sif S (2011) Bromodomain protein 7 interacts with PRMT5 and PRC2, and is involved in transcriptional repression of their target genes. *Nucleic acids research* **39**: 5424-5438

Tamburini BA, Tyler JK (2005) Localized histone acetylation and deacetylation triggered by the homologous recombination pathway of double-strand DNA repair. *Molecular and cellular biology* **25**: 4903-4913

Tan CP, Nakielny S (2006) Control of the DNA methylation system component MBD2 by protein arginine methylation. *Molecular and cellular biology* **26**: 7224-7235

Tang J, Frankel A, Cook RJ, Kim S, Paik WK, Williams KR, Clarke S, Herschman HR (2000) PRMT1 is the predominant type I protein arginine methyltransferase in mammalian cells. *The Journal of biological chemistry* **275**: 7723-7730

Tang J, Gary JD, Clarke S, Herschman HR (1998) PRMT 3, a type I protein arginine N-methyltransferase that differs from PRMT1 in its oligomerization, subcellular localization, substrate specificity, and regulation. *The Journal of biological chemistry* **273**: 16935-16945

Tarighat SS, Santhanam R, Frankhouser D, Radomska HS, Lai H, Anghelina M, Wang H, Huang X, Alinari L, Walker A, Caligiuri MA, Croce CM, Li L, Garzon R, Li C, Baiocchi RA, Marcucci G (2016) The dual epigenetic role of PRMT5 in acute myeloid leukemia: gene activation and repression via histone arginine methylation. *Leukemia* **30**: 789-799

Tee WW, Pardo M, Theunissen TW, Yu L, Choudhary JS, Hajkova P, Surani MA (2010) Prmt5 is essential for early mouse development and acts in the cytoplasm to maintain ES cell pluripotency. *Genes & development* **24**: 2772-2777

Troffer-Charlier N, Cura V, Hassenboehler P, Moras D, Cavarelli J (2007) Functional insights from structures of coactivator-associated arginine methyltransferase 1 domains. *The EMBO journal* **26**: 4391-4401

Uhart M, Bustos DM (2013) Human 14-3-3 paralogs differences uncovered by cross-talk of phosphorylation and lysine acetylation. *PLoS one* **8**: e55703

Uhlen M, Fagerberg L, Hallstrom BM, Lindskog C, Oksvold P, Mardinoglu A, Sivertsson A, Kampf C, Sjostedt E, Asplund A, Olsson I, Edlund K, Lundberg E, Navani S, Szigartyo CA, Odeberg J, Djureinovic D, Takanen JO, Hober S, Alm T, Edqvist PH, Berling H, Tegel H, Mulder J, Rockberg J, Nilsson P, Schwenk JM, Hamsten M, von Feilitzen K, Forsberg M, Persson L, Johansson F, Zwahlen M, von Heijne G, Nielsen J, Ponten F (2015) Proteomics. Tissue-based map of the human proteome. *Science* **347**: 1260419

Uitley RT, Lacoste N, Jobin-Robitaille O, Allard S, Cote J (2005) Regulation of NuA4 histone acetyltransferase activity in transcription and DNA repair by phosphorylation of histone H4. *Molecular and cellular biology* **25**: 8179-8190

Volkmer E, Karnitz LM (1999) Human homologs of *Schizosaccharomyces pombe* rad1, hus1, and rad9 form a DNA damage-responsive protein complex. *The Journal of biological chemistry* **274**: 567-570

Wade JB, Liu J, Coleman RA, Cunningham R, Steplock DA, Lee-Kwon W, Pallone TL, Shenolikar S, Weinman EJ (2003) Localization and interaction of NHERF isoforms in the renal proximal tubule of the mouse. *American journal of physiology Cell physiology* **285**: C1494-1503

Waldmann T, Izzo A, Kamieniarz K, Richter F, Vogler C, Sarg B, Lindner H, Young NL, Mittler G, Garcia BA, Schneider R (2011) Methylation of H2AR29 is a novel repressive PRMT6 target. *Epigenetics & chromatin* **4**: 11

Walport LJ, Hopkinson RJ, Chowdhury R, Schiller R, Ge W, Kawamura A, Schofield CJ (2016) Arginine demethylation is catalysed by a subset of JmjC histone lysine demethylases. *Nature communications* **7**: 11974

Walsh CT, Garneau-Tsodikova S, Gatto GJ, Jr. (2005) Protein posttranslational modifications: the chemistry of proteome diversifications. *Angewandte Chemie* **44**: 7342-7372

Wang C, Sun H, Zou R, Zhou T, Wang S, Sun S, Tong C, Luo H, Li Y, Li Z, Wang E, Chen Y, Cao L, Li F, Zhao Y (2015) MDC1 functionally identified as an androgen receptor co-activator participates in suppression of prostate cancer. *Nucleic acids research* **43**: 4893-4908

Weimann M, Grossmann A, Woodsmith J, Ozkan Z, Birth P, Meierhofer D, Benlasfer N, Valovka T, Timmermann B, Wanker EE, Sauer S, Stelzl U (2013) A Y2H-seq approach defines the human protein methyltransferase interactome. *Nature methods* **10**: 339-342

Weiss VH, McBride AE, Soriano MA, Filman DJ, Silver PA, Hogle JM (2000) The structure and oligomerization of the yeast arginine methyltransferase, Hmt1. *Nature structural biology* **7**: 1165-1171

Wilker EW, Grant RA, Artim SC, Yaffe MB (2005) A structural basis for 14-3-3sigma functional specificity. *The Journal of biological chemistry* **280**: 18891-18898

Williamson EA, Wray JW, Bansal P, Hromas R (2012) Overview for the histone codes for DNA repair. *Prog Mol Biol Transl Sci* **110**: 207-227

Xiao A, Li H, Shechter D, Ahn SH, Fabrizio LA, Erdjument-Bromage H, Ishibe-Murakami S, Wang B, Tempst P, Hofmann K, Patel DJ, Elledge SJ, Allis CD (2009) WSTF regulates the H2A.X DNA damage response via a novel tyrosine kinase activity. *Nature* **457**: 57-62

Xiao B, Smerdon SJ, Jones DH, Dodson GG, Soneji Y, Aitken A, Gamblin SJ (1995) Structure of a 14-3-3 protein and implications for coordination of multiple signalling pathways. *Nature* **376**: 188-191

Yadav N, Lee J, Kim J, Shen J, Hu MC, Aldaz CM, Bedford MT (2003) Specific protein methylation defects and gene expression perturbations in coactivator-associated arginine methyltransferase 1-deficient mice. *Proceedings of the National Academy of Sciences of the United States of America* **100**: 6464-6468

Yaffe MB (2002) Phosphotyrosine-binding domains in signal transduction. *Nature reviews Molecular cell biology* **3**: 177-186

Yaffe MB, Rittinger K, Volinia S, Caron PR, Aitken A, Leffers H, Gamblin SJ, Smerdon SJ, Cantley LC (1997) The structural basis for 14-3-3:phosphopeptide binding specificity. *Cell* **91**: 961-971

Yan F, Alinari L, Lustberg ME, Martin LK, Cordero-Nieves HM, Banasavadi-Siddegowda Y, Virk S, Barnholtz-Sloan J, Bell EH, Wojton J, Jacob NK, Chakravarti A, Nowicki MO, Wu X, Lapalombella R, Datta J, Yu B, Gordon K, Haseley A, Patton JT, Smith PL, Ryu J, Zhang X, Mo X, Marcucci G, Nuovo G, Kwon CH, Byrd JC, Chiocca EA, Li C, Sif S, Jacob S, Lawler S, Kaur B, Baiocchi RA (2014) Genetic validation of the protein arginine methyltransferase PRMT5 as a candidate therapeutic target in glioblastoma. *Cancer research* **74**: 1752-1765

Yan Q, Dutt S, Xu R, Graves K, Juszczynski P, Manis JP, Shipp MA (2009) BBAP monoubiquitylates histone H4 at lysine 91 and selectively modulates the DNA damage response. *Molecular cell* **36**: 110-120

Yanagida M, Hayano T, Yamauchi Y, Shinkawa T, Natsume T, Isobe T, Takahashi N (2004) Human fibrillarin forms a sub-complex with splicing factor 2-associated p32,

protein arginine methyltransferases, and tubulins alpha 3 and beta 1 that is independent of its association with preribosomal ribonucleoprotein complexes. *The Journal of biological chemistry* **279**: 1607-1614

Yang C, Wang H, Xu Y, Brinkman KL, Ishiyama H, Wong ST, Xu B (2012) The kinetochore protein Bub1 participates in the DNA damage response. *DNA repair* **11**: 185-191

Yang D, Liang T, Gu Y, Zhao Y, Shi Y, Zuo X, Cao Q, Yang Y, Kan Q (2016) Protein N-arginine methyltransferase 5 promotes the tumor progression and radioresistance of nasopharyngeal carcinoma. *Oncology reports* **35**: 1703-1710

Yang J, Sarker R, Singh V, Sarker P, Yin J, Chen TE, Chaerkady R, Li X, Tse CM, Donowitz M (2015) The NHERF2 sequence adjacent and upstream of the ERM-binding domain affects NHERF2-ezrin binding and dexamethasone stimulated NHE3 activity. *The Biochemical journal* **470**: 77-90

Yang M, Sun J, Sun X, Shen Q, Gao Z, Yang C (2009) Caenorhabditis elegans protein arginine methyltransferase PRMT-5 negatively regulates DNA damage-induced apoptosis. *PLoS genetics* **5**: e1000514

Yang Y, Lu Y, Espejo A, Wu J, Xu W, Liang S, Bedford MT (2010) TDRD3 is an effector molecule for arginine-methylated histone marks. *Molecular cell* **40**: 1016-1023

Yoo BK, Yanda MK, No YR, Yun CC (2012) Human intestinal epithelial cell line SK-CO15 is a new model system to study Na(+)/H(+) exchanger 3. *American journal of physiology Gastrointestinal and liver physiology* **303**: G180-188

Yoshimoto T, Boehm M, Olive M, Crook MF, San H, Langenickel T, Nabel EG (2006) The arginine methyltransferase PRMT2 binds RB and regulates E2F function. *Experimental cell research* **312**: 2040-2053

Yu X, Chini CC, He M, Mer G, Chen J (2003) The BRCT domain is a phospho-protein binding domain. *Science* **302**: 639-642

Yu Z, Chen T, Hebert J, Li E, Richard S (2009) A mouse PRMT1 null allele defines an essential role for arginine methylation in genome maintenance and cell proliferation. *Molecular and cellular biology* **29**: 2982-2996

Yue WW, Hassler M, Roe SM, Thompson-Vale V, Pearl LH (2007) Insights into histone code syntax from structural and biochemical studies of CARM1 methyltransferase. *The EMBO journal* **26**: 4402-4412

Zachos NC, Tse M, Donowitz M (2005) Molecular physiology of intestinal Na⁺/H⁺ exchange. *Annual review of physiology* **67**: 411-443

Zhang HT, Zhang D, Zha ZG, Hu CD (2014) Transcriptional activation of PRMT5 by NF-Y is required for cell growth and negatively regulated by the PKC/c-Fos signaling in prostate cancer cells. *Biochimica et biophysica acta* **1839**: 1330-1340

Zhang M, Wang W (2003) Organization of signaling complexes by PDZ-domain scaffold proteins. *Accounts of chemical research* **36**: 530-538

Zhang T, Gunther S, Looso M, Kunne C, Kruger M, Kim J, Zhou Y, Braun T (2015) Prmt5 is a regulator of muscle stem cell expansion in adult mice. *Nature communications* **6**: 7140

Zhang X, Zhou L, Cheng X (2000) Crystal structure of the conserved core of protein arginine methyltransferase PRMT3. *The EMBO journal* **19**: 3509-3519

Zhang Z, Lotti F, Dittmar K, Younis I, Wan L, Kasim M, Dreyfuss G (2008) SMN deficiency causes tissue-specific perturbations in the repertoire of snRNAs and widespread defects in splicing. *Cell* **133**: 585-600

Zhao Q, Rank G, Tan YT, Li H, Moritz RL, Simpson RJ, Cerruti L, Curtis DJ, Patel DJ, Allis CD, Cunningham JM, Jane SM (2009) PRMT5-mediated methylation of histone H4R3 recruits DNMT3A, coupling histone and DNA methylation in gene silencing. *Nature structural & molecular biology* **16**: 304-311

Zou R, Zhong X, Wang C, Sun H, Wang S, Lin L, Sun S, Tong C, Luo H, Gao P, Li Y, Zhou T, Li D, Cao L, Zhao Y (2015) MDC1 Enhances Estrogen Receptor-mediated Transactivation and Contributes to Breast Cancer Suppression. *International journal of biological sciences* **11**: 992-1005

Zurita-Lopez CI, Sandberg T, Kelly R, Clarke SG (2012) Human protein arginine methyltransferase 7 (PRMT7) is a type III enzyme forming omega-NG-monomethylated arginine residues. *The Journal of biological chemistry* **287**: 7859-7870

Chapter: 8 Vita

Alexsandra B. Espejo Lataillade was born in Santiago, Chile on July 25, 1974, the daughter of Ivette Lataillade Meza and German Espejo Castro. After completing her work at Alexander Fleming High School, Santiago, Chile in 1993, she entered University of Concepcion, Concepcion, Chile. She received the degree of Bachelor of Science in Marine Biology from University of Concepcion in March 2000. For the next nine years, she worked as a Research Investigator in the Department of Epigenetic and Molecular Carcinogenesis at University of Texas, M.D. Anderson Cancer Center. In May of 2010 she entered The University of Texas Graduate School of Biomedical Sciences at Houston.

Permanent address:

193 Piney Ridge
Bastrop, TX 78602

APPENDIX A



KINEXUS

SUBSTRATE PROFILING SERVICES

PROFILING OF 1 PEPTIDE SUBSTRATE

AGAINST 295 PROTEIN KINASES

ORDER 3220

Principal Investigator: Dr. Mark Bedford

Institution: M.D. Anderson Cancer Center

Completion Date: March 6, 2015

Report Contact: Ms. Catherine Sutter

Telephone: 604-323-2547, Ext 11

Email: info@kinexus.ca

8755 Ash Street, Suite 1, Vancouver, B.C. Canada V6P 6T3

T: 604.323.2547 • F: 604.323.2548 • E: info@kinexus.ca • www.kinexus.ca

Table of Contents

1. OVERVIEW OF SERVICE

Introduction	3
Enzyme and Substrate Targets	3
Confidentiality	4

2. OBJECTIVES

Service Requested	4
-------------------------	---

3. MATERIALS

Quality Control & Reagents	4
----------------------------------	---

4. RESULTS

Evaluation	4-5
Activity.....	6-13

5. DISCUSSION

Conclusion	13-14
------------------	-------

6. APPENDIX A - METHODOLOGY

Protein Kinase Assays	15
Raw Data	16-22

1. OVERVIEW OF PROFILING SERVICE

Introduction

The Kinexus Kinase/Phosphatase Profiling Services access a large and diverse panel of highly active protein kinases and protein phosphatases for screening substrates and bioactive compounds. These active enzyme preparations are subjected to rigorous quality control analyses and are extensively assayed against a panel of biologically relevant substrates and optimized synthetic peptides to ensure that all test reactions are performed under optimal assay conditions. These protein kinase/phosphatase profiling services determine the extent of phosphorylation or dephosphorylation of a selected substrate to understand the putative mechanisms of action of bioactive compounds and to support the identification of the upstream protein kinases and protein phosphatases and their substrate proteins in signalling networks. All of the protein kinases and phosphatases can be profiled against a given compound or substrate using a single concentration of the compound/substrate or at multiple concentrations. In addition, the protein kinase assays can be performed under varying ATP concentrations to evaluate potential competition of test inhibitory compounds with respect to the ATP substrate.

The protein kinase and phosphatase activity profiling services offered by Kinexus use a very economical and convenient approach to facilitate the drug discovery continuum with a three to four-week turnaround of your specific profiling results. Substrates (proteins or peptides) can be supplied by the client as stock solutions of known concentration, as solid material in vials, or in 96-well plates.

Enzyme and Substrate Targets

Kinexus has a diverse and ever-expanding range of target proteins that are actively being pursued from a drug development perspective, with a main focus on signalling proteins, including active protein kinases and protein phosphatases. Except for receptor-tyrosine protein kinases, these highly purified active enzymes are usually generated from the full-length human genes and are based on wild-type sequences, unless explicitly stated. Most of these preparations of recombinant enzymes do not harbor activating mutations. We also produce antibodies for the detection of these enzymes and substrate peptides for assaying their enzymatic activities. With most proteins featuring on average 40 or more potential phosphosites, synthetic substrate peptides can be valuable probes to investigate specific phosphosites and the kinases and phosphatases that target them. We can produce analogues of target substrate sequences that can be useful to confirm the actual sites of phosphorylation in cases where multiple candidate phosphosites are clustered close together. In addition, peptide substrate analogues are helpful to define critical surrounding amino acids for specific protein kinase recognition. Kinexus' In Silico Kinase Substrate Prediction Services can be useful for narrowing down protein kinases that may target a specific phosphosite.

Confidentiality

Kinexus maintains all information under strict confidentiality. All information and or materials supplied will be used as directed by the client. Upon completion of the project, all materials will be either returned to the client or disposed of accordingly. Kinexus is pleased to execute confidentiality agreements with its clients.

2. OBJECTIVES

Service Requested

The client has requested that Kinexus provide the following service:

- Synthesis of two peptide substrates based on the PRMT5 [T634] site and a corresponding peptide with the threonine mutated to an alanine PRMT5 [A634].
- Profile the PRMT5 [T634] peptide against 295 protein kinases at one concentration (500 μ M) in single measurements using a radiometric assay method with $[\gamma\text{-}^{33}\text{P}]\text{ATP}$.

3. MATERIALS

Quality Control & Reagents

The recombinant protein kinases employed in the substrate profiling process were cloned, expressed and purified using proprietary methods. Quality control testing is routinely performed on each of the kinases to ensure compliance to acceptable standards. The $[\gamma\text{-}^{33}\text{P}]\text{ATP}$ was purchased from PerkinElmer. All other materials were of standard laboratory grade. Approximately 10 mg of the PRMT5 [T634] peptide and 3-5 mg of the PRMT5 [A634] peptide were synthesized based on the peptide sequences listed below. Normally, additional C-terminal amino acid sequences would also be included to improve kinase substrate recognition. However, this particular sequence was located at the C-terminus of PRMT5.

No.	Peptide Code	Site	Name	Peptide Sequence	Purity
1	KSP01-CKS	PRMT5 [T634]	Wild type (WT)	KKPTGRSY T IGL	>98%
2	KSP01-CKT	PRMT5 [A634]	Mutant (MT)	KKPTGRSY A IGL	>97%

4. RESULTS

Evaluation

Kinexus evaluated the activity of 295 protein kinases against the the PRMT5 [T634] peptide by employing the standardized assay methodology outlined in Appendix A. The results observed as activity of each peptide substrate are presented in Table 1, while Appendix B contains all the raw data for the protein kinases. The intra-assay variability was determined to be less than 10%.

Comparison of Substrates

For comparisons of kinase substrates, the proteins or peptides should be of similar size, number of phosphosites, and concentrations whenever possible. There are two common approaches for comparing substrates. One is to measure the level of phosphorylation from the test substrate against a known control substrate. The disadvantage of this method is that the control substrates are normally optimized proteins or peptides that may be used at higher concentrations than the test substrate (typically 1 mg/ml), making a direct comparison difficult. Protein substrates usually have higher affinity and lower K_m values than peptide substrates for most protein kinases. Control substrates may also have multiple phosphorylation sites or they may be used at saturating conditions, and therefore a high count from a control substrate, while showing the kinase is active, may not directly be compared to a test substrate.

The other approach for comparing substrate profiling is to place greater emphasis on the highest counts for the test substrate by many diverse protein kinases, as this indicates how well the lead kinases phosphorylates the substrate relative to other tested kinases. **This is the approach taken for this order.** It should, however, be appreciated that the specific enzyme activities of different preparations of the same kinase may show some variability when assayed at different times and direct comparison of different kinases for the same substrate can be misleading. If there is a wild type and mutant version of the same peptide, then a comparison of the difference in counts between these two peptides and the % change from control (CFC) can be particularly instructive for determining the effect of the mutation. Once a short-list of the top kinases has been selected based on the results from this assay, they can be assayed against both the WT and MT peptides.

The profiling data for the PRMT5 [T634] wild type peptide when assayed against 295 protein kinases, using the radiometric assay method with [γ - ^{33}P]-ATP, showed low to excellent phosphorylation with counts ranging from 102 cpm up to as high as 412,000 cpm. (Table 1 provides a listing of the counts observed for the kinases selected). Of the 295 kinases tested, there were 55 kinases (representing about 20% of the total number selected) that generated signals greater than 100,000 cpm. From this subset, 31 kinases produced counts between 100,000 to 200,000 cpm (highlighted in light blue), 14 kinases had counts between 200,000 to 300,000 cpm (highlighted in dark blue), 9 kinases gave counts between 300,000 to 400,000 cpm (highlighted in light purple) and 1 kinase (SGK2) with a count greater than 400,000 cpm. It is often observed that kinases from the same families act on substrates in a similar manner. In this order, SGK1, SGK2 and SGK3 gave the highest counts collectively of all the groups, ranging from 333,000 cpm to 412,000 cpm. The CAMK2 alpha, beta, delta and gamma kinases were also observed with high counts ranging from 341,000 to 384,000 cpm. Other kinase groups which gave reasonably high counts included DAPK1/2/3, MAPKAP2/3, MRCK alpha and beta, RSK1/2/3, ROCK1/2, PIM 1/2/3, PKAc alpha, beta, gamma, TTBK1/2 and TLK1/2.

Activity

Table 1. Activity of protein kinases in the presence of the WT peptide substrate using a radiometric assay method. The table is arranged alphabetically by kinase.

No.	Protein Kinase	Activity (CPM)
1	ACVR2A Protein	26,135
2	ACVR2B Protein	665
3	AKT1	184,332
4	AKT2	12,004
5	AKT3	256,989
6	ALK1	1,059
7	ALK2	1,540
8	ALK3 (BMPR1A)	1,631
9	ALK4	4,674
10	ALK6 (BMPR1B)	6,843
11	ALK7 Protein	922
12	AMPK (A1/B1/G1)	120,531
13	AMPK (A1/B1/G2)	137,047
14	AMPK (A1/B1/G3)	57,751
15	AMPK (A1/B2/G1)	44,378
16	AMPK (A2/B1/G1)	48,194
17	AMPK (A2/B2/G1)	19,964
18	AMPK (A2/B2/G2)	14,142
19	ASK1	28,529
20	AURORA A	9,545
21	AURORA B	112,213
22	AURORA C	39,025
23	BMPR2	18,119
24	BRAF	1,696
25	BRSK1	19,064
26	BRSK2	20,527
27	BUB1B	1,160
28	CAMK1	9,476
29	CAMK1 beta	106,825
30	CAMK1 delta	15,024
31	CAMK1 gamma	3,686
32	CAMK2 alpha	384,870
33	CAMK2 beta	341,444
34	CAMK2 delta	364,345
35	CAMK2 gamma	382,030
36	CAMK4	10,920

No.	Protein Kinase	Activity (CPM)
37	CAMKK1	8,797
38	CAMKK2	3,311
39	CASK	5,970
40	CDC7/DBF4	21,880
41	CDK1/CyclinA1	4,147
42	CDK1/CyclinA2	4,605
43	CDK1/CyclinB1	3,514
44	CDK2/CyclinA1	1,132
45	CDK2/CyclinA2	1,572
46	CDK2/CyclinE1	789
47	CDK2/CyclinO	2,995
48	CDK3/CyclinE1	790
49	CDK4/CyclinD1	504
50	CDK4/CyclinD3	453
51	CDK5/p25	1,745
52	CDK5/p29	102
53	CDK5/p35	3,187
54	CDK6/CyclinD1	3,012
55	CDK6/CyclinD3	7,910
56	CDK7/CyclinH1	11,595
57	CDK8/CyclinC	311
58	CDK9/CyclinK	1,150
59	CHK1	209,670
60	CHK2	98,578
61	CK1 alpha 1	9,572
62	CK1 alpha 1L	6,839
63	CK1 delta	11,638
64	CK1 epsilon	9,286
65	CK1 gamma 1	24,862
66	CK1 gamma 2	19,223
67	CK1 gamma 3	16,547
68	CK2 alpha 1	4,683
69	CK2 alpha 2	525
70	CLK1	21,102
71	CLK2	118,274
72	CLK3	12,714
73	CLK4	6,897
74	COT	3,193
75	DAPK1	238,228
76	DAPK2	163,564
77	DAPK3	229,886

No.	Protein Kinase	Activity (CPM)
78	DCAMKL1	11,853
79	DCAMKL2	140,301
80	DMPK	17,202
81	DRAK1 (STK17A)	32,897
82	DYRK1 alpha Pro	9,143
83	DYRK2	19,414
84	DYRK3	3,114
85	DYRK4 Pro	434
86	EEF2K	8,055
87	EIF2AK1 (HRI)	5,441
88	EIF2AK2	30,549
89	EIF2AK3	59,022
90	EIF2AK4 (GCN2)	19,515
91	ERK1	1,948
92	ERK2	403
93	ERK5	30,371
94	ERN2 (IRE2)	1,761
95	FASTK	708
96	GCK	338,874
97	GLK	161,367
98	GRK1	18,300
99	GRK2	2,006
100	GRK3	3,136
101	GRK5	3,744
102	GRK6	6,634
103	GRK7	2,628
104	GSK3 alpha	2,068
105	GSK3 beta	4,264
106	Haspin (GSG2)	18,918
107	HGK	158,934
108	HIPK1	9,861
109	HIPK2	5,237
110	HIPK3	4,703
111	HIPK4	2,381
112	HPK1	257,198
113	HUNK	2,823
114	ICK	4,394
115	IKK alpha	4,263
116	IKK beta	7,049
117	IKK epsilon	2,677
118	IRAK2	708

No.	Protein Kinase	Activity (CPM)
119	IRAK4	176,708
120	JNK1	3,856
121	JNK2	2,303
122	JNK3	1,050
123	KHS1	74,819
124	KSR1	5,444
125	LATS1	699
126	LATS2	8,596
127	LIMK1	4,119
128	LKB1/M025 alpha	2,494
129	LOK	1,811
130	LRRK2	794
131	MAK	2,456
132	MAPKAPK2	200,518
133	MAPKAPK3	166,463
134	MAPKAPK5	11,164
135	MARK1	2,877
136	MARK2	7,781
137	MARK3	4,839
138	MARK4	7,588
139	MEK1	564
140	MEK2	171
141	MEK5	1,974
142	MEK6	120
143	MEKK1	8,134
144	MEKK2	8,170
145	MEKK3	9,812
146	MEKK6	3,174
147	MELK	9,853
148	MINK1	8,291
149	MLCK	271,797
150	MLK1	59,642
151	MLK2	12,752
152	MLK3	2,540
153	MLK4	5,181
154	MNK1	16,754
155	MNK2	42,325
156	MRCK alpha	160,763
157	MRCK beta	207,336
158	MSK1	140,815
159	MSK2	15,148

No.	Protein Kinase	Activity (CPM)
160	MSSK1	2,765
161	MST1	142,975
162	MST3	45,762
163	MST4	29,240
164	MYLK2	278,395
165	MYLK3	8,609
166	MYLK4	22,478
167	MYO3 alpha	15,278
168	MYO3 beta	43,265
169	MYT1 Protein	2,892
170	NDR	2,333
171	NDR2 (STK38L)	1,085
172	NEK1	23,457
173	NEK11	54,326
174	NEK2	108,865
175	NEK3	38,946
176	NEK4 Pro	2,900
177	NEK5	58,817
178	NEK6	5,999
179	NEK7	1,867
180	NEK8	4,113
181	NEK9	23,797
182	NIK	8,706
183	NIM1	22,839
184	NLK	2,245
185	NUAK1	3,780
186	NUAK2	7,583
187	p38 alpha	857
188	p38 beta	361
189	p38 delta	1,390
190	p38 gamma	602
191	p70S6K	93,764
192	p70S6Kb	109,597
193	PAK1/CDC42	10,296
194	PAK2 Protein	1,005
195	PAK3	100,876
196	PAK4	1,554
197	PAK6	2,244
198	PAK7	4,425
199	PASK	352,063
200	PCTK1(CDK16)Cyclin Y	2,100

No.	Protein Kinase	Activity (CPM)
201	PCTK2 (CDK17)/CyclinY	2,214
202	PDHK1	1,922
203	PDHK2	1,318
204	PDHK3	1,841
205	PDHK4	605
206	PDK1	30,164
207	PEAK1	1,016
208	PFTK1(CDK14)	15,215
209	PHKG1	7,385
210	PHKG2	61,583
211	PIM1	102,288
212	PIM2	131,639
213	PIM3	102,646
214	PKAc alpha	178,738
215	PKAc beta	265,847
216	PKAc gamma	256,765
217	PKC alpha	62,585
218	PKC beta I	58,112
219	PKC beta II	230,541
220	PKC delta	4,927
221	PKC epsilon	11,107
222	PKC eta	28,880
223	PKC gamma	16,134
224	PKC iota	10,008
225	PKC mu	38,445
226	PKC nu	47,811
227	PKC theta	15,137
228	PKC zeta	22,727
229	PKD2	92,839
230	PKN1/PRK1	4,971
231	PKN2/PRK2	7,881
232	PKN3/PRK3	6,675
233	PLK1	7,423
234	PLK2	3,576
235	PLK3	2,029
236	PLK4	31,058
237	PRKG1	30,700
238	PRKG2	57,214
239	PRKX	11,241
240	QIK	6,809
241	RAF1	41,713

No.	Protein Kinase	Activity (CPM)
242	RIPK1	4,714
243	RIPK2	1,508
244	RIPK3	19,575
245	RIPK5	510
246	ROCK1	173,333
247	ROCK2	372,820
248	RSK1	286,017
249	RSK2	158,034
250	RSK3	152,511
251	RSK4	61,611
252	SBK1	20,183
253	SGK1	358,728
254	SGK2	412,655
255	SGK3	333,447
256	SIK	15,673
257	SIK3	3,800
258	SLK	59,362
259	SNRK	9,686
260	SOK1	60,021
261	SRPK1	6,587
262	SRPK2	11,749
263	STK19	12,902
264	STK3	47,144
265	STK32B(YANK2)	32,399
266	STK32C (YANK3)	9,053
267	STK33	9,030
268	STK36	2,875
269	STK39 (STLK3)	34,778
270	TAK1-TAB1	5,334
271	TAOK1	123,780
272	TAOK2	94,068
273	TAOK3	249,457
274	TBK1	36,231
275	TESK1 Pro	1,359
276	TGFBR1 (ALK5)	1,551
277	TGFBR2	6,348
278	TLK1	135,948
279	TLK2	153,824
280	TNIK	110,261
281	TOPK	23,323
282	TSSK1B	11,969

No.	Protein Kinase	Activity (CPM)
283	TSSK2	14,897
284	TTBK1	186,494
285	TTBK2	193,036
286	TTK	47,019
287	TYK2 (JTK1)	5,578
288	ULK1	34,710
289	ULK2	44,553
290	ULK3	34,499
291	VRK1	5,902
292	VRK2	2,897
293	WEE1 Protein	4,348
294	WNK1	7,347
295	ZAK	53,677

Legend

> 400,000 CPM
300,000 - 400,000 CPM
200,000 - 300,000 CPM
100,000 - 200,000 CPM

5. DISCUSSION

Conclusion

Kinexus evaluated the activity of 295 protein kinases in the presence of a peptide derived from the C-terminus of the protein PRMT5 [T634]. The aim was to monitor the level of phosphorylation of the peptide by the protein kinases and narrow down a subset of the best kinase candidates to test further against both the PRMT5 [T634] wild-type, and a corresponding peptide with the threonine mutated to an alanine PRMT5 [A634]. Marked reductions in the phosphorylation of the A634 mutated peptide would permit identification of those kinases that primarily target the T634 site.

The protein kinases tested were serine/threonine-specific or dual specificity kinases that are also known to target tyrosine residues for phosphorylation. This was reasonable, since the site that was targeted was a threonine residue. The substrate peptide contained two other amino acids that are potentially phosphorylatable, which corresponds to serine [S632] and tyrosine [Y633]. However, with high concentrations of peptide substrates, we have often observed that protein-serine/threonine kinases (e.g. CK2) can also phosphorylate peptides that only feature tyrosine and no serine or threonine residues at appreciable levels. Likewise, many protein-tyrosine kinases have appreciable activity towards serine and threonine residues (e.g. EGFR and JAK's). In view of the 4000-fold range

of phosphorylation of the substrate obtained with the 295 different protein kinases, the lower range of phosphorylation, i.e. less than 25,000, should be discounted.

From the assay results, 55 protein kinases (representing approximately 20% of all the kinases tested) showed a strong preference for the PRMT5 [T634] peptide. This was based on the higher counts observed, from 100,000 up to 412,000 cpm. There were a further 46 kinases (representing 15% of the kinases), with moderate counts ranging from 25,000 to 100,000. The remaining 194 kinases (representing 65% of the kinases) gave counts less than 25,000 cpm. The next step would be to assay a subset of these kinases against both the PRMT5 [T634] and [A634] peptides to determine the effect of phosphorylation that can be attributed to the threonine at position 634.

In comparing the top candidates for the protein kinases that specifically target the T634 site, it should be appreciated that each of these preparations of protein kinases were generated as recombinant proteins and every attempt was made to produce them in the most active states. Nonetheless, we cannot rule out the possibility that additional phosphorylation or other covalent modifications of these enzymes or the presence of other as yet unidentified activating subunits or compounds that are available physiologically are still needed for their maximal specific enzyme activity. Furthermore, during the expression and purification procedures, there may be varying levels of the ratios of active compared to inactive enzyme molecules for each kinase preparation. This can result in variable V_{max} values for each protein kinase from one preparation to another. However, the relative affinity of a purified protein kinase for a purified substrate is less variable, and determination of the relative K_m of the top ranked protein kinases for the same peptide substrate could provide a better assessment of the protein kinases that are likely to target the T634 site physiologically.

It should also be appreciated that there may be protein kinases that demonstrate higher affinities for PRMT5 and phosphorylate the T634 site than apparent from this study with the peptide based on the amino acid sequences surrounding this site. Certain protein kinases and substrates feature additional sequences that act as secondary docking sites to further improve kinase-substrate recognition. However, these experiments with the synthetic peptide substrates should markedly narrow down the candidate proteins kinases, which can be tested later against recombinant PRMT5. In preparation for this, it may be worthwhile to develop a phosphosite-specific antibody for the T634 site. To our knowledge, phosphorylation of the C-terminus of PRMT5 has not been previously reported, nor has it been predicted with our Kinase Substrate Predictor algorithms. If a substantial drop in phosphorylation of the A634 site is observed with the lead protein kinases identified from this study, then the development of a phosphosite-specific antibody is warranted, and Kinexus could assist you for such an objective. We have recently developed over 400 phosphosite-specific antibodies in-house.

APPENDIX A - METHODOLOGY

The assay condition for the various protein kinase targets were optimized to yield acceptable enzymatic activity. In addition, the assays were optimized to give high signal-to-noise ratio.

Protein Kinase Assays

A radioisotope assay format was used for profiling evaluation of the kinase activities towards their substrates and all assays are performed in a designated radioactive working area. Protein kinase assays were performed at ambient temperature for 20-40 minutes (depending on the kinase) in a final volume of 25 μ l according to the following assay reaction recipe:

- Component 1.** 5 μ l of diluted active protein kinase (~10-50 nM final protein concentration in the assay)
- Component 2.** 5 μ l of assay solution of peptide substrate
- Component 3.** 10 μ l of kinase assay buffer
- Component 4.** 5 μ l of [γ -³³P] ATP (250 μ M stock solution, 0.8 μ Ci)

The assay was initiated by the addition of [γ -³³P] ATP and the reaction mixture incubated at ambient temperature for 20-40 minutes, depending on the protein kinase tested. After the incubation period, the assay was terminated by spotting 10 μ l of the reaction mixture onto a multiscreen phosphocellulose P81 plate. The multiscreen phosphocellulose P81 plate was washed 3 times for approximately 15 minutes each in a 1% phosphoric acid solution. The radioactivity on the P81 plate was counted in the presence of scintillation fluid in a Trilux scintillation counter.

Appendix B - Raw Data

Counts from the PRMT5 [T634] Peptide

No.	Protein Kinase	Original Counts	Blank	Activity (CPM)
1	ALK1	1,414	355	1,059
2	CAMKK2	3,734	423	3,311
3	DCAMKL1	12,439	586	11,853
4	EIF2AK4 (GCN2)	19,948	433	19,515
5	FASTK	1,085	377	708
6	PCTK2 (CDK17)/CyclinY	2,626	412	2,214
7	RIPK1	5,268	554	4,714
8	RIPK3	20,246	671	19,575
9	SOK1	60,795	774	60,021
10	STK32B(YANK2)	32,967	568	32,399
11	TNIK	110,739	478	110,261
12	VRK2	3,296	399	2,897
13	WNK1	7,785	438	7,347
14	AMPK (A1/B1/G1)	120,876	345	120,531
15	AMPK (A1/B1/G2)	137,461	414	137,047
16	AMPK (A1/B1/G3)	58,270	519	57,751
17	AMPK (A1/B2/G1)	44,884	506	44,378
18	AMPK (A2/B1/G1)	48,684	490	48,194
19	AMPK (A2/B2/G1)	20,442	478	19,964
20	AMPK (A2/B2/G2)	14,640	498	14,142
21	CAMK1	10,021	545	9,476
22	CAMK1 beta	107,288	463	106,825
23	CAMK1 delta	15,529	505	15,024
24	CAMK1 gamma	4,241	555	3,686
25	CAMK2 alpha	385,448	578	384,870
26	CAMK2 beta	341,953	509	341,444
27	CAMK2 delta	364,932	587	364,345
28	CAMK2 gamma	382,628	598	382,030
29	CAMK4	11,385	465	10,920
30	CAMKK1	9,205	408	8,797
31	CASK	6,329	359	5,970
32	DAPK1	238,772	544	238,228
33	DAPK2	163,963	399	163,564
34	DCAMKL2	140,976	675	140,301
35	EEF2K	8,653	598	8,055
36	MLCK	272,462	665	271,797
37	MYLK2	279,134	739	278,395
38	MYLK3	9,102	493	8,609

39	MYLK4	22,995	517	22,478
40	NIM1	23,362	523	22,839
41	PKN2/PRK2	8,357	476	7,881
42	PRKG1	31,218	518	30,700
43	PRKG2	57,702	488	57,214
44	PKC alpha	63,234	649	62,585
45	PKC beta I	58,868	756	58,112
46	PKC beta II	230,971	430	230,541
47	PKC delta	5,364	437	4,927
48	PKC epsilon	11,596	489	11,107
49	PKC eta	29,446	566	28,880
50	PKC gamma	16,603	469	16,134
51	PKC iota	10,586	578	10,008
52	PKC theta	15,836	699	15,137
53	PAK1/CDC42	10,764	468	10,296
54	ACVR2A Protein	26,635	500	26,135
55	ACVR2B Protein	1,231	566	665
56	AKT1	184,959	627	184,332
57	AKT2	12,433	429	12,004
58	AKT3	257,538	549	256,989
59	ALK2	1,973	433	1,540
60	ALK3 (BMPR1A)	2,179	548	1,631
61	ALK4	5,074	400	4,674
62	ALK6 (BMPR1B)	7,432	589	6,843
63	ALK7 Protein	1,427	505	922
64	ASK1	29,008	479	28,529
65	AURORA A	10,109	564	9,545
66	AURORA B	112,766	553	112,213
67	AURORA C	39,424	399	39,025
68	BMPR2	18,775	656	18,119
69	BRAF	2,174	478	1,696
70	BRSK1	19,619	555	19,064
71	BRSK2	21,155	628	20,527
72	BUB1B	1,639	479	1,160
73	CDC7/DBF4	22,449	569	21,880
74	CDK1/CyclinA1	4,610	463	4,147
75	CDK1/CyclinA2	5,117	512	4,605
76	CDK1/CyclinB1	4,103	589	3,514
77	CDK2/CyclinA1	1,683	551	1,132
78	CDK2/CyclinA2	2,076	504	1,572
79	CDK2/CyclinE1	1,288	499	789
80	CDK2/CyclinO	3,566	571	2,995
81	CDK3/CyclinE1	1,149	359	790

82	CDK4/CyclinD1	907	403	504
83	CDK4/CyclinD3	982	529	453
84	CDK5/p25	2,378	633	1,745
85	CDK5/p29	569	467	102
86	CDK5/p35	3,716	529	3,187
87	CDK6/CyclinD1	3,608	596	3,012
88	CDK6/CyclinD3	8,522	612	7,910
89	CDK7/CyclinH1	12,102	507	11,595
90	CDK8/CyclinC	809	498	311
91	CDK9/CyclinK	1,798	648	1,150
92	CHK1	210,205	535	209,670
93	CHK2	99,045	467	98,578
94	CK1 alpha 1	10,017	445	9,572
95	CK1 alpha 1L	7,371	532	6,839
96	CK1 delta	12,127	489	11,638
97	CK1 epsilon	9,763	477	9,286
98	CK1 gamma 1	25,407	545	24,862
99	CK1 gamma 2	19,697	474	19,223
100	CK1 gamma 3	17,083	536	16,547
101	CK2 alpha 1	5,062	379	4,683
102	CK2 alpha 2	1,084	559	525
103	CLK1	21,728	626	21,102
104	CLK2	118,742	468	118,274
105	CLK3	13,239	525	12,714
106	CLK4	7,438	541	6,897
107	COT	3,748	555	3,193
108	DAPK3	230,541	655	229,886
109	DMPK	17,551	349	17,202
110	DRAK1 (STK17A)	33,520	623	32,897
111	DYRK1 alpha Pro	9,739	596	9,143
112	DYRK2	19,942	528	19,414
113	DYRK3	3,653	539	3,114
114	DYRK4 Pro	950	516	434
115	EIF2AK1 (HRI)	6,007	566	5,441
116	EIF2AK2	31,138	589	30,549
117	EIF2AK3	59,548	526	59,022
118	ERK1	2,503	555	1,948
119	ERK2	878	475	403
120	ERK5	31,027	656	30,371
121	ERN2 (IRE2)	2,305	544	1,761
122	GCK	339,562	688	338,874
123	GLK	162,112	745	161,367
124	GRK1	19,154	854	18,300

125	GRK2	2,639	633	2,006
126	GRK5	4,332	588	3,744
127	GRK6	7,091	457	6,634
128	GRK7	3,195	567	2,628
129	GSK3 alpha	2,611	543	2,068
130	GSK3 beta	4,793	529	4,264
131	Haspin (GSG2)	19,563	645	18,918
132	HGK	159,611	677	158,934
133	HIPK1	10,249	388	9,861
134	HIPK2	5,806	569	5,237
135	HIPK3	5,213	510	4,703
136	HIPK4	2,876	495	2,381
137	HPK1	257,847	649	257,198
138	HUNK	3,476	653	2,823
139	ICK	4,983	589	4,394
140	IKK alpha	4,743	480	4,263
141	IKK beta	7,507	458	7,049
142	IKK epsilon	3,163	486	2,677
143	IRAK2	1,167	459	708
144	IRAK4	177,356	648	176,708
145	JNK1	4,300	444	3,856
146	JNK2	2,818	515	2,303
147	JNK3	1,597	547	1,050
148	KHS1	75,444	625	74,819
149	KSR1	5,995	551	5,444
150	LATS1	1,225	526	699
151	LATS2	9,232	636	8,596
152	LIMK1	4,594	475	4,119
153	LKB1/M025 alpha	3,011	517	2,494
154	LOK	2,345	534	1,811
155	LRRK2	1,470	676	794
156	MAK	3,022	566	2,456
157	MAPKAPK2	200,974	456	200,518
158	MAPKAPK3	166,901	438	166,463
159	MAPKAPK5	11,683	519	11,164
160	MARK1	3,376	499	2,877
161	MARK2	8,334	553	7,781
162	MARK3	5,378	539	4,839
163	MARK4	8,153	565	7,588
164	MEK1	1,039	475	564
165	MEK2	709	538	171
166	MEK6	680	560	120
167	MEKK1	8,563	429	8,134

168	MEKK2	8,682	512	8,170
169	MEKK3	10,340	528	9,812
170	MEKK6	3,807	633	3,174
171	MELK	10,379	526	9,853
172	MINK1	8,767	476	8,291
173	MLK1	60,286	644	59,642
174	MLK2	13,272	520	12,752
175	MLK3	3,018	478	2,540
176	MLK4	5,718	537	5,181
177	MNK1	17,368	614	16,754
178	MNK2	42,864	539	42,325
179	MRCK alpha	161,286	523	160,763
180	MRCK beta	207,962	626	207,336
181	MSK1	141,334	519	140,815
182	MSK2	15,640	492	15,148
183	MSSK1	3,446	681	2,765
184	MST1	143,512	537	142,975
185	MST3	46,290	528	45,762
186	MST4	29,854	614	29,240
187	MYO3 alpha	15,796	518	15,278
188	MYO3 beta	43,757	492	43,265
189	MYT1 Protein	3,525	633	2,892
190	NDR	3,016	683	2,333
191	NDR2 (STK38L)	1,673	588	1,085
192	NEK1	23,983	526	23,457
193	NEK11	54,857	531	54,326
194	NEK2	109,414	549	108,865
195	NEK3	39,624	678	38,946
196	NEK4 Pro	3,469	569	2,900
197	NEK5	59,451	634	58,817
198	NEK6	6,511	512	5,999
199	NEK7	2,337	470	1,867
200	NEK8	4,557	444	4,113
201	NEK9	24,390	593	23,797
202	NIK	9,344	638	8,706
203	NLK	2,773	528	2,245
204	NUAK1	4,200	420	3,780
205	NUAK2	8,101	518	7,583
206	p38 alpha	1,395	538	857
207	p38 beta	929	568	361
208	p38 delta	1,836	446	1,390
209	p38 gamma	1,124	522	602
210	p70S6K	94,339	575	93,764

211	p70S6Kb	110,186	589	109,597
212	PAK2 Protein	1,480	475	1,005
213	PAK3	101,509	633	100,876
214	PAK4	2,203	649	1,554
215	PAK6	2,787	543	2,244
216	PAK7	4,937	512	4,425
217	PASK	352,653	590	352,063
218	PCTK1(CDK16)Cyclin Y	2,523	423	2,100
219	PDHK1	2,456	534	1,922
220	PDHK2	1,842	524	1,318
221	PDHK3	2,349	508	1,841
222	PDHK4	1,037	432	605
223	PDK1	30,725	561	30,164
224	PEAK1	1,595	579	1,016
225	PFTK1(CDK14)	15,762	547	15,215
226	PHKG1	7,860	475	7,385
227	PHKG2	62,052	469	61,583
228	PIM1	102,821	533	102,288
229	PIM2	132,196	557	131,639
230	PIM3	103,235	589	102,646
231	PKAc alpha	179,415	677	178,738
232	PKAc beta	266,334	487	265,847
233	PKAc gamma	257,313	548	256,765
234	PKC mu	38,992	547	38,445
235	PKC nu	48,384	573	47,811
236	PKC zeta	23,285	558	22,727
237	PKD2	93,492	653	92,839
238	PKN1/PRK1	5,438	467	4,971
239	PKN3/PRK3	7,251	576	6,675
240	PLK1	7,910	487	7,423
241	PLK2	3,954	378	3,576
242	PLK3	2,485	456	2,029
243	PLK4	31,591	533	31,058
244	PRKX	11,770	529	11,241
245	QIK	7,309	500	6,809
246	RAF1	42,244	531	41,713
247	RIPK2	2,030	522	1,508
248	RIPK5	996	486	510
249	ROCK1	173,900	567	173,333
250	ROCK2	373,406	586	372,820
251	RSK1	286,594	577	286,017
252	RSK2	158,605	571	158,034
253	RSK3	153,085	574	152,511

254	RSK4	62,177	566	61,611
255	SBK1	20,661	478	20,183
256	SGK1	359,318	590	358,728
257	SGK2	413,507	852	412,655
258	SGK3	334,212	765	333,447
259	SIK	16,235	562	15,673
260	SLK	59,897	535	59,362
261	SNRK	10,156	470	9,686
262	SRPK1	7,155	568	6,587
263	SRPK2	12,273	524	11,749
264	STK19	13,414	512	12,902
265	STK3	47,674	530	47,144
266	STK32C (YANK3)	9,528	475	9,053
267	STK33	9,488	458	9,030
268	STK36	3,462	587	2,875
269	STK39 (STLK3)	35,322	544	34,778
270	TAK1-TAB1	5,913	579	5,334
271	TAOK1	124,379	599	123,780
272	TAOK2	94,544	476	94,068
273	TAOK3	250,114	657	249,457
274	TBK1	36,775	544	36,231
275	TESK1 Pro	1,948	589	1,359
276	TGFBR1 (ALK5)	2,134	583	1,551
277	TGFBR2	6,864	516	6,348
278	TLK1	136,414	466	135,948
279	TLK2	154,368	544	153,824
280	TOPK	23,905	582	23,323
281	TSSK1B	12,457	488	11,969
282	TSSK2	15,372	475	14,897
283	TTBK1	187,091	597	186,494
284	TTBK2	193,626	590	193,036
285	TTK	47,653	634	47,019
286	TYK2 (JTK1)	6,088	510	5,578
287	ULK1	35,196	486	34,710
288	ULK2	45,081	528	44,553
289	ULK3	35,135	636	34,499
290	VRK1	6,391	489	5,902
291	WEE1 Protein	4,946	598	4,348
292	ZAK	54,155	478	53,677
293	GRK3	3,597	461	3,136
294	MEK5	2,540	566	1,974
295	SIK3	4,198	398	3,800



KINEXUS

SUBSTRATE PROFILING SERVICES

PROFILING OF 2 PEPTIDE SUBSTRATES

AGAINST 18 PROTEIN KINASES

ORDER 3272

Principal Investigator: Dr. Mark Bedford / Alexandra Espejo

Institution: M.D. Anderson Cancer Center

Completion Date: May 7, 2015

Report Contact: Ms. Catherine Sutter

Telephone: 604-323-2547, Ext 11

Email: info@kinexus.ca

8755 Ash Street, Suite 1, Vancouver, B.C. Canada V6P 6T3

T: 604.323.2547 • F: 604.323.2548 • E: info@kinexus.ca • www.kinexus.ca

Table of Contents

1. OVERVIEW OF SERVICE

Introduction	3
Enzyme and Substrate Targets	3
Confidentiality	4

2. OBJECTIVES

Service Requested	4
-------------------------	---

3. MATERIALS

Quality Control & Reagents	4
----------------------------------	---

4. RESULTS

Evaluation	5-6
Activity.....	6

5. DISCUSSION

Conclusion	7-8
------------------	-----

6. APPENDIX A - METHODOLOGY

Protein Kinase Assays	9
-----------------------------	---

1. OVERVIEW OF PROFILING SERVICE

Introduction

The Kinexus Kinase/Phosphatase Profiling Services provide access to a large and diverse panel of highly active protein kinases and protein phosphatases for screening substrates and bioactive compounds. These active enzyme preparations are subjected to rigorous quality control analyses and are extensively assayed against a panel of biologically relevant substrates and optimized synthetic peptides to ensure that all test reactions are performed under optimal assay conditions. These protein kinase/phosphatase profiling services determine the extent of phosphorylation or dephosphorylation of a selected substrate to understand the putative mechanisms of action of bioactive compounds and to support the identification of the upstream protein kinases and protein phosphatases and their substrate proteins in signalling networks. All of the protein kinases and phosphatases can be profiled against a given compound or substrate using a single concentration of the compound/substrate or at multiple concentrations. In addition, the protein kinase assays can be performed under varying ATP concentrations to evaluate potential competition of test inhibitory compounds with respect to the ATP substrate. The protein kinase and phosphatase activity profiling services offered by Kinexus use a very economical and convenient approach to facilitate the drug discovery continuum with a three to four-week turnaround of your specific profiling results. Substrates (proteins or peptides) can be supplied by the client as stock solutions of known concentration, as solid material in vials, or in 96-well plates.

Enzyme and Substrate Targets

Kinexus has a diverse and ever-expanding range of enzymes that are actively being pursued from a drug development perspective, with a main focus on signalling proteins, including active protein kinases and protein phosphatases. Except for receptor-tyrosine protein kinases, these highly purified active enzymes are usually generated from the full-length human genes and are based on wild-type sequences, unless explicitly stated. Most of these preparations of recombinant enzymes do not harbor activating mutations. We also produce antibodies for the detection of these enzymes and substrate peptides for assaying their enzymatic activities. With most proteins featuring on average 40 or more potential phosphosites, synthetic substrate peptides can be valuable probes to investigate specific phosphosites and the kinases and phosphatases that target them. Our open-access PhosphoNET (www.phosphonet.ca) provides predictions of the most likely protein kinases that target over 960,000 known or predicted phosphosites in human proteins. We can produce analogues of target substrate sequences that can be useful to confirm the actual sites of phosphorylation in cases where multiple candidate phosphosites are clustered close together. In addition, peptide substrate analogues are helpful to define critical surrounding amino acids for specific protein kinase recognition. Our In Silico Kinase Substrate Prediction Services can be useful for narrowing down non-human protein kinases that target specific phosphosites in other species.

Confidentiality

Kinexus maintains all information under strict confidentiality. All information and or materials supplied will be used as directed by the client. Upon completion of the project, all materials will be either returned to the client or disposed of accordingly. Kinexus is pleased to execute confidentiality agreements with its clients.

2. OBJECTIVES

Service Requested

The client has requested that Kinexus provide the following service:

- Profile the PRMT5 [T634] peptide and a corresponding peptide with the threonine mutated to an alanine PRMT5 [A634] against 18 protein kinases at one concentration (500 μ M) in single measurements using the radiometric assay method with [γ -³³P]ATP.

3. MATERIALS

Quality Control & Reagents

The recombinant protein kinases employed in the substrate profiling process were cloned, expressed and purified using proprietary methods. Quality control testing is routinely performed on each of the kinases to ensure compliance to acceptable standards. The [γ -³³P]ATP was purchased from PerkinElmer. All other materials were of standard laboratory grade. The PRMT5 [T634] and [A634] peptides were synthesized at Kinexus based on the sequences listed below. Normally, additional C-terminal amino acid sequences would also be included to improve kinase substrate recognition. However, this particular sequence was located at the C-terminus of PRMT5. Note that although the KSP01-CKS and KSP01-CKT peptides were subjected to rigorous purification prior to their deployment in the kinase assays, it is possible that a small percentage of the peptides may have a slightly altered sequence in which an extra serine or tyrosine residue has been incorporated due to differences in coupling efficiencies with different amino acids during the synthesis step.

No.	Peptide Code	Site	Name	Peptide Sequence	Purity
1	KSP01-CKS	PRMT5 [T634]	Wild type (WT)	KKPTGRSY T IGL	>98%
2	KSP01-CKT	PRMT5 [A634]	Mutant (MT)	KKPTGRSY A IGL	>97%

4. RESULTS

Evaluation

Kinexus evaluated the activity of 18 protein kinases against the two peptides by employing the standardized assay methodology outlined in Appendix A. The results observed as activity of each peptide substrate are presented in Table 1. The intra-assay variability was determined to be less than 10%.

Comparison of Substrates

For comparisons of kinase substrates, the proteins or peptides should be of similar size, number of phosphosites, and concentrations whenever possible. There are two common approaches for comparing substrates. One is to measure the level of phosphorylation from the test substrate against a known control substrate. The disadvantage of this method is that the control substrates are normally optimized proteins or peptides that may be used at higher concentrations than the test substrate (typically 1 mg/ml), making a direct comparison difficult. Protein substrates usually have higher affinity and lower K_m values than peptide substrates for most protein kinases. Control substrates may also have multiple phosphorylation sites or they may be used at saturating conditions, and therefore a high count from a control substrate, while showing the kinase is active, may not directly be compared to a test substrate.

The other approach for comparing substrate profiling is to place greater emphasis on the highest counts for the test substrate by many diverse protein kinases, as this indicates how well the lead kinases phosphorylates the substrate relative to other tested kinases. It should, however, be appreciated that the specific enzyme activities of different preparations of the same kinase may show some variability when assayed at different times and direct comparison of different kinases for the same substrate can be misleading. If there is a wild type and mutant version of the same peptide, then a comparison of the difference in counts between these two peptides and the % change from control (CFC) can be particularly instructive for determining the effect of the mutation.

This is the approach taken for this order.

The first screening of the PRMT5 [T634] wild type peptide was against 295 protein-serine-threonine and dual-specificity kinases (Order #3220). The objective was to determine the best candidate kinases which showed the greatest affinity (as measured by the highest counts) for the peptide substrate. From that study, 18 kinases, with counts from 249,000 to 412,000 cpm, were selected for further examination against the wild type PRMT5 [T634] and its mutated peptide, PRMT5 [A634].

Of the 18 kinases tested, the majority generated high signals with the PRMT5 [T634] wild type (WT) peptide, with counts ranging from 205,000 to 530,000 cpm. However, there were 2 kinases which gave lower counts than what was observed in the previous study, including AKT3 at 87,994 cpm and MLCK with 42,473 cpm (in the last study both of these kinases had counts >250,000 cpm).

In contrast, the profiling data for the PRMT5 [A634] mutant (MT) peptide showed significantly reduced levels of phosphorylation for all of the kinases tested in comparison to the WT peptide. AKT3 and MLCK gave the lowest counts for the MT peptide in the range of 4,000 to 5,000 cpm, and the remaining 16 kinases had counts from 15,000 up to 274,000 cpm with ROCK2. Overall, the counts for the MT peptide were approximately 80% lower than what was observed for the WT peptide, indicating a preference of the kinases towards the T634 site than the T629 or S632 sites. Based on the protein kinases tested, these results are consistent with the general observation that an arginine residue at the -3 position relative to the phosphoacceptor amino acid is commonly a strong positive determinant for protein-serine/threonine kinase recognition.

Activity

Table 1. Activity of 18 protein kinases in the presence of the WT and MT peptide substrates using the radiometric assay method. The table is arranged alphabetically by kinase name.

No.	Protein Kinase	Counts (CPM) PRMT5 [T634]	Counts (CPM) PRMT5 [A634]	% Change
1	AKT3	87,994	5,082	-94%
2	CAMK2 alpha	214,728	23,413	-89%
3	CAMK2 beta	315,127	36,406	-88%
4	CAMK2 delta	460,424	52,995	-88%
5	CAMK2 gamma	205,755	15,296	-93%
6	GCK	530,961	102,459	-81%
7	HPK1	360,910	58,049	-84%
8	MLCK	42,473	4,337	-90%
9	MYLK2	436,816	47,171	-89%
10	PASK	302,878	51,385	-83%
11	PKAc beta	368,281	97,185	-74%
12	PKAc gamma	335,295	128,075	-62%
13	ROCK2	528,311	274,183	-48%
14	RSK1	355,043	34,110	-90%
15	SGK1	361,446	55,225	-85%
16	SGK2	328,678	106,394	-68%
17	SGK3	496,925	118,683	-76%
18	TAOK3	306,202	29,544	-90%

5. DISCUSSION

Conclusion

Kinexus evaluated the activity of 18 protein kinases in the presence of a peptide derived from the C-terminus of the protein PRMT5 [T634] and a corresponding peptide with the threonine mutated to an alanine PRMT5 [A634]. The objective was to observe which kinases show marked reductions in the phosphorylation of the A634 mutated peptide for the identification of those kinases that primarily target the T634 site. The WT peptide also contained three other amino acids that could be potentially phosphorylatable, corresponding to threonine [T629], serine [S632] and tyrosine [Y633].

From the assay results, it appears that all of the protein kinases tested showed a significantly stronger preference for the PRMT5 [T634] peptide than the corresponding [A634] peptide. This is based on the significantly higher counts observed for the WT peptide compared to the MT peptide (on average 80% higher counts). For the purposes of identifying and selecting the kinases that specifically target the PRMT5 [T634] site, the % difference observed between the WT vs. MT peptide should also be considered. In general, the effect of the alanine substitution of the PRMT5 [A634] peptide revealed a significant decrease in the level of phosphorylation for the kinases tested when compared to the corresponding wild type PRMT5 [T634] peptide. The differences observed between the peptides ranged from 48% (with ROCK2) to up to 94% (with AKT3). All of the kinases tested gave relatively high % CFC values. In particular, the CAMK2 family of kinases (alpha, beta, delta and gamma) gave strong results with differences of 88-93% between the peptides and high counts of the WT peptide (205,000 to 460,000 cpm). However, all of the kinases could be candidates for further studies.

Table 2. Subset of protein kinases with counts > 200,000 and changes > 80% of the WT compared to the MT peptide, arranged based on the greatest changes.

No.	Protein Kinase	Count (CPM) PRMT5 [T634]	Count (CPM) PRMT5 [A634]	% Change WT-MT
1	CAMK2g	205,755	15,296	-93%
2	RSK1	355,043	34,110	-90%
3	TAOK3	306,202	29,544	-90%
4	MYLK2	436,816	47,171	-89%
5	CAMK2a	214,728	23,413	-89%
6	CAMK2d	460,424	52,995	-88%
7	CAMK2b	315,127	36,406	-88%
8	SGK1	361,446	55,225	-85%
9	HPK1	360,910	58,049	-84%
10	PASK	302,878	51,385	-83%
11	GCK	530,961	102,459	-81%

In comparing the top candidates for the protein kinases that specifically target the T634 site, it should be appreciated that each of these preparations of protein kinases were generated as recombinant proteins and every attempt was made to produce them in the most active states. Nonetheless, we cannot rule out the possibility that additional phosphorylation or other covalent modifications of these enzymes or the presence of other as yet unidentified activating subunits or compounds that are available physiologically are still needed for their maximal specific enzyme activity. Furthermore, during the expression and purification procedures, there may be varying levels of the ratios of active compared to inactive enzyme molecules for each kinase preparation. This can result in variable V_{max} values for each protein kinase from one preparation to another. However, the relative affinity of a purified protein kinase for a purified substrate is less variable, and determination of the relative K_m of the top ranked protein kinases for the same peptide substrate could provide a better assessment of the protein kinases that are likely to target the T634 site physiologically.

It should also be appreciated that there may still be protein kinases that demonstrate higher affinities for PRMT5 and phosphorylate the T634 site than those that were apparent from this study with the peptide based on the amino acid sequences surrounding this site. Certain protein kinases and substrates feature additional sequences that act as secondary docking sites to further improve kinase-substrate recognition. However, these experiments with the synthetic peptide substrates should markedly narrow down the candidate proteins kinases, which can be tested later against recombinant PRMT5. In preparation for this, it may be worthwhile to develop a phosphosite-specific antibody for the T634 site. To our knowledge, phosphorylation of the C-terminus of PRMT5 has not been previously reported, nor has it been predicted with our Kinase Substrate Predictor algorithms. With the substantial drop in phosphorylation of the A634 site as observed with the lead protein kinases identified from this study, we believe that the development of a phosphosite-specific antibody is warranted, and Kinexus could assist you for such an objective. We have recently developed over 400 phosphosite-specific antibodies in-house.

APPENDIX A - METHODOLOGY

The assay condition for the various protein kinase targets were optimized to yield acceptable enzymatic activity. In addition, the assays were optimized to give high signal-to-noise ratio.

Protein Kinase Assays

A radioisotope assay format was used for profiling evaluation of the kinase activities towards their substrates and all assays are performed in a designated radioactive working area. Protein kinase assays were performed at ambient temperature for 20-40 minutes (depending on the kinase) in a final volume of 25 μ l according to the following assay reaction recipe:

- Component 1.** 5 μ l of diluted active protein kinase (~10-50 nM final protein concentration in the assay)
- Component 2.** 5 μ l of assay solution of peptide substrate
- Component 3.** 10 μ l of kinase assay buffer
- Component 4.** 5 μ l of [γ -³³P] ATP (250 μ M stock solution, 0.8 μ Ci)

The assay was initiated by the addition of [γ -³³P] ATP and the reaction mixture incubated at ambient temperature for 20-40 minutes, depending on the protein kinase tested. After the incubation period, the assay was terminated by spotting 10 μ l of the reaction mixture onto a multiscreen phosphocellulose P81 plate. The multiscreen phosphocellulose P81 plate was washed 3 times for approximately 15 minutes each in a 1% phosphoric acid solution. The radioactivity on the P81 plate was counted in the presence of scintillation fluid in a Trilux scintillation counter.

APPENDIX B

GST-PDZ Domains

	Protein	Domain	Acc #	Size	AA sequence
1	a-1-syntrophin(1/1)	DPZ	Q61234	81-164 = 84	RVTVRKADAGGLGISIKGGRENKMPILIS KIFKGLAADQTEALFVGDAILSVNGEDLS SATHDEAVQALKKTGKEVVLEVKYMK
2	β1-syntrophin (1/1)	PDZ	Q99L88	111-194 = 84	GVKVLKQELGGLGISIKGGKENKMPILIS KIFKGLAADQTQALYVGDAILSVNGADL RDATHDEAVQALKRAGKEVLLLEVKYMR
3	γ 1-syntrophin (1/1)	PDZ	Q925E1	57-140 = 84	TVTIRRQTVGGFGLSIKGGAEHNIPVVIS KISKEQRAELSGLLFIGDAILQINGINVRK CRHEEVVQVLRNAGEEVTITVSFLK
4	γ2-syntrophin (1/1)	PDZ	Q925E0	73-156 = 84	TVTLRRQPVGGGLGLSIKGGAEHGVVVI SKIFKDQAADQTEMLFIGDAVLQVNGIN VENATHEEVHLLRNAGDDVTITVEYLR
5	Chapsyn-110 (2/3)	PDZ	Q91XM9	193-280 = 88	EIKLFKGPGLGFSIAGGVGNQHIPGDN SIYVTKIIDGGAAQKDGRLQVGDRLLMV NNYSLEEVTHEEAVAILKNTSDVVYLKV GKPT
6	Chapsyn-110 (3/3)	PDZ	Q91XM9	421-502 = 82	KVVLHKGSTGLGFNIVGGEDGEGIFVSFI LAGGPADLSGELQRGDQILSVNGIDLRG ASHEQAAAALKGAGQTVTIIAQYQP
7	Cipp (3/10)	PDZ	Q63ZW7	365-453 = 89	SVELVKKDQSLGIRIVGYVGT AHPGEAS GIYVKSIIPGSAAAHNGQIQVNDKIVAVD GVNIQGFANQDVVEVLRNAGQVVHLLT VRRK
8	Cipp (5/10)	PDZ	Q63ZW7	688-774 = 87	TVELVKDCKGLGFSILDYQDPLDPTRSVIV RSLVADGVAERSGELLPGDRLVSVNEFSL DNATLAEAVEVLKAVPPGVVHLGICKP
9	Cipp (8/10)	PDZ	Q63ZW7	1472-1555 = 84	IIEISKGRSGLSIVGGKDTPLDAIVIHEVY EEGAAARDGRLWAGDQILEVNGVDLRSS SHEEAITALRQTPQKVRLVVYRDE
10	Cipp (9/10)	PDZ	Q63ZW7	1568-1650 = 83	LVDLQKKTGRGLSIVGKRSVGSVFI VKGGAADLDGRLIRGDQILSVNGEDMRH ASQETVATILKCVQGLVQLEIGRLR
11	Cipp (10/10)	PDZ	Q63ZW7	1709-1795 = 87	TVEIIRELSDALGSIAGGKGSPLGDIPIFIA MIQANGVAARTQKLKVGDRIVSINGQPL DGLSHTDAVNLLKNAFGRILQVVADT
12	Radil (1/1)	PDZ	Q69Z89	1000-1085 = 86	MVELERGPSGLGMGLIDGMHTPLGAQG LYIQTLLPGSPAASDGRSLGDQILEVNGS SLRGVSYMRAVDLIRHGGKKMRFLVAKS D
13	Dlgh3 (1/1)	PDZ	Q6XE40	135-218 = 84	VKIVRLVKNKEPLGATIRRDEHSGA VVVARIMRGGAAADRSGLVHVGDEL EVNGIAVLHKRPDEISQILAQSQGS ITLKIIPAT
14	Dvl1 (1/1)	PDZ	Q3U2D3	251-323 = 73	TVTLNMRHHFLGISIVGQSNDRGDGGIY IGSIMKGGAVAADGRIEPGDMLLQVNDV NFENMSNDDAVRVLRE
15	Dvl2 (1/1)	PDZ	Q60838	267-339 = 73	TVTLNMEKYNFLGISIVGQSNERGDGGIYI GSIMKGGAVAADGRIEPGDMLLQVND

GST-PDZ Domains

					MNFENMSNDDAVRVLRD
16	Dvl3 (1/1)	PDZ	Q61062	249-321 = 73	TVTLNMEKYNFLGISIVGQSNERGDGGIYI GSIMKGGAVAADGRIEPGDMLLQVNEIN FENMSNDDAVRVLRE
17	Erbin (1/1)	PDZ	Q80TH2	1311-1400 = 90	EIRVRVEKDPPELGFSGVGGVGGRRGNPFRP DDDGFVTRVQPEGPASKLLQPGDKIIQA NGYSFINIEHGQAVSLLKTFHNAVDLIIVR EV
18	GRASP55 (1/1)	PDZ	Q99JX3	5-75 = 71	QSVEIPGGGTEGYHVLRVQENSPGHRAG LEPFFDFIVSINGSRLNKDNDTLKDLLKAN VEKPVKMLIYSSK
19	Grip1 (6/7)	PDZ	Q925T6	672-754 = 83	TVELKRYGGPLGITISGTEEPFDPIISSLTK GGLAERTGAIHIGDRILAINSSSLKKGKPLSE AIHLLQMAGETVTLKIKKQT
20	Grip2 (5/7)	PDZ	E0CX54	555-638 = 84	TFHVKLPKRSVELGITISSaSRKR GEPLIISDIKKGSVAHRTGtLEPGD KLLAIDNIRLDNCPMEDAVQILRQC EDLVKLRIR
21	Harmonin (2/3)	PDZ	Q9ES64	211-295 = 85	KVFISLVGSRGLGCSISSGPIQKPGIFVSHV KPGSLSAEVLETGDQIVEVNGIDFTNLD HKEAVNVLKSSRSLTISIVAGAGRE
22	HtrA1 (1/1)	PDZ	Q9QZK6	365-467 = 103	TESHDRQAKGKAVTKKKYIGIRMMSLTSS KAKELKDRHRDFPDVLSGAYIIEVIPDTPA EAGGLKENDVIISINGQSVVTANDVSDVI KKENTLNMVVRGNE
23	HtrA3 (1/1)	PDZ	Q9D236	365-450 = 86	IRMRTITPSLVEELKAANPDFPAVSSGIYV QEVVPNSPSQRGGIQDGDIIVKVNGRPL ADSELQEAVLNESSLLEVRRGNDLL
24	Interleukin 16 (1/4)	PDZ	Q9QZP6	213-299 = 87	NIVLMKGOAKGLGFSIVGGKDSIYGPIGIY VKSIFAGGAAAADGRLQEGDEILELNGES MAGLTHQDALQKFKQAKKGLLTLVTRTR
25	LARG (1/1)	PDZ	Q8R4H2	72-151 = 80	CVIIKQDDNGFGLTVSGDNPVVFQSVKE DGAAMRAGVQTGDRIIKVNGTLVTHSN HLEVVKLIRSGSYVALTVQGRPPGS
26	LIN-7A (1/1)	PDZ	Q8JZ50	108-190 = 83	VVELPKTDEGLGFNVMGGKEQNSPIYISR IIPGGVAERHGGKRGDQLLSVNGVSVE GEHHEKAVELLKAAKDSVKLVVRYTP
27	Lin7c (1/1)	PDZ	O88952	93-175 = 83	VVELPKTEEGLGFNIMGGKEQNSPIYISRII PGGIADRHGGLKRGDQLLSVNGVSVEGE HHEKAVELLKAAQGVKLVVRYTP
28	LnX1 (2/4)	PDZ	O70263	385-467 = 83	HVILNKSSPEEQLGIKLVRVDEPGVFIFN VLNGGVADRHGQLEENDRVLAINGHDL RFGSPESAHLIQASERRVHLVVSQR
29	LnX1 (3/4)	PDZ	O70263	508-593 = 86	VVSVWKDPSESLGMTVGGGASHREWDL

GST-PDZ Domains

					PIYVISVEPGGVISRDGRIKTGDILLNVNGI ELTEVSRTAEAVAILKSAPSSVVLKALEV
30	Lrrc7 (1/1)	PDZ	Q80TE7	1398-1488 = 91	EQFCVRIEKNPGLGFSISGGISGQGNPFKP SDKGIFVTRVQPDGPASNLLQPGDKILQA NGHSFVHMEHEKAVLLLKSFQNTVDLVI QREL
31	Magi-1 (2/6)	PDZ	Q6RHR9	464-546 = 83	HTKLRKSSRGFGFTVVGDEPDEFLQIKSL VLDGPAALDGMETGDVIVSVNDTCVLG HTHAQVVKIFQSIPIGASVDLELCR
32	Magi-1 (4/6)	PDZ	Q6RHR9	833-915 = 83	DIFLWRKETGFGFRILGGNEPGEPIYIGHI VPLGAADTDGRLRSGDELICVDGTPVIGK SHQLVVQLMQQAAKQGHVNLTVRR
33	Magi-1 (6/6)	PDZ	Q6RHR9	1132-1214 = 83	TVELERGAKGFGFSLRGGREYNMDLYVL RLAEDGPAERCCKMRIGDEILEINGETTK NMKHSRAIELIKNGGRRVRLFLRRGD
34	Magi-2 (2/6)	PDZ	Q9WVQ1	425-509 = 85	STTLKSNMGFGFTIIGGDEPDEFLQVKS VIPDGPAAQDGKMETGDVIVYINEVCVL GHTHADVVKLFQSVPIGQSVNLVLCRGY
35	Magi-2 (5/6)	PDZ	Q9WVQ1	919-1009 = 91	DVVIHRKENEGFGFVIISSLNRPESGATITV PHKIGRIIDGSPADRCALKVGDRLAVNG QSIINMPHADIVKLIKDAGLSVTLRIIPQE
36	Magi-2 (6/6)	PDZ	Q9WVQ1	1139-1221 = 83	TVDMEKGAKGFGFSIRGGREYKMDLYVL RLAEDGPAIRNGRMRVGDQIIEINGESTR DMTHARAIELIKSGGRRVRLLLKRGD
37	Magi-3 (1/6)	PDZ	Q9EQJ9	18-108 = 91	CAVSWAGPPGDLGAEIRGGAERGEFPYL GRLRDEAGGGGGTCCVVS GKAPSPGDVL LEVNGTPVSGLTNRDTLAVIRHFREPIRLK TVKPG
38	Magi-3 (2/6)	PDZ	Q9EQJ9	413-495 = 83	RASLKKSTMGFGFTIIGGDRPDEFLQVKN VLKDGPAAQDGKIAPGDVIVDINGNCVL GHTHADVVQMFQLVPVNQYVNLTLCR
39	Magi-3 (5/6)	PDZ	Q9EQJ9	852-939 = 88	DVTLQRKENEGFGFVILTSKSKPPPVIPIH KIGRVIDGSPADRCGGLKVGDDHISAVNG QSIVDLSHDNIVQLIKDAGVTVTLTVVAEE
40	Mals2 (1/1) / lin-7	PDZ	Q9HAP6	93-175 = 83	VVELPKTDEGLGFNIMGGKEQNSPIYISR VIPGGVADRHGGLKRGDQLLSVNGVSVE GEQHEKAVELLKAAQGSVKLVVRYTP
41	Mpp7 (1/1)	PDZ	Q8BVD5	139-220 = 82	IIRLVKNSEPLGATIKKDEQTGAITVARIM RGGAADRSGLIHVGDDELREVNIPVEDK RPEEIIKILSQSKGAIKFIIIPST
42	MUPP1 (1/13)	PDZ	Q8VBX6	138-225 = 88	IFELLKPPCGGLGFSVVGRLRSENREGELGIF VQEIQEGSVAHRDGRDKETDQILAINGQV LDQTITHQQAISILQKAKDTVQLVIARGS
43	MUPP1 (5/13)	PDZ	Q8VBX6	693-779 = 87	SIELEKGSRGLGFSILDYQDPIDPANTVIVI

GST-PDZ Domains

					RSLVPGGIAEKDGRFLPGDRLMFVNDINL ENSTLEEAVEALKGAPSGMVRIGVAKP
44	MUPP1 (10/13)	PDZ	Q8VBX6	1614-1697 = 84	TIEISKGQTGLGLSIVGGSDTLGAIHHEVY EEGAACKDGRLWAGDQILEVNGIDLKRA THDEAINVLRQTPQVRVRLTYRDE
45	MUPP1 (11/13)	PDZ	Q8VBX6	1710-1792 = 83	TIELQKRPKGKGLGLSIVGKRNDTGVFVSDI VKGGIADADGRMLMQGDQILMVNGEDV RHATQEAVAALLKCSLGAVTLEVGRVK
46	MUPP1 (12/13)	PDZ	Q8VBX6	1847-1933 = 87	TVEIKKGPADSLGLSIAGGVGSPGLDVPIFI AMMHPNGVAAQTQKLRVGDRIVTICGT STDGMTHTQAVNLMKNASGSIEVQVVA GG
47	MUPP1 (13/13)	PDZ	Q8VBX6	1972-2055 = 84	TITLDRGPDGLGFSIVGGYGSPLHGLPIYV KTVFAKGGAAEDGRLKRGDQIIAVNGQS LEGVTHEEAVAILKRTKGTVTLMVLS
48	NHERF-1 (1/2)	PDZ	P70441	14-94 = 81	LCCLEKGPNGYGFHLHGEKGVGQFIRLV EPGSPAESGLLAGDRLVEVNGENVEKET HQQVVSRIRAALNAVRLLVVDPE
49	NHERF-1 (2/2)	PDZ	P70441	149-229 = 81	LCTMKKGPNGYGFNLHSDKSKPGQFIRA VDPDSPAESGLRAQDRIVEVNGVCME GKQHGDVVSAIKGGGDEAKLLVVDKE
50	NHERF-2 (1/2)	PDZ	Q9JHL1	11-91 = 81	LCRLVRGEQGYGFHLHGEKGRRGQFIRR VEPGSPAEEAALRAGDRLVEVNGVNVEG ETHHQVVQRIKAVEGQTQLLVVDKE
51	NHERF-2 (2/2)	PDZ	Q9JHL1	151-231 = 81	LCHLRRGPQGYGFNLHSDKSRPGQYIRSV DPGSPASHSGLRAQDRLIEVNGQNVEGL RHAEVVARIKAQEDEARLLVVDPE
52	nNOS (1/1)	PDZ	Q9Z0J4	17-99 = 83	SVRLFKRKVGGLGFLVKERVSKPPVIISDLI RGGAAEQSGLIQAGDIILAVNDRPLVDLS YDSALEVLRGIASETHVVLILRG
53	OMP25 (1/1)	PDZ	Q8K4F3	13-100 = 88	EINLTRGPSGLGFNIVGGTDQQYVSNDS GIYVSRIKEDGAAAQDGRLQEGDKILSVN GQDLKNLLHQDAVDLFRNAGCAVSLRV QHRL
54	PAR-3 (3/3)	PDZ	Q99NH2	590-677 = 88	EVPLNDSGSAGLGVSVKGNRSKENHADL GIFVKSIINGGAASKDGRRLRVNDQLIAVN GESLLGKANQEAMETLRRSMSTEGNKRG MIQ
55	PAR3B (1/3)	PDZ	Q5SV53	201-289 = 89	TRAVEISGEGDPLGIHVVPFFSSLSGRILGL FIRGIEENSRCQEGFLQENECIVKINNVE LLDKTFAQAQDVFRQAMKSPSIVLHVLL
56	PAR6B (1/1)	PDZ	Q9JK83	157-250 = 94	RVRLYKYGTEKPLGFYIRDGSSVRVTPHGL EKVPGIFISRLVPGGLAQSTGLLAVNDEVL EVNGIEVSGKSLDQVTDMMIANSRNLIT

GST-PDZ Domains

						VRPAN
57	Pdlim5 (1/1)	PDZ	Q3UGD0	2-85	= 84	SNYSVSLVGPAPWGFRLQGGKDFNMPL TISSLKDGGKASQAHVRIGDVVLSIDGISA QGMTHLEAQNKIKACTGSLNMTLQRAS
58	Pdzk1 (1/4) / NHRF3/ NaPiCap1	PDZ	Q9JIL4	9-90	= 82	ECKLSKQEGQNYGFFLRIEKDTDGHLIRVI EEGSPAEEKAGLLDGRVLRINGVFVDKKEE HAQVVELVRKSGNSVTLLVLDGD
59	Pdzk1 (3/4) / NHRF3/ NaPiCap1	PDZ	Q9JIL4	243-323	= 81	VVVIKKGSGNGYGFYLRAGPEQKQIIEK PGSPAEEAAGLKNNDLVAVNGKSVEALD HDGVVEMIRKGGDQTTLLVLDKE
60	Pdzk11 (1/1)	PDZ	Q9CZG9	47-129	= 83	IVTLKKPPGAQLGFNIRGGKASQLGIFISK VIPSDAHRAGLQEGDQVLAVNDVDFQ DIEHSCAVEILKTAREISMRVRFPPY
61	Pdzk3 (1/4) /NHRF4/NaPiCap2	PDZ	Q99MJ6	49-130	= 82	FCLLSKEEEKTFGFHLQQLHGKADHVVCR VDPGTSARQQLREGDRILAVNNNIVAH EDHAVVVRYIRASGPRVLLTVLAQH
62	Pdzk3 (3/4) / /NHRF4/NaPiCap2	PDZ	Q99MJ6	263-346	= 84	CLNIEKGPEGFGFLLREEKGLDGRGQFL WDVDPGLPADKAGMKAGDRLVAVAGE SVDGLGHEETVSRIRAQGSCVSLIVVDPE
63	Pdzk3 (1/6)	PDZ	E9Q1M1	81- 179	= 99	ETVGLSFGNIPVFGDYGEKRRGGKKR KTHQGPVLDVGCIVWTELKRNPAK KSGKVRRLRDEILSLNGQLMVGVDVSG ASYLAEQCWNGGFIYLIIMLRRF
64	Pdzk3 (2/6)	PDZ	E9Q1M1	342- 419	= 78	DGLGIQVSGGRGSKRSPHAIIVVTQVK EGGAAHRDGRSLGDELLVINGHLLV GLSHEEAVAILRSATGMVQLVVASKE
65	PDZ-RGS3 (1/1)	PDZ	Q9DC04	18-95	= 78	QITIRRGKDGFGFTICCDSPVRVQAVDSG GPAERAGLQQLDVLQNLNERPVEHWKC VELAHEIRSCPSEIILLVWRVV
66	PSD95 (1/3)	PDZ	Q62108	65-151	= 87	EITLERGNSGLGFSIAGGTDNPHIGDDPSI FITKIIPGGAAQDGRRLRVNDSILFVNEVD VREVTHSAAVEALKEAGSIVRLVMRR
67	PSD95 (2/3)	PDZ	Q62108	160-246	= 87	EIKLIKGPKGLGFSIAGGVGNQHIPGDNSI YVTKIIEGGAAHKDGRQLQIGDKILAVNSV GLEDVMHEDAVAALKNTYDVVYLKVAKP
68	PSD95 (3/3)	PDZ	Q62108	313-393	= 81	RIVIHGSGTGLGFNIVGGEDGEGIFISFILA GGPADLSGELRKGQILSVNGVDLRNAS HEQAAIALKNAGQVTIIAQYK
69	PTP-BL (2/5)	PDZ	Q64512	1357-1442	= 86	EVELAKTDGSLGISVTGGVNTSVRHGGIY VKAIIPKGAAESDGRHKGDRVLAVNGVS LEGATHKQAVETLRNTGQVVHLLLEKGGQ
70	SAP102 (2/3)	PDZ	P70175	244-330	= 87	EVNLLKGPGLGFSIAGGIGNQHIPGDNSI IYTKIIEGGAAQKDGRLQIGDRLLAVNNT NLQDVRHEEAVASLKNTSMDMVYLKVAKP

GST-PDZ Domains

71	SAP102 (3/3)	PDZ	P70175	404-484 = 81	KIILHKGSTGLGFNIVGGEDGEGIFVSVILA GGPADLSGELRRGDRILSVNGVNLRNAT HEQAAAALKRAGQSVTIVAQYR
72	SAP97 (1/3)	PDZ	Q811D0	224-311 = 88	EITLERGNSGLGFSIAGGTDNPHIGDDSSI FITKIITGGAAAQDGRLRVNDCILRVNEA DVRDVTHSKAVEALKEAGSIVRLYVKRRK
73	SAP97 (2/3)	PDZ	Q811D0	319-406 = 88	EIKLIKGPKGLGFSIAGGVGNQHIPGDNSI YVTKIIEGGAAHKDGKLIQIDKLLAVNSV CLEEVTHEEAVTALKNTSDFVYLKVAKPT
74	SAP97 (3/3)	PDZ	Q811D0	466-547 = 82	KVVLHRGSTGLGFNIVGGEDGEGIFISFIL AGGPADLSGELRKGDRIISVNSVDLRAAS HEQAAAALKNAGQAVTIVAQYRP
75	Scrb1 (1/4)	PDZ	Q80U72	714-801 = 88	TLTIVRQTGGLGISIAGGKGSTPYKGDDE GIFISRVSEEGPAARAGVRVGDKLEEVNG VALQDAEHHEAVEALRGAGAAVQMRV WRER
76	Scrb1 (2/4)	PDZ	Q80U72	848-936 = 89	AACLVRSEKGLGFSIAGGKGSTPYRAGDG GIFISRIAEGGAAHRAGTLQVGDRVLSIN GVDMTEARHDHAVSLTAASPTISLLER ET
77	Scrb1 (3/4)	PDZ	Q80U72	990-1079 = 90	EICLPRAGGPLGLSIVGGSDHSSHFPVQ DPGVFISKVLPRGLAARCGLRVGDRILAV NGQDVREATHQEAVSALLRPCLELCLLVR RDP
78	Semcap3 (1/2)	PDZ	Q69ZS0	249-339 = 91	TLVLHRDSGSLGFNIIGRPCVDNQDSS SEGIFVSKIVDSGPAAKEGGLQIHDRIIEV NGKDLRATHDQAVEAFKTAKEPIVVQV LRRT
79	Shank1 (1/1)	PDZ	D3YZU1	663-757 = 95	TVLLQKKDSEGFVLRGAKAQTPIEEFTP TPAFPALQYLESVDEGGVAWRAGLRMG DFLIEVNGQNVVKVGHQRQVNMIRQGG NTLMVKVVMVT
80	Shank3 (1/1)	PDZ	Q4ACU6	570-664 = 95	VAILQKRDHEGFGVLRGAKAETPIEFTFP TPAFPALQYLESVDVEGVAVWRAGLRTGD FLIEVNGVNVVKVGHKQVVGLIRQGGNR LVMKVVSVT
81	Shroom (1/1)	PDZ	Q9QXN0	24-109 = 86	FVYLEALLEGGAPWGFTLKGGLERGEPLII SKIEEGGKADSVSSGLQAGDEVIHINEVAL SSPREAVSLVKGSYKTLRLVRRDV
82	SLIM (1/1)	PDZ	Q8R1G6	1-84 = 84	MALTVDVAGPAPWGFRISSGRDFHTPII VTKVTERGKAEAADLRPGDIIVAINGQSA ENMLHAEAQSKIRQSASPLRLQLDRSQ

GST-PDZ Domains

83	Tiam2 (1/1)	PDZ	Q6ZPF3	911-997 = 87	DVQLTKTGDMTDFGFAVTVQVDEHQHL NRIFISDVLPSLAYGGGLRKGNEITSLNG EPVSDLDIQQMEALFSEKSVGLTLVARPV T
84	TIP-1 (1/1)	PDZ	Q9DBG9	15-112 = 98	RVEIHKLRQGENLILGFSIGGGIDQDPSQ NPFSEDKTDKGIYVTRVSEGGPAEIAGLQI GDKIMQVNGWDMTMVTHDQARKRLT KRSEEVVRLLVTRQ
85	Whirlin (3/3)	PDZ	Q5MLF8	827-910 = 84	LVRVRKSAATLGIAIEGGANTRQPLPRIVT IQRGGSANCGQLKVGHVILEVNGQTLR GKEHKEAARIAEAFKTKERDYIDFL
86	ZO-1 (1/3)	PDZ	P39447	23-110 = 88	TVTLHRAPGFGFGIAISGGRDNPHFQSGE TSIVISDVLKGGPAEGQLQENDRVAMVN GVSMMDNVEHAFVQQLRKSGKNAKITIR RKK
87	ZO-1 (2/3)	PDZ	P39447	186-264 = 79	KVTLVKSRKNEEYGLRLASHIFVKEISQDSL AARDGNIQEGDVVLKINGTVTENMSLTD AKTLIERSKGKLMVVQRDE
88	ZO-2 (1/3)	PDZ	Q9ZOU1	10-97 = 88	TVTLQKDSKRGFGIAVSGGRDNPHFENG ETSIVISDVLPGGPADGLLQENDRVVMV NGTPMEDVLHSFAVQQLRKSGKIAAIVV KRPR
89 1	ZO-3 (1/3)	PDZ	Q9QXY1	287-365 = 79	GVLLTKSKANEEYGLRLGSQIFIKEMTRTG LATKDGNLHEGDIIKINGTVTENMSLTD ARKLIEKSRGKLQLVVLDRS

APPENDIX C

Certificate of Analysis

Product Name: Microinjection Ready Validated

Product Number: CRSPMVA

Lot Number: 879

Target Gene: PRMT5 *mus musculus*

Description of Product:

5 x 50uL of ready-to-inject CRISPR/Cas9*

*premixed Cas9 and sgRNA in microinjection buffer

sgRNA Target Site Sequence 5'→3':

gRNA/PAM Site: atggtataggagcggccggtagg (complementary)

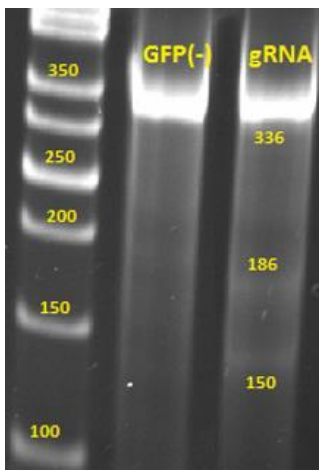
Validated Primers:

Primer Name	Sequence 5'-3'
sgRNA #1 Forward	cgcctgtgtcttctgatt
sgRNA #1 Reverse	gtggccacatgacattag

Please store all reagents at: -80°C. Spin down reagents before opening.

For microinjection guidelines please reference our tech bulletin at
<http://www.sageresearchlabs.com/crisprtech>

CRISPR/Cas9 Validation:



Cel-1 assay resolved on 10% TBE-PAGE

All gRNAs were transfected into Mouse Neuro2A cells and genomic DNA was harvested 24 hours post transfection. This DNA was used as template for a mismatch sensitive PCR assay to detect CRISPR/Cas9-mediated mutations.

Genotyping Protocol:

1. Prepare a PCR reaction with the following reaction components:

Reaction components	Volume (µL)	Final concentration
DNA template	1	--
10 uM Primer F	5	1 uM
10 uM Primer R	5	1 uM
Sigma JumpStart Taq ReadyMix (P2893)	25	1X
H ₂ O	14	--
	50 µl reaction	

2. PCR cycling conditions

Cycle Step	Temp (°C)	Time	
1	95	5 min	
2	95	30s	x35 cycles
3	60	30s	
4	68	40s	
5	68	5 min	

3. Sequencing the PCR Product / Mutation Analysis

Send all PCR product to sequencing for mutation analysis. For best results it is recommended that the PCR products undergo a purification step to remove residual dNTPs and primers prior to sequencing.

Expected wild type band size: 336bp

APPENDIX D

**ELSEVIER LICENSE
TERMS AND CONDITIONS**

Aug 25, 2016

This Agreement between Aleksandra B Espejo ("You") and Elsevier ("Elsevier") consists of your license details and the terms and conditions provided by Elsevier and Copyright Clearance Center.

License Number	3936090062382
License date	Aug 25, 2016
Licensed Content Publisher	Elsevier
Licensed Content Publication	Molecular Cell
Licensed Content Title	Protein Arginine Methylation in Mammals: Who, What, and Why
Licensed Content Author	Mark T. Bedford, Steven G. Clarke
Licensed Content Date	16 January 2009
Licensed Content Volume Number	33
Licensed Content Issue Number	1
Licensed Content Pages	13
Start Page	1
End Page	13
Type of Use	reuse in a thesis/dissertation
Intended publisher of new work	other
Portion	figures/tables/illustrations
Number of figures/tables /illustrations	2
Format	print
Are you the author of this Elsevier article?	No
Will you be translating?	No
Order reference number	
Original figure numbers	1 and 2
Title of your thesis/dissertation	Role of phosphorylation in the regulation of PRMT5
Expected completion date	Jun 2016
Estimated size (number of pages)	100
Elsevier VAT number	GB 494 6272 12

Requestor Location Alexsandra B Espejo
 1808 Park Road 1-C

 SMITHVILLE, TX 78957
 United States
 Attn: Alexsandra B Espejo

Total 0.00 USD

Terms and Conditions

INTRODUCTION

1. The publisher for this copyrighted material is Elsevier. By clicking "accept" in connection with completing this licensing transaction, you agree that the following terms and conditions apply to this transaction (along with the Billing and Payment terms and conditions established by Copyright Clearance Center, Inc. ("CCC"), at the time that you opened your Rightslink account and that are available at any time at <http://myaccount.copyright.com>).

GENERAL TERMS

2. Elsevier hereby grants you permission to reproduce the aforementioned material subject to the terms and conditions indicated.

3. Acknowledgement: If any part of the material to be used (for example, figures) has appeared in our publication with credit or acknowledgement to another source, permission must also be sought from that source. If such permission is not obtained then that material may not be included in your publication/copies. Suitable acknowledgement to the source must be made, either as a footnote or in a reference list at the end of your publication, as follows:

"Reprinted from Publication title, Vol /edition number, Author(s), Title of article / title of chapter, Pages No., Copyright (Year), with permission from Elsevier [OR APPLICABLE SOCIETY COPYRIGHT OWNER]." Also Lancet special credit - "Reprinted from The Lancet, Vol. number, Author(s), Title of article, Pages No., Copyright (Year), with permission from Elsevier."

4. Reproduction of this material is confined to the purpose and/or media for which permission is hereby given.

5. Altering/Modifying Material: Not Permitted. However figures and illustrations may be altered/adapted minimally to serve your work. Any other abbreviations, additions, deletions and/or any other alterations shall be made only with prior written authorization of Elsevier Ltd. (Please contact Elsevier at permissions@elsevier.com)

6. If the permission fee for the requested use of our material is waived in this instance, please be advised that your future requests for Elsevier materials may attract a fee.

7. Reservation of Rights: Publisher reserves all rights not specifically granted in the combination of (i) the license details provided by you and accepted in the course of this licensing transaction, (ii) these terms and conditions and (iii) CCC's Billing and Payment terms and conditions.

8. License Contingent Upon Payment: While you may exercise the rights licensed immediately upon issuance of the license at the end of the licensing process for the transaction, provided that you have disclosed complete and accurate details of your proposed use, no license is finally effective unless and until full payment is received from you (either by publisher or by CCC) as provided in CCC's Billing and Payment terms and conditions. If full payment is not received on a timely basis, then any license preliminarily granted shall be

deemed automatically revoked and shall be void as if never granted. Further, in the event that you breach any of these terms and conditions or any of CCC's Billing and Payment terms and conditions, the license is automatically revoked and shall be void as if never granted. Use of materials as described in a revoked license, as well as any use of the materials beyond the scope of an unrevoked license, may constitute copyright infringement and publisher reserves the right to take any and all action to protect its copyright in the materials.

9. **Warranties:** Publisher makes no representations or warranties with respect to the licensed material.

10. **Indemnity:** You hereby indemnify and agree to hold harmless publisher and CCC, and their respective officers, directors, employees and agents, from and against any and all claims arising out of your use of the licensed material other than as specifically authorized pursuant to this license.

11. **No Transfer of License:** This license is personal to you and may not be sublicensed, assigned, or transferred by you to any other person without publisher's written permission.

12. **No Amendment Except in Writing:** This license may not be amended except in a writing signed by both parties (or, in the case of publisher, by CCC on publisher's behalf).

13. **Objection to Contrary Terms:** Publisher hereby objects to any terms contained in any purchase order, acknowledgment, check endorsement or other writing prepared by you, which terms are inconsistent with these terms and conditions or CCC's Billing and Payment terms and conditions. These terms and conditions, together with CCC's Billing and Payment terms and conditions (which are incorporated herein), comprise the entire agreement between you and publisher (and CCC) concerning this licensing transaction. In the event of any conflict between your obligations established by these terms and conditions and those established by CCC's Billing and Payment terms and conditions, these terms and conditions shall control.

14. **Revocation:** Elsevier or Copyright Clearance Center may deny the permissions described in this License at their sole discretion, for any reason or no reason, with a full refund payable to you. Notice of such denial will be made using the contact information provided by you. Failure to receive such notice will not alter or invalidate the denial. In no event will Elsevier or Copyright Clearance Center be responsible or liable for any costs, expenses or damage incurred by you as a result of a denial of your permission request, other than a refund of the amount(s) paid by you to Elsevier and/or Copyright Clearance Center for denied permissions.

LIMITED LICENSE

The following terms and conditions apply only to specific license types:

15. **Translation:** This permission is granted for non-exclusive world **English** rights only unless your license was granted for translation rights. If you licensed translation rights you may only translate this content into the languages you requested. A professional translator must perform all translations and reproduce the content word for word preserving the integrity of the article.

16. **Posting licensed content on any Website:** The following terms and conditions apply as follows: Licensing material from an Elsevier journal: All content posted to the web site must maintain the copyright information line on the bottom of each image; A hyper-text must be included to the Homepage of the journal from which you are licensing at <http://www.sciencedirect.com/science/journal/xxxxx> or the Elsevier homepage for books at <http://www.elsevier.com>; Central Storage: This license does not include permission for a

scanned version of the material to be stored in a central repository such as that provided by Heron/XanEdu.

Licensing material from an Elsevier book: A hyper-text link must be included to the Elsevier homepage at <http://www.elsevier.com> . All content posted to the web site must maintain the copyright information line on the bottom of each image.

Posting licensed content on Electronic reserve: In addition to the above the following clauses are applicable: The web site must be password-protected and made available only to bona fide students registered on a relevant course. This permission is granted for 1 year only. You may obtain a new license for future website posting.

17. For journal authors: the following clauses are applicable in addition to the above:

Preprints:

A preprint is an author's own write-up of research results and analysis, it has not been peer-reviewed, nor has it had any other value added to it by a publisher (such as formatting, copyright, technical enhancement etc.).

Authors can share their preprints anywhere at any time. Preprints should not be added to or enhanced in any way in order to appear more like, or to substitute for, the final versions of articles however authors can update their preprints on arXiv or RePEc with their Accepted Author Manuscript (see below).

If accepted for publication, we encourage authors to link from the preprint to their formal publication via its DOI. Millions of researchers have access to the formal publications on ScienceDirect, and so links will help users to find, access, cite and use the best available version. Please note that Cell Press, The Lancet and some society-owned have different preprint policies. Information on these policies is available on the journal homepage.

Accepted Author Manuscripts: An accepted author manuscript is the manuscript of an article that has been accepted for publication and which typically includes author-incorporated changes suggested during submission, peer review and editor-author communications.

Authors can share their accepted author manuscript:

- immediately
 - o via their non-commercial person homepage or blog
 - o by updating a preprint in arXiv or RePEc with the accepted manuscript
 - o via their research institute or institutional repository for internal institutional uses or as part of an invitation-only research collaboration work-group
 - o directly by providing copies to their students or to research collaborators for their personal use
 - o for private scholarly sharing as part of an invitation-only work group on commercial sites with which Elsevier has an agreement
- after the embargo period
 - o via non-commercial hosting platforms such as their institutional repository
 - o via commercial sites with which Elsevier has an agreement

In all cases accepted manuscripts should:

- link to the formal publication via its DOI
- bear a CC-BY-NC-ND license - this is easy to do
- if aggregated with other manuscripts, for example in a repository or other site, be

shared in alignment with our hosting policy not be added to or enhanced in any way to appear more like, or to substitute for, the published journal article.

Published journal article (JPA): A published journal article (PJA) is the definitive final record of published research that appears or will appear in the journal and embodies all value-adding publishing activities including peer review co-ordination, copy-editing, formatting, (if relevant) pagination and online enrichment.

Policies for sharing publishing journal articles differ for subscription and gold open access articles:

Subscription Articles: If you are an author, please share a link to your article rather than the full-text. Millions of researchers have access to the formal publications on ScienceDirect, and so links will help your users to find, access, cite, and use the best available version.

Theses and dissertations which contain embedded PJAs as part of the formal submission can be posted publicly by the awarding institution with DOI links back to the formal publications on ScienceDirect.

If you are affiliated with a library that subscribes to ScienceDirect you have additional private sharing rights for others' research accessed under that agreement. This includes use for classroom teaching and internal training at the institution (including use in course packs and courseware programs), and inclusion of the article for grant funding purposes.

Gold Open Access Articles: May be shared according to the author-selected end-user license and should contain a [CrossMark logo](#), the end user license, and a DOI link to the formal publication on ScienceDirect.

Please refer to Elsevier's [posting policy](#) for further information.

18. **For book authors** the following clauses are applicable in addition to the above:

Authors are permitted to place a brief summary of their work online only. You are not allowed to download and post the published electronic version of your chapter, nor may you scan the printed edition to create an electronic version. **Posting to a repository:** Authors are permitted to post a summary of their chapter only in their institution's repository.

19. **Thesis/Dissertation:** If your license is for use in a thesis/dissertation your thesis may be submitted to your institution in either print or electronic form. Should your thesis be published commercially, please reapply for permission. These requirements include permission for the Library and Archives of Canada to supply single copies, on demand, of the complete thesis and include permission for Proquest/UMI to supply single copies, on demand, of the complete thesis. Should your thesis be published commercially, please reapply for permission. Theses and dissertations which contain embedded PJAs as part of the formal submission can be posted publicly by the awarding institution with DOI links back to the formal publications on ScienceDirect.

Elsevier Open Access Terms and Conditions

You can publish open access with Elsevier in hundreds of open access journals or in nearly 2000 established subscription journals that support open access publishing. Permitted third party re-use of these open access articles is defined by the author's choice of Creative Commons user license. See our [open access license policy](#) for more information.

Terms & Conditions applicable to all Open Access articles published with Elsevier:

Any reuse of the article must not represent the author as endorsing the adaptation of the article nor should the article be modified in such a way as to damage the author's honour or reputation. If any changes have been made, such changes must be clearly indicated.

The author(s) must be appropriately credited and we ask that you include the end user

license and a DOI link to the formal publication on ScienceDirect.

If any part of the material to be used (for example, figures) has appeared in our publication with credit or acknowledgement to another source it is the responsibility of the user to ensure their reuse complies with the terms and conditions determined by the rights holder.

Additional Terms & Conditions applicable to each Creative Commons user license:

CC BY: The CC-BY license allows users to copy, to create extracts, abstracts and new works from the Article, to alter and revise the Article and to make commercial use of the Article (including reuse and/or resale of the Article by commercial entities), provided the user gives appropriate credit (with a link to the formal publication through the relevant DOI), provides a link to the license, indicates if changes were made and the licensor is not represented as endorsing the use made of the work. The full details of the license are available at <http://creativecommons.org/licenses/by/4.0>.

CC BY NC SA: The CC BY-NC-SA license allows users to copy, to create extracts, abstracts and new works from the Article, to alter and revise the Article, provided this is not done for commercial purposes, and that the user gives appropriate credit (with a link to the formal publication through the relevant DOI), provides a link to the license, indicates if changes were made and the licensor is not represented as endorsing the use made of the work. Further, any new works must be made available on the same conditions. The full details of the license are available at <http://creativecommons.org/licenses/by-nc-sa/4.0>.

CC BY NC ND: The CC BY-NC-ND license allows users to copy and distribute the Article, provided this is not done for commercial purposes and further does not permit distribution of the Article if it is changed or edited in any way, and provided the user gives appropriate credit (with a link to the formal publication through the relevant DOI), provides a link to the license, and that the licensor is not represented as endorsing the use made of the work. The full details of the license are available at <http://creativecommons.org/licenses/by-nc-nd/4.0>. Any commercial reuse of Open Access articles published with a CC BY NC SA or CC BY NC ND license requires permission from Elsevier and will be subject to a fee.

Commercial reuse includes:

- Associating advertising with the full text of the Article
- Charging fees for document delivery or access
- Article aggregation
- Systematic distribution via e-mail lists or share buttons

Posting or linking by commercial companies for use by customers of those companies.

20. Other Conditions:

v1.8

Questions? customer@copyright.com or +1-855-239-3415 (toll free in the US) or +1-978-646-2777.

Subject: RE: Request permission for thesis/disertation
Date: Thursday, August 25, 2016 3:47:06 PM Central Daylight Time
From: Ballen, Karen
To: Espejo,Alexsandra B

Dear Alexsandra:

Copyright permission is granted for this request.

Kind regards,

Karen Ballen
Manager

From: Espejo,Alexsandra B [mailto:abespejo@mdanderson.org]
Sent: Thursday, August 25, 2016 4:22 PM
To: Ballen, Karen
Subject: Request permission for thesis/disertation

Hello,

I am preparing my thesis and I would like to use the figure 1 of the following publication:

Title: Redox Regulation of DNA
Repair: Implications for
Human Health and Cancer
Therapeutic Development
Author: Meihua Luo, Hongzhen He,
Mark R. Kelley, et al
Publication: Antioxidants & Redox
Signaling
Publisher: Mary Ann Liebert, Inc.
Date: Jun 1, 2010

Please let me know how this could be arranged,

Thank you,

Alexsandra

The information contained in this e-mail message may be privileged, confidential, and/or protected from disclosure. This e-mail message may contain protected health information (PHI); dissemination of PHI should comply with applicable federal and state laws. If you are not the intended recipient, or an authorized representative of the intended recipient, any further review, disclosure, use, dissemination, distribution, or copying of this message or any attachment (or the information contained therein) is strictly prohibited. If you think that you have received this e-mail message in error, please notify the sender by return e-mail and delete all references to it and its contents from your systems.

**NATURE PUBLISHING GROUP LICENSE
TERMS AND CONDITIONS**

Aug 25, 2016

This Agreement between Aleksandra B Espejo ("You") and Nature Publishing Group ("Nature Publishing Group") consists of your license details and the terms and conditions provided by Nature Publishing Group and Copyright Clearance Center.

License Number	3936100851999
License date	Aug 25, 2016
Licensed Content Publisher	Nature Publishing Group
Licensed Content Publication	Nature Structural and Molecular Biology
Licensed Content Title	A mediator methylation mystery: JMJD1C demethylates MDC1 to regulate DNA repair
Licensed Content Author	Jian Lu, Michael J Matunis
Licensed Content Date	Dec 4, 2013
Licensed Content Volume Number	20
Licensed Content Issue Number	12
Type of Use	reuse in a dissertation / thesis
Requestor type	academic/educational
Format	print and electronic
Portion	figures/tables/illustrations
Number of figures/tables /illustrations	1
High-res required	no
Figures	1
Author of this NPG article	no
Your reference number	
Title of your thesis / dissertation	Role of phosphorylation in the regulation of PRMT5
Expected completion date	Jun 2016
Estimated size (number of pages)	100
Requestor Location	Aleksandra B Espejo 1808 Park Road 1-C SMITHVILLE, TX 78957 United States

Attn: Alexsandra B Espejo

Billing Type Invoice

Billing Address Alexsandra B Espejo
1808 Park Road 1-C

SMITHVILLE, TX 78957
United States
Attn: Alexsandra B Espejo

Total 0.00 USD

Terms and Conditions

Terms and Conditions for Permissions

Nature Publishing Group hereby grants you a non-exclusive license to reproduce this material for this purpose, and for no other use, subject to the conditions below:

1. NPG warrants that it has, to the best of its knowledge, the rights to license reuse of this material. However, you should ensure that the material you are requesting is original to Nature Publishing Group and does not carry the copyright of another entity (as credited in the published version). If the credit line on any part of the material you have requested indicates that it was reprinted or adapted by NPG with permission from another source, then you should also seek permission from that source to reuse the material.
2. Permission granted free of charge for material in print is also usually granted for any electronic version of that work, provided that the material is incidental to the work as a whole and that the electronic version is essentially equivalent to, or substitutes for, the print version. Where print permission has been granted for a fee, separate permission must be obtained for any additional, electronic re-use (unless, as in the case of a full paper, this has already been accounted for during your initial request in the calculation of a print run). NB: In all cases, web-based use of full-text articles must be authorized separately through the 'Use on a Web Site' option when requesting permission.
3. Permission granted for a first edition does not apply to second and subsequent editions and for editions in other languages (except for signatories to the STM Permissions Guidelines, or where the first edition permission was granted for free).
4. Nature Publishing Group's permission must be acknowledged next to the figure, table or abstract in print. In electronic form, this acknowledgement must be visible at the same time as the figure/table/abstract, and must be hyperlinked to the journal's homepage.
5. The credit line should read:
Reprinted by permission from Macmillan Publishers Ltd: [JOURNAL NAME] (reference citation), copyright (year of publication)
For AOP papers, the credit line should read:
Reprinted by permission from Macmillan Publishers Ltd: [JOURNAL NAME], advance online publication, day month year (doi: 10.1038/sj.[JOURNAL ACRONYM].XXXXX)

Note: For republication from the *British Journal of Cancer*, the following credit lines apply.

Reprinted by permission from Macmillan Publishers Ltd on behalf of Cancer Research UK: [JOURNAL NAME] (reference citation), copyright (year of publication) For AOP papers, the credit line should read:

Reprinted by permission from Macmillan Publishers Ltd on behalf of Cancer Research UK: [JOURNAL NAME], advance online publication, day month year (doi: 10.1038/sj.[JOURNAL

ACRONYM].XXXXX)

6. Adaptations of single figures do not require NPG approval. However, the adaptation should be credited as follows:

Adapted by permission from Macmillan Publishers Ltd: [JOURNAL NAME] (reference citation), copyright (year of publication)

Note: For adaptation from the *British Journal of Cancer*, the following credit line applies.

Adapted by permission from Macmillan Publishers Ltd on behalf of Cancer Research UK: [JOURNAL NAME] (reference citation), copyright (year of publication)

7. Translations of 401 words up to a whole article require NPG approval. Please visit <http://www.macmillanmedicalcommunications.com> for more information. Translations of up to a 400 words do not require NPG approval. The translation should be credited as follows:

Translated by permission from Macmillan Publishers Ltd: [JOURNAL NAME] (reference citation), copyright (year of publication).

Note: For translation from the *British Journal of Cancer*, the following credit line applies.

Translated by permission from Macmillan Publishers Ltd on behalf of Cancer Research UK: [JOURNAL NAME] (reference citation), copyright (year of publication)

We are certain that all parties will benefit from this agreement and wish you the best in the use of this material. Thank you.

Special Terms:

v1.1

Questions? customercare@copyright.com or +1-855-239-3415 (toll free in the US) or +1-978-646-2777.
